

L. Koorevaar

Spectral Calibration of Time- Inhomogeneous Exponential Lévy Models

with Asymptotic Normality, Confidence Intervals,
Simulations, and Empirical Results

December 7, 2022

Spectral Calibration of Time-Inhomogeneous Exponential Lévy Models

**with Asymptotic Normality, Confidence Intervals,
Simulations, and Empirical Results**

by

L. Koorevaar

to obtain the degree of Master of Science in Applied Mathematics
at the EEMCS faculty of Delft University of Technology,
to be defended publicly on Thursday December 15th, 2022 at 1:00 PM.

Student number: 4598474
Project duration: August 1, 2021 – December 15, 2022
Thesis committee: Prof. dr. A. Papantoleon, TU Delft
Dr. J. Söhl, TU Delft, supervisor

An electronic version of this thesis is available at <http://repository.tudelft.nl/>.

Abstract

In this thesis, the problem of calibrating *time-inhomogeneous* exponential Lévy models with finite jump activity based on market prices of plain vanilla options is studied. Belomestny and Reiß [7] introduced an estimation procedure for calibration in the homogeneous case with one maturity. The open-ended question that will be addressed is if we can extend this model to use all listed plain vanilla options with multiple maturities. This opens a way to use all available data to create a time-inhomogeneous model with time-dependent Lévy triplets between subsequent intervals based on the maturities.

We establish via an adapted Lévy-Khintchine representation an estimation procedure on the explicit inversion of the option price formulas in the spectral domain with a cut-off scheme for the regularisation of high frequencies. The estimation procedure will be shown to be well-defined and the parameters to be normally distributed asymptotically.

Practical implications imply that using the asymptotic variances of the normal distributions leads to insufficient confidence intervals for non-asymptotical cases. We, therefore, construct confidence intervals using an approximated finite sample variance.

Monte Carlo simulations are implemented in the computational software R to evaluate the stability and accuracy of the estimation procedure. Furthermore, the finite sample confidence intervals are assessed with coverage probabilities. The estimations and confidence intervals are sufficient concerning coverage probabilities when the underlying error magnitudes are estimated by a penalized least squares method. Otherwise, undersmoothing must be employed to counteract the bias term.

In the end, the estimation procedure is evaluated by calibrating to market data of plain vanilla S&P500 options, which contain numerous maturities. The estimated parameters with confidence intervals between maturities support time-dependency and the constructed time-inhomogeneous exponential Lévy models appear favorable in contrast to the time-homogeneous model.

Preface

It is with this thesis that I conclude my period as a Master's student in Applied Mathematics at the EEMCS faculty. In fact, this thesis ends a fruitful, revealing, and much enjoyed period as a student at the Delft University of Technology. Initially, I entered the mathematics faculty as a freshman to complement my bachelor of Applied Physics — what I still naively thought was my favorite child. However, after the strange physical quantity of time moved on, I realized that my interest lies principally in mathematics.

From a teenager onward, my mind was intrigued by watching the fast-paced never settling stock market on television. I wanted to know what moved these stocks upwards or downwards. I never found out unfortunately what actually moved these stocks (otherwise I would not be sitting here writing but stealing the oracle title from Warren Buffett himself). However, I did find out after my bachelor's that these stocks can be modeled using data with my beloved mathematics. In the past year, I was therefore privileged to research a new model that exactly had all these elements combined.

I would like to take this moment to thank Dr. Jakob Söhl for the opportunity and guidance to complete my thesis under his supervision. I enjoyed our weekly meetings in which he patiently helped me with encountered difficulties and general insights into the project. Doing research goes in steps. First, you make two steps forward, and then one step backward, where you meet with — what seems to be — a hopeless problem. His guidance always helped me to make the next steps forward again, for which I want to express my gratitude. I would also like to thank Ms. Rianne Smits for her patience and guidance in making my exchange in my master's program happen. A lot of complications were present due to the corona crisis, which resulted in a two-time cancellation of my exchange. This made me sorrowful, but she always provided me with fresh insights and new options. I am grateful for the last-minute opportunity to go to Hong Kong and her help in making this precipitate. Last but not least, I would like to thank Prof. Dr. Antonis Papapantoleon for the time and engagement he is willing to spend studying this project and for taking a seat on my thesis committee.

I thank the university and all its engaging teachers for all the wisdom and knowledge that I have attained in both my bachelor's and master's programs. I would like to thank my family, (student) friends, and roommates (both in Delft and Rotterdam). They helped me become a more responsible and professional person on the journey from adolescence to adulthood.

Rotterdam,
December 2022

Loek Koorevaar

Contents

Introduction	1
1 Theory	5
1.1 Time-Homogeneous Lévy Processes	5
1.2 Additive Processes and Time-Inhomogeneous Lévy Processes	6
2 The Statistical Model	9
2.1 Exponential Time-Inhomogeneous Lévy Models and Plain Vanilla Options ..	10
2.2 Observations of the Option Prices	11
2.2.1 Data Transformation	11
2.2.2 Estimation of \mathcal{O}_j	12
2.3 Statistical Estimation Approach	12
2.3.1 Relation between \mathcal{O}_j and φ_{T_j}	13
2.3.2 Calibration Function ψ_j and Calibration Estimator $\tilde{\psi}_j$	14
2.4 Spectral Estimation of the Lévy Triplet	16
3 Theoretical Results	21
3.1 Underlying Assumptions	21
3.2 The Estimator $\tilde{\psi}_j$ for ψ_j	23
3.2.1 Choice of Trimmed Value $\kappa(v, T_{j-l})$	24
3.2.2 Asymptotically Well-Definedness of $\tilde{\psi}_j$ for ψ_j	24
3.3 Asymptotic Normality of $(\tilde{\sigma}_j^2, \tilde{\gamma}_j, \tilde{\lambda}_j)$	28
3.3.1 Error Decomposition	28
3.3.2 Asymptotic Normality of Linear Terms $\mathcal{L}_{\xi_j}^l$	30
3.3.3 Bias Term \mathcal{B}_{ξ_j}	38
3.3.4 Remainder Terms $\mathcal{R}_{\xi_j}^l$	39
3.3.5 Normality of $\tilde{\sigma}_j$	46
3.3.6 Normality of $\tilde{\gamma}_j$	48
3.3.7 Normality of $\tilde{\lambda}_j$	49
3.4 Asymptotic Normality of $\tilde{\mu}_j(x)$	50
3.5 Concluding Theorem of Normality Results	53
3.6 Difficulty of Inverse Calibration Problem	54
3.7 Convergence Rates	55
4 Confidence Intervals with Finite Sample Variance	59
4.1 Confidence Intervals for $\tilde{\sigma}_j$	60
4.2 Confidence Intervals for $\tilde{\gamma}_j$	62
4.3 Confidence Intervals for $\tilde{\lambda}_j$	63
4.4 Confidence Intervals for $\tilde{\nu}_j(x)$	65

5	Simulations	71
5.1	Simulation Settings	71
5.1.1	Choice of Cut-off Parameters U_j and U_{ν_j}	71
5.1.2	Choice of Weight Functions	72
5.1.3	Simulation of Exponential Time-Inhomogeneous Lévy Model	73
5.1.4	Simulation of Noised Option Prices from Models	75
5.1.5	Numerical Approximation Fourier Transform	75
5.2	Simulation Results	76
5.2.1	Estimating $(\tilde{\psi}_j)_{j=1,2,3}$ for $(\psi_j)_{j=1,2,3}$	77
5.2.2	Estimating $(\tilde{\sigma}_j, \tilde{\gamma}_j, \tilde{\lambda}_j)_{j=1,2,3}$ for $(\sigma_j, \gamma_j, \lambda_j)_{j=1,2,3}$	78
5.2.3	Estimating $(\tilde{\nu}_j)_{j=1,2,3}$ for $(\nu_j)_{j=1,2,3}$	80
5.2.4	Confidence Intervals and Coverage Probabilities	83
6	Empirical Results	91
6.1	Empirical Settings	91
6.1.1	Underlying Data Set	91
6.1.2	Interest Rate r	92
6.1.3	Smoothness Parameter s_j	93
6.1.4	Choice of Cut-Off Parameters U_j and U_{ν_j}	93
6.2	Empirical Results	93
6.3	Real-Life Parameters over Time	98
7	Conclusion	103
	References	105
A	Proofs of Lemmata	109
B	Additional Details Asymptotic Normality $\tilde{\mu}_j(x)$	113
B.1	Bias Term \mathcal{B}	113
B.2	Decomposition of Ψ Term	113
B.3	Normality of Terms $\mathcal{L}_{\mu_j}^l(v)$ in Ψ	114
B.4	Remainder Terms $\mathcal{R}_{\mu_j}^l$ in Ψ	120

Introduction

Model calibration is essential to the pricing and hedging of financial products. A key question when calibrating a model based on prices of European call and put options is how all the information contained in the option prices can be merged into one model. On the one hand, the model needs to be large enough to allow for sufficient flexibility and to be able to integrate all the available information. On the other hand, the model needs to be identifiable from the options traded on the market. The frequently observed volatility smile or skew is an indication that the Black–Scholes model is not flexible enough to account for the prices of options with different strike prices. Exponential Lévy models are flexible enough to model the volatility smile or skew and can therefore incorporate the information of options with different strike prices. However, empirical evidence shows that calibrating exponential Lévy models by options with different maturities leads to conflicting information, see Cont and Tankov [17], Belomestny and Reiß [9] or Söhl and Trabs [43]. In other words, the stationarity implicitly assumed in the exponential Lévy model is not satisfied. We propose an identifiable time-inhomogeneous Lévy model that does not assume stationarity and that can be calibrated based on option prices from different maturities and different strike prices without leading to conflicting information.

We model an asset price (S_t) by

$$S_t = S e^{rt + X_t} \quad \text{for } t \geq 0, \quad (0.1)$$

where r is the riskless interest rate and (X_t) is a time-inhomogeneous Lévy process in the sense that on each interval between two consecutive maturities T_{j-1} and T_j , the process (X_t) follows a Lévy process which may be different from interval to interval. We focus on the nonparametric calibration of the model to reduce the risk of model misspecification. We model small fluctuations through the volatility and restrict ourselves to Lévy processes of finite jump intensity.

Our estimation is based on European call and put options on the asset S_t , which are traded at time $t = 0$ with maturities T_1, \dots, T_n and different strike prices. In the considered asymptotics the maturities T_1, \dots, T_n are fixed, while for each maturity the range of the strike prices grows and the mesh size of the strike prices decreases. This reflects that options are traded typically only for a few maturities but with many different strike prices for each maturity. Since we base our inference on option prices, the calibration is for the risk-neutral price process.

In the time-inhomogeneous Lévy model, we derive the convergence rates and show confidence intervals for the estimators of the volatility, the drift, the intensity, and the Lévy density. Previously, confidence intervals have been constructed for time-homogeneous Lévy models in an idealized Gaussian white noise model by Söhl [42]. In the idealized Gaussian white noise model, it is assumed that the observations are Gaussian and given continuously across the strike prices. This simplifies the analysis significantly. Here we construct the confidence intervals in a discrete observation setting for time-inhomogeneous Lévy models and the only assumption on the errors is that they are sub-Gaussian, in particular, all bounded errors with arbitrary distributions are covered. Our additional results on the con-

vergence rates extend the paper by Belomestny and Reiß [8] from time-homogeneous to time-inhomogeneous Lévy models.

Three strands of literature are relevant to the thesis at hand. The first strand covers exponential Lévy models. They were first introduced by Merton [32] and have been studied in a variety of pricing and optimization problems in finance, see e.g. Boyarchenko and Levendorskiĭ [12], Cont and Voltchkova [20], Emmer and Klüppelberg [22], Kallsen [28], Mordecki [34], Tankov [45] and the references therein. Pricing and hedging in time-inhomogeneous Lévy models have been treated in Cont and Voltchkova [19] and Zheng and Kwok [52].

The second strand studies the nonparametric estimation of Lévy processes. Nonparametric confidence sets have been studied for Lévy processes observed at high-frequency by Figueroa-López [23] and by Kato and Kurisu [29]. The difference in our work is twofold. Instead of observing the Lévy process directly, we base our inference on option prices. Furthermore, even if compared to the direct observation setting, our observation scheme with fixed maturities corresponds to observations at low frequency and not at high frequency. Estimation of Lévy processes from low-frequency observations has been studied from a frequentist perspective, e.g. by Neumann and Reiß [35], Gugushvili [26], Nickl and Reiß [36] and Coca [15]. From a Bayesian perspective, Lévy processes were studied by Gugushvili et al. [27], Belomestny et al. [5], and Nickl and Söhl [37].

The third strand is closest to the paper at hand and treats the nonparametric calibration of exponential Lévy models based on option prices. It comprises the works Cont and Tankov [18], Belomestny [3], Belomestny and Reiß [11] and Trabs [48, 49]. These works have in common that they assume homogeneity in time and a fixed maturity. Qin and Todorov [38] and Todorov [47] consider a maturity tending to zero in an Itô semimartingale model and study the estimation of the Lévy density at time zero and the spot volatility, respectively.

The thesis at hand is a continuation of the work by Tendijck [46]. The theoretical results of Tendijck [46] have been heavily revised, clarified, and reworked. Next to the revisions, the emphasis of this work has been on confidence intervals, simulations, and empirical results. This work therefore additionally provides a thorough simulation study and brings the method into practice by addressing all the issues needed for the calibration of time-inhomogeneous Lévy models to market data. The computer code is made in the computational software R and can be found publicly at the GitHub page: <https://github.com/Loek44/Spectral-Calibration-of-Time-Inhomogeneous-Levy-processes>.

This thesis can be decomposed into six themed chapters. Chapter 1 provides an overview of the required underlying theory that is required for the subsequent chapters. Section 1.1 elucidates the established results of (homogeneous) Lévy processes. Then, in Section 1.2, additive processes are introduced by dropping the stationary assumption of Section 1.1. The time-inhomogeneous Lévy process will be defined as a discrete additive process based on the observation of option prices with a finite number of maturities.

Chapter 2 is devoted to the statistical estimation procedure. Section 2.1 introduces the risk-neutral setting of the price process and the plain-vanilla options used for calibration. A regression model is made in Section 2.2 to account for the noise in the option prices. Section 2.3 then shows how the characteristic function of the process can be linked via a Fourier transform to the observed noised option prices. Finally, Section 2.4 elucidates how the underlying parameters of the process can be estimated non-parametrically via a cut-off regularisation procedure from the characteristic function.

In Chapter 3 the main theoretical results of the estimators will be derived. First, in Section 3.1 the underlying assumptions prior to the results will be introduced. Section 3.2 establishes when the estimation procedure is well-defined, this happens whenever the estimator of the characteristic function can be bounded from below. Then, in Section 3.3 and Section 3.4, we show via an error decomposition and the Lyapunov central limit theorem that the estimators asymptotically tend to a normal distribution. We provide a summary of all the results and conditions in a main theorem in Section 3.5. Finally, Section 3.6 and Section 3.7 respectively inspect the difficulty of the calibration procedure based on this main theorem and establishes optimal convergence rates.

The derived asymptotic standard deviation of the normal distribution in Chapter 3 is not generally sufficient for confidence intervals in finite sample cases. Chapter 4, therefore, establishes confidence intervals for the case of a non-asymptotic/discrete observation scheme. The different sections in this chapter treat the different estimators one by one.

Chapter 5 tests the stability and accuracy of the estimation procedure via simulations. Section 5.1 first answers to open-ended questions about how the to-be-calibrated model should be built and how the cut-off scheme should be chosen. The calibration results of the estimators are inspected using multiple Monte-Carlo simulations in Section 5.2. Furthermore, the confidence intervals will be assessed with coverage probabilities.

In the final Chapter, Chapter 6, we employ calibration to empirical data of the S&P500 index. Section 6.1 addresses the underlying data set and the assumptions that differ from the simulations in Chapter 5. Then, Section 6.2 shows the results of calibration in a similar setting as the simulations for comparison. Finally, Section 6.3 shows the results if the calibration has been done on all options prices with numerous maturities and we discuss the favorability of the inhomogeneous model to the homogeneous model.

Chapter 1

Theory

Recalling that random walks — sums of independent identically distributed random variables — provide the simplest examples of stochastic processes in discrete time. A natural question that arises is if for continuous times we can also make processes with independent stationary increments. These continuous-time relatives to random walks are called Lévy processes – in honor of the French mathematician Paul Lévy. These Lévy processes provide important examples of stochastic processes in continuous time and provide ingredients for building continuous-time stochastic models. Fundamental examples of Lévy processes are the Brownian motion (or equivalently Wiener process) and the Poisson process. It can even be shown, e.g. Cont and Tankov [16, Chapter 3], that Brownian motion and the Poisson process can be thought of as building blocks for Lévy processes because every Lévy process can be written as a superposition of a Brownian motion and a (may be infinite) number of independent Poisson processes.

In this chapter, the main facts about Lévy processes and more general stochastic processes needed for the statistical analysis will be reviewed. The theory displayed here will be fundamental for the subsequent statistical analysis and the reader is advised to pay close attention. Especially the second subsection, where the *time-inhomogeneous Lévy process* is defined, is not considered omnipresent theory, while it is essential for the rest of the thesis.

1.1 Time-Homogeneous Lévy Processes

The Lévy process must be defined as a continuous counterpart to the discrete random walks that keeps the properties of stationary and independent increments. The exact assumptions and imposed properties underlying Lévy processes are given below in Definition 1.1.

Definition 1.1 An \mathbb{R} -valued process $X = (X_t)_{t \geq 0}$ defined on a filtered probability space $(\Omega, \mathcal{F}, (\mathcal{F})_{t \geq 0}, \mathbb{P})$ is called a Lévy process if it is (\mathcal{F}_t) -adapted and if it has the following properties

- (i) X is continuous in probability, i.e., for fixed $s \geq 0$, $\mathbb{P}(|X_t - X_s| > \varepsilon) \rightarrow 0$ holds as $t \rightarrow s$ for all $\varepsilon > 0$.
- (ii) $\mathbb{P}(X_0 = 0) = 1$.
- (iii) For $0 \leq s \leq t$, $X_t - X_s$ is equal in distribution to X_{t-s} .
- (iv) For $0 \leq s \leq t$, $X_t - X_s$ is independent of \mathcal{F}_s .

As a remark, notice that all Lévy processes have a càdlàg modification. Without loss of generality, we will assume that all sample paths of Lévy processes are càdlàg.

In Definition 1.1 condition (ii) makes sure that the process starts at 0, condition (iii) makes sure of the stationary increments, and condition (iv) makes sure of the independent increments. Condition (i) is called *Stochastic Continuity* and it does not imply that the sample paths are continuous. The main reason for stochastic continuity is to exclude jumps at nonrandom (fixed) times that can be regarded as scheduled events and are not interesting for our purpose.

The generalization of Brownian motion to Lévy processes mostly lies in the fact that in Lévy processes, as with Poisson processes, a jump component is present. This jump component for all Lévy processes can be described by the *Lévy measure* and is defined in Definition 1.2.

Definition 1.2 A Lévy measure on \mathbb{R} is a σ -finite measure ν on \mathbb{R} such that $\nu(\{0\}) = 0$ and

$$\int_{\mathbb{R}} (1 \wedge |x|^2) d\nu(x) < \infty.$$

The Lévy measure $\nu(A)$ can be interpreted as the expected number, per unit time, of jumps whose size belong to A . Having this in mind, the Lévy measure ν will also be called and referred to as the jump measure.

Lévy processes X are generally easy to work with because the characteristic function φ_t can be found in closed form. This important result is called the Lévy-Khintchine representation and is given in Theorem 1.1.

Theorem 1.1 (*Lévy-Khintchine representation*) Let X be a Lévy process taking values in \mathbb{R} . Then for each $t \geq 0$ the characteristic function φ_t of X_t satisfies

$$\varphi_t(v) := \mathbb{E} [e^{ivX_t}] = e^{t\xi(v)}, \quad v \in \mathbb{R},$$

with characteristic exponent $\xi(v)$ given by

$$\xi(v) = -\frac{\sigma^2 v^2}{2} + i\gamma v + \int_{\mathbb{R}} (e^{ivx} - 1 - ivx \mathbb{1}_{|x| \leq 1}) d\nu(x),$$

where $\gamma \in \mathbb{R}$, $\sigma \in \mathbb{R}^+$ and ν is a Lévy measure on \mathbb{R} .

We can find a proof of the Theorem above in [16]. The quantity (σ^2, γ, ν) is called the characteristic triplet of the Lévy process X . This characteristic triplet characterizes the complete Lévy process because it completely determines the characteristic function $\varphi_t(v)$.

In this thesis, we shall restrict ourselves to Lévy processes X with a jump component of finite activity and absolutely continuous jump measure. With some abuse of notation, the jump density will also be denoted as $\nu(x) \in L^1(\mathbb{R})$. The characteristic function of X_t can then be given by the Lévy-Khintchine representation

$$\varphi_t(v) = \exp \left(t \left(-\frac{\sigma^2 v^2}{2} + i\gamma v + \int_{\mathbb{R}} (e^{ivx} - 1) \nu(x) dx \right) \right). \quad (1.1)$$

The parameter $\sigma \in \mathbb{R}^+$ is called the volatility, $\gamma \in \mathbb{R}$ is called the drift, and $\lambda := \|\nu\|_{L^1(\mathbb{R})} < \infty$ is called the intensity.

The volatility σ can be thought of as the measure of change over time of the process. For example, when thinking of a financial process, volatility quantifies a stock's lack of stability or the tendency of its prices to move up and down. The drift γ is the tendency of the process to move up or down in the long run and the intensity λ is the expected amount of jumps the process exhibits in a unit of time.

As mentioned earlier, the statistical analysis has already been done for ordinary Lévy processes [16, 7]. In this thesis, a more complex model build-up from multiple Lévy processes will be inspected. The theory around this more complex model is given in the next section.

1.2 Additive Processes and Time-Inhomogeneous Lévy Processes

Although Lévy processes supply nice features in terms of analytical tractability, the assumptions of stationary and independent increments prove to be rather restrictive. Cont and Tankov [16, Chapter 7] show that the stationarity of increments of Lévy processes leads to rigid scaling properties for the marginal distributions, which are not observed in empirical

time series of returns. Furthermore, Cont and Tankov [16, Chapter 13] also show that (exponential) Lévy models allow calibrating to implied volatility patterns for a single maturity, but fail to reproduce option prices over a range of differing maturities.

To address these problems, a new process X called an *Additive Process* will be introduced. Additive processes are processes with independent but not stationary increments. This generalization takes into account deterministic time inhomogeneities, i.e., the parameters that describe the behavior of the process X may now be time-dependent, however, they are not random. The big upside of this new model is that it allows us to preserve almost all the nice tractability of Lévy processes, while it also enables us to reproduce the whole range of option prices across multiple strikes and maturities.

An additive process X – which is made by dropping condition (iii) in Definition 1.1 – is presented in Definition 1.3.

Definition 1.3 An \mathbb{R} -valued process $X = (X_t)_{t \geq 0}$ defined on a filtered probability space $(\Omega, \mathcal{F}, (\mathcal{F}_t)_{t \geq 0}, \mathbb{P})$ is called an additive process if it is (\mathcal{F}_t) -adapted and if it has the following properties

1. X is continuous in probability, i.e., for fixed $s \geq 0$, $\mathbb{P}(|X_t - X_s| > \varepsilon) \rightarrow 0$ holds as $t \rightarrow s$ for all $\varepsilon > 0$.
2. $\mathbb{P}(X_0 = 0) = 1$.
3. For $0 \leq s \leq t$, $X_t - X_s$ is independent of \mathcal{F}_s .

All additive processes have a càdlàg modification. Without loss of generality, we will assume that all sample paths of additive processes are càdlàg. More specifics about additive processes can be found in, for example, Cont and Tankov [16, Chapter 14].

The main advantage of these additive processes is that the underlying parameters that describe the motion can now be time-dependent and time inhomogeneities can now more easily be taken into account. The calibration of the parameters will be done by using option prices at maturities T_j , $j = 1, \dots, n$. To use all available data to reconstruct the option prices over all maturities, we want to create a model where the dynamics on every interval $(T_j - T_{j-1})_{j=1, \dots, n}$ is governed by an independent Lévy process. Then the whole process on the interval $(T_n - T_0)$ is an additive process with time-dependent parameters. We will call this subset of additive processes *time-inhomogeneous Lévy processes*. Definition 1.4 defines this subset X of additive processes based on observations at the finite number of maturities $(T_j)_{j=1, \dots, n}$.

Definition 1.4 An \mathbb{R} -valued additive process $X = (X_t)_{t \geq 0}$ defined on a filtered probability space $(\Omega, \mathcal{F}, (\mathcal{F}_t)_{t \geq 0}, \mathbb{P})$ will be called a *time-inhomogeneous Lévy process* if it can be written as a composition of independent Lévy processes $(X_t - X_{T_j})_{T_{j-1} \leq t \leq T_j}$ with Lévy triplet $(\sigma_j^2, \gamma_j, \nu_j)$ where T_j , $j = 0, \dots, n$, with $T_0 = 0$ and $T_n = T$.

To track these time-inhomogeneous Lévy processes a new Lévy-Khintchine representation for the characteristic function $\varphi_{T_j}(v)$ of the process X can be made.

Using the independent increments property (iii) in Definition 1.3 and making the assumption that all $(X_t - X_{T_j})_{T_{j-1} \leq t \leq T_j}$ have a jump component of finite activity and absolutely continuous jump measure, the characteristic function can be written as

$$\varphi_{T_j}(v) := \mathbb{E} \left[e^{ivX_{T_j}} \right] = \mathbb{E} \left[e^{iv(X_{T_j} - X_{T_{j-1}})} e^{ivX_{T_{j-1}}} \right] = \mathbb{E} \left[e^{iv(X_{T_j} - X_{T_{j-1}})} \right] \varphi_{T_{j-1}}(v),$$

where $\varphi_{T_0}(v) = 1$. Notice that $(X_{T_j} - X_{T_{j-1}})$ is the Lévy process with characteristic triplet $(\sigma_j^2, \gamma_j, \nu_j)$, thus with the Lévy-Khintchine representation (1.1) we can write

$$\frac{\varphi_{T_j}(v)}{\varphi_{T_{j-1}}(v)} = \exp \left((T_j - T_{j-1}) \left(-\frac{\sigma_j^2 v^2}{2} + i\gamma_j v + \int_{\mathbb{R}} (e^{ivx} - 1) \nu_j(x) dx \right) \right). \quad (1.2)$$

The combination of all Lévy triplets $(\sigma_j^2, \gamma_j, \nu_j)_{j=1, \dots, n}$ completely determines the characteristic function and, thereby, the time-inhomogeneous Lévy model.

Chapter 2

The Statistical Model

The statistical model used here is an extension of the homogeneous model developed by Cont and Tankov [16], Belomestny and Reiß [7], Söhl and Trabs [44], and a clarified and improved version of the introduced time-inhomogeneous model by Tendijck [46].

As portrayed in the introduction, all models in this thesis correspond to incomplete markets, which implies that we can not make perfect hedges and options prices can not be uniquely identified from the underlying price process by arbitrage arguments only. These difficulties of incomplete markets illustrate that the approach of using historical data for the calibration of the parameters of (exponential) Lévy models is not satisfactory — due to the incomplete market, knowledge of the historical price process alone does not bear a way to compute option prices uniquely [21, 2].

Furthermore, Cont and Tankov [16, Chapter 9] show that in a market that is free of arbitrage all prices of securities can be written as discounted conditional expectations concerning a certain risk-neutral measure \mathbb{Q} for which discounted asset prices are martingales. When markets are incomplete, the risk-neutral measure \mathbb{Q} bears only a weak relation to the time-series behavior described by \mathbb{P} . With weak relation we mean that \mathbb{Q} cannot be identified from \mathbb{P} , it only inherits some qualitative properties, e.g., variation is finite or infinite, presence of jumps. This modeling of \mathbb{Q} from \mathbb{P} is called implied or risk-neutral modeling. However, the problem still exists that, if \mathbb{Q} is modeled in this way, then \mathbb{Q} does not give values consistent with listed options — assuming, of course, that listed options are present.

So, if option prices are available, a market-consistent pricing model \mathbb{Q} can not be obtained by only looking at the historical time series of the underlying asset. When option prices are quoted on the market for the underlying, these listed options can provide an additional source of information for selecting \mathbb{Q} . The practice of choosing \mathbb{Q} such that the options prices can be reproduced is called *model calibration*.

Model calibration is known as the choice of a risk-neutral model such that the prices of traded options are reproduced, i.e., given market prices $(C_i)_{i \in I}$ at $t = 0$ for a set of benchmark options, a risk-neutral measure \mathbb{Q} needs to be found such that the options are correctly priced

$$\forall i \in I, C_i^0 = e^{-rT} \mathbb{E}^{\mathbb{Q}} [C_i^T], \quad (2.1)$$

where C_i^T is the payoff function of $i \in I$ at time T . The benchmark options that are mostly used, and that will also be used in this thesis, are plain-vanilla options, e.g, call options C_i^t with strike K_i and maturity T_i , such that with the general pricing formula $C_i^T = \max(0, S_{T_i} - K_i)$. The way of thinking is that after the calibration has been done, one could use the risk-neutral measure \mathbb{Q} for the pricing of more exotic, illiquid, or OTC options and to compute hedge ratios.

Because we are interested in finding parameters that describe the risk-neutral dynamics from observed option prices, instead of using the dynamics to price options, the calibration procedure is the *inverse problem* associated with the pricing problem. This inverse problem is, however, ill-posed, i.e., there may be many pricing models that generate these option prices, therefore, the solution is not necessarily unique [16].

In general, one needs to assume for calibrating purposes that the measure \mathbb{Q} belongs to a certain prespecified class of models. In this thesis, we will assume that \mathbb{Q} belongs to the class of exponential time-inhomogeneous Lévy models. When such an assumption is made, however, there is no guarantee that an exact solution for \mathbb{Q} even exists, i.e., there might be no model that exactly reproduces the option prices. Thus, a better way to look at the calibration problem is to achieve the best approximation of the option prices within a given class of models.

In this chapter, the goal is to find a statistical manner to approximate the best exponential time-inhomogeneous Lévy model that reproduces the option prices for some underlying asset. The model will be found by nonparametrically calibrating all characteristic triplets $(\sigma_j^2, \gamma_j, \nu_j)_{j=1, \dots, n}$ from observed plain-vanilla option prices with different maturities. Between every two maturities, the assumption is thus made that an independent Lévy model governs the dynamics. The exact calibration is done in the spectral/Fourier domain and is therefore also called *spectral calibration*.

2.1 Exponential Time-Inhomogeneous Lévy Models and Plain Vanilla Options

Since our calibration is based on option prices, we are in a risk-neutral world, portrayed by a filtered probability space $(\Omega, \mathcal{F}, (\mathcal{F})_{t \geq 0}, \mathbb{Q})$, on which the price process of an asset $S = (S_t)_{t \geq 0}$ after discounting needs to be a martingale. It is common practice in calibration literature to assume that the risk-neutral measure \mathbb{Q} is settled by the market.

Consider European call $\mathcal{C}(K_{j,k}, T_j)$ and put options $\mathcal{P}(K_{j,k}, T_j)$ with maturities at T_j and strikes at these maturities $K_{j,k}$ with $j = 1, \dots, n$ and $k = 1, \dots, m_j$. These maturities will define the time grid on which the time-inhomogeneous Lévy model will be defined, i.e., between every two maturities, T_{j-1} and T_j an independent Lévy process with triplet $(\sigma_j^2, \gamma_j, \nu_j)$ exists that governs the dynamics.

The price process of the asset S_t with time $0 \leq t \leq T$ is modelled by an exponential time-inhomogeneous Lévy process, that is

$$S_t = S_0 e^{rt + X_t}, \quad (2.2)$$

where X_t is a time-inhomogeneous Lévy process as in Definition 1.4 with characteristic triplets $(\sigma_j^2, \gamma_j, \nu_j)_{j=1, \dots, n}$, $r \geq 0$ the risk free rate, and S_0 the initial price.

Using the assumption that only finite variation Lévy processes are considered, the martingale condition for the discounted price process $e^{-rt} S_t$ under the risk-neutral measure \mathbb{Q} gives that for all $t \geq 0$

$$S_0 = \mathbb{E}[S_t | \mathcal{F}_0] \iff 1 = \mathbb{E}[e^{X_t}]. \quad (2.3)$$

Now applying the Lévy-Khintchine representation (1.2) results that for all the triplets $(\sigma_j^2, \gamma_j, \nu_j)_{j=1, \dots, n}$ it must hold that

$$\frac{\sigma_j^2}{2} + \gamma_j + \int_{-\infty}^{\infty} (e^x - 1) \nu_j(x) dx = 0, \quad \text{for all } j = 1, \dots, n. \quad (2.4)$$

To facilitate the results in the following sections, a mild assumption must be made on the price process, namely that the price process has finite second moment $\mathbb{E}[S_T^2] < \infty$, this is equivalent to

$$\mathbb{E}[e^{2X_{T_j}}] < \infty, \quad \text{for all } j = 1, \dots, n. \quad (2.5)$$

As a remark, notice that this assumption is rather intuitive for a financial security – financial securities with infinite variance are rather uncommon.

The risk-neutral prices for the call options $\mathcal{C}(K_{j,k}, T_j)$ and put options $\mathcal{P}(K_{j,k}, T_j)$ at $t = 0$ with underlying price process S_t are given by

$$\mathcal{C}(K_{j,k}, T_j) = e^{-rT_j} \mathbb{E}[(S_{T_j} - K_{j,k})^+] \quad \text{and} \quad \mathcal{P}(K_{j,k}, T_j) = e^{-rT_j} \mathbb{E}[(K_{j,k} - S_{T_j})^+],$$

where $(Y)^+ := \max(0, Y)$. The number of parameters can be reduced by defining the negative log-forward moneyness

$$x_{j,k} := \log(K_{j,k}/S_0) - rT_j,$$

then the call and put prices can be expressed as

$$\mathcal{C}(x_{j,k}, T_j) = S_0 \mathbb{E} \left[(e^{X_{T_j}} - e^{x_{j,k}})^+ \right] \quad \text{and} \quad \mathcal{P}(x_{j,k}, T_j) = S_0 \mathbb{E} \left[(e^{x_{j,k}} - e^{X_{T_j}})^+ \right].$$

Using no-arbitrage arguments, the well-known put-call parity in terms of the negative log-forward moneyness can easily be derived

$$\mathcal{C}(x_{j,k}, T_j) - \mathcal{P}(x_{j,k}, T_j) = S_0 \mathbb{E} \left[e^{X_{T_j}} - e^{x_{j,k}} \right] = S_0 (1 - e^{x_{j,k}}). \quad (2.6)$$

2.2 Observations of the Option Prices

The model will be calibrated using option prices. These option prices can exhibit noise and we need to deal with this noise in a certain way. The observations of the option prices will therefore be made using a regression model. Next to that, there are complications with the fact that call and put option prices as functions of the strike are not Fourier transformable, this is also a problem we need to deal with in this section. In the end, we will show a manner how the desired regression function will be estimated.

2.2.1 Data Transformation

Due to imperfections of the markets and bid-ask spreads, the observed risk-neutral prices of the options will exhibit noise. We will employ a regression model in the modeling of this noise factor. The prices of m_j call options $Y_{j,k}$ (or, equivalently, put options by the parity (2.6)) observed at strikes $K_{j,k}$, $k = 1, \dots, m_j$ with maturity T_j and corrupted by noise ([39] motivates this model), are modelled by

$$Y_{j,k} = \mathcal{C}(K_{j,k}, T_j) + \zeta_{j,k} \varepsilon_{j,k}, \quad k = 1, \dots, m_j, \quad (2.7)$$

with $\zeta_{j,k} > 0$ and random variables $\varepsilon_{j,k}$. We assume that the observed noise $(\varepsilon_{j,k})$ consists of independent centered sub-Gaussian random variables with variance $\mathbb{V}[\varepsilon_{j,k}] = 1$. Sub-Gaussianity means that the tails of the distribution are dominated by Gaussian tails, which ensures that the tails of $(\varepsilon_{j,k})$ do not have too much mass.

By the moment condition for sub-Gaussian tails, we have that all moments are finite, in particular $\mathbb{E}[\varepsilon_{j,k}^4] < \infty$ — which is the assumption Belomestny and Reiß [7] used for their time-homogeneous work. Belomestny and Reiß [7] then show that minimax results hold for the assumed noise.

As discussed in the introduction of this chapter, the calibration procedure will be done using option prices listed for S_t on the market. For the calibration procedure, we need to employ Fourier techniques. Note that the options functions $\mathcal{C}(x, T_j)$ and $\mathcal{P}(x, T_j)$ do not converge to 0, when $x \rightarrow \infty$ and $x \rightarrow -\infty$, respectively. Thus, the Fourier transforms of these functions do not exist. However, if we use the fact that $\lim_{x \rightarrow \infty} \mathcal{C}(x, T_j) = 0 = \lim_{x \rightarrow -\infty} \mathcal{P}(x, T_j)$, then, in the spirit of Carr and Madan [14], we can define the Fourier transformable function

$$\mathcal{O}_j(x) := \begin{cases} \mathcal{C}(x, T_j)/S_0, & x \geq 0, \\ \mathcal{P}(x, T_j)/S_0, & x < 0. \end{cases} \quad (2.8)$$

With the put-call parity (2.6), one can always ensure that all option information is used for $\mathcal{O}_j(x)$ by transforming the call options to put options and vice versa.

Now it is favourable to write the regression model (2.7) in terms of the negative log-forward moneyness $x_{j,k}$ and the Fourier transformable function $\mathcal{O}(x_{j,k})$, this results in

$$\mathcal{O}_{j,k} = \mathcal{O}_j(x_{j,k}) + \delta_{j,k} \varepsilon_{j,k}, \quad k = 1, \dots, m_j, \quad (2.9)$$

where we defined $\mathcal{O}_{j,k} := \mathcal{C}(x_{j,k}, T_j)/S_0$ and $\delta_{j,k} := \zeta_{j,k}/S_0$.

2.2.2 Estimation of \mathcal{O}_j

From the regression model (2.9) it can be seen that we do not observe the function $\mathcal{O}_j(x_{j,k})$ directly, but the version $\mathcal{O}_{j,k}$ corrupted by noise. Therefore, a way to approximate the $\mathcal{O}_j(x_{j,k})$ using the observations $\mathcal{O}_{j,k}$, given by the function $\tilde{\mathcal{O}}_j$, needs to be implemented. In the spirit of [10], the problem can be formulated as

Problem 2.1 Find function $\tilde{\mathcal{O}}_j$ among all functions \mathcal{O}_j with two continuous derivatives that minimize the penalized residual sum of squares

$$\text{RSS}(\mathcal{O}_j, \alpha) = \sum_{k=0}^{N+1} (\mathcal{O}_{j,k} - \mathcal{O}_j(x_k))^2 + \alpha \int_{x_0}^{x_{N+1}} [\mathcal{O}_j''(u)]^2 du, \quad (2.10)$$

where $x_0 \ll x_1$ and $x_{N+1} \gg x_N$ are two artificial points and $\mathcal{O}_{j,N+1} = \mathcal{O}_{j,0} = 0$.

The first term in expression (2.10) measures the closeness of the data, whereas the second term penalizes the non-smoothness of the function, and α defines the trade-off between the two.

The solution of Problem 2.1 can be proven to be a unique natural cubic spline with knots at the unique values $x_{j,k}$, $k = 1, \dots, m_j$ (proven in, for example, [25]), i.e., $\tilde{\mathcal{O}}_j$ can be written as

$$\tilde{\mathcal{O}}_j(x) = \sum_{k=1}^{m_j} \mathcal{O}_{j,k} e_{j,k}(x), \quad x \in \mathbb{R}, \quad (2.11)$$

where $e_{j,k}(x)$ with $k = 1, \dots, m_j$ are the set of basis functions for representing the family of cubic smoothing splines.

However, the asymptotic theoretical results become more concise and comprehensible using interpolation with linear splines – all the preliminary theoretical work of [7] and [46] were also done using linear splines. Furthermore, if the theoretical results hold for linear splines, they will also hold for cubic splines, which are better approximations. The cubic splines will be implemented in the practical calibration part of the thesis.

Therefore, in the theoretical part, just the linear cubic spline interpolation scheme will be used

$$\tilde{\mathcal{O}}_j(x) = \beta_{j,0}(x) + \sum_{k=1}^{m_j} \mathcal{O}_{j,k} b_{j,k}(x), \quad x \in \mathbb{R}, \quad (2.12)$$

where $(b_{j,k})$ are linear splines and the function $\beta_{j,0}$ is added to take care of the jump in the derivative of \mathcal{O}_j at zero: $\beta'_{j,0}(0+) - \beta'_{j,0}(0-) = -1$. In particular, $b_{j,k}$ is chosen as the triangular function, i.e., $b_{j,k}(x) = \Lambda(\frac{x-x_{j,k}}{x_{j,k+1}-x_{j,k}})$ with $\Lambda(x) = (1 - |x|)\mathbb{1}_{|x| \leq 1}$.

Due to the non-smooth behavior of $\mathcal{O}_j(x)$ at 0 (see [6]), it is recommended to fit smoothing splines — in both approximations (2.12) and (2.11) — separately for $x \geq 0$ and $x < 0$, and combine them thereafter.

As mentioned, in the theoretical results, the basis of the linear spline scheme (2.12) will be used, whereas in the practical results both spline schemes linear (2.12) and cubic (2.11) will be implemented and investigated.

2.3 Statistical Estimation Approach

Now, after we have implemented a manner how the data in the form of call $\mathcal{C}(K_{j,k}, T_j)$ and put option prices $\mathcal{P}(K_{j,k}, T_j)$ can be transformed and observed through the interpolated linear splines estimator $\tilde{\mathcal{O}}_j$, the question arises how this can be coupled to the underlying time-inhomogeneous Lévy model. In the first subsection, we will see that there exists a natural relation between $\mathcal{O}_j(x)$ and the characteristic function $\varphi_{T_j}(v)$ using the Fourier transform. However, we observe the interpolated version $\tilde{\mathcal{O}}_j(x)$, and therefore we also need

to define an estimator $\tilde{\varphi}_{T_j}(v)$ for $\varphi_{T_j}(v)$. Thereafter, in the next subsection, the actual calibration method for finding the Lévy triplet $(\sigma_j, \gamma_j, \nu_j)_{j=1, \dots, n}$ will be extracted from this relation.

2.3.1 Relation between \mathcal{O}_j and φ_{T_j}

Using the martingale condition (2.4) and the put-call parity (2.6), Carr and Madan [14] proposed and Belomestny and Reiß [6, p.4] proved and derived some important properties of the function $\mathcal{O}_j(x)$ for $j = 1$, i.e., the homogeneous case. In Proposition 2.1 these properties will be extended and proved for the inhomogeneous case.

Proposition 2.1 *The function $\mathcal{O}_j(x)$, defined in (2.8), satisfies the following properties:*

- (i) For all $x \in \mathbb{R}$, it holds that $\mathcal{O}_j(x) = \mathcal{C}(x, T_j)/S_0 - (1 - e^x)^+$.
- (ii) For all $x \in \mathbb{R}$, it holds that $\mathcal{O}_j(x) \in [0, 1 \wedge e^x]$.
- (iii) $C_\alpha := \mathbb{E}[e^{\alpha X_{T_j}}]$ is finite for some $\alpha \geq 1 \implies \mathcal{O}_j(x) \leq C_\alpha e^{(1-\alpha)x}$ for all $x \geq 0$.
- (iv) The Fourier transform of \mathcal{O}_j satisfies

$$\mathcal{F}(\mathcal{O}_j(x))(v) = \int_{-\infty}^{\infty} \mathcal{O}_j(x) e^{ivx} dx = \frac{1 - \varphi_{T_j}(v - i)}{v(v - i)}$$

for all $v \in \mathbb{C}$ with $\text{Im}(v) \in [0, 1]$.

Proof All the different properties will be proven individually:

- (i) If $x \geq 0$, then trivially $\mathcal{O}_j(x) = C_j(x, T_j)/S_0 = C_j(x, T_j)/S_0 - (1 - e^x)^+$. If $x < 0$, then with the put-call parity (2.6) we have

$$\begin{aligned} C_j(x, T_j) - S_0 \mathcal{O}_j(x) &= S_0(1 - e^x) \Leftrightarrow \mathcal{O}_j(x) = \mathcal{C}(x, T_j)/S_0 - (1 - e^x) \\ &= \mathcal{C}(x, T_j)/S_0 - (1 - e^x)^+. \end{aligned}$$

Hence, the result follows.

- (ii) $\mathcal{O}_j(x) \geq 0$ follows directly from the definition while $\mathcal{O}_j(x) \leq \mathbb{E}[e^{X_{T_j}}] - (1 - e^x)^+ = 1 \wedge e^x$ follows from (i) and the martingale condition (2.3).
- (iii) By Hölder's and Markov's inequality for $x \geq 0$,

$$\begin{aligned} \mathcal{O}_j(x) &= C_j(x, T_j)/S_0 \leq \mathbb{E}[e^{X_{T_j}} \mathbb{1}_{\{X_{T_j} > x\}}] \leq C_\alpha^{1/\alpha} \mathbb{P}(X_{T_j} > x)^{\alpha/(1-\alpha)} \\ &\leq C_\alpha^{1/\alpha} \left(\frac{C_\alpha}{e^{\alpha x}} \right)^{(\alpha-1)/\alpha} = C_\alpha e^{(1-\alpha)x}. \end{aligned}$$

- (iv) By the definition of $\mathcal{O}_j(v)$ it follows that

$$\begin{aligned} \mathcal{F}(\mathcal{O}_j(x))(v) &= \frac{1}{S_0} \left(\int_{-\infty}^0 e^{ivx} \mathcal{P}(x, T_j) dx + \int_0^{\infty} e^{ivx} \mathcal{C}(x, T_j) dx \right) \\ &= \int_{-\infty}^0 e^{ivx} \mathbb{E}[\mathbb{1}_{\{X_{T_j} \leq x\}} (e^x - e^{X_{T_j}})] dx + \int_0^{\infty} e^{ivx} \mathbb{E}[\mathbb{1}_{\{X_{T_j} > x\}} (e^{X_{T_j}} - e^x)] dx. \end{aligned}$$

Using partial integration, we find the results

$$\begin{aligned} \int_{-\infty}^0 e^{(iv+1)x} \mathbb{P}(X_{T_j} \leq x) dx &= \frac{1}{1+iv} \mathbb{P}(X_{T_j} \leq 0) - \frac{1}{1+iv} \mathbb{E}[\mathbb{1}_{\{X_{T_j} \leq 0\}} e^{(1+iv)X_{T_j}}] \\ \int_{-\infty}^0 e^{ivx} \mathbb{E}[\mathbb{1}_{\{X_{T_j} \leq x\}} e^{X_{T_j}}] dx &= \frac{1}{iv} \mathbb{E}[\mathbb{1}_{\{X_{T_j} \leq 0\}} e^{X_{T_j}}] - \frac{1}{iv} \mathbb{E}[\mathbb{1}_{\{X_{T_j} \leq 0\}} e^{(1+iv)X_{T_j}}] \end{aligned}$$

and therefore

$$\begin{aligned} \int_{-\infty}^0 e^{ivx} \mathbb{E}[\mathbb{1}_{\{X_{T_j} \leq x\}} (e^x - e^{X_{T_j}})] dx &= \frac{1}{1+iv} \mathbb{P}(X_{T_j} \leq 0) - \frac{1}{1+iv} \mathbb{E}[\mathbb{1}_{\{X_{T_j} \leq 0\}} e^{(1+iv)X_{T_j}}] \\ &\quad - \frac{1}{iv} \mathbb{E}[\mathbb{1}_{\{X_{T_j} \leq 0\}} e^{X_{T_j}}] + \frac{1}{iv} \mathbb{E}[\mathbb{1}_{\{X_{T_j} \leq 0\}} e^{(1+iv)X_{T_j}}]. \end{aligned}$$

In a similar fashion

$$\begin{aligned} \int_0^{\infty} e^{ivx} \mathbb{E}[\mathbb{1}_{\{X_{T_j} > x\}} (e^{X_{T_j}} - e^x)] dx &= -\frac{1}{iv} \mathbb{E}[\mathbb{1}_{\{X_{T_j} > 0\}} e^{X_{T_j}}] + \frac{1}{iv} \mathbb{E}[\mathbb{1}_{\{X_{T_j} > 0\}} e^{(1+iv)X_{T_j}}] \\ &\quad + \frac{1}{1+iv} \mathbb{P}(X_{T_j} > 0) - \frac{1}{1+iv} \mathbb{E}[\mathbb{1}_{\{X_{T_j} > 0\}} e^{(1+iv)X_{T_j}}]. \end{aligned}$$

Combining these results and using the martingale condition $\mathbb{E}[e^{X_{T_j}}] = 1$ (2.3) gives

$$\mathcal{F}(\mathcal{O}_j(x))(v) = \frac{1}{1+iv} - \frac{1}{1+iv} \mathbb{E}[e^{(1+iv)X_{T_j}}] - \frac{1}{iv} + \frac{1}{iv} \mathbb{E}[e^{(1+iv)X_{T_j}}] = \frac{1 - \varphi_{T_j}(v-i)}{v(v-i)}.$$

□

The assumption of the finite second moment of the price process $C_2 := \mathbb{E}[e^{2X_{T_j}}] < \infty$ given in (2.5) guarantees by Proposition 2.1 (ii), (iii) the exponential decay of $\mathcal{O}_j(x)$, which in turn guarantees that the Fourier transform of $\mathcal{O}_j(x)$ exists.

This is the first time we encountered the Fourier transform and because many different definitions exist, let us make sure the definition of the Fourier transform used in this thesis is clear. In the rest of the thesis, the following definition of Fourier pairs will be used

$$\begin{aligned} \mathcal{F}f(v) &:= \mathcal{F}(f(x))(v) = \int_{-\infty}^{\infty} f(x) e^{-ivx} dx \quad \text{and} \\ \mathcal{F}^{-1}F(x) &:= \mathcal{F}^{-1}(F(v))(x) = \frac{1}{2\pi} \int_{-\infty}^{\infty} F(v) e^{ivx} dv. \end{aligned}$$

The last relation (iv) in Proposition 2.1 is the most important and will be crucial in the estimation procedure. Note that this relation couples the characteristic function $\varphi_{T_j}(v-i)$ to observed plain-vanilla option prices through a Fourier transform of the $\mathcal{O}_j(x)$ function. This opens a way to estimate the characteristic function $\varphi_{T_j}(v-i)$ through the option price function $\mathcal{O}_j(x)$,

$$\varphi_{T_j}(v-i) = 1 - v(v-i) \mathcal{F}\mathcal{O}_j(v) = 1 + iv(1+iv) \mathcal{F}\mathcal{O}_j(v). \quad (2.13)$$

The function $\varphi_{T_j}(v-i)$ was the characteristic function of the Lévy process that governed the dynamics between T_{j-1} and T_j . Recall that in the Theory expression (1.2) we found the Lévy-Khintchine representation for time-inhomogeneous Lévy processes was given by

$$\frac{\varphi_{T_j}(v)}{\varphi_{T_{j-1}}(v)} = \exp \left((T_j - T_{j-1}) \left(-\frac{\sigma_j^2 v^2}{2} + i\gamma_j v + \int_{\mathbb{R}} (e^{ivx} - 1) \nu_j(x) dx \right) \right).$$

Therefore, to calibrate the characteristic triplet $(\sigma_j^2, \gamma_j, \lambda_j)$, we need two characteristic functions, namely $\varphi_{T_j}(v)$ and $\varphi_{T_{j-1}}(v)$, which can both be extracted by the option price functions $\mathcal{O}_j(x)$ and $\mathcal{O}_{j-1}(x)$ by expression (2.13). This calibration is the topic of the next subsection.

2.3.2 Calibration Function ψ_j and Calibration Estimator $\tilde{\psi}_j$

To signify the important relation in Proposition 2.1 (iv), the functions ψ_j^l for $j = 1, \dots, n$ and $l = 0, 1$ will be defined as

$$\psi_j^l(v) := \frac{1}{T_j - T_{j-1}} \log [1 + iv(1+iv) \mathcal{F}\mathcal{O}_{j-l}(v)] \stackrel{(iv)}{=} \frac{1}{T_j - T_{j-1}} \log [\varphi_{T_{j-l}}(v-i)],$$

where the complex logarithm is taken such that $\psi_j^l(0) = 0$ and such that ψ_j^l is continuous on $(-v_0, v_0)$ with v_0 being the smallest positive zero of $\varphi_{T_{j-l}}$.

In the calibration procedure, we would like to find all Lévy triplets $(\sigma_j^2, \gamma_j, \nu_j)_{j=1, \dots, n}$ for calibrating the time-inhomogeneous Lévy model. These Lévy triplets are coupled to the characteristic functions using the derived Lévy-Khintchine representation (1.2), this suggests defining the calibration function ψ_j as

$$\begin{aligned} \psi_j(v) &:= \psi_j^0(v) - \psi_j^1(v), \\ &= \frac{1}{T_j - T_{j-1}} \log \left[\frac{1 + iv(1 + iv) \mathcal{F} \mathcal{O}_j(v)}{1 + iv(1 + iv) \mathcal{F} \mathcal{O}_{j-1}(v)} \right], \\ &= \frac{1}{T_j - T_{j-1}} \log \left[\frac{\varphi_{T_j}(v - i)}{\varphi_{T_{j-1}}(v - i)} \right], \\ &= -\frac{\sigma_j^2(v - i)^2}{2} + i\gamma_j(v - i) + \int_{\mathbb{R}} (e^{i(v-i)x} - 1)\nu_j(x)dx, \\ &= -\frac{\sigma_j^2 v^2}{2} + i(\sigma_j^2 + \gamma_j)v^2 + (\sigma_j^2/2 + \gamma_j - \lambda_j) + \mathcal{F} \mu_j(v), \end{aligned} \quad (2.14)$$

with $\mu_j(x) := e^x \nu_j(x)$ called the exponentially weighted jump density.

Due to the Riemann-Lebesgue Lemma $\mathcal{F} \mu_j(v)$ tends to 0 when $|v| \rightarrow \infty$, such that ψ_j is, at least for large $|v|$, the sum of a quadratic polynomial and a function vanishing at 0. Therefore, formula (2.14) shows that the Lévy triplet $(\sigma_j^2, \gamma_j, \mu_j)$ (Lévy triplets will equivalently be parametrized with ν_j and μ_j) is uniquely identifiable given the whole option price functions \mathcal{O}_j and \mathcal{O}_{j-1} without noise. The parameters σ_j^2 , γ_j and λ_j can be identified as parameters of the polynomial for arguments tending to infinity, thereafter $\mathcal{F} \mu_j(v)$ can be obtained as the difference between the polynomial and ψ_j . The exact nonparametric statistical approach to this estimation will be examined later.

In subsection 2.2.2 we argued that, because of noise, the option function $\mathcal{O}_j(x)$ is not observed, but an approximated version $\tilde{\mathcal{O}}_j(x)$. Therefore we need to approximate the function ψ_j by some estimator $\tilde{\psi}_j$. After observing the definition of the function ψ , a natural choice for the estimator $\tilde{\psi}_j$ of the function ψ_j can be given by

$$\begin{aligned} \tilde{\psi}_j(v) &:= \tilde{\psi}_j^0(v) - \tilde{\psi}_j^1(v) \\ &:= \frac{1}{T_j - T_{j-1}} \log_{\geq \kappa(v, T_j)} [\tilde{\varphi}_{T_j}(v - i)] - \frac{1}{T_j - T_{j-1}} \log_{\geq \kappa(v, T_{j-1})} [\tilde{\varphi}_{T_{j-1}}(v - i)], \\ &:= \frac{1}{T_j - T_{j-1}} \log_{\geq \kappa(v, T_j)} \left[1 + iv(1 + iv) \mathcal{F} \tilde{\mathcal{O}}_j(v) \right] \\ &\quad - \frac{1}{T_j - T_{j-1}} \log_{\geq \kappa(v, T_{j-1})} \left[1 + iv(1 + iv) \mathcal{F} \tilde{\mathcal{O}}_{j-1}(v) \right], \end{aligned}$$

where after calibration using the interpolated observations $\tilde{\mathcal{O}}_{j-l}$ instead of \mathcal{O}_{j-l} for $l = 0, 1$ we find the approximated version $(\tilde{\sigma}_j, \tilde{\gamma}_j, \tilde{\mu}_j(x))$ of $(\sigma_j, \gamma_j, \mu_j(x))$. Note that a trimmed logarithm $\log_{\geq \kappa(v, T_{j-l})}$, $l = 0, 1$, defined by

$$\log_{\geq \kappa(v, T_{j-l})}(z) := \begin{cases} \log(z), & |z| \geq \kappa(v, T_{j-l}), \\ \log(\kappa(v, T_{j-l})z/|z|), & |z| < \kappa(v, T_{j-l}), \end{cases}$$

was used instead of the normal logarithm. The reason for this is that small errors in the argument of the normal logarithm close to zero could result in large statistical errors. This stabilization of the logarithm is mainly used for theoretical reasons; its practical importance is minor [7, p. 8].

The complex trimmed logarithms are again taken such that $\tilde{\psi}_j^l$ is continuous on $(-v_0, v_0)$ with $\tilde{\psi}_j^l(0) = 0$ and v_0 being the smallest positive zero of $\tilde{\varphi}_{T_{j-l}}$.

In the first section of the theoretical part, we will show a reasonable choice for the trimmed value $\kappa(v, T_{j-l})$, and a proof will be given that with this trimmed value the estimator $\tilde{\psi}_j$ for ψ_j is asymptotically well-defined.

2.4 Spectral Estimation of the Lévy Triplet

The exact estimation method of the parametric part $(\tilde{\sigma}_j^2, \tilde{\gamma}_j, \tilde{\lambda}_j)$ and the exponentially weighted jump density $\tilde{\mu}_j(x) = e^x \tilde{\nu}_j(x)$ for $j = 1, \dots, n$ will now be worked out. The exact problem is summarized below.

Problem 2.2 Given the approximated option price functions $\tilde{O}_j(x)$ and $\tilde{O}_{j-1}(x)$, nonparametrically find best estimates of $\tilde{\sigma}_j^2$, $\tilde{\gamma}_j$, $\tilde{\lambda}_j$ and $\tilde{\mu}_j$ from

$$\begin{aligned} \tilde{\psi}_j(v) &= \frac{1}{T_j - T_{j-1}} \log_{\geq \kappa(v, T_j)} \left[1 + iv(1 + iv) \mathcal{F} \tilde{O}_j(v) \right] \\ &\quad - \frac{1}{T_j - T_{j-1}} \log_{\geq \kappa(v, T_{j-1})} \left[1 + iv(1 + iv) \mathcal{F} \tilde{O}_{j-1}(v) \right] \\ &= -\frac{\tilde{\sigma}_j^2 v^2}{2} + i(\tilde{\sigma}_j^2 + \tilde{\gamma}_j)v + (\tilde{\sigma}_j^2/2 + \tilde{\gamma}_j - \tilde{\lambda}_j) + \mathcal{F} \tilde{\mu}_j(v). \end{aligned} \quad (2.15)$$

In the first chapter, it was already explained that for the Lévy-Khintchine representation (1.2) we made the underlying assumption that $\tilde{\mu}_j$ is absolutely continuous and of finite activity. Then with the Riemann-Lebesgue lemma it can be shown that $\mathcal{F} \tilde{\mu}_j(v) \rightarrow 0$ as $|v| \rightarrow \infty$ (See, for example, Kawata [30, p. 43]).

Consequently, $\tilde{\psi}$ in expression (2.15) can be viewed, at least for large $|v|$, as a quadratic polynomial in v with coefficients $(\tilde{\sigma}_j^2/2 + \tilde{\gamma}_j - \tilde{\lambda}_j, i(\tilde{\sigma}_j^2 + \tilde{\gamma}_j), -\tilde{\sigma}_j^2/2)$, plus a part $\mathcal{F} \tilde{\mu}_j(v)$ that vanishes for arguments tending to infinity. Using the decaying effect of $\mathcal{F} \tilde{\mu}_j(v)$, we will regularize the problem by cutting off frequencies $|v|$ higher than a certain “cutoff frequency” $U_j > 0$, which may depend on smoothness assumptions and noise levels of the underlying jump density.

Thus, the parametric part can be estimated using the following general optimization problem, where the term $\mathcal{F} \tilde{\mu}_j(v)$ squared and weighted will be minimized,

$$\inf_{(\tilde{\sigma}_j^2, \tilde{\gamma}_j, \tilde{\lambda}_j)} \int_{\{|v| > U_j\}} \tilde{w}^{U_j}(v) \left| \tilde{\psi}_j(v) + \frac{1}{2} \tilde{\sigma}_j^2 v^2 - i(\tilde{\sigma}_j^2 + \tilde{\gamma}_j)v - (\tilde{\sigma}_j^2/2 + \tilde{\gamma}_j - \tilde{\lambda}_j) \right|^2 dv,$$

where \tilde{w}^{U_j} is some nonnegative weight function that satisfies

$$\tilde{w}^{U_j}(v) := \frac{1}{U_j} \tilde{w}^1 \left(\frac{v}{U_j} \right)$$

with $\tilde{w}^1(v)$ continuous, $\text{supp } \tilde{w}^1 \subseteq [0, 1]$ and $\tilde{w}^1(u) > 0$ on $(0, 1)$. The estimation of the parametric part can be understood as an orthogonal projection with respect to a weighted L^2 scalar product.

Let us expand on the exact reason why the weight function $\tilde{w}^{U_j}(v)$ is introduced. Belomestny et al. [4] show that the deviation of $\tilde{\psi}_j(v)$ from $\psi_j(v)$ increases exponentially in v whenever $\tilde{\sigma}_j > 0$. It is therefore advised to restrict the range of frequencies v used for estimating the parametric part $(\tilde{\sigma}_j^2/2 + \tilde{\gamma}_j - \tilde{\lambda}_j, i(\tilde{\sigma}_j^2 + \tilde{\gamma}_j), -\tilde{\sigma}_j^2/2)$. This task can be accomplished by introducing the weight function $\tilde{w}^{U_j}(u)$.

The optimisation problem can be simplified by splitting the integrand in a real and imaginary part

$$\begin{aligned} &\inf_{(\tilde{\sigma}_j^2, \tilde{\gamma}_j, \tilde{\lambda}_j)} \int_{\{|v| > U_j\}} \tilde{w}^{U_j}(v) \left| \tilde{\psi}_j(v) + \frac{1}{2} \tilde{\sigma}_j^2 v^2 - i(\tilde{\sigma}_j^2 + \tilde{\gamma}_j)v - (\tilde{\sigma}_j^2/2 + \tilde{\gamma}_j - \tilde{\lambda}_j) \right|^2 dv \\ &= \inf_{(\tilde{\sigma}_j^2, \tilde{\gamma}_j, \tilde{\lambda}_j)} \int_{\{|v| > U_j\}} \tilde{w}^{U_j}(v) \left\{ \left(\text{Re}(\tilde{\psi}_j(v)) + \frac{1}{2} \tilde{\sigma}_j^2 v^2 - (\tilde{\sigma}_j^2/2 + \tilde{\gamma}_j - \tilde{\lambda}_j) \right)^2 \right. \\ &\quad \left. + \left(\text{Im}(\tilde{\psi}_j(v)) - (\tilde{\sigma}_j^2 + \tilde{\gamma}_j)v \right)^2 \right\} dv \end{aligned}$$

$$\left. + \left(\operatorname{Im}(\tilde{\psi}_j(v)) - (\tilde{\sigma}_j^2 + \tilde{\gamma}_j)v \right)^2 \right\} dv,$$

where we used that for $z \in \mathbb{C}$ it holds that $|z|^2 = \operatorname{Re}(z)^2 + \operatorname{Im}(z)^2$.

Now using the linearity of the integral and the reparametrization

$$(\hat{\sigma}^2, \hat{\gamma}, \hat{\lambda}) = (\tilde{\sigma}_j^2, (\tilde{\sigma}_j^2 + \tilde{\gamma}_j), (\tilde{\sigma}_j^2/2 + \tilde{\gamma}_j - \tilde{\lambda}_j)), \quad (2.16)$$

the optimisation problem can be separated into two parts, namely

$$\begin{aligned} (\hat{\sigma}_j^2, \hat{\lambda}_j) &:= \arg \min_{(\sigma_j^2, \lambda_j)} \int_{-U_j}^{U_j} \tilde{w}^{U_j}(v) \left(\operatorname{Re}(\tilde{\psi}_j(v)) + \frac{1}{2}\sigma_j^2 v^2 - \lambda_j \right)^2 dv \quad \text{and} \\ \hat{\gamma}_j &:= \arg \min_{\gamma_j} \int_{-U_j}^{U_j} \tilde{w}^{U_j}(v) \left(\operatorname{Im}(\tilde{\psi}_j(v)) - \gamma_j v \right)^2 dv. \end{aligned}$$

The solutions are found by straightforward calculations by taking partial derivatives and identifying the minimum. For completeness, these calculations are done in the next subsections.

Solving for $\hat{\sigma}_j^2$ and $\hat{\lambda}_j$

For solving the problem

$$(\hat{\sigma}_j^2, \hat{\lambda}_j) := \arg \min_{(\sigma_j^2, \lambda_j)} \int_{-U_j}^{U_j} \tilde{w}^{U_j}(v) \left(\operatorname{Re}(\tilde{\psi}_j(v)) + \frac{1}{2}\sigma_j^2 v^2 - \lambda_j \right)^2 dv,$$

define the function g by

$$g(v) = \int_{-U_j}^{U_j} \tilde{w}^{U_j}(v) \left(\operatorname{Re}(\tilde{\psi}_j(v)) + \frac{1}{2}\sigma_j^2 v^2 - \lambda_j \right)^2 dv.$$

By taking the partial derivatives $\frac{\partial g(v)}{\partial \sigma_j^2}$ and $\frac{\partial g(v)}{\partial \lambda_j}$, and setting these to zero, the following results can be found

$$\begin{aligned} 0 &= \frac{\partial g(v)}{\partial \sigma_j^2} = \int_{-U_j}^{U_j} \tilde{w}^{U_j}(v) \operatorname{Re}(\tilde{\psi}_j(v)) v^2 dv + \frac{1}{2}\sigma_j^2 \int_{-U_j}^{U_j} \tilde{w}^{U_j}(v) v^4 dv - \lambda_j \int_{-U_j}^{U_j} \tilde{w}^{U_j}(v) v^2 dv, \\ 0 &= \frac{\partial g(v)}{\partial \lambda_j} = -2 \int_{-U_j}^{U_j} \tilde{w}^{U_j}(v) \operatorname{Re}(\tilde{\psi}_j(v)) dv - \sigma_j^2 \int_{-U_j}^{U_j} \tilde{w}^{U_j}(v) v^2 dv + 2\lambda_j \int_{-U_j}^{U_j} \tilde{w}^{U_j}(v) dv. \end{aligned}$$

These are two linear equations in σ_j^2 and λ_j that can easily be solved to find isolated expressions for σ_j^2 and λ_j .

Solving for σ_j^2 and verifying that this is indeed a minimum gives

$$\hat{\sigma}_j^2 = \int_{-U_j}^{U_j} w_{\sigma_j}^{U_j} \operatorname{Re}(\tilde{\psi}_j(v)) dv,$$

where we defined $w_{\sigma_j}^{U_j}$ in terms of w^{U_j} as

$$w_{\sigma_j}^{U_j}(v) := \tilde{w}^{U_j}(v) \frac{2 \left[\left(\int_{-U_j}^{U_j} \tilde{w}^{U_j}(s) ds \right) v^2 - \int_{-U_j}^{U_j} \tilde{w}^{U_j}(s) s^2 ds \right]}{\left(\int_{-U_j}^{U_j} \tilde{w}^{U_j}(s) s^2 ds \right)^2 - \int_{-U_j}^{U_j} \tilde{w}^{U_j}(s) s^4 ds \cdot \int_{-U_j}^{U_j} \tilde{w}^{U_j}(s) ds}.$$

The new weight function $w_{\sigma_j}^{U_j}(v)$ inherits from $\tilde{w}^{U_j}(v)$ some rather natural conditions, first of all, it is symmetric, and secondly

$$\int_{-U_j}^{U_j} (-v^2/2)w_{\sigma_j}^{U_j} dv = 1 \quad \text{and} \quad \int_{-U_j}^{U_j} w_{\sigma_j}^{U_j} dv = 0.$$

Furthermore, it can be seen that $w_{\sigma_j}^{U_j}(v) = \frac{1}{U_j^3} w_{\sigma_j}^1(v/U_j)$, where $w_{\sigma_j}^1$ is supported on $[0, 1]$, symmetric and bounded, because

$$\left(\int_{-U_j}^{U_j} \tilde{w}^{U_j}(s) s^2 ds \right)^2 - \int_{-U_j}^{U_j} \tilde{w}^{U_j}(s) s^4 ds \cdot \int_{-U_j}^{U_j} \tilde{w}^{U_j}(s) ds > 0$$

by the Cauchy-Schwarz inequality.

Now solving for λ_j and verifying that it is a minimum gives

$$\hat{\lambda}_j = \int_{-U_j}^{U_j} w_{\lambda_j}^{U_j}(v) \operatorname{Re}(\psi_j(v)) dv,$$

where we defined $w_{\lambda_j}^{U_j}$ in terms of \tilde{w}^{U_j} as

$$w_{\lambda_j}^{U_j}(v) := \tilde{w}^{U_j}(v) \frac{\int_{-U_j}^{U_j} \tilde{w}^{U_j}(s) s^4 ds - \left(\int_{-U_j}^{U_j} \tilde{w}^{U_j}(v) s^2 ds \right) v^2}{\int_{-U_j}^{U_j} \tilde{w}^{U_j}(s) s^4 ds \cdot \int_{-U_j}^{U_j} \tilde{w}^{U_j}(s) ds - \left(\int_{-U_j}^{U_j} \tilde{w}^{U_j}(v) s^2 ds \right)^2}.$$

The weight functions $w_{\lambda_j}^{U_j}(v)$ again inherits some natural conditions, it is symmetric, and

$$\int_{-U_j}^{U_j} w_{\lambda_j}^{U_j}(v) dv = 1 \quad \text{and} \quad \int_{-U_j}^{U_j} (v^2/2) w_{\lambda_j}^{U_j}(v) dv = 1.$$

Next to this, the weight function can be written as $w_{\lambda_j}^{U_j}(v) = \frac{1}{U_j} w_{\lambda_j}^1(v/U_j)$ where $w_{\lambda_j}^1$ is supported on $[0, 1]$ and bounded, again by the Cauchy-Schwarz inequality.

Solving for $\hat{\gamma}_j$

For solving the problem for $\hat{\gamma}_j$,

$$\hat{\gamma}_j := \arg \min_{\gamma_j} \int_{-U_j}^{U_j} \tilde{w}^{U_j}(v) \left(\operatorname{Im}(\tilde{\psi}_j(v)) - \gamma_j v \right)^2 dv,$$

define the function h by

$$h(v) = \int_{-U_j}^{U_j} \tilde{w}^{U_j}(v) \left(\operatorname{Im}(\tilde{\psi}_j(v)) - \gamma_j v \right)^2 dv.$$

Setting the partial derivative $\partial h / \partial \gamma$ to 0, we find

$$0 = \frac{\partial h}{\partial \gamma} = -2 \int_{-U_j}^{U_j} v \tilde{w}^{U_j}(v) \operatorname{Im}(\tilde{\psi}_j(v)) dv + 2\gamma \int_{-U_j}^{U_j} \tilde{w}^{U_j}(v) v^2 dv.$$

Solving for γ and verifying that this is indeed a minimum gives the solution

$$\hat{\gamma}_j = \int_{-U_j}^{U_j} \tilde{w}_{\gamma_j}^{U_j}(v) \operatorname{Im}(\tilde{\psi}_j(v)) dv,$$

where we defined $\tilde{w}_{\gamma_j}^{U_j}$ as

$$\tilde{w}_{\gamma_j}^{U_j}(v) = \tilde{w}^{U_j}(v) \frac{v}{\int_{-U_j}^{U_j} \tilde{w}^{U_j}(s) s^2 ds}.$$

The weight function $\tilde{w}_{\gamma_j}^{U_j}(v)$ fulfills

$$\int_{-U_j}^{U_j} v w_{\gamma_j}^{U_j}(v) dv = 1,$$

and $\tilde{w}_{\gamma_j}^{U_j}(v) = \frac{1}{U_j^2} w_{\gamma_j}^1(v/U_j)$, where $w_{\gamma_j}^1$ is an anti-symmetric function, supported on $[0, 1]$ and bounded.

End Results for $\tilde{\sigma}_j^2, \tilde{\gamma}_j, \tilde{\lambda}_j$ and $\tilde{\nu}_j$

The solutions for the original estimators $(\tilde{\sigma}_j^2, \tilde{\gamma}_j, \tilde{\lambda}_j)$ can be found after plugging back the reparametrization $(\hat{\sigma}^2, \hat{\gamma}, \hat{\lambda}) = (\tilde{\sigma}_j^2, (\tilde{\sigma}_j^2 + \tilde{\gamma}_j), (\tilde{\sigma}_j^2/2 + \tilde{\gamma}_j - \tilde{\lambda}_j))$ as in expression (2.16), this results in

$$\begin{aligned} \tilde{\sigma}_j^2 &= \int_{-U_j}^{U_j} w_{\sigma_j}^{U_j}(v) \operatorname{Re}(\tilde{\psi}_j(v)) dv, \\ \tilde{\gamma}_j &= -\tilde{\sigma}_j^2 + \int_{-U_j}^{U_j} w_{\gamma_j}^{U_j}(v) \operatorname{Im}(\tilde{\psi}_j(v)) dv, \\ \tilde{\lambda}_j &= \frac{\tilde{\sigma}_j^2}{2} + \tilde{\gamma}_j - \int_{-U_j}^{U_j} w_{\lambda_j}^{U_j}(v) \operatorname{Re}(\tilde{\psi}_j(v)) dv, \end{aligned}$$

where the weight functions $w_{\sigma_j}^{U_j}(v)$, $w_{\gamma_j}^{U_j}(v)$ and $w_{\lambda_j}^{U_j}(v)$ satisfy

$$\begin{aligned} \int_{-U_j}^{U_j} \frac{-v^2}{2} w_{\sigma_j}^{U_j}(v) dv &= 1, \quad \int_{-U_j}^{U_j} v w_{\gamma_j}^{U_j}(v) dv = 1, \quad \int_{-U_j}^{U_j} w_{\lambda_j}^{U_j}(v) dv = 1, \\ \int_{-U_j}^{U_j} w_{\sigma_j}^{U_j}(v) dv &= 0, \quad \int_{-U_j}^{U_j} v^2 w_{\lambda_j}^{U_j}(v) dv = 0. \end{aligned}$$

Furthermore, $w_{\sigma_j}^{U_j}(v) = \frac{1}{U_j^3} w_{\sigma_j}^1(v/U_j)$ is symmetric, $w_{\gamma_j}^{U_j}(v) = \frac{1}{U_j^2} w_{\gamma_j}^1(v/U_j)$ is antisymmetric, and $w_{\lambda_j}^{U_j}(v) = \frac{1}{U_j} w_{\lambda_j}^1(v/U_j)$ is symmetric, with all normalised functions $w_{\sigma_j}^1$, $w_{\gamma_j}^1$, and $w_{\lambda_j}^1$ bounded and supported on $[0, 1]$.

The exponentially weighted jump density $\tilde{\mu}_j$ can, thereafter, be estimated by the smoothed inverse Fourier transform of the weighted difference of the quadratic polynomial and $\tilde{\psi}_j$ with the found parameters, that is,

$$\tilde{\mu}_j(x) = \mathcal{F}^{-1} \left[\left(\tilde{\psi}_j(\cdot) + \frac{\tilde{\sigma}_j^2}{2} (\cdot - i)^2 - i \tilde{\gamma}_j (\cdot - i) + \tilde{\lambda}_j \right) w_{\mu_j}(\cdot) \right] (x), \quad x \in \mathbb{R},$$

where $w_{\mu_j}^{U_j}(v) = w_{\mu_j}^1(v/U_j)$ is a symmetric weight function supported on $[-U_j, U_j]$.

From practical applications, it is found that estimating the jump measure $\nu_j(x)$ directly – instead of the exponentially weighted jump measure $\mu(x) = e^x \nu_j(x)$ – leads to more stable results,

$$\tilde{\nu}_j(x) = \mathcal{F}^{-1} \left[\left(\tilde{\psi}_j(\cdot + i) + \frac{\tilde{\sigma}_j^2}{2} (\cdot)^2 - i \tilde{\gamma}_j (\cdot) + \tilde{\lambda}_j \right) w_{\nu_j}(\cdot) \right] (x), \quad x \in \mathbb{R}.$$

For practical purposes, we define the shifted ψ_j by

$$\begin{aligned} \tilde{\psi}_{\nu_j}(v) := \tilde{\psi}_j(v + i) &= \frac{1}{T_j - T_{j-1}} \log_{\geq \kappa(v+i, T_j)} \left[1 - v(v+i) \mathcal{F} \tilde{\mathcal{O}}_j(v+i) \right] \\ &\quad - \frac{1}{T_j - T_{j-1}} \log_{\geq \kappa(v+i, T_{j-1})} \left[1 - v(v+i) \mathcal{F} \tilde{\mathcal{O}}_{j-1}(v+i) \right]. \end{aligned}$$

The version $\tilde{\psi}_{\nu_j}$ has more stability in practical cases for estimating the density. The estimation procedure for $\tilde{\nu}_j(x)$ then becomes

$$\tilde{\nu}_j(x) = \mathcal{F}^{-1} \left[\left(\tilde{\psi}_{\nu_j}(\cdot) + \frac{\tilde{\sigma}_j^2}{2}(\cdot)^2 - i\tilde{\gamma}_j(\cdot) + \tilde{\lambda}_j \right) w_{\nu_j}(\cdot) \right] (x), \quad x \in \mathbb{R}. \quad (2.17)$$

Due to the estimation error and the cut-off procedure, the estimated jump density $\tilde{\nu}_j(x)$ might take negative values and needs correction. Belomestny and Reiß [10, Section 2.6] provide the following, a posteriori, correction procedure: find $\tilde{\nu}_j^+$ such that

$$\|\tilde{\nu}_j^+ - \tilde{\nu}_j\| \rightarrow \min, \quad \inf_{x \in \mathbb{R}} \tilde{\nu}_j^+ \geq 0 \quad \text{subject to} \quad \int_{\mathbb{R}} \tilde{\nu}_j^+(x) dx = \int_{\mathbb{R}} \tilde{\nu}_j(x) dx.$$

The solution can easily be shown to be

$$\tilde{\nu}_j^+(x; \varrho) := \max(0, \tilde{\nu}_j(x) - \varrho),$$

where ϱ is chosen to satisfy the equation

$$\int_{\mathbb{R}} \tilde{\nu}_j^+(u; \varrho) du = \int_{\mathbb{R}} \tilde{\nu}_j(u; \varrho) du = \tilde{\lambda}_j. \quad (2.18)$$

This corrected density $\tilde{\nu}_j^+$ can be thought of as the density that is nonnegative and the closest to $\tilde{\nu}_j(x)$.

Now we have found a statistical method to calibrate all Lévy processes between two maturities T_{j-1} and T_j . Note that to find the whole time-inhomogeneous Lévy model we need to do the calibration of $(\tilde{\sigma}_j^2, \tilde{\gamma}_j, \tilde{\lambda}_j, \tilde{\nu}_j(x))$ for all $j = 1, \dots, n$ and thereafter “glue” them all together.

Chapter 3

Theoretical Results

As is common in statistical estimation procedures, we are interested in the performance and distribution of the created estimators of the last chapter. The calibration results on real-life data and simulations are presented in the second half of this thesis. Before we tackle the calibration from simulations and real-life data, it is good practice to investigate the theoretical properties of the estimators. Therefore, in this chapter, the well-definedness and asymptotic normality of the estimators will be proven.

First, the underlying assumptions for the results will be elucidated. We then show a satisfactory parameter $\kappa(v, T_{j-l})$ of the complex trimmed logarithm and prove that the estimator $\tilde{\psi}_j$ for ψ_j is asymptotically well-defined. Recall that this estimator is the basis of the estimation of the Lévy triplet. Thereafter, the most important theoretical result will be proven, namely that the estimators $(\tilde{\sigma}_j^2, \tilde{\gamma}_j, \tilde{\lambda}_j)$ are asymptotically normal. The asymptotic normality of $\tilde{\mu}_j$ will be proven afterward because the derivation differs from $(\tilde{\sigma}_j^2, \tilde{\gamma}_j, \tilde{\lambda}_j)$ by the fact that it was obtained by an inverse Fourier transform of the remainder. Finally, the optimal convergence rates of the parameters will also be looked upon.

We shall use throughout this chapter the notation $A \lesssim B$ if A is bounded by a constant multiple of B, independently of the parameters involved, that is, in the Landau notation $A = O(B)$.

3.1 Underlying Assumptions

Before these derivations are done we need to impose some important underlying assumptions that will be the basis of all theoretical results.

Assumptions of the Lévy Triplets

The assumptions we will lay upon the underlying parameters of the time-inhomogeneous Lévy process $(\sigma_j^2, \gamma_j, \lambda_j, \mu_j)$ are presented below in Definition 3.1.

Definition 3.1 For integers $s_j \geq 0$, and $R, \sigma_{\max} > 0$, let $\mathcal{G}_{s_j}^n(R, \sigma_{\max})$ denote the set of all Lévy triplets $\tau = (\sigma_j^2, \gamma_j, \mu_j)_{j=1, \dots, n}$ such that for all $j = 1, \dots, n$, μ_j is s_j -times (weakly) differentiable, the martingale condition (2.4) and finite second moment assumption (2.5) are satisfied, and

$$\sigma_j \in (0, \sigma_{\max}), \quad |\gamma_j|, \lambda_j \in [0, R], \quad \max_{k=0, \dots, s} \|\mu_j^{(k)}\|_{L^2(\mathbb{R})} \leq R, \quad \text{and} \quad \|\mu_j^{(s_j)}\|_{\infty} \leq R.$$

This definition makes multiple assumptions, some may be directly clear to one reader and unclear to another. The reasoning behind these assumptions will, therefore, now be discussed.

Recall that expression (2.4) was the martingale condition and is the basis of the fact that the model is a martingale under the risk-neutral measure \mathbb{Q} . Expression (2.5) was the assumption that the variance of the path of the underlying security S_t , which is modeled by an exponential time-inhomogeneous Lévy model, must be finite. This reassured that the Fourier transform of \mathcal{O}_j exists and is well-defined.

The parameters R and σ_{\max} are introduced to bound the to-be-estimated parameters — we do not want the underlying parameters to be “too large”. In the case that the parameters become too large, it is difficult to construct a statistically stable estimation method because then we will not have any guarantee that the argument in the logarithm of ψ_j is bounded from below by a positive constant. This can result in two undesirable outcomes: 1) a statistically unstable estimation method, and/or, 2) an extra bias term.

The assumption is imposed that μ_j is s_j times differentiable. Recall that the jump density ν_j was coupled to the exponentially weighted jump density μ_j by $\mu_j(x) = e^x \nu_j(x)$, such that ν_j is also s_j times differentiable. To show the theoretical results, the exact value of the integer $s_j \geq 0$ does not matter that much, even for small values the results still hold. The value matters most for the speed of convergence and performance of the statistical model, the smoother μ_j , i.e. the bigger s_j , the faster the convergence rate. Next to that the value s_j also plays a crucial role in the determination of the optimal cut-off values U_j . In empirical results, s_j is, of course, not known a priori, and here we need to assume the smoothness of the underlying security. This will be elaborated at the empirical results.

Assumptions of the Weight Functions

The exact choice of the weight functions $w_{\sigma_j^2}^1(v)$, $w_{\gamma_j}^1(v)$, $w_{\lambda_j}^1(v)$, and $w_{\mu_j}^1(v)$ will not matter for the theoretical results. Definition 3.2 will only impose some conditions the considered weight functions need to obey.

Definition 3.2 For an integer $s_j \geq 0$, let $\mathcal{W}_{s_j}^n$ denote the set of all weight function $w_{\sigma_j^2}^1$, $w_{\gamma_j}^1$, $w_{\lambda_j}^1$ and $w_{\mu_j}^1$ that satisfy the implied conditions of section 2.4, and

$$\begin{aligned} w_{\sigma_j^2}^1(v)/v^{s_j}, w_{\gamma_j}^1(v)/v^{s_j}, w_{\lambda_j}^1(v)/v^{s_j}, (1 - w_{\mu_j}^1(v))/v^{s_j} &\in L^2(\mathbb{R}), \\ \mathcal{F}[w_{\sigma_j^2}^1(v)/v^{s_j}], \mathcal{F}[w_{\gamma_j}^1(v)/v^{s_j}], \mathcal{F}[w_{\lambda_j}^1(v)/v^{s_j}], \mathcal{F}[(1 - w_{\mu_j}^1(v))/v^{s_j}] &\in L^1(\mathbb{R}). \end{aligned}$$

In Definition 3.2 the smoothness parameter s_j for μ_j is the same as in Definition 3.1.

The implied conditions of section 2.4 were the conditions that these weight functions inherited from the statistical estimation procedure. Of course, if we choose weight functions ourselves, we want those conditions to be valid. Otherwise, the estimation procedure can be invalid.

The $L^2(\mathbb{R})$ -integrability assumptions of the weight functions $w_{\sigma_j^2}^1$, $w_{\gamma_j}^1$, $w_{\lambda_j}^1$ divided by v^{s_j} , and also the $L^1(\mathbb{R})$ -integrability of their Fourier transforms, are necessary to make sure that the integrals in the theoretical results will be well behaved.

Assumptions of the Interpolation Scheme

Recall the underlying regression model (2.9)

$$\mathcal{O}_{j,k} = \mathcal{O}_j(x_{j,k}) + \delta_{j,k} \varepsilon_{j,k}, \quad k = 1, \dots, m_j.$$

By the noise introduced in this regression model, we can not observe $\mathcal{O}_j(x)$ directly and called the empirical observed counterpart $\tilde{\mathcal{O}}_j(x)$. In the theoretical results, out of simplification and previous work by Tendijck [46], Belomestny and Reiß [7], a linear spline will be used to construct $\tilde{\mathcal{O}}_j(x)$, i.e.

$$\tilde{\mathcal{O}}_j(x) = \beta_{0,j}(x) + \sum_{k=1}^{m_j} \mathcal{O}_{j,k} b_{j,k}(x), \quad x \in \mathbb{R},$$

where $(b_{j,k})$ are linear splines and the function β_0 is added to take care of the jump in the derivative of \mathcal{O} at zero: $\beta_0'(0+) - \beta_0'(0-) = -1$. In particular, $b_{j,k}$ is chosen as the triangular function, i.e., $b_{j,k}(x) = \Lambda(\frac{x-x_{j,k}}{x_{j,k+1}-x_{j,k}})$ with $\Lambda(x) = (1 - |x|)\mathbb{1}_{|x| \leq 1}$.

It is important to keep in mind that in the statistical estimation model we already made the underlying assumption that $(\varepsilon_{j,k})$ are independent (in j and k) centered sub-Gaussian random variables with $\mathbb{V}[\varepsilon_{j,k}] = 1$.

The magnitude of the error is modeled by the factor $\delta_{j,k} > 0$. For this $\delta_{j,k}$ we assume that it can be modeled by a certain $L^{2+\eta}(\mathbb{R})$ -integrable function δ_j with $\eta > 0$ such that at the design points $\delta_{j,k} = \delta_j(x_{j,k})$. This assumption must be made to make sure the asymptotic variance of the to-be-found asymptotic normal distribution of the parameters does exist.

For the asymptotics in the theoretical results, we need a growing number of observations to identify the whole option function $\mathcal{O}_j(x)$ for all $x \in \mathbb{R}$,

$$\Delta_j := \max_{k=2,\dots,m_j} |x_{j,k} - x_{j,k-1}| \rightarrow 0 \quad \text{and} \quad A_j := \min(x_{j,m_j}, -x_{j,1}) \rightarrow \infty. \quad (3.1)$$

These conditions ensure that the observations will now contain the whole x -axis.

Another assumption that will be made in the theoretical results is that the log-forward moneyness grid $\{x_{j,k} : k = 1, \dots, m_j\}$ will be equidistant such that

$$\Delta_j = |x_{j,k} - x_{j,k-1}| \quad \text{for all } k = 2, \dots, m_j,$$

is a constant. This will make the theoretical calculations easy and concise without seriously affecting the model and the results.

Using the interpolation scheme (2.12), a useful result that relates the error of the estimator of the characteristic function $\tilde{\varphi}_{T_{j-l}}$ to $\varphi_{T_{j-l}}$ can be found

$$\begin{aligned} \tilde{\varphi}_{T_{j-l}}(v-i) - \varphi_{T_{j-l}}(v-i) &= iv(1+iv)\mathcal{F}(\tilde{\mathcal{O}}_{j-l}(x) - \mathcal{O}_{j-l}(x))(v) \\ &= iv(1+iv)\mathcal{F}\left(\sum_{k=1}^{m_{j-l}} (\mathcal{O}_{j-l,k} - \mathcal{O}_{j-l}(x_{j,k}))b_{j-l,k}(x)\right)(v) \\ &= iv(1+iv)\sum_{k=1}^{m_{j-l}} \delta_{j,k}\varepsilon_{j,k}\mathcal{F}b_{j,k}(v). \end{aligned} \quad (3.2)$$

For calculating $\mathcal{F}b_{j,k}(v)$, recall that in the interpolation scheme (2.12), $(b_{j,k})$ were chosen as $b_{j,k}(x) = \Lambda\left(\frac{x-x_{j,k}}{x_{j,k+1}-x_{j,k}}\right)$ with $\Lambda(x) = (1-|x|)\mathbb{1}_{|x|\leq 1}$. Remember that the triangular function $\Lambda(x)$ is the convolution of two box functions $\Pi(x) = \mathbb{1}_{|x|\leq 1/2}$, and that the Fourier transform of the box function is $\mathcal{F}\Pi(v) = \text{sinc}(v/2) = \sin(v/2)/(v/2)$. This convolution transforms into a product in the spectral domain, therefore

$$\mathcal{F}\Lambda(v) = \mathcal{F}(\Pi * \Pi)(v) = \text{sinc}^2(v/2).$$

Now the Fourier transform of $b_{j,k}(x) = \Lambda\left(\frac{x-x_{j,k}}{x_{j,k+1}-x_{j,k}}\right)$ is found by using the scale- and time-shift properties of the Fourier transform

$$\mathcal{F}b_{j,k}(v) = \Delta_j e^{ivx_{j,k}} \text{sinc}^2(\Delta_j v/2), \quad (3.3)$$

where we use the assumption of an equidistant grid.

3.2 The Estimator $\tilde{\psi}_j$ for ψ_j

The estimator $\tilde{\psi}_j$ of ψ_j in the model section was defined as

$$\begin{aligned} \tilde{\psi}_j(v) &= \frac{1}{T_j - T_{j-1}} \log_{\geq \kappa(v, T_j)} \left[1 + iv(1+iv)\mathcal{F}\tilde{\mathcal{O}}_j(v) \right] \\ &\quad - \frac{1}{T_j - T_{j-1}} \log_{\geq \kappa(v, T_{j-1})} \left[1 + iv(1+iv)\mathcal{F}\tilde{\mathcal{O}}_{j-1}(v) \right]. \end{aligned}$$

There were still two theoretical open-ended questions that needed to be answered for the estimator $\tilde{\psi}_j$, namely:

1. how to choose the trimmed value $\kappa(v, T_{j-l})$,
2. is the estimator "well-defined".

3.2.1 Choice of Trimmed Value $\kappa(v, T_{j-l})$

The martingale condition in expression (2.4) can also be written as

$$\frac{\sigma_j^2}{2} + \gamma_j + \int_{\mathbb{R}} (e^x - 1) \nu_j(x) dx = 0 \iff \frac{\sigma_j^2}{2} + \gamma_j - \lambda_j = -\mathcal{F}\mu_j(0). \quad (3.4)$$

The general idea of the trimmed value $\kappa(v, T_{j-l})$ was to prevent unboundedness in the case of large stochastic errors, with this in mind we introduced the trimmed logarithm which ensures that $|\tilde{\psi}_j(v)| \geq \left| \log \left(\frac{\kappa(v, T_j)}{\kappa(v, T_{j-1})} \right) \right|$, this result trivially follows from the definition of the trimmed logarithm.

The goal of this section is that for Lévy triplets in $\mathcal{G}_{s_j}^n(R, \sigma_{\max})$ we want to define a lower bound for $|\tilde{\varphi}_{T_j}(v - i)|$. Using expression (3.4) and the fact that $\operatorname{Re}(\mathcal{F}\mu_j(v)) = \int_{\mathbb{R}} \mu_j(x) \cos(x) dx \geq -\|\mu_j\|_{L^1}$ we can first find

$$\begin{aligned} \left| \frac{\varphi_{T_j}(v - i)}{\varphi_{T_{j-1}}(v - i)} \right| &= \left| e^{(T_j - T_{j-1})\psi_j(v)} \right| = \left| e^{(T_j - T_{j-1})\left(-\frac{\sigma_j^2 v^2}{2} + i(\sigma_j + \gamma_j)v + \left(\frac{\sigma_j^2}{2} + \gamma_j - \lambda_j\right) + \mathcal{F}\mu_j(v)\right)} \right| \\ &= e^{(T_j - T_{j-1})\left(-\frac{\sigma_j^2 v^2}{2} + \left(\frac{\sigma_j^2}{2} + \gamma_j - \lambda_j\right) + \operatorname{Re}(\mathcal{F}\mu_j(v))\right)} \\ &\stackrel{(3.4)}{=} e^{(T_j - T_{j-1})\left(-\frac{\sigma_j^2 v^2}{2} - \mathcal{F}\mu_j(0) + \operatorname{Re}(\mathcal{F}\mu_j(v))\right)} \\ &= e^{(T_j - T_{j-1})\left(-\frac{\sigma_j^2 v^2}{2} - \|\mu_j\|_{L^1} + \operatorname{Re}(\mathcal{F}\mu_j(v))\right)} \\ &\geq e^{(T_j - T_{j-1})\left(-\frac{\sigma_j^2 v^2}{2} - 2\|\mu_j\|_{L^1}\right)} \\ &\stackrel{\text{def 3.1}}{\geq} e^{(T_j - T_{j-1})\left(-\frac{\sigma_j^2 v^2}{2} - 2R\right)} =: 2K(T_j - T_{j-1}, \sigma_j, R, v) \end{aligned} \quad (3.5)$$

The factor two in the definition is useful for mathematical tractability in the bound later on in Proposition 3.1. With expression (3.5), it is easy to find a desired lower bound

$$\begin{aligned} |\varphi_{T_j}(v - i)| &= \prod_{r=1}^j \left| \frac{\varphi_{T_r}(v - i)}{\varphi_{T_{r-1}}(v - i)} \right| \geq \prod_{r=1}^j 2K(T_r - T_{r-1}, \sigma_r, R, v) \\ &= e^{-\sum_{r=1}^j \frac{(T_r - T_{r-1})\sigma_r^2 v^2}{2} - (\sum_{r=1}^j T_r - T_{r-1})2R} \\ &\stackrel{\text{def 3.1}}{\geq} e^{-T_j \left(\frac{\sigma_{\max}^2 v^2}{2} - 2R\right)} =: 2\kappa(v, T_j). \end{aligned} \quad (3.6)$$

Hence, the trimmed value for $l = 0, 1$ can be chosen as $\kappa(v, T_{j-l}) = \frac{1}{2}e^{-T_{j-l}\left(\frac{\sigma_{\max}^2 v^2}{2} - 2R\right)}$. Note that $\kappa(v, T_{j-l})$ is a decreasing function in the first argument. The bound in expressions (3.5) will also be of great importance in the rest of the theoretical results.

3.2.2 Asymptotically Well-Definedness of $\tilde{\psi}_j$ for ψ_j

For the estimation procedure to work properly, the estimator $\tilde{\psi}_j$ does not need to *blow up*, this happens whenever $\tilde{\varphi}_{T_j}(v - i) = 0$ for some $j = 1, \dots, n$ [40, p.8]. In this section, we will therefore prove that $\mathbb{P}(\tilde{\varphi}_{T_j}(v - i) = 0) = 0$ for all $j = 1, \dots, n$. This result will be proven to be asymptotically true if the cut-off value U_j does not converge too quickly to infinity, when the maximum distance between the observations Δ_j converges to zero, i.e., one quantity can be expressed as an intermediate sequence with respect to the other quantity.

The result $\mathbb{P}(\tilde{\varphi}_{T_j}(v - i) = 0) = 0$ for all $j = 1, \dots, n$ will be shown by stating the result of Proposition 3.1. The proof of Proposition 3.1 can be found at the end of this section.

Proposition 3.1 *Let $j \in \{1, \dots, n\}$ and $k \in \{1, \dots, m_j\}$. Assume that the error distributions $(\varepsilon_{j,k})$ consists of independent centered sub-Gaussian random variables with $\mathbb{V}[\varepsilon_{j,k}] = 1$. Choose the cut-off value U_j and grid size Δ_j such that*

$$\Delta_j U_j^4 \log U_j e^{U_j^2 \sum_{r=1}^j (T_r - T_{r-1}) \sigma_r^2} \rightarrow 0 \quad \text{when } U_j \rightarrow \infty \text{ and } \Delta_j \rightarrow 0.$$

If there exists a constant $p > 1$ with $\lim_{U_j \rightarrow \infty} \Delta_j \sum_{k=1}^{m_j} \delta_{j,k}^2 (1 + |x_{j,k}|^p) < \infty$, then

$$\lim_{U_j \rightarrow \infty} \mathbb{P} \left(\sup_{v \in [0, U_j]} |\tilde{\varphi}_{T_j}(v - i) - \varphi_{T_j}(v - i)| > \inf_{v \in [0, U_j]} \prod_{r=1}^j K(T_r - T_{r-1}, \sigma_r, R, v) \right) = 0.$$

To show the well-definedness of the complex logarithm, the result of Lemma 3.1 below will be utilized.¹

Lemma 3.1 *Let $f, g : [0, T] \rightarrow \mathbb{C}$ be two continuous functions with $|f(t)| > C$, $|f(t) - g(t)| \leq C$ for all $t \in [0, T]$ and $\arg f(0) = \arg g(0)$. If \arg is chosen such that $t \rightarrow \arg \gamma(t)$ is continuous for a continuous function $\gamma(t)$, then*

$$\sup_{t \in [0, T]} |\arg g(t) - \arg f(t)| \leq \pi.$$

In expression (3.6) it was deduced that $2^{j-1} \prod_{r=1}^j K(T_r - T_{r-1}, \sigma_r, R, v) \geq \kappa(v, T_j)$. Proposition 3.1 then states that asymptotically with probability tending to one

$$\sup_{v \in [0, U_j]} |\tilde{\varphi}_{T_j}(v - i) - \varphi_{T_j}(v - i)| \leq \inf_{v \in [0, U_j]} \kappa(v, T_j) = \kappa(U_j, T_j),$$

where we used that κ is a decreasing function in the first argument. Moreover (3.6) gives $|\varphi_{T_j}(v - i)| > 2\kappa(v, T_j) > \kappa(U_j, T_j)$ and it is easy to see that $\arg \tilde{\varphi}_{T_j}(-i) = \arg \varphi_{T_j}(-i) = 0$. All the conditions of Lemma 3.1 are satisfied, thus asymptotically with probability one,

$$\sup_{v \in [0, U_j]} |\arg \tilde{\varphi}_{T_j}(v - i) - \arg \varphi_{T_j}(v - i)| \leq \pi$$

and, thereby,

$$\lim_{U_j \rightarrow \infty} \mathbb{P} \left(\sup_{v \in [0, U_j]} |\arg \tilde{\varphi}_{T_j}(v - i) - \arg \varphi_{T_j}(v - i)| > \pi \right) = 0. \quad (3.7)$$

Expression (3.7) shows that the branches of the complex logarithms are taken similarly and that the estimated characteristic function is distinct from zero everywhere.

Proof (Proposition 3.1) Applying Markov's inequality with the convex function x^2 we get

$$\begin{aligned} & \mathbb{P} \left(\sup_{v \in [0, U_j]} |\tilde{\varphi}_{T_j}(v - i) - \varphi_{T_j}(v - i)| > 2^{j-1} \inf_{v \in [0, U_j]} \prod_{i=r}^j K(T_r - T_{r-1}, \sigma_r, R, v) \right) \\ & \leq \frac{\mathbb{E} \left[\sup_{v \in [0, U_j]} |\tilde{\varphi}_{T_j}(v - i) - \varphi_{T_j}(v - i)|^2 \right]}{\left(2^{j-1} \inf_{v \in [0, U_j]} \prod_{r=1}^j K(T_r - T_{r-1}, \sigma_r, R, v) \right)^2}. \end{aligned}$$

The main difficulty in simplification of the expression above is in the term $|\tilde{\varphi}_{T_j}(v - i) - \varphi_{T_j}(v - i)|^2$. Using (3.2) we can write

$$|\tilde{\varphi}_{T_j}(v - i) - \varphi_{T_j}(v - i)|^2 = |iv(1 + iv) \sum_{k=1}^{m_j} \delta_{j,k} \varepsilon_{j,k} \mathcal{F} b_{j,k}|^2 =: \Delta_j (v^4 + v^2) |G(v)|^2$$

¹ In the rest of the thesis, all proofs of the intermediate lemmata can be found in the appendix.

with $G(v) := \frac{1}{\sqrt{\Delta_j}} \sum_{k=1}^{m_j} \delta_{j,k} \varepsilon_{j,k} \mathcal{F} b_{j,k}(v)$. We will bound the function $G(v)$ using an entropy argument and Dudley's theorem, i.e., we will bound the difference $|G(v) - G(w)|$ in terms of $|v - w|$. Let $q \in [0, 1]$, then

$$\begin{aligned}
\Delta_j \mathbb{E}[|G(v) - G(w)|^2] &= \mathbb{E} \left[\left| \sum_{k=1}^{m_j} \delta_{j,k} \varepsilon_{j,k} \int_{\mathbb{R}} b_{j,k}(x) (e^{ixv} - e^{ixw}) dx \right|^2 \right] \\
&\stackrel{\text{IND}}{=} \sum_{k=1}^{m_j} \delta_{j,k}^2 \left| \int_{\mathbb{R}} b_{j,k}(x) (e^{ixv} - e^{ixw}) dx \right|^2 \leq \sum_{k=1}^{m_j} \delta_{j,k}^2 \left(\int_{\mathbb{R}} b_{j,k}(x) \min(2, |v - w||x|) dx \right)^2 \\
&= \sum_{k=1}^{m_j} \delta_{j,k}^2 \left(\int_{|x| > 2/(v-w)} 2b_{j,k}(x) dx + \int_{|x| \leq 2/(v-w)} b_{j,k}(x) |v - w||x| dx \right)^2 \\
&\leq \sum_{k=1}^{m_j} \delta_{j,k}^2 \left(\int_{|x| > 2/(v-w)} 2b_{j,k}(x) \left(\frac{|x||v - w|}{2} \right)^q dx \right. \\
&\quad \left. + \int_{|x| \leq 2/(v-w)} b_{j,k}(x) |v - w||x| \left(\frac{2}{|x||v - w|} \right)^{1-q} dx \right)^2 \\
&= \sum_{k=1}^{m_j} \delta_{j,k}^2 \left(\int_{\mathbb{R}} 2^{1-q} b_{j,k}(x) |x|^q |v - w|^q dx \right)^2 = |v - w|^{2q} 2^{2-2q} \sum_{k=1}^{m_j} \delta_{j,k}^2 \left(\int_{\mathbb{R}} b_{j,k}(x) |x|^q dx \right)^2 \\
&\leq |v - w|^{2q} 2^{2-2q} \sum_{k=1}^{m_j} \delta_{j,k}^2 \left(\int_{x_{j,k-1}}^{x_{j,k+1}} b_{j,k}(x) |x|^q dx \right)^2 \\
&\leq |v - w|^{2q} 2^{2-2q} \sum_{k=1}^{m_j} \delta_{j,k}^2 (x_{j,k+1} - x_{j,k-1})^2 |\max\{x_{j,k+1}, x_{j,k-1}\}|^{2q} \\
&\leq |v - w|^{2q} 2^{4-2q} \Delta_j^2 \sum_{k=1}^{m_j} \delta_{j,k}^2 (|x_{j,k}| + \Delta_j)^{2q}
\end{aligned}$$

Lemma 3.2 below can simplify this last expression even further.

Lemma 3.2 *Let $q, x \in \mathbb{R}$ and $c > 0$, then $(x^2 + c)^{2q} \leq \max\{2^{2q-1}, 1\}((x^2)^{2q} + c^{2q})$, where in the case of $x = 0$ it should be read as $(x^2)^{2q} = 1$.*

For some $q \in [0, 1]$ we have that $\max\{2^{2q-1}, 1\} \leq 2$, and we can then finally bound the difference

$$\Delta_j \mathbb{E}[|G(v) - G(w)|^2] \leq |v - w|^{2q} 2^{5-2q} \Delta_j^2 \sum_{k=1}^{m_j} \delta_{j,k}^2 (|x_{j,k}|^{2q} + \Delta_j^{2q}) < \infty,$$

where the finiteness follows from the second assumption of the proposition with $q = \min\{p/2, 1\}$.

With regards to the entropy argument, there thus exists a $c > 0$ such that

$$d(v, w) := \sqrt{\mathbb{E}[|G(v) - G(w)|^2]} \leq c|v - w|^H =: \rho(v, w),$$

with $H = q = \min\{p/2, 1\}$. So, $B_\rho(x, r) \subset B_d(x, r)$ for all $x \in \mathbb{R}$ and $r > 0$, and thus $N_d(X, r) \leq N_\rho(X, r)$ for sets X and all $r > 0$.

Before we can apply Dudley's theorem, the metric entropy needs to be estimated. Firstly, notice that there exists a $D \in \mathbb{R}$ such that $d(v, w) \leq D$ for all $v, w \in \mathbb{R}$. This is immediate when one applies the inequality $|e^{ix} - e^{iy}| \leq 2$ for $x, y \in \mathbb{R}$.

The covering number of $[0, U_j]$ of the metric ρ given a radius r is equal to

$$N_\rho([0, U_j], r) = \left\lceil U_j (c/r)^{1/H} / 2 \right\rceil$$

The asymptotic assumption is made that U_j is large enough such that $U_j \geq (eD/c)^{1/H}$, then

$$N_\rho([0, U_j], r) \leq U_j(c/r)^{1/H}.$$

We can now estimate the metric entropy

$$\begin{aligned} J([0, U_j], d) &:= \int_0^\infty \sqrt{\log(N_d([0, U_j], r))} dr = \int_0^D \sqrt{\log(N_d([0, U_j], r))} dr \\ &\leq \int_0^D \sqrt{\log(N_\rho([0, U_j], r))} dr \leq \int_0^D \sqrt{\log(U_j(c/r)^{1/H})} dr \\ &= H^{-1/2} \int_0^D \sqrt{\log(U_j^H(c/r))} dr = cH^{-1/2} U_j^H \int_0^{D/(U_j^H c)} \sqrt{\log(1/s)} ds \\ &\leq cH^{-1/2} U_j^H \cdot D / (U_j^H c) \sqrt{\log((U_j^H c) / D)} = \sqrt{\log(U_j) + \log(c^{1/H} / D^{1/H})} \\ &\lesssim \sqrt{\log U_j}. \end{aligned}$$

Some further explanation about the steps in this derivation needs to be given. Firstly, note that if $x := D / (U_j^H c) \leq e^{-1}$, then $\log x^{-1} \geq 1$. Now the integral is solved and estimated as follows

$$\int_0^x \sqrt{\log(1/s)} ds = \frac{\sqrt{\pi}}{2} \cdot \left(1 - \operatorname{Erf}\left(\sqrt{\log x^{-1}}\right)\right) + x \sqrt{\log x^{-1}},$$

with

$$\operatorname{Erf}(x) := \frac{2}{\sqrt{\pi}} \int_0^x e^{-s^2} ds.$$

This can be further simplified using

$$1 - \operatorname{Erf}\left(\sqrt{\log x^{-1}}\right) \leq \exp(-\log x^{-1}) / \left(\sqrt{\pi} \sqrt{\log x^{-1}}\right) = \frac{x}{\sqrt{\pi}} \cdot \frac{1}{\sqrt{\log x^{-1}}}.$$

Then if we use $\log x^{-1} \geq 1$,

$$\int_0^x \sqrt{\log(1/s)} ds \leq \frac{x}{2} \cdot \left(\frac{1}{\sqrt{\log x^{-1}}} + \sqrt{\log x^{-1}}\right) \leq x \sqrt{\log x^{-1}}.$$

Dudley's theorem now states that for all $U_j > 0$ we have a version of the process which is almost surely continuous on $[0, U_j]$ for the metric d . Moreover, it provides the following bound [50, Corollary 2.2.8] for all $a \geq 1$

$$\mathbb{E} \left[\sup_{v \in [0, U_j]} |G(v)|^a \right] \lesssim (\log U_j)^{a/2}.$$

Note that we now found a way to bound the described difficult term in Markov's inequality

$$\begin{aligned} &\mathbb{P}\left(\sup_{v \in [0, U_j]} |\tilde{\varphi}_{T_j}(v-i) - \varphi_{T_j}(v-i)| > 2^{j-1} \inf_{v \in [0, U_j]} \prod_{r=1}^j K(T_r - T_{r-1}, \sigma_r, R, v) \right) \\ &\leq \mathbb{E} \left[\sup_{v \in [0, U_j]} |\tilde{\varphi}_{T_j}(v-i) - \varphi_{T_j}(v-i)|^2 \right] \cdot \left(2^{j-1} \inf_{v \in [0, U_j]} \prod_{r=1}^j K(T_r - T_{r-1}, \sigma_r, R, v) \right)^{-2} \\ &\leq \Delta_j (U_j^4 + U_j^2) \mathbb{E} \left[\sup_{v \in [0, U_j]} |G(v)|^2 \right] \cdot 2^{2-2j} \prod_{r=1}^j (K(T_r - T_{r-1}, \sigma_r, R, U_j))^{-2} \\ &\leq \Delta_j (U_j^4 + U_j^2) \mathbb{E} \left[\sup_{v \in [0, U_j]} |G(v)|^2 \right] \cdot 4 \exp \left(U_j^2 \cdot \sum_{r=1}^j (T_r - T_{r-1}) \sigma_r^2 - 4RT_j \right) \end{aligned}$$

$$\lesssim \Delta_j U_j^4 \log(U_j) \cdot \exp\left(U_j^2 \cdot \sum_{r=1}^j (T_r - T_{r-1}) \sigma_r^2\right),$$

where we used that asymptotically when $U_j \rightarrow \infty$ the U_j^4 term dominates the U_j^2 term. By the assumption of the proposition, the last bound found converges to 0. \square

3.3 Asymptotic Normality of $(\tilde{\sigma}_j^2, \tilde{\gamma}_j, \tilde{\lambda}_j)$

This section is devoted to the main theoretical result of this thesis, namely that the estimators $(\tilde{\sigma}_j, \tilde{\gamma}_j, \tilde{\lambda}_j)_{j=1, \dots, n}$ for $(\sigma_j, \gamma_j, \lambda_j)_{j=1, \dots, n}$ are asymptotically normal. As can be seen in the spectral estimation part, the estimators $(\tilde{\sigma}_j, \tilde{\gamma}_j, \tilde{\lambda}_j)_{j=1, \dots, n}$ bear great resemblance and are therefore treated together. Whereas $(\tilde{\mu}_j(x))_{j=1, \dots, n}$ has a different estimation procedure with an inverse Fourier transform, and will therefore be treated separately afterward.

To the end of showing the normality of $(\tilde{\sigma}_j, \tilde{\gamma}_j, \tilde{\lambda}_j)_{j=1, \dots, n}$, we will first make a decomposition of the errors of the estimators in Bias terms, Linear terms, and Remainder terms. Thereafter, it will be shown that asymptotically, the Bias and Remainder terms are negligible to the Linear terms, and that the Linear terms asymptotically admit a normal distribution.

For conciseness, the case of the volatility estimator $\tilde{\sigma}_j$ will be completely evaluated, and because the estimators $\tilde{\gamma}_j$ and $\tilde{\lambda}_j$ bear great resemblance, the differences in the proofs of these estimators will be given at the end of every section.

The Greek letter ξ_j will sometimes be used to generalize that a given expression is valid for all $\xi_j \in \{\sigma_j, \gamma_j, \lambda_j\}$

3.3.1 Error Decomposition

The error analysis will be exemplified by considering $\tilde{\sigma}_j^2 - \sigma_j^2$. By expressions (2.14) and the properties of the weight functions, we can decompose the error into

$$\begin{aligned} \tilde{\sigma}_j^2 - \sigma_j^2 &= \int_{-U_j}^{U_j} w_{\sigma_j}^{U_j}(v) \operatorname{Re}(\tilde{\psi}_j(v) - \psi_j(v)) dv + \int_{-U_j}^{U_j} w_{\sigma_j}^{U_j}(v) \operatorname{Re}(\psi_j(v)) dv - \sigma_j^2 \\ &= \int_{-U_j}^{U_j} w_{\sigma_j}^{U_j}(v) \operatorname{Re}(\tilde{\psi}_j(v) - \psi_j(v)) dv + \int_{-U_j}^{U_j} w_{\sigma_j}^{U_j}(v) \operatorname{Re}(\mathcal{F}\mu_j(v)) dv \\ &= \underbrace{\int_{-U_j}^{U_j} w_{\sigma_j}^{U_j}(v) \operatorname{Re}(\tilde{\psi}_j^0(v) - \psi_j^0(v)) dv + \int_{-U_j}^{U_j} w_{\sigma_j}^{U_j}(v) \operatorname{Re}(\tilde{\psi}_j^1(v) - \psi_j^1(v)) dv}_{\text{Stochastic Error}} \\ &\quad + \underbrace{\int_{-U_j}^{U_j} w_{\sigma_j}^{U_j}(v) \operatorname{Re}(\mathcal{F}\mu_j(v)) dv}_{\text{Bias}}. \end{aligned}$$

In the first line to the second line, we used the conditions of the weight functions $\int_{-U_j}^{U_j} (-v^2/2) w_{\sigma_j}^{U_j}(v) dv = 1$ and $\int_{-U_j}^{U_j} w_{\sigma_j}^{U_j}(v) dv = 0$ such that with expression (2.15) it follows that

$$\begin{aligned} &\int_{-U_j}^{U_j} w_{\sigma_j}^{U_j}(v) \operatorname{Re}(\psi_j(v)) dv - \sigma_j^2 \\ &= \int_{-U_j}^{U_j} w_{\sigma_j}^{U_j}(v) \operatorname{Re}(\psi_j(v)) dv - \sigma_j^2 \int_{-U_j}^{U_j} (-v^2/2) w_{\sigma_j}^{U_j}(v) dv - \left(\frac{\sigma_j^2}{2} + \gamma_j - \lambda_j\right) \int_{-U_j}^{U_j} w_{\sigma_j}^{U_j}(v) dv \\ &= \int_{-U_j}^{U_j} w_{\sigma_j}^{U_j}(v) \left\{ \operatorname{Re}(\psi_j(v)) + \frac{\sigma_j^2 v^2}{2} - \left(\frac{\sigma_j^2}{2} + \gamma_j - \lambda_j\right) \right\} dv \\ &\stackrel{(2.15)}{=} \int_{-U_j}^{U_j} w_{\sigma_j}^{U_j}(v) \operatorname{Re}(\mathcal{F}\mu_j(v)) dv. \end{aligned}$$

Recall that for $l = 0, 1$, we did define

$$\tilde{\psi}_j^l(v) - \psi_j^l(v) = \frac{1}{T_j - T_{j-1}} \left[\log_{\geq \kappa(v, T_{j-l})}(\tilde{\varphi}_{j-l}(v-i)) - \log(\varphi_{j-l}(v-i)) \right].$$

Neglecting the stabilisation of $\kappa(v, T_{j-l})$, we will split the Taylor approximation of the logarithm $\log(\tilde{\varphi}_{j-l}(v-i)/\varphi_{j-l}(v-i))$ into a first-order term (linearisation) $\mathcal{L}_j^l(v)$ and a remainder term $\mathcal{R}_j^l(v)$:

$$\mathcal{L}_j^l(v) = \frac{1}{T_j - T_{j-1}} \frac{\tilde{\varphi}_{T_{j-l}}(v-i) - \varphi_{T_{j-l}}(v-i)}{\varphi_{T_{j-l}}(v-i)} \quad \text{and} \quad \mathcal{R}_j^l(v) = \tilde{\psi}_j^l(v) - \psi_j^l(v) - \mathcal{L}_j^l(v). \quad (3.8)$$

Using the terms of (3.8), the error decomposition becomes

$$\begin{aligned} \tilde{\sigma}_j^2 - \sigma_j^2 &= \int_{-U_j}^{U_j} w_{\sigma_j^{U_j}}^{U_j}(v) \operatorname{Re}(\mathcal{L}_j^0(v)) dv - \int_{-U_j}^{U_j} w_{\sigma_j^{U_j}}^{U_j}(v) \operatorname{Re}(\mathcal{L}_j^1(v)) dv \\ &\quad + \int_{-U_j}^{U_j} w_{\sigma_j^{U_j}}^{U_j}(v) \operatorname{Re}(\mathcal{R}_j^0(v)) dv - \int_{-U_j}^{U_j} w_{\sigma_j^{U_j}}^{U_j}(v) \operatorname{Re}(\mathcal{R}_j^1(v)) dv \\ &\quad + \int_{-U_j}^{U_j} w_{\sigma_j^{U_j}}^{U_j}(v) \operatorname{Re}(\mathcal{F}\mu_j(v)) dv \\ &=: \mathcal{L}_{\sigma_j^2}^0 - \mathcal{L}_{\sigma_j^2}^1 + \mathcal{R}_{\sigma_j^2}^0 - \mathcal{R}_{\sigma_j^2}^1 + \mathcal{B}_{\sigma_j^2}. \end{aligned} \quad (3.9)$$

The idea is that we will show that the difference of the linear terms $\mathcal{L}_{\sigma_j^2}^0 - \mathcal{L}_{\sigma_j^2}^1$ is asymptotically normal with some standard deviation s_n and, secondly, we will show that the bias term $\mathcal{B}_{\sigma_j^2}$ and remainder terms $\mathcal{R}_{\sigma_j^2}^0, \mathcal{R}_{\sigma_j^2}^1$ divided by s_n are asymptotically negligible with respect to the Linear terms $\mathcal{L}_{\sigma_j^2}^0, \mathcal{L}_{\sigma_j^2}^1$. Then we can conclude

$$\frac{\tilde{\sigma}_j^2 - \sigma_j^2}{s_n} = \frac{\mathcal{L}_{\sigma_j^2}^0 - \mathcal{L}_{\sigma_j^2}^1}{s_n} + \frac{\mathcal{R}_{\sigma_j^2}^0 - \mathcal{R}_{\sigma_j^2}^1}{s_n} + \frac{\mathcal{B}_{\sigma_j^2}}{s_n} \xrightarrow{d} \mathcal{N}(0, 1),$$

where d stands for convergence in distribution.

From the spectral estimators of $\tilde{\gamma}_j$ and $\tilde{\lambda}_j$ it can be seen that it is useful — in the same manner as in the estimating part — to restrict the error decomposition of these estimators to the parametrizations $\hat{\gamma}_j := \tilde{\gamma}_j + \tilde{\sigma}_j^2$ and $\hat{\lambda}_j := \tilde{\lambda}_j - \tilde{\sigma}_j^2/2 - \tilde{\gamma}_j$ instead of simply $\tilde{\gamma}_j$ and $\tilde{\lambda}_j$. Following a similar line of thought of first decomposing the bias term and stochastic error term, and then writing the stochastic error term in a first order and remainder term, we get

$$\begin{aligned} (\tilde{\gamma}_j + \tilde{\sigma}_j^2) - (\gamma_j + \sigma_j^2) &= \int_{-U_j}^{U_j} w_{\gamma_j^{U_j}}^{U_j}(v) \operatorname{Im}(\mathcal{L}_j^0(v)) dv - \int_{-U_j}^{U_j} w_{\gamma_j^{U_j}}^{U_j}(v) \operatorname{Im}(\mathcal{L}_j^1(v)) dv \\ &\quad + \int_{-U_j}^{U_j} w_{\gamma_j^{U_j}}^{U_j}(v) \operatorname{Im}(\mathcal{R}_j^0(v)) dv - \int_{-U_j}^{U_j} w_{\gamma_j^{U_j}}^{U_j}(v) \operatorname{Im}(\mathcal{R}_j^1(v)) dv + \int_{-U_j}^{U_j} w_{\sigma_j^{U_j}}^{U_j}(v) \operatorname{Im}(\mathcal{F}\mu_j(v)) dv \\ &=: \mathcal{L}_{\gamma_j}^0 - \mathcal{L}_{\gamma_j}^1 + \mathcal{R}_{\gamma_j}^0 - \mathcal{R}_{\gamma_j}^1 + \mathcal{B}_{\gamma_j}, \quad \text{and} \end{aligned} \quad (3.10)$$

$$\begin{aligned} (\tilde{\lambda}_j - \tilde{\sigma}_j^2/2 - \tilde{\gamma}_j) - (\lambda_j - \sigma_j^2/2 - \gamma_j) &= \int_{-U_j}^{U_j} w_{\lambda_j^{U_j}}^{U_j}(v) \operatorname{Re}(\mathcal{L}_j^0(v)) dv - \int_{-U_j}^{U_j} w_{\lambda_j^{U_j}}^{U_j}(v) \operatorname{Re}(\mathcal{L}_j^1(v)) dv \\ &\quad + \int_{-U_j}^{U_j} w_{\lambda_j^{U_j}}^{U_j}(v) \operatorname{Re}(\mathcal{R}_j^0(v)) dv - \int_{-U_j}^{U_j} w_{\lambda_j^{U_j}}^{U_j}(v) \operatorname{Re}(\mathcal{R}_j^1(v)) dv + \int_{-U_j}^{U_j} w_{\lambda_j^{U_j}}^{U_j}(v) \operatorname{Re}(\mathcal{F}\mu_j(v)) dv \\ &=: \mathcal{L}_{\lambda_j}^0 - \mathcal{L}_{\lambda_j}^1 + \mathcal{R}_{\lambda_j}^0 - \mathcal{R}_{\lambda_j}^1 + \mathcal{B}_{\lambda_j}. \end{aligned} \quad (3.11)$$

Note that the main differences between the error decompositions are due to the properties of the different weight functions $w_{\sigma_j}^{U_j}, w_{\gamma_j}^{U_j}, w_{\lambda_j}^{U_j} \in \mathcal{W}_{s_j}^n$ and the different use of Re and Im.

3.3.2 Asymptotic Normality of Linear Terms $\mathcal{L}_{\xi_j}^l$

The asymptotic normality of the linear terms $\mathcal{L}_{\xi_j}^0, \mathcal{L}_{\xi_j}^1$ for $\xi_j \in \{\sigma_j^2, \gamma_j, \lambda_j\}$ will be shown. The whole derivation of $\mathcal{L}_{\sigma_j^2}^l$ is presented, and the deviations of $\mathcal{L}_{\gamma_j}^l, \mathcal{L}_{\lambda_j}^l$ will be noted at the end of the section.

First of all for $l = 0, 1$ recall that

$$\mathcal{L}_j^l(v) = \frac{1}{T_j - T_{j-1}} \frac{\tilde{\varphi}_{T_{j-1}}(v-i) - \varphi_{T_{j-1}}(v-i)}{\varphi_{T_{j-1}}(v-i)} \quad \text{and} \quad \mathcal{L}_{\sigma_j^2}^l = \int_{-U_j}^{U_j} w_{\sigma_j}^{U_j} \operatorname{Re}(\mathcal{L}_j^l(v)) \, dv.$$

The asymptotic normality will be shown by writing $\mathcal{L}_{\sigma_j^2}^l$ as a sum of the error distribution of the regression model $(\varepsilon_{j,k})$, which were centered independent sub-Gaussian random variables with $\mathbb{V}[\varepsilon_{j,k}] = 1$. Thereafter, we will show that the conditions of Theorem 3.1 below hold ², and conclude that $\mathcal{L}_{\sigma_j^2}^l$ is asymptotically normal.

Theorem 3.1 (Lyapunov CLT)

Let X_1, X_2, \dots, X_n be independent random variables such that $\mathbb{E}[X_i] = 0$ and $\mathbb{V}[X_i] = \sigma_i^2 < \infty$ for all $i = 1, \dots, n$. Define $T_n = \sum_{i=1}^n X_i$ and $s_n^2 = \sum_{i=1}^n \sigma_i^2$, then the following relation holds

$$\left(\exists \eta > 0 : \lim_{n \rightarrow \infty} \frac{1}{s_n^{2+\eta}} \sum_{i=1}^n \mathbb{E}[|X_i|^{2+\eta}] = 0 \right) \implies \left(\frac{1}{s_n} T_n \rightarrow^d \mathcal{N}(0, 1) \right). \quad (3.12)$$

The condition on the left-hand side is known as the Lyapunov condition.

Using (3.2), we can first write $\mathcal{L}_j^l(v)$ as

$$\mathcal{L}_j^l(v) = \frac{1}{T_j - T_{j-1}} \frac{iv(1+iv) \sum_{k=1}^{m_{j-l}} \delta_{j,k} \varepsilon_{j-l,k} \mathcal{F} b_{j-l,k}(v)}{\varphi_{T_{j-l}}(v)}. \quad (3.13)$$

Note that all the randomness is portrayed in the distribution $(\varepsilon_{j-l,k})$. Next to that, with the Lévy-Khintchine expression (1.2), the deterministic function $\varphi_{T_{j-l}}$ can be written as

$$\begin{aligned} \varphi_{T_{j-l}}(v-i) &= \prod_{r=1}^{j-l} \frac{\varphi_{T_r}(v-i)}{\varphi_{T_{r-1}}(v-i)} \\ &= \exp \left(\frac{-v^2}{2} \left(\sum_{r=1}^{j-l} (T_r - T_{r-1}) \sigma_r^2 \right) + iv \left(\sum_{r=1}^{j-l} (T_r - T_{r-1}) (\sigma_r^2 + \gamma_r) \right) \right. \\ &\quad \left. + \left(\sum_{r=1}^{j-l} (T_r - T_{r-1}) \left(\frac{\sigma_r^2}{2} + \gamma_r - \lambda_r \right) \right) + \left(\sum_{r=1}^{j-l} (T_r - T_{r-1}) \mathcal{F} \mu_r(v) \right) \right) \\ &=: \exp \left(-\frac{v^2}{2} A_{j-l} + iv B_{j-l} + C_{j-l} + D_{j-l}(v) \right). \end{aligned} \quad (3.14)$$

At this moment, the goal is to write $\mathcal{L}_{\sigma_j^2}^l$ as a sum of the independent $(\varepsilon_{j,k})$, such that we are in the form of Theorem 3.1. Using the properties of the weight function $w_{\sigma_j} \in \mathcal{W}_{s_j}^n$ and expression (3.13) gives the result

² Theorem 3.1 is the so-called Lyapunov Central Limit Theorem, which is generalized by the famous Lindeberg Central Limit Theorem.

$$\begin{aligned}
\mathcal{L}_{\sigma_j^2}^l &= \int_{-U_j}^{U_j} \operatorname{Re}(\mathcal{L}_j^l(v)) w_{\sigma_j}^{U_j}(v) dv = U_j \int_{-1}^1 \operatorname{Re}(\mathcal{L}_j^l(vU_j)) w_{\sigma_j}^{U_j}(vU_j) dv \\
&= U_j^{-2} \int_{-1}^1 \operatorname{Re}(\mathcal{L}_j^l(vU_j)) w_{\sigma_j}^1(v) dv \\
&= U_j^{-2} \int_0^1 \operatorname{Re}(\mathcal{L}_j^l(vU_j)) w_{\sigma_j}^1(v) dv + U_j^{-2} \int_0^1 \operatorname{Re}(\mathcal{L}_j^l(-vU_j)) w_{\sigma_j}^1(-v) dv \\
&= U_j^{-2} \int_0^1 \operatorname{Re}(\mathcal{L}_j^l(vU_j)) w_{\sigma_j}^1(v) dv + U_j^{-2} \int_0^1 \operatorname{Re}(\overline{\mathcal{L}_j^l(vU_j)}) w_{\sigma_j}^1(v) dv \\
&= 2U_j^{-2} \int_0^1 \operatorname{Re}(\mathcal{L}_j^l(vU_j)) w_{\sigma_j}^1(v) dv \\
&= \frac{2U_j^{-2}}{T_j - T_{j-1}} \sum_{k=1}^{m_{j-l}} \delta_{j-l,k} \varepsilon_{j-l,k} \operatorname{Re} \left(\int_0^1 \frac{ivU_j (1 + ivU_j) \mathcal{F}b_{j-l,k}(vU_j)}{\varphi_{T_{j-l}}(vU_j - i)} w_{\sigma_j}^1(v) dv \right).
\end{aligned} \tag{3.15}$$

If, for $k = 1, \dots, m_{j-l}$, we define random variables

$$X_k := \frac{2U_j^{-2}}{T_j - T_{j-1}} \delta_{j-l,k} \varepsilon_{j-l,k} \operatorname{Re} \left(\int_0^1 \frac{ivU_j (1 + ivU_j) \mathcal{F}b_{j-l,k}(vU_j)}{\varphi_{T_{j-l}}(vU_j - i)} w_{\sigma_j}^1(v) dv \right),$$

then, from the properties that $(\varepsilon_{j,k})$ are independent centered random variables with $\mathbb{V}[\varepsilon_{j,k}] = 1$, it follows that (X_k) are independent centred random variables with $\mathbb{V}[X_k] = \sigma_k^2 < \infty$. Note that this is exactly the setting of Theorem 3.1 where $\mathcal{L}_{\sigma_j^2}^l = T_{m_{j-l}} = \sum_{k=1}^{m_{j-l}} X_k$.

Now for the normality of $\mathcal{L}_{\sigma_j^2}^l = \sum_{k=1}^{m_{j-l}} X_k$ the Lyapunov condition needs to be shown. Firstly, the asymptotic variance $s_{n,l}^2$ of $\mathcal{L}_{\sigma_j^2}^l$ will be looked upon. The result is stated as a proposition because the proof is rather tedious and enduring.

Proposition 3.2 *Let $s_{n,l}^2 = \sum_{k=1}^{m_j} \sigma_k^2$ with $\sigma_k^2 = \mathbb{V}[X_k] < \infty$ for $k = 1, \dots, m_j$ and let $\delta_{j-l} \in L^\eta(\mathbb{R})$ for $\eta \geq 2$ and $l = 0, 1$. As U_j tends to infinity, then*

$$s_{n,l}^2 = w_{\sigma_j}^1(1)^2 d_{j,j-l} \Delta_{j-l} U_j^{-4} \exp(A_{j-l} U_j^2),$$

where we defined the constant

$$d_{j,j-l} := 2 \|\delta_{j-l}\|_{L^2}^2 (T_j - T_{j-1})^{-2} A_{j-l}^{-2} \exp(-2C_{j-l}),$$

and the terms A_{j-l} and C_{j-l} are as in expression (3.14).

Proof (Proposition 3.2) Using that $\mathbb{V}[\varepsilon_{j-l,k}] = 1$, it follows that

$$s_{n,l}^2 = \sum_{k=1}^{m_{j-l}} \sigma_k^2 = \frac{4U_j^{-4}}{(T_j - T_{j-1})^2} \sum_{k=1}^{m_{j-l}} \delta_{j-l,k}^2 \operatorname{Re}^2 \left(\int_0^1 \frac{ivU_j (1 + ivU_j) \mathcal{F}b_{j-l,k}(vU_j)}{\varphi_{T_{j-l}}(vU_j - i)} w_{\sigma_j}^1(v) dv \right).$$

Instead of computing the real part immediately, we will make use of the following identity

$$\operatorname{Re}^2 z = \left(\frac{z + \bar{z}}{2} \right)^2 = \frac{1}{4} (z^2 + 2z\bar{z} + \bar{z}^2),$$

and compute the three different parts instead. The problem can then be decomposed to

$$s_{n,l}^2 = \frac{U_j^{-4}}{(T_j - T_{j-1})^2} \sum_{k=1}^{m_{j-l}} \delta_{j-l,k}^2 (\mathcal{I}_v^2 + 2\mathcal{I}_v \mathcal{I}_{\bar{v}} + \mathcal{I}_{\bar{v}}^2) \tag{3.16}$$

with $\mathcal{I}_v := \int_0^1 f(v) dv$ and $\mathcal{I}_{\bar{v}} := \overline{\int_0^1 f(v) dv}$ for function $f(v) = \frac{ivU_j(1+ivU_j)\mathcal{F}b_{j-l,k}(vU_j)}{\varphi_{T_{j-l}}(vU_j-i)} w_{\sigma_j}^1(v)$.

Let us start with \mathcal{I}_v^2 , using expression (3.14) for $\varphi_{T_{j-l}}(vU_j - i)$ we have

$$\begin{aligned} \mathcal{I}_v^2 &:= \left(\int_0^1 \frac{ivU_j(1+ivU_j)\mathcal{F}b_{j-l,k}(vU_j)}{\exp(-v^2U_j^2A_{j-l}/2 + ivU_jB_{j-l} + C_{j-l} + D_{j-l}(vU_j))} w_{\sigma_j}^1(v)dv \right)^2 \\ &= \int_0^1 \int_0^1 \frac{ivU_j(1+ivU_j)iwU_j(1+iwU_j)\mathcal{F}b_{j-l,k}(vU_j)\mathcal{F}b_{j-l,k}(wU_j)}{\exp(-(v^2+w^2)U_j^2A_{j-l}/2 + i(v+w)U_jB_{j-l} + 2C_{j-l} + D_{j-l}(vU_j) + D_{j-l}(wU_j))} \\ &\quad w_{\sigma_j}^1(v)w_{\sigma_j}^1(w)dvdw \\ &= -U_j^2 \exp(-2C_{j-l}) \int_0^1 \int_0^1 vw \exp(A_{j-l}(v^2+w^2)U_j^2/2) (1+ivU_j)(1+iwU_j)g(v,w)dvdw \\ &= -U_j^2 \exp(-2C_{j-l}) \left(\int_0^1 \int_0^1 vw \exp(A_{j-l}(v^2+w^2)U_j^2/2) g(v,w)dvdw \right. \\ &\quad \left. + iU_j \int_0^1 \int_0^1 vw \exp(A_{j-l}(v^2+w^2)U_j^2/2) (v+w)g(v,w)dvdw \right. \\ &\quad \left. - U_j^2 \int_0^1 \int_0^1 vw \exp(A_{j-l}(v^2+w^2)U_j^2/2) \cdot vwg(v,w)dvdw \right), \end{aligned}$$

with g defined as

$$g(v,w) := g_{U_j}(v,w) := \frac{\mathcal{F}b_{j-l,k}(vU_j)\mathcal{F}b_{j-l,k}(wU_j)}{\exp(i(v+w)U_jB_{j-l} + D_{j-l}(vU_j) + D_{j-l}(wU_j))} w_{\sigma_j}^1(v)w_{\sigma_j}^1(w).$$

Note that we can decompose $g_{U_j}(v,w) = h_{U_j}(v)h_{U_j}(w)$ and that $h_{U_j}(-x)$ is the complex conjugate of $h_{U_j}(x)$.

In a similar manner, the terms $\mathcal{I}_{\bar{v}}^2$ and $\mathcal{I}_v\mathcal{I}_{\bar{v}}$ can be expressed as

$$\begin{aligned} \mathcal{I}_{\bar{v}}^2 &= -U_j^2 \exp(-2C_{j-l}) \left(\int_0^1 \int_0^1 vw \exp(A_{j-l}(v^2+w^2)U_j^2/2) g(-v,-w)dvdw \right. \\ &\quad \left. + iU_j \int_0^1 \int_0^1 vw \exp(A_{j-l}(v^2+w^2)U_j^2/2) (-v-w)g(-v,-w)dvdw \right. \\ &\quad \left. - U_j^2 \int_0^1 \int_0^1 vw \exp(A_{j-l}(v^2+w^2)U_j^2/2) vwg(-v,-w)dvdw \right) \end{aligned}$$

and

$$\begin{aligned} \mathcal{I}_v\mathcal{I}_{\bar{v}} &= U_j^2 \exp(-2C_{j-l}) \cdot \left(\int_0^1 \int_0^1 vw \exp(A_{j-l}(v^2+w^2)U_j^2/2) \cdot g(v,-w)dvdw \right. \\ &\quad \left. + iU_j \int_0^1 \int_0^1 vw \exp(A_{j-l}(v^2+w^2)U_j^2/2) \cdot (v-w)g(v,-w)dvdw \right. \\ &\quad \left. - U_j^2 \int_0^1 \int_0^1 vw \exp(A_{j-l}(v^2+w^2)U_j^2/2) \cdot -vwg(v,-w)dvdw \right). \end{aligned}$$

For evaluating these integrals further Lemma 3.3 below will be used.

Lemma 3.3 *Let $g_U(v,w)$ be a bounded function on the unit square $0 \leq |g_U(v,w)| \leq C$ for $(v,w) \in [0,1]^2$, let $h(x)$ be a function such that $h(x) \downarrow 0$ as $x \rightarrow \infty$, and let $f_U(v,w)$ be a positive function such that*

$$\lim_{U \rightarrow \infty} \int_0^1 \int_0^1 f_U(v,w)dvdw = 1 \quad \text{and} \quad \lim_{U \rightarrow \infty} \int_{1-h(U)}^1 \int_{1-h(U)}^1 f_U(v,w)dvdw = 1.$$

If the function $g_U(v,w)$ satisfies

$$\lim_{U \rightarrow \infty} \sup_{(v,w) \in [1-h(U),1]^2} |g_U(v,w) - g_U(1,1)| = 0,$$

then

$$\lim_{U \rightarrow \infty} \int_0^1 \int_0^1 f_U(v, w) g_U(v, w) dv dw = \lim_{U_j \rightarrow \infty} g_U(1, 1).$$

Remembering the solution of the Fourier transform $\mathcal{F}b_{j,k}(v)$ in expression (3.3), we can show that $\lim_{U_j \rightarrow \infty} g_{U_j}(v, w)$ is not necessarily finite.

For applying Lemma 3.3 a new function $\tilde{g}_{U_j}(v, w)$, defined by

$$\tilde{g}_{U_j}(v, w) := vw \exp(2iU_j B_{j-l}) \mathcal{F}b_{j,k}(U_j)^{-2} g_{U_j}(v, w),$$

will be used. With this new addition, $\lim_{U_j \rightarrow \infty} \tilde{g}_{U_j}(1, 1)$ exists and is finite. Hence, we need to check the conditions on \tilde{g}_{U_j} and we need to find functions f_{U_j} which converge to a Dirac delta function at $(1, 1)$. Rescaling the other factors in the integrals, such that these integrals are in the form of Lemma 3.3, gives

$$f_{U_j}(v, w) := A_{j-l}^2 U_j^4 \exp(-A_{j-l} U_j^2) vw \exp(A_{j-l}(v^2 + w^2) U_j^2 / 2) =: F(v) \cdot F(w).$$

The $h(x)$ function in Lemma 3.3 will be chosen as $h(x) = x^{-3/2}$, it is easy to see that $h(x) \downarrow 0$ as $x \rightarrow \infty$. Now the conditions of Lemma 3.3 will be checked on this particular $f_{U_j}(w, v)$ function

$$\begin{aligned} \lim_{U_j \rightarrow \infty} \int_{1-U_j^{-3/2}}^1 \int_{1-U_j^{-3/2}}^1 f_{U_j}(v, w) dv dw &= \lim_{U_j \rightarrow \infty} \left(\int_{1-U_j^{-3/2}}^1 F(v) dv \right)^2 = 1, \\ \lim_{U \rightarrow \infty} \int_0^1 \int_0^1 f_U(v, w) dv dw &= \lim_{U_j \rightarrow \infty} \left(\int_0^1 F(v) dv \right)^2 = 1, \end{aligned}$$

where it was used that for a certain function $b(v)$,

$$\begin{aligned} \int_{b(U_j)}^1 F(v) dv &= \exp(-A_{j-l} U_j^2 / 2) \int_{b(U_j)}^1 v A_{j-l} U_j^2 \exp(A_{j-l} v^2 U_j^2 / 2) dv \\ &= \exp(-A_{j-l} U_j^2 / 2) \cdot \left[\exp(A_{j-l} v^2 U_j^2 / 2) \right]_{b(U_j)}^1 \\ &= \exp(-A_{j-l} U_j^2 / 2) \cdot \left[\exp(A_{j-l} U_j^2 / 2) - \exp\left(A_{j-l} (b(U_j))^2 U_j^2 / 2\right) \right] \\ &= 1 - \exp(-A_{j-l} U_j^2 [1 - b(U_j)^2] / 2). \end{aligned}$$

The function f is thus satisfactory. What remains to check is the boundedness of \tilde{g}_U on the unit square and we need to check that

$$\lim_{U_j \rightarrow \infty} \sup_{(v,w) \in [1-U^{-3/2}, 1]^2} |\tilde{g}_{U_j}(v, w) - \tilde{g}_{U_j}(1, 1)| = 0.$$

First of all recall

$$\begin{aligned} \tilde{g}_U(v, w) &:= vw \exp(2iU_j B_{j-l}) \mathcal{F}b_{j,k}(U_j)^{-2} g(v, w) \\ &= vw \frac{\mathcal{F}b_{j-l,k}(vU_j) \mathcal{F}b_{j-l,k}(wU_j)}{\mathcal{F}b_{j-l,k}(U_j)^2} w_{\sigma_j}^1(v) w_{\sigma_j}^1(w) \frac{\exp(2iU_j B_{j-l})}{\exp(i(v+w)U_j B_{j-l})} e^{-D_{j-l}(vU_j) - D_{j-l}(wU_j)} \end{aligned}$$

The mild assumption is made that $U_j > c$ for a certain $c > 0$. For ease of notation let

$$\begin{aligned} \tilde{g}_1(v, w) &= vw, \quad \tilde{g}_2(v, w) = \frac{\mathcal{F}b_{j-l,k}(vU_j) \mathcal{F}b_{j-l,k}(wU_j)}{\mathcal{F}b_{j-l,k}(U_j)^2}, \quad \tilde{g}_3(v, w) = w_{\sigma_j}^1(v) w_{\sigma_j}^1(w) \\ \tilde{g}_4(v, w) &= \exp(i(2-v-w)U_j B_{j-l}), \quad \tilde{g}_5(v, w) = \exp(-D_{j-l}(vU_j) - D_{j-l}(wU_j)) \end{aligned}$$

Note that \tilde{g}_1, \tilde{g}_3 and \tilde{g}_4 are uniformly bounded on the unit square. Also, note that by the Riemann-Lebesgue lemma $\mathcal{F}\mu_j(x) \rightarrow 0$ when $x \rightarrow \infty$. Hence, $D_{j-l}(vU_j) =$

$\sum_{r=1}^{j-l} (T_r - T_{r-1}) \mathcal{F} \mu_r(vU_j)$ is a bounded function, which implies that \tilde{g}_5 is bounded uniformly. Proving boundedness of \tilde{g}_2 , recall expression (3.3), then

$$\tilde{g}_2(v, w) = \exp(i(v + w - 2)U_j x_{j,k} \Delta_{j-l}) \cdot \frac{\text{sinc}^2(vU_j \Delta_{j-l}/2) \text{sinc}^2(wU_j \Delta_{j-l}/2)}{\text{sinc}^2(U_j \Delta_{j-l}/2)} \quad (3.17)$$

where Δ_{j-l} was the grid size. Since $U_j \Delta_{j-l} \rightarrow 0$, a $c > 0$ can be found such that for all $U_j > c$ we have $\text{sinc}^2(U_j \Delta_{j-l}/2) \geq 1/2$, which leads to the bound

$$|\tilde{g}_2(v, w)| \leq \left| \frac{\text{sinc}^2(vU_j \Delta_{j-l}/2) \text{sinc}^2(wU_j \Delta_{j-l}/2)}{\text{sinc}^2(U_j \Delta_{j-l}/2)} \right| \leq \left| \frac{1}{\text{sinc}^2(U_j \Delta_{j-l}/2)} \right| \leq 2,$$

So, \tilde{g}_2 is bounded on the unit square. Putting everything together we can conclude that $\tilde{g}_{U_j}(v, w)$ is bounded on the unit square.

We note that $\tilde{g}_1 \cdot \tilde{g}_3$ is continuous on $[0, 1]^2$. Moreover, the second part of \tilde{g}_2 in expression (3.17) also behaves satisfactorily. Thus, these factors can be taken out of the equation. Note that, \tilde{g}_5 converges uniformly to 1 for $U_j \rightarrow \infty$ because of the smoothness of $\mu_j(x)$. The only problems thus occur in the first part of \tilde{g}_2 in expression (3.17) and in \tilde{g}_4 ,

$$\begin{aligned} \sup_{(v,w) \in [1-U_j^{-3/2}, 1]^2} |\tilde{g}_4(v, w) - 1| &= \left| \exp\left(i\left(2 - \left(1 - U_j^{-3/2}\right) - \left(1 - U_j^{-3/2}\right)\right)U_j B_{j-l}\right) - 1 \right| \\ &= \left| \exp\left(i \cdot U_j^{-1/2} B_{j-l}\right) - \exp(i \cdot 0) \right| \leq \left| U_j^{-1/2} B_{j-l} \right| \rightarrow 0. \end{aligned}$$

Similarly, the first part of \tilde{g}_2 can be controlled. This completes all the conditions of the function $\tilde{g}_{U_j}(v, w)$ in Lemma 3.3. To conclude, now we have found and checked the functions $f_{U_j}(v, w)$ and $\tilde{g}_{U_j}(v, w)$ in Lemma 3.3 and we can use these functions to solve the desired integrals.

From this Lemma, it appears that all the integrals in the final expressions for \mathcal{I}_v^2 , $\mathcal{I}_{\bar{v}}^2$ and $\mathcal{I}_v \mathcal{I}_{\bar{v}}$ converge equally fast to 0 and the dominating asymptotic term is the last one with the U_j^4 factor in front of it. Henceforth, the first two integrals will be left out of the equation. Reminding the extra term of $\tilde{g}_{U_j}(v, w)$ with respect to $g(v, w)$, then using Lemma 3.3 the limit is found to be

$$\begin{aligned} &\lim_{U_j \rightarrow \infty} \mathcal{I}_{\bar{v}}^2 A_{j-l}^2 \exp(-A_{j-l} U_j^2) \mathcal{F} b_{j,k}(U_j)^{-2} \exp(2iU_j B_{j-l}) \\ &= \lim_{U_j \rightarrow \infty} \exp(-2C_{j-l}) \int_0^1 \int_0^1 f_{U_j}(v, w) \tilde{g}_{U_j}(v, w) dv dw = \exp(-2C_{j-l}) \lim_{U_j \rightarrow \infty} \tilde{g}_{U_j}(1, 1) \\ &= \exp(-2C_{j-l}) w_{\sigma_j}^1(1)^2 \lim_{U_j \rightarrow \infty} \exp(-2D_{j-l}(U_j)) = \exp(-2C_{j-l}) w_{\sigma_j}^1(1)^2. \end{aligned} \quad (3.18)$$

In a similar manner, the other terms $\mathcal{I}_{\bar{v}}^2$ and $\mathcal{I}_v \mathcal{I}_{\bar{v}}$ their convergence can be deduced

$$\begin{aligned} &\lim_{U_j \rightarrow \infty} \mathcal{I}_{\bar{v}}^2 A_{j-l}^2 \exp(-A_{j-l} U_j^2) \overline{\mathcal{F} b_{j,k}(U_j)^{-2}} \exp(-2iU_j B_{j-l}) = \exp(-2C_{j-l}) w_{\sigma_j}^1(1)^2, \\ &\lim_{U_j \rightarrow \infty} \mathcal{I}_v \mathcal{I}_{\bar{v}} A_{j-l}^2 \exp(-A_{j-l} U_j^2) |\mathcal{F} b_{j,k}(U_j)|^{-2} = \exp(-2C_{j-l}) w_{\sigma_j}^1(1)^2. \end{aligned}$$

Recalling expression (3.16) for $s_{n,l}^2$, the asymptotic variance $s_{n,l}^2$ will be found by considering the following adapted limit

$$\begin{aligned} &\lim_{U_j \rightarrow \infty} \frac{s_{n,l}^2}{\Delta_{j-l} U_j^{-4} A_{j-1}^{-2} \exp(A_{j-1} U_j^2)} \\ &= \frac{1}{(T_j - T_{j-1})^2} \lim_{U_j \rightarrow \infty} \Delta_{j-l}^{-1} \sum_{k=1}^{m_{j-l}} \delta_{j-l,k}^2 A_{j-1}^2 e^{-A_{j-1} U_j^2} (\mathcal{I}_v^2 + 2\mathcal{I}_v \mathcal{I}_{\bar{v}} + \mathcal{I}_{\bar{v}}^2). \end{aligned} \quad (3.19)$$

An important remark to make is that when $U_j \rightarrow \infty$ the maximum distance between the grid points needs to go to zero $\Delta_{j-l} \rightarrow 0$, and thereby the number of observations needs to go infinity $m_{j-l} \rightarrow \infty$.

All the different limits for $\mathcal{I}_v^2, \mathcal{I}_v \mathcal{I}_{\bar{v}}$ and $\mathcal{I}_{\bar{v}}^2$ will be individually considered by replacing the summands by their respective asymptotic behavior. Note that this is not a trivial step and should be proven. The result is given in Lemma (3.4).

Lemma 3.4 *Under the assumptions of Proposition 3.2,*

$$\begin{aligned} \lim_{U_j \rightarrow \infty} \Delta_{j-l}^{-1} \sum_{k=1}^{m_{j-l}} \delta_{j-l,k}^2 A_{j-l}^2 e^{-A_{j-l} U_j^2} \mathcal{I}_v^2 \\ = \lim_{U_j \rightarrow \infty} \Delta_{j-l}^{-1} \sum_{k=1}^{m_{j-l}} \delta_{j-l,k}^2 e^{-2C_{j-l}} w_{\sigma_j}^1(1)^2 \mathcal{F} b_{j-l,k}(U_j)^2 e^{-2iB_{j-l} U_j} \end{aligned}$$

Recalling the Fourier transform $\mathcal{F} b_{j-l,k}(v)$ in (3.3), the underlying assumption that the magnitudes of the errors $\delta_{j-l,k}$ can be modeled by a function $\delta_{j-l} \in L^{2+\eta}(\mathbb{R})$ with $\eta > 0$, and the definition of the Riemann integral, then with Lemma 3.4 it follows that

$$\begin{aligned} \lim_{U_j \rightarrow \infty} \Delta_{j-l}^{-1} \sum_{k=1}^{m_{j-l}} \delta_{j-l,k}^2 A_{j-l}^2 e^{-A_{j-l} U_j^2} \mathcal{I}_v^2 \\ = e^{-2C_{j-l}} w_{\sigma_j}^1(1)^2 \lim_{U_j \rightarrow \infty} e^{-2iB_{j-l} U_j} \Delta_{j-l}^{-1} \sum_{k=1}^{m_{j-l}} \delta_{j-l,k}^2 \mathcal{F} b_{j-l,k}(U_j)^2 \\ = e^{-2C_{j-l}} w_{\sigma_j}^1(1)^2 \lim_{U_j \rightarrow \infty} e^{-2iB_{j-l} U_j} \text{sinc}^4(U_j \Delta_{j-l}/2) \sum_{k=1}^{m_{j-l}} \delta_{j-l,k}^2 e^{2iU_j x_{j-l,k}} \Delta_{j-l} \\ = e^{-2C_{j-l}} w_{\sigma_j}^1(1)^2 \lim_{U_j \rightarrow \infty} e^{-2iB_{j-l} U_j} \text{sinc}^4(U_j \Delta_{j-l}/2) \int_{-\infty}^{\infty} \delta_{j-l}(x)^2 e^{2iU_j x} dx \\ = e^{-2C_{j-l}} w_{\sigma_j}^1(1)^2 \lim_{U_j \rightarrow \infty} e^{-2iB_{j-l} U_j} \text{sinc}^4(U_j \Delta_{j-l}/2) \mathcal{F} \delta_{j-l}^2(2U_j). \end{aligned} \quad (3.20)$$

In a similar manner, the following asymptotics for the other terms $\mathcal{I}_{\bar{v}}^2$ and $\mathcal{I}_v \mathcal{I}_{\bar{v}}$ can be found

$$\begin{aligned} \lim_{U_j \rightarrow \infty} \Delta_{j-l}^{-1} \sum_{k=1}^{m_{j-l}} \delta_{j-l,k}^2 A_{j-l}^2 e^{-A_{j-l} U_j^2} \mathcal{I}_{\bar{v}}^2 \\ = e^{-2C_{j-l}} w_{\sigma_j}^1(1)^2 \lim_{U_j \rightarrow \infty} e^{2iB_{j-l} U_j} \Delta_{j-l}^{-1} \sum_{k=1}^{m_{j-l}} \delta_{j-l,k}^2 \mathcal{F} b_{j-l,k}(-U_j)^2 \\ = e^{-2C_{j-l}} w_{\sigma_j}^1(1)^2 \lim_{U_j \rightarrow \infty} e^{2iB_{j-l} U_j} \text{sinc}^4(-U_j \Delta_{j-l}/2) \mathcal{F} \delta_{j-l}^2(-2U_j) \end{aligned} \quad (3.21)$$

$$\begin{aligned} \lim_{U_j \rightarrow \infty} \Delta_{j-l}^{-1} \sum_{k=1}^{m_{j-l}} \delta_{j-l,k}^2 A_{j-l}^2 e^{-A_{j-l} U_j^2} \mathcal{I}_v \mathcal{I}_{\bar{v}} \\ = e^{-2C_{j-l}} w_{\sigma_j}^1(1)^2 \lim_{U_j \rightarrow \infty} \Delta_{j-l}^{-1} \sum_{k=1}^{m_{j-l}} \delta_{j-l,k}^2 |\mathcal{F} b_{j-l,k}(U_j)|^2 \\ = e^{-2C_{j-l}} w_{\sigma_j}^1(1)^2 \lim_{U_j \rightarrow \infty} \text{sinc}^4(U_j \Delta_{j-l}/2) \int_{-\infty}^{\infty} \delta_{j-l}(x)^2 dx \\ = e^{-2C_{j-l}} w_{\sigma_j}^1(1)^2 \lim_{U_j \rightarrow \infty} \text{sinc}^4(U_j \Delta_{j-l}/2) \|\delta_{j-l}\|_{L^2(\mathbb{R})}^2. \end{aligned} \quad (3.22)$$

We have assumed that δ_{j-l} is an $L^2(\mathbb{R})$ integrable function, therefore $\mathcal{F} \delta_{j-l}^2(2U_j) \rightarrow 0$. Moreover, $U_j \Delta_{j-l} \rightarrow 0$, thus $\text{sinc}^4(U_j \Delta_{j-l}) \rightarrow 1$ as $U_j \rightarrow \infty$. So, we can conclude that expressions (3.20) and (3.21) are equal to 0 in the limit. Furthermore, expression (3.22)

becomes

$$\begin{aligned} \lim_{U_j \rightarrow \infty} \Delta_{j-l}^{-1} \sum_{k=1}^{m_{j-l}} \delta_{j-l,k}^2 A_{j-l}^2 e^{-A_{j-l} U_j^2} \mathcal{I}_v \mathcal{I}_{\bar{v}} \\ = e^{-2C_{j-l}} w_{\sigma_j}^1(1)^2 \lim_{U_j \rightarrow \infty} \operatorname{sinc}^4(U_j \Delta_{j-l}/2) \|\delta_{j-l}\|_{L^2(\mathbb{R})}^2. \end{aligned}$$

Using expression (3.19) the asymptotic variance $s_{n,l}^2$ is then found to be

$$\begin{aligned} s_{n,l}^2 &= \Delta_{j-l} U_j^{-4} A_{j-l}^{-2} e^{A_{j-l} U_j^2} \cdot \frac{1}{4} \left(0 + 2 \cdot 4 (T_j - T_{j-1})^{-2} e^{-2C_{j-l}} w_{\sigma_j}^1(1)^2 \|\delta_{j-l}\|_{L^2}^2 + 0 \right) \\ &= 2 \|\delta_{j-l}\|_{L^2}^2 (T_j - T_{j-1})^{-2} A_{j-l}^{-2} \exp(-2C_{j-l}) w_{\sigma_j}^1(1)^2 \cdot \Delta_{j-l} U_j^{-4} e^{A_{j-l} U_j^2} \\ &= w_{\sigma_j}^1(1)^2 d_{j,j-l} \Delta_{j-l} U_j^{-4} e^{A_{j-l} U_j^2} \end{aligned}$$

where we defined the constant

$$d_{j,j-l} := 2 \|\delta_{j-l}\|_{L^2}^2 (T_j - T_{j-1})^{-2} A_{j-l}^{-2} e^{-2C_{j-l}}.$$

□

Now the asymptotic variance $s_{n,l}^2$ in the Lyapunov condition is found. Next to that, an expression or bound for $\mathbb{E}|X_r|^{2+\eta}$ is needed. Note that $(\varepsilon_{j,k})$ were sub-Gaussian random variables. The moment condition for sub-Gaussian random variables states that for some $K > 0$:

$$\mathbb{E}[\varepsilon_{j,k}^{2+\eta}] \leq K^{2+\eta} (2+\eta)^{(2+\eta)/2}.$$

Using the moment condition, the following bound is found

$$\begin{aligned} \mathbb{E}|X_k|^{2+\eta} &= \mathbb{E} \left\{ \left| \frac{2U_j^{-2}}{T_j - T_{j-1}} \delta_{j-l,k} \varepsilon_{j-l,k} \operatorname{Re} \left(\int_0^1 \frac{ivU_j (1+ivU_j) \mathcal{F}b_{j-l,k}(vU_j) w_{\sigma_j}^1(v) dv}{\varphi_{T_{j-l}}(v-i)} \right) \right|^{2+\eta} \right\} \\ &\lesssim U_j^{-2(2+\eta)} |\delta_{j-l,k}|^{2+\eta} \left| \operatorname{Re} \left(\int_0^1 \frac{ivU_j (1+ivU_j) \mathcal{F}b_{j-l,k}(vU_j) w_{\sigma_j}^1(v)}{\exp(-v^2 U_j^2 A_{j-l}/2 + ivU_j B_{j-l} + C_{j-l} + D_{j-l}(vU_j))} dv \right) \right|^{2+\eta} \\ &\leq U_j^{-2(2+\eta)} |\delta_{j-l,k}|^{2+\eta} \left| \int_0^1 \frac{ivU_j (1+ivU_j) \mathcal{F}b_{j-l,k}(vU_j) w_{\sigma_j}^1(v)}{\exp(-v^2 U_j^2 A_{j-l}/2 + ivU_j B_{j-l} + C_{j-l} + D_{j-l}(vU_j))} dv \right|^{2+\eta}. \end{aligned}$$

Note that the integral looks similar to \mathcal{I}_v in the proof of Proposition 3.2. In avoidance of repeating arguments, the integral behaved in the limit as

$$\lim_{U_j \rightarrow \infty} |\mathcal{I}_v| \cdot A_{j-l} e^{-A_{j-l} U_j^2/2} |\mathcal{F}b_{j-l,k}(U_j)|^{-1} = e^{-C_{j-l}} w_{\sigma_j}^1(1).$$

Now using expression (3.3), it can be found that the limit behaves asymptotically as

$$\begin{aligned} |\mathcal{I}_v| &\lesssim A_{j-l}^{-1} e^{A_{j-l} U_j^2/2} |\mathcal{F}b_{j-l,k}(U_j)| e^{-C_{j-l}} w_{\sigma_j}^1(1) \\ &= A_{j-l}^{-1} e^{A_{j-l} U_j^2/2} \Delta_{j-l} \operatorname{sinc}^2(U_j \Delta_{j-l}/2) e^{-C_{j-l}} w_{\sigma_j}^1(1). \end{aligned}$$

Then the following bound is found

$$\mathbb{E}|X_k|^{2+\eta} \lesssim U_j^{-2\eta} |\delta_{j-l,k}|^{2+\eta} e^{A_{j-l} U_j^2 \cdot \eta/2} \Delta_{j-l}^{2+\eta}. \quad (3.23)$$

With the expression for s_n^2 in Proposition 3.2 and the bound in expression (3.23), the Lyapunov condition can be verified

$$\begin{aligned}
& \lim_{n \rightarrow \infty} s_{n,l}^{-(2+\eta)} \sum_{k=1}^{m_{j-l}} \mathbb{E} \left\{ |X_k|^{2+\eta} \right\} \\
& \lesssim \lim_{m_{j-l} \rightarrow \infty} U_j^{2(2+\eta)} \Delta_{j-l}^{-(2+\eta)/2} e^{-A_{j-l} U_j^2 (2+\eta)/2} \sum_{k=1}^{m_{j-l}} U_j^{-2(2+\eta)} |\delta_{j-l,k}|^{2+\eta} e^{A_{j-l} U_j^2 (2+\eta)/2} \Delta_{j-l}^{2+\eta} \\
& = \lim_{m_{j-l} \rightarrow \infty} \Delta_{j-l}^{(2+\eta)/2-1} \sum_{k=1}^{m_{j-l}} |\delta_{j-l,k}|^{2+\eta} \Delta_{j-l} = \lim_{m_{j-l} \rightarrow \infty} \Delta_{j-l}^{(2+\eta)/2-1} \int_{-\infty}^{\infty} |\delta_{j-l}(x)|^{2+\eta} dx \\
& = \|\delta_{j-l}\|_{L^{2+\eta}} \lim_{m_{j-l} \rightarrow \infty} \Delta_{j-l}^{(2+\eta)/2-1} = 0
\end{aligned}$$

where in the last step, it is used that $\eta > 0$, $\delta_{j-l} \in L^{2+\eta}$ and δ_{j-l} Riemann integrable.

Hence, Theorem 3.1 implies that

$$\frac{\mathcal{L}_{\sigma_j^2}^l}{s_{n,l}} = \frac{T_m}{s_{n,l}} \xrightarrow{d} \mathcal{N}(0, 1), \quad \text{for } l = 0, 1.$$

Now, let us look at the terms $\mathcal{L}_{\gamma_j}^l$ and $\mathcal{L}_{\lambda_j}^l$, as given in the error decompositions (3.10) and (3.11), by pointing out the differences and arguing how this does affect the derivation. For $\mathcal{L}_{\gamma_j}^l$ three main differences in the derivation occur:

1. $w_{\gamma_j}^{U_j} = \frac{1}{U_j^2} w_{\gamma_j}^1$ instead of $w_{\sigma_j}^{U_j} = \frac{1}{U_j^3} w_{\sigma_j}^1$,
2. $w_{\gamma_j}^1$ is antisymmetric instead of $w_{\sigma_j}^{U_j}$ which was symmetric, and
3. we have $\text{Im}(\tilde{\psi}_j(v))$ instead of $\text{Re}(\psi_j(v))$.

Point (i) does not change the essence of the proof but does affect the convergence rate, which is now a factor U_j slower. Point (ii) will mostly give a minus sign instead of a plus sign in the simplification of the integral at (3.15), this minus sign is, however, canceled because we also have the Im of point (iii) and a conjugation in the second integral. For finding the expression (3.19) we used the identity $\text{Re}^2(z) = ((z + \bar{z})/2)^2 = (z^2 + 2\bar{z}z + \bar{z}^2)/4$. From point (iii), Re is replaced by Im , we should now use the identity $\text{Im}^2(z) = ((z - \bar{z})/2i)^2 = -(z^2 - 2\bar{z}z + \bar{z}^2)/4$. This does not affect the result, because in the proof we showed that the factor $z\bar{z}$ is the factor that defined the asymptotics, and this factor is the same in Re^2 and Im^2 .

The term $\mathcal{L}_{\lambda_j}^l$ is less complicated, here only one main difference occurs $w_{\lambda_j}^{U_j} = \frac{1}{U_j} w_{\lambda_j}^1$ instead of $w_{\sigma_j}^{U_j} = \frac{1}{U_j^3} w_{\sigma_j}^1$, which only affects the convergence to be U_j^2 slower.

To summarize this section, the results will be presented in Proposition 3.3.

Proposition 3.3 *Let $\varepsilon_{j-l,k}$ be independent centered sub-Gaussian random variables with $\mathbb{V}[\varepsilon_{j-l,k}] = 1$ for all $k = 1, \dots, m_{j-l}$, $l = 0, 1$ and let $\delta_{j-l} \in L^{2+\eta}$ for $\eta > 0$, $l = 0, 1$. Furthermore, let the Levy triplets $(\sigma_j, \gamma_j, \lambda_j)$ belong to $\mathcal{G}_{s_j}^n$ and the weight function $(w_{\sigma_j}^1, w_{\gamma_j}^1, w_{\lambda_j}^1)$ belong to $\mathcal{W}_{s_j}^n$. As U_j tends to infinity, then for $l = 0, 1$ we have the asymptotic normality*

$$\frac{\mathcal{L}_{\sigma_j^2}^l}{s_{n,l}} \xrightarrow{d} \mathcal{N}(0, 1), \quad \frac{\mathcal{L}_{\gamma_j}^l}{U_j s_{n,l}} \xrightarrow{d} \mathcal{N}(0, 1) \quad \text{and} \quad \frac{\mathcal{L}_{\lambda_j}^l}{U_j^2 s_{n,l}} \xrightarrow{d} \mathcal{N}(0, 1),$$

with

$$s_{n,l}^2 = w_{\sigma_j}^1(1)^2 d_{j,j-l} \Delta_{j-l} U_j^{-4} e^{A_{j-l} U_j^2},$$

where we defined the constant

$$d_{j,j-l} := 2 \|\delta_{j-l}\|_{L^2}^2 (T_j - T_{j-1})^{-2} A_{j-l}^{-2} e^{-2C_{j-l}},$$

and the terms A_{j-l} and C_{j-l} are as in expression (3.14).

3.3.3 Bias Term \mathcal{B}_{ξ_j}

In this section we will bound the bias terms \mathcal{B}_{ξ_j} for $\xi_j \in \{\sigma_j^2, \gamma_j, \lambda_j\}$ from above. Again we first derive it for $\mathcal{B}_{\sigma_j^2}$, and then investigate where \mathcal{B}_{γ_j} and \mathcal{B}_{λ_j} differ, and show how this affects the results.

In the derivation, a couple of results about Fourier transforms are needed, which are stated in Remark 3.1 below.

Remark 3.1 1. The definition of the Fourier transform can be extended from $L^1(\mathbb{R})$ to $L^1(\mathbb{R}) \cup L^2(\mathbb{R})$ and the **Plancherel identity** states that for all $f, g \in L^2(\mathbb{R})$

$$\int_{\mathbb{R}} f(x)\overline{g(x)}dx = \frac{1}{2\pi} \int_{\mathbb{R}} \mathcal{F}f(v)\overline{\mathcal{F}g(v)}dv.$$

2. Let $f \in L^2(\mathbb{R})$ be such that for all $k \in \{0, 1, \dots, s\}$ the (weak) derivative $f^{(k)}$ satisfies $f^{(k)} \in L^2(\mathbb{R})$. Then for all $k \in \{1, \dots, s\}$

$$\mathcal{F}[f^{(k)}](v) = (iv)^k \mathcal{F}f(v).$$

3. For $U > 0$ we have

$$\mathcal{F}f(v) = U \mathcal{F}[f(U\cdot)](Uv) \quad \text{and} \quad \mathcal{F}^{-1}f(v) = U \mathcal{F}^{-1}[f(U\cdot)](Uv)$$

Assume that $(\sigma_j^2, \gamma_j, \lambda_j) \in \mathcal{G}_{s_j}^n(R, \sigma_{\max})$ and $(w_{\sigma_j}, w_{\gamma_j}, w_{\lambda_j}) \in \mathcal{W}_{s_j}^n$ as given in Definitions 3.1 and 3.2. From these assumptions we have that for an integer $s_j > 0$ it holds that $w_{\sigma_j}^1(v)/v^{s_j} \in L^2(\mathbb{R})$, $w_{\sigma_j}^1(v)/v^{s_j} \in L^1(\mathbb{R})$ and for some $R > 0$ we have $\max_{k=0, \dots, s} \|\mu_j^{(k)}\|_{L^2(\mathbb{R})} \leq R$ and $\|\mu_j^{(s_j)}\|_{\infty} \leq R$. Firstly, using the triangle inequality (normal and for integrals), $\overline{w_{\sigma_j}^{U_j}} = w_{\sigma_j}^{U_j}$, and Remark 4.1, the dependency of $\mu_j(x)$ can be abstracted

$$\begin{aligned} |\mathcal{B}_{\sigma_j^2}| &= \left| \int_{-U_j}^{U_j} \operatorname{Re}(\mathcal{F}\mu_j(v)) w_{\sigma_j}^{U_j} dv \right| \leq \left| \int_{-U_j}^{U_j} \mathcal{F}\mu_j(v) w_{\sigma_j}^{U_j}(v) dv \right| = \left| \int_{-\infty}^{\infty} \mathcal{F}\mu_j(v) w_{\sigma_j}^{U_j}(v) dv \right| \\ &\stackrel{(ii)}{=} \left| \int_{-\infty}^{\infty} \mathcal{F}\mu_j^{(s_j)}(v) \frac{w_{\sigma_j}^{U_j}(v)}{(iv)^{s_j}} dv \right| = \left| \int_{-\infty}^{\infty} \mathcal{F}\mu_j^{(s_j)}(v) \overline{\left(\frac{w_{\sigma_j}^{U_j}(v)}{(-iv)^{s_j}} \right)} dv \right| \\ &\stackrel{(i)}{=} 2\pi \left| \int_{-\infty}^{\infty} \mu_j^{(s_j)}(x) \mathcal{F}^{-1} \left(\frac{w_{\sigma_j}^{U_j}(v)}{(-iv)^{s_j}} \right) (x) dx \right| \leq 2\pi \int_{-\infty}^{\infty} |\mu_j^{(s_j)}(x)| \left| \mathcal{F}^{-1} \left(\frac{w_{\sigma_j}^{U_j}(v)}{(-iv)^{s_j}} \right) (x) \right| dx \\ &\leq \|\mu_j^{(s_j)}(x)\|_{\infty} 2\pi \int_{-\infty}^{\infty} \left| \mathcal{F}^{-1} \left(\frac{w_{\sigma_j}^{U_j}(v)}{(-iv)^{s_j}} \right) (x) \right| dx. \end{aligned}$$

The properties of the weight function $w_{\sigma_j}^{U_j}(v)$ can now be used to see the dependency of the resulting integral to the cut-off U_j and the weight function $w_{\sigma_j}^1(v)$,

$$\begin{aligned} 2\pi \int_{-\infty}^{\infty} \left| \mathcal{F}^{-1} \left(\frac{w_{\sigma_j}^{U_j}(v)}{(-iv)^{s_j}} \right) (x) \right| dx &= 2\pi \int_{-\infty}^{\infty} \left| \frac{1}{2\pi} \int_{-\infty}^{\infty} \frac{w_{\sigma_j}^{U_j}(v)}{(-iv)^{s_j}} e^{-ivx} dv \right| dx \\ &= \int_{-\infty}^{\infty} \left| \int_{-\infty}^{\infty} \frac{w_{\sigma_j}^{U_j}(v)}{(iv)^{s_j}} e^{ivx} dv \right| dx = \int_{-\infty}^{\infty} \left| \int_{-\infty}^{\infty} \frac{U_j^{-3} w_{\sigma_j}^1(v/U_j)}{(iv)^{s_j}} e^{ivx} dv \right| dx \\ &\stackrel{u=v/U_j}{=} U_j^{-2} \int_{-\infty}^{\infty} \left| \int_{-\infty}^{\infty} \frac{w_{\sigma_j}^1(u)}{(iuU_j)^{s_j}} e^{iuU_jx} du \right| dx = U_j^{-(2+s_j)} \int_{-\infty}^{\infty} \left| \int_{-\infty}^{\infty} \frac{w_{\sigma_j}^1(u)}{u^{s_j}} e^{iuU_jx} du \right| dx \\ &\stackrel{y=xU_j}{=} U_j^{-(2+s_j)} \int_{-\infty}^{\infty} \left| \int_{-\infty}^{\infty} \frac{w_{\sigma_j}^1(u)}{u^{s_j}} e^{iuy} du \right| U_j^{-1} dy = U_j^{-(3+s_j)} \int_{-\infty}^{\infty} \left| \mathcal{F} \left(\frac{w_{\sigma_j}^1(u)}{u^{s_j}} \right) (y) \right| dy \end{aligned}$$

$$= U_j^{-(3+s_j)} \left\| \mathcal{F} \left(\frac{w_{\sigma_j}^1(u)}{u^{s_j}} \right) \right\|_{L^1},$$

where this last norm exists by the assumptions of the class $\mathcal{W}_{s_j}^n$. Hence, it follows that

$$|\mathcal{B}_{\sigma_j^2}| \leq U_j^{-(s_j+3)} \|\mu^{(s_j)}\|_{\infty} \|\mathcal{F}(w_{\sigma_j}^1(v)/v^{s_j})\|_{L^1(\mathbb{R})},$$

or, with $\|\mu^{(s_j)}\|_{\infty} < R$ and $\|\mathcal{F}(w_{\sigma_j}^1(v)/v^{s_j})\|_{L^1(\mathbb{R})} < \infty$,

$$|\mathcal{B}_{\sigma_j^2}| \lesssim U_j^{-(s_j+3)}.$$

The main differences between the term \mathcal{B}_{γ_j} as in the error decomposition (3.10) and $\mathcal{B}_{\sigma_j^2}$ are that we have $\text{Im}(\mathcal{F}\mu_j(v))$ instead of $\text{Re}(\mathcal{F}\mu_j(v))$, the weight functions $w_{\gamma_j}^{U_j}$ is antisymmetric instead of $w_{\sigma_j}^{U_j}$ which was symmetric, and $w_{\gamma_j}^{U_j}(v) = U_j^{-2}w_{\gamma_j}^{U_j}(v)$ instead of $w_{\sigma_j}^{U_j}(v) = U_j^{-3}w_{\sigma_j}^{U_j}(v)$. Note that it was used that $|\text{Re}(\mathcal{F}\mu_j(v))| \leq |\mathcal{F}\mu_j(v)|$, and that this will just be replaced with $|\text{Im}(\mathcal{F}\mu_j(v))| \leq |\mathcal{F}\mu_j(v)|$, so the first point does not matter. The second point was never used in the derivation, so this does also not matter. The third point is the only difference that matters in the derivation, the result is that the upper bound is a factor U_j smaller.

For \mathcal{B}_{λ_j} as in (3.11) the only difference is $w_{\lambda_j}^{U_j}(v) = U_j^{-1}w_{\lambda_j}^{U_j}(v)$ instead of $w_{\sigma_j}^{U_j}(v) = U_j^{-3}w_{\sigma_j}^{U_j}(v)$, so the upper bound will be a factor U_j^2 smaller.

All the assumptions and results are summarized in Proposition 3.4

Proposition 3.4 *Suppose the Lévy triplets belong to $\mathcal{G}_{s_j}^n(R, \sigma_{\max})$ and the weight functions belong to $\mathcal{W}_{s_j}^n$, then*

$$\begin{aligned} |\mathcal{B}_{\sigma_j^2}| &\leq U_j^{-(s_j+3)} \|\mu_j^{(s_j)}\|_{\infty} \|\mathcal{F}(w_{\sigma_j}(v)/v^{s_j})\|_{L^1}, \\ |\mathcal{B}_{\gamma_j}| &\leq U_j^{-(s_j+2)} \|\mu_j^{(s_j)}\|_{\infty} \|\mathcal{F}(w_{\sigma_j}(v)/v^{s_j})\|_{L^1}, \\ |\mathcal{B}_{\lambda_j}| &\leq U_j^{-(s_j+1)} \|\mu_j^{(s_j)}\|_{\infty} \|\mathcal{F}(w_{\sigma_j}(v)/v^{s_j})\|_{L^1}, \end{aligned}$$

such that, using the definitions of the classes $\mathcal{G}_{s_j}^n(R, \sigma_{\max})$ and $\mathcal{W}_{s_j}^n$,

$$|\mathcal{B}_{\sigma_j^2}| \lesssim U_j^{-(s_j+3)}, \quad |\mathcal{B}_{\gamma_j}| \lesssim U_j^{-(s_j+2)}, \quad \text{and} \quad |\mathcal{B}_{\lambda_j}| \lesssim U_j^{-(s_j+1)}.$$

3.3.4 Remainder Terms $\mathcal{R}_{\xi_j}^l$

In this section, we want to investigate if and under which conditions the asymptotic remainder term will be asymptotically negligible. We first investigate $\mathcal{R}_{\sigma_j^2}^l$, and thereafter look at the differences of $\mathcal{R}_{\gamma_j}^l$ and $\mathcal{R}_{\lambda_j}^l$ with the derivation of $\mathcal{R}_{\sigma_j^2}^l$.

Before we begin, recall that we did define

$$\mathcal{R}_j^l(v) = \tilde{\psi}_j^l(v) - \psi_j^l(v) - \mathcal{L}_j^l(v) \quad \text{and} \quad \mathcal{R}_{\sigma_j^2}^l = \int_{-U_j}^{U_j} \text{Re}(\mathcal{R}_j^l(v)) w_{\sigma_j}^{U_j}(v) dv.$$

Note that $\mathcal{R}_{\sigma_j^2}^l$ is a random variable with $\mathbb{E}[\mathcal{R}_{\sigma_j^2}^l] = 0$, because it is connected to the error terms $(\varepsilon_{j,k})$ without a bias term.

The idea is going to be that we are going to look at certain conditions such that asymptotically when $U_j \rightarrow \infty$ and $\Delta_j \rightarrow 0$ we have

$$\mathcal{R}_{\sigma_j^2}^l f_{\sigma_j^2}(U_j, \Delta_j) \xrightarrow{\mathbb{P}} 0,$$

where the function $f_{\sigma_j^2}(U_j, \Delta_j)$ is given by

$$f_{\sigma_j^2}(U_j, \Delta_j) = \frac{U_j^2 e^{-U_j^2 \sum_{i=1}^j (T_i - T_{i-1}) \sigma_i^2 / 2}}{\sqrt{d_{j,j} \Delta_j + d_{j,j-1} \Delta_{j-1} e^{-U_j^2 (T_j - T_{j-1}) \sigma_j^2}}}.$$

Note that $f_{\sigma_j^2}(U_j, \Delta_j)$ is a positive deterministic function and \mathbb{P} stands for convergence in probability.

This function $f_{\sigma_j^2}(U_j, \Delta_j)$ may feel arbitrary now, but it will be shown that this function is coupled to the asymptotic standard deviation s_n of $\tilde{\sigma}_j^2$ by $f_{\sigma_j^2}(U_j, \Delta_j) = \frac{|w_{\sigma_j^2}^1(1)|}{s_n}$. We actually want $\frac{\mathcal{R}_{\sigma_j^2}^l}{s_n}$ to become 0, because then we can conclude that $\frac{\tilde{\sigma}_j^2 - \sigma_j^2}{s_n^2} \xrightarrow{d} \mathcal{N}(0, 1)$. This will be elucidated in the next section.

Markov's inequality will be used with the convex function x^2 to bound the convergence in probability, i.e., let $\varepsilon > 0$ then

$$\mathbb{P}\left(\left|\mathcal{R}_{\sigma_j^2}^l f_{\sigma_j^2}(U_j, \Delta_j)\right| > \varepsilon\right) \leq \frac{1}{\varepsilon^2} \mathbb{E}\left[\left|\mathcal{R}_{\sigma_j^2}^l f_{\sigma_j^2}(U_j, \Delta_j)\right|^2\right] = \frac{\left|f_{\sigma_j^2}(U_j, \Delta_j)\right|^2}{\varepsilon^2} \mathbb{E}\left[\left|\mathcal{R}_{\sigma_j^2}^l\right|^2\right].$$

So we want to find a bound for $\mathbb{E}\left[\left|\mathcal{R}_{\sigma_j^2}^l\right|^2\right]$, this will be a tedious task in the next two pages.

Bounding $\mathbb{E}\left[\left|\mathcal{R}_{\sigma_j^2}^l\right|^2\right]$

It is advised to first find a bound for the term $|\mathcal{R}_j^l(v)|$. In the persuasion of this, first remember the definition

$$\tilde{\psi}_j^l(v) := \frac{1}{T_j - T_{j-1}} \log_{\geq \kappa(v, T_{j-1})}(\tilde{\varphi}_{T_{j-1}}(v - i)).$$

Using that $\tilde{\psi}_j^l(v) = e^{\log \tilde{\psi}_j^l(v)}$ and the triangle inequality, we can write the remainder term as a second order Taylor expansion of the logarithm

$$\begin{aligned} (T_j - T_{j-1}) |\mathcal{R}_j^l(v)| &= \left| (T_j - T_{j-1}) \tilde{\psi}_j^l(v) - (T_j - T_{j-1}) \psi_j^l(v) - (T_j - T_{j-1}) \mathcal{L}_j^l(v) \right| \\ &= \left| \log e^{(T_j - T_{j-1}) \tilde{\psi}_j^l(v)} - \log e^{(T_j - T_{j-1}) \psi_j^l(v)} - \frac{\tilde{\varphi}_{T_{j-1}}(v - i) - \varphi_{T_{j-1}}(v - i)}{\varphi_{T_{j-1}}(v - i)} \right| \\ &\leq \left| \log e^{(T_j - T_{j-1}) \tilde{\psi}_j^l(v)} - \log e^{(T_j - T_{j-1}) \psi_j^l(v)} - \frac{e^{(T_j - T_{j-1}) \tilde{\psi}_j^l(v)} - \varphi_{T_{j-1}}(v - i)}{\varphi_{T_{j-1}}(v - i)} \right| \\ &\quad + \left| \frac{\tilde{\varphi}_{T_{j-1}}(v - i) - e^{(T_j - T_{j-1}) \tilde{\psi}_j^l(v)}}{\varphi_{T_{j-1}}(v - i)} \right| \\ &= \left| \log e^{(T_j - T_{j-1}) \tilde{\psi}_j^l(v)} - \log e^{(T_j - T_{j-1}) \psi_j^l(v)} - \frac{e^{(T_j - T_{j-1}) \tilde{\psi}_j^l(v)} - e^{(T_j - T_{j-1}) \psi_j^l(v)}}{e^{(T_j - T_{j-1}) \psi_j^l(v)}} \right| \\ &\quad + \left| \varphi_{T_{j-1}}(v - i)^{-1} (\tilde{\varphi}_{T_{j-1}}(v - i) - e^{(T_j - T_{j-1}) \tilde{\psi}_j^l(v)}) \right|. \end{aligned}$$

Recall that in expression (3.6) it was found that

$$|\varphi_{T_{j-l}}(v - i)| \geq \prod_{r=1}^{j-l} 2K(T_r - T_{r-1}, \sigma_r, R, v) =: 2K_{j-l}(v)$$

where $K_{j-l}(v)$ is defined for ease of notation later on. A consequence of Proposition 3.1 with this notation is that asymptotically with probability one we have $|\tilde{\varphi}_{T_{j-l}}(v - i) - \varphi_{T_{j-l}}(v - i)| \leq$

$K_{j-l}(v)$. From this, it can be derived that

$$\lim_{U_j \rightarrow \infty} \mathbb{P} \left(|\tilde{\varphi}_{T_{j-l}}(v-i)| \geq K_{j-l}(v) \right) = 1, \quad (3.24)$$

which implies with the definition of the trimmed complex logarithm that,

$$\lim_{U_j \rightarrow \infty} \mathbb{P} \left(e^{(T_j - T_{j-1})\tilde{\psi}_j^l(v)} = \tilde{\varphi}_{T_{j-l}}(v-i) \right) = 1. \quad (3.25)$$

Therefore, the second term in $(T_j - T_{j-1}) |\mathcal{R}_j^l(v)|$,

$$\left| \varphi_{T_{j-l}}(v-i)^{-1} (\tilde{\varphi}_{T_{j-l}}(v-i) - e^{(T_j - T_{j-1})\tilde{\psi}_j^l(v)}) \right|,$$

is asymptotically zero. The first term of $(T_j - T_{j-1}) |\mathcal{R}_j^l(v)|$ will be bounded with Lemma 3.5.

Lemma 3.5 *Let $z \in \mathbb{C}$. If $|\tilde{z}| > C$, $|z| > 2C$, and $|\arg(z) - \arg(\tilde{z})| \leq \pi$, then*

$$\left| \log(\tilde{z}) - \log(z) - \frac{\tilde{z} - z}{z} \right| \leq \frac{|\tilde{z} - z|^2}{2C^2}$$

From (3.31) we already know that $|\varphi_{T_j}(v-i)| = |e^{(T_j - T_{j-1})\psi_j^l(v)}| \geq 2K_j(v)$. From expressions (3.25) and (3.24) it then follows for the estimator that with probability tending to one

$$\left| \exp \left((T_j - T_{j-1}) \tilde{\psi}_j^l(v) \right) \right| = |\tilde{\varphi}_{T_{j-l}}(v-i)| \geq K_{j-l}(v).$$

Furthermore, in expression (3.7) it was also shown that with probability tending to one,

$$\left| \arg \varphi_{T_{j-l}}(v-i) - \arg \tilde{\varphi}_{T_{j-l}}(v-i) \right| \leq \pi.$$

Hence, we can apply Lemma 3.5 with probability tending to one to bound the first term and find the result

$$\begin{aligned} & \left| \log e^{(T_j - T_{j-1})\tilde{\psi}_j^l(v)} - \log e^{(T_j - T_{j-1})\psi_j^l(v)} - e^{-(T_j - T_{j-1})\psi_j^l(v)} \left(e^{(T_j - T_{j-1})\tilde{\psi}_j^l(v)} - e^{(T_j - T_{j-1})\psi_j^l(v)} \right) \right| \\ & \leq \frac{1}{2} K_{j-l}(v)^{-2} \left| e^{(T_j - T_{j-1})\tilde{\psi}_j^l(v)} - e^{(T_j - T_{j-1})\psi_j^l(v)} \right|^2 \\ & = \frac{1}{2} K_{j-l}(v)^{-2} (v^4 + v^2) \left| \mathcal{F}(\tilde{\mathcal{O}}_{j-l} - \mathcal{O}_{j-l})(v) \right|^2. \end{aligned}$$

To summarize, the following important bound with probability tending to one is found

$$\begin{aligned} |\mathcal{R}_j^l| & \leq \frac{1}{2} (T_j - T_{j-1})^{-1} K_{j-l}(v)^{-2} (v^4 + v^2) \left| \mathcal{F}(\tilde{\mathcal{O}}_{j-l} - \mathcal{O}_{j-l})(v) \right|^2 \\ & \lesssim K_{j-l}(v)^{-2} (v^4 + v^2) \left| \mathcal{F}(\tilde{\mathcal{O}}_{j-l} - \mathcal{O}_{j-l})(v) \right|^2. \end{aligned} \quad (3.26)$$

The original problem was to find an estimate of the upper bound of the quadratic remainder term $|\mathcal{R}_{\sigma_j^2}^l|^2$. Using the normal and integral triangle inequality, we first find

$$\begin{aligned} \mathbb{E} \left[|\mathcal{R}_{\sigma_j^2}^l|^2 \right] & = \mathbb{E} \left[\left| \int_{-U_j}^{U_j} \operatorname{Re}(\mathcal{R}_j^l(v)) w_{\sigma_j}^{U_j}(v) dv \right|^2 \right] \\ & \leq \mathbb{E} \left[\left| \int_{-U_j}^{U_j} \mathcal{R}_j^l(v) w_{\sigma_j}^{U_j}(v) dv \right|^2 \right] \leq \mathbb{E} \left[\left(\int_{-U_j}^{U_j} |\mathcal{R}_j^l(v)| |w_{\sigma_j}^{U_j}(v)| dv \right)^2 \right]. \end{aligned}$$

Note that for $|\mathcal{R}_j^l(v)|$ the upper bound of (3.26) can be used and that the quadratic integral can be extended,

$$\begin{aligned}
\mathbb{E} \left[|\mathcal{R}_{\sigma_j^l}^l|^2 \right] &\lesssim \mathbb{E} \left[\left(\int_{-U_j}^{U_j} (v^4 + v^2) \left| \mathcal{F}(\tilde{\mathcal{O}}_{j-l} - \mathcal{O}_{j-l})(v) \right|^2 \frac{|w_{\sigma_j^l}^{U_j}(v)|}{K_{j-l}(v)^2} dv \right)^2 \right] \\
&\lesssim \mathbb{E} \left[\int_{-U_j}^{U_j} \int_{-U_j}^{U_j} (v^4 + v^2)(w^4 + w^2) \left| \mathcal{F}(\tilde{\mathcal{O}}_{j-l} - \mathcal{O}_{j-l})(v) \right|^2 \left| \mathcal{F}(\tilde{\mathcal{O}}_{j-l} - \mathcal{O}_{j-l})(w) \right|^2 \right. \\
&\quad \left. \frac{|w_{\sigma_j^l}^{U_j}(v)| |w_{\sigma_j^l}^{U_j}(w)|}{K_{j-l}(v)^2 K_{j-l}(w)^2} dv dw \right] \\
&\lesssim \int_{-U_j}^{U_j} \int_{-U_j}^{U_j} \mathbb{E} \left[\left| \mathcal{F}(\tilde{\mathcal{O}}_{j-l} - \mathcal{O}_{j-l})(v) \mathcal{F}(\tilde{\mathcal{O}}_{j-l} - \mathcal{O}_{j-l})(w) \right|^2 \right] \frac{v^4 |w_{\sigma_j^l}^{U_j}(v)| w^4 |w_{\sigma_j^l}^{U_j}(w)|}{K_{j-l}(v)^2 K_{j-l}(w)^2} dv dw
\end{aligned}$$

where in the last expression all the lower order terms of $(v^4 + v^2)(w^4 + w^2)$ are neglected, because asymptotically when $U_j \rightarrow \infty$ the term $v^4 w^4$ dominates.

In the subsequent analysis, we frequently use the following norm bounds for the B-splines $b_{j,k}$ in the interpolation scheme (2.12),

$$\|\mathcal{F}b_{j,k}\|_{L^2} = \sqrt{2\pi} \|b_{j,k}\|_{L^2} \leq (4\pi\Delta_j)^{1/2}, \quad \|\mathcal{F}b_{j,k}\|_{\infty} \leq \|b_{j,k}\|_{L^1} \leq 2\Delta_j \quad (3.27)$$

which follows from expression (3.3), $\|b_{j,k}\|_{\infty} = 1$ and $|x_{j,k+1} - x_{j,k-1}| \leq 2\Delta_j$.

Using the interpolation scheme, the term

$$\mathbb{E} \left[\left| \mathcal{F}(\tilde{\mathcal{O}}_{j-l} - \mathcal{O}_{j-l})(v) \mathcal{F}(\tilde{\mathcal{O}}_{j-l} - \mathcal{O}_{j-l})(w) \right|^2 \right]$$

will be bounded. The idea is that the terms will be split into a bias and variance term by addition and subtraction of the expected values $\mathbb{E}\tilde{\mathcal{O}}_{j-l}$. After working out the terms and using the triangle inequality, the following simplified expression can be found

$$\begin{aligned}
&\mathbb{E} \left[\left| \mathcal{F}(\tilde{\mathcal{O}}_{j-l} - \mathcal{O}_{j-l})(v) \mathcal{F}(\tilde{\mathcal{O}}_{j-l} - \mathcal{O}_{j-l})(w) \right|^2 \right] \\
&= \mathbb{E} \left[\left| \mathcal{F}(\tilde{\mathcal{O}}_{j-l} - \mathbb{E}\tilde{\mathcal{O}}_{j-l} + \mathbb{E}\tilde{\mathcal{O}}_{j-l} - \mathcal{O}_{j-l})(v) \mathcal{F}(\tilde{\mathcal{O}}_{j-l} - \mathbb{E}\tilde{\mathcal{O}}_{j-l} + \mathbb{E}\tilde{\mathcal{O}}_{j-l} - \mathcal{O}_{j-l})(w) \right|^2 \right] \\
&\leq 4\mathbb{E} \left[\left| \mathcal{F}(\tilde{\mathcal{O}}_{j-l} - \mathbb{E}\tilde{\mathcal{O}}_{j-l})(v) \mathcal{F}(\tilde{\mathcal{O}}_{j-l} - \mathbb{E}\tilde{\mathcal{O}}_{j-l})(w) \right|^2 \right] \\
&\quad + 4\|\mathcal{F}(\mathcal{O}_{j-l} - \mathbb{E}\tilde{\mathcal{O}}_{j-l})\|_{\infty}^2 \mathbb{E} \left[\left| \mathcal{F}(\tilde{\mathcal{O}}_{j-l} - \mathbb{E}\tilde{\mathcal{O}}_{j-l})(v) \right|^2 \right] \\
&\quad + 4\|\mathcal{F}(\mathcal{O}_{j-l} - \mathbb{E}\tilde{\mathcal{O}}_{j-l})\|_{\infty}^2 \mathbb{E} \left[\left| \mathcal{F}(\tilde{\mathcal{O}}_{j-l} - \mathbb{E}\tilde{\mathcal{O}}_{j-l})(w) \right|^2 \right] \\
&\quad + 4\|\mathcal{F}(\mathcal{O}_{j-l} - \mathbb{E}\tilde{\mathcal{O}}_{j-l})\|_{\infty}^4. \quad (3.28)
\end{aligned}$$

Note that in the expression (3.28) the second and third terms are constants multiplied with the variance of $\mathcal{F}\tilde{\mathcal{O}}_{j-l}$. Now, let us estimate this variance by using the interpolation scheme (2.12) and the properties imposed on the distributions of $(\varepsilon_{j-l,k})$ and the magnitude $(\delta_{j-l,k})$, this results in

$$\begin{aligned}
\mathbb{V} \left[\mathcal{F}\tilde{\mathcal{O}}_{j-l}(v) \right] &= \mathbb{V} \left[\mathcal{F} \left(\beta_{j-l,0}(x) + \sum_{k=1}^{m_{j-l}} \mathcal{O}_{j-l,k} b_{j-l,k}(x) \right) (v) \right] \\
&= \mathbb{V} \left[\mathcal{F} \beta_{0,j-l}(v) + \sum_{k=1}^{m_{j-l}} \mathcal{O}_{j-l,k} \mathcal{F} b_{j-l,k}(v) \right] \\
&= \mathbb{V} \left[\sum_{k=1}^{m_{j-l}} \mathcal{O}_{j-l,k} \mathcal{F} b_{j-l,k}(v) \right] = \mathbb{V} \left[\sum_{k=1}^{m_{j-l}} (\mathcal{O}_{j-l}(x_{j,k}) + \delta_{j-l,k} \varepsilon_{j-l,k}) \mathcal{F} b_{j-l,k}(v) \right]
\end{aligned}$$

$$\begin{aligned}
&= \mathbb{V} \left[\sum_{k=1}^{m_{j-l}} \delta_{j-l,k} \varepsilon_{j-l,k} \mathcal{F} b_{j-l,k}(w) \right] = \sum_{k=1}^{m_{j-l}} |\delta_{j-l,k} \mathcal{F} b_{j-l,k}(v)|^2 \mathbb{V} [\varepsilon_{j-l,k}] \\
&= \sum_{k=1}^{m_{j-l}} |\delta_{j-l,k} \mathcal{F} b_{j-l,k}(v)|^2 \leq \sum_{k=1}^{m_{j-l}} |\delta_{j-l,k}|^2 \|\mathcal{F} b_{j-l,k}\|_\infty^2 \leq \sum_{k=1}^{m_{j-l}} |\delta_{j-l,k}|^2 \|b_{j-l,k}\|_{L^1}^2 \\
&\leq 4\Delta_{j-l}^2 \sum_{k=1}^{m_{j-l}} |\delta_{j-l,k}|^2 = 4\Delta_{j-l}^2 \|\delta_{j-l}\|_{l^2}^2 \lesssim \Delta_{j-l} \|\delta_{j-l}\|_\infty^2, \tag{3.29}
\end{aligned}$$

where we made the assumption that $\Delta_{j-l} \|\delta_{j-l}\|_{l^2}^2 \leq \|\delta_{j-l}\|_\infty^2$, which is rather intuitive because $\Delta_{j-l} \rightarrow 0$.

Substituting expression (3.29) in (3.28) then gives the intermediate bound

$$\begin{aligned}
&\mathbb{E} \left[\left| \mathcal{F} \left(\tilde{\mathcal{O}}_{j-l} - \mathcal{O}_{j-l} \right) (v) \mathcal{F} \left(\tilde{\mathcal{O}}_{j-l} - \mathcal{O}_{j-l} \right) (w) \right|^2 \right] \\
&\lesssim \mathbb{E} \left[\left| \mathcal{F} \left(\tilde{\mathcal{O}}_{j-l} - \mathbb{E} \tilde{\mathcal{O}}_{j-l} \right) (v) \mathcal{F} \left(\tilde{\mathcal{O}}_{j-l} - \mathbb{E} \tilde{\mathcal{O}}_{j-l} \right) (w) \right|^2 \right] + \|\delta_{j-l}\|_\infty^2 \mathbb{E} \left[\left| \mathcal{F} \left(\tilde{\mathcal{O}}_{j-l} - \mathbb{E} \tilde{\mathcal{O}}_{j-l} \right) (v) \right|^2 \right] \\
&\quad + \|\delta_{j-l}\|_\infty^2 \mathbb{E} \left[\left| \mathcal{F} \left(\tilde{\mathcal{O}}_{j-l} - \mathbb{E} \tilde{\mathcal{O}}_{j-l} \right) (w) \right|^2 \right] + \|\mathcal{F}(\mathcal{O}_{j-l} - \mathbb{E} \tilde{\mathcal{O}}_{j-l})\|_\infty^4 \\
&\lesssim \mathbb{E} \left[\left| \mathcal{F} \left(\tilde{\mathcal{O}}_{j-l} - \mathbb{E} \tilde{\mathcal{O}}_{j-l} \right) (v) \mathcal{F} \left(\tilde{\mathcal{O}}_{j-l} - \mathbb{E} \tilde{\mathcal{O}}_{j-l} \right) (w) \right|^2 \right] + \|\delta_{j-l}\|_\infty^2 \Delta_{j-l}^4 + \Delta_{j-l}^8 \tag{3.30}
\end{aligned}$$

Furthermore, we also want to find a simplified bound for

$$\mathbb{E} \left[\left| \mathcal{F} \left(\tilde{\mathcal{O}}_{j-l} - \mathbb{E} \tilde{\mathcal{O}}_{j-l} \right) (v) \mathcal{F} \left(\tilde{\mathcal{O}}_{j-l} - \mathbb{E} \tilde{\mathcal{O}}_{j-l} \right) (w) \right|^2 \right]. \tag{3.31}$$

First, again with the interpolation scheme (2.12), we can write

$$\tilde{\mathcal{O}}_{j-l} - \mathbb{E} \tilde{\mathcal{O}}_{j-l} = \sum_{k=1}^{m_{j-l}} (\mathcal{O}_{j-l,k} - \mathcal{O}_{j-l}(x_{j-l,k})) b_{j-l,k}(x) = \sum_{k=1}^{m_{j-l}} \delta_{j-l,k} \varepsilon_{j-l,k} b_{j-l,k}(x).$$

Substituting the above expression into (3.31), then provides the bound

$$\begin{aligned}
&\mathbb{E} \left[\left| \mathcal{F} \left(\tilde{\mathcal{O}}_{j-l} - \mathbb{E} \tilde{\mathcal{O}}_{j-l} \right) (v) \mathcal{F} \left(\tilde{\mathcal{O}}_{j-l} - \mathbb{E} \tilde{\mathcal{O}}_{j-l} \right) (w) \right|^2 \right] \\
&= \mathbb{E} \left[\left| \mathcal{F} \left(\sum_{k=1}^{m_{j-l}} \delta_{j-l,k} \varepsilon_{j-l,k} b_{j-l,k} \right) (v) \mathcal{F} \left(\sum_{k=1}^{m_{j-l}} \delta_{j-l,k} \varepsilon_{j-l,k} b_{j-l,k} \right) (w) \right|^2 \right] \\
&= \mathbb{E} \left[\left| \sum_{k=1}^{m_{j-l}} \delta_{j-l,k} \varepsilon_{j-l,k} \mathcal{F} b_{j-l,k}(v) \sum_{k=1}^{m_{j-l}} \delta_{j-l,k} \varepsilon_{j-l,k} \mathcal{F} b_{j-l,k}(w) \right|^2 \right] \\
&= \mathbb{E} \left[\sum_{i=1}^{m_{j-l}} \sum_{k=1}^{m_{j-l}} \delta_{j-l,i}^2 \delta_{j-l,k}^2 \varepsilon_{j-l,i}^2 \varepsilon_{j-l,k}^2 |\mathcal{F} b_{j-l,i}(v)|^2 |\mathcal{F} b_{j-l,k}(w)|^2 \right] \\
&= \sum_{i=1}^{m_{j-l}} \sum_{k=1}^{m_{j-l}} \delta_{j-l,i}^2 \delta_{j-l,k}^2 \mathbb{E} [\varepsilon_{j-l,i}^2 \varepsilon_{j-l,k}^2] |\mathcal{F} b_{j-l,i}(v)|^2 |\mathcal{F} b_{j-l,k}(w)|^2
\end{aligned}$$

Now we use that $(\varepsilon_{j-l,k})$ are independent sub-Gaussian centered random variables with $\mathbb{V}[\varepsilon_{j-l,i}] = 1$, this results in

$$= \sum_{i=1}^{m_{j-l}} \delta_{j-l,i}^4 \mathbb{E} [\varepsilon_{j-l,i}^4] |\mathcal{F} b_{j-l,i}(v)|^2 |\mathcal{F} b_{j-l,k}(w)|^2$$

$$\begin{aligned}
& + \sum_{i=1}^{m_{j-l}} \sum_{k=1, k \neq i}^{m_{j-l}} \delta_{j-l,i}^2 \delta_{j-l,k}^2 \mathbb{E}[\varepsilon_{j-l,i}^2] \mathbb{E}[\varepsilon_{j-l,k}^2] |\mathcal{F}b_{j-l,i}(v)|^2 |\mathcal{F}b_{j-l,k}(w)|^2 \\
& \lesssim \sum_{i=1}^{m_{j-l}} \delta_{j-l,i}^4 |\mathcal{F}b_{j-l,i}(v)|^2 |\mathcal{F}b_{j-l,k}(w)|^2 + \sum_{i=1}^{m_{j-l}} \sum_{k=1, k \neq i}^{m_{j-l}} \delta_{j-l,i}^2 \delta_{j-l,k}^2 |\mathcal{F}b_{j-l,i}(v)|^2 |\mathcal{F}b_{j-l,k}(w)|^2 \\
& = \sum_{i=1}^{m_{j-l}} \sum_{k=1}^{m_{j-l}} \delta_{j-l,i}^2 \delta_{j-l,k}^2 |\mathcal{F}b_{j-l,i}(v)|^2 |\mathcal{F}b_{j-l,k}(w)|^2 \\
& = \left(\sum_{i=1}^{m_{j-l}} \delta_{j-l,i}^2 |\mathcal{F}b_{j-l,i}(v)|^2 \right) \left(\sum_{k=1}^{m_{j-l}} \delta_{j-l,k}^2 |\mathcal{F}b_{j-l,k}(w)|^2 \right). \tag{3.32}
\end{aligned}$$

For finding the final bound for $\mathbb{E} \left[\left| \mathcal{R}_{\sigma_j^2}^l \right|^2 \right]$ we first substitute (3.32) in (3.30), and then (3.30) back into the original expression, this gives

$$\begin{aligned}
\mathbb{E} \left[\left| \mathcal{R}_{\sigma_j^2}^l \right|^2 \right] & \lesssim \int_{-U_j}^{U_j} \int_{-U_j}^{U_j} \mathbb{E} \left[\left| \mathcal{F}(\tilde{\mathcal{O}}_{j-l} - \mathcal{O}_{j-l})(v) \mathcal{F}(\tilde{\mathcal{O}}_{j-l} - \mathcal{O}_{j-l})(w) \right|^2 \right] \\
& \quad \cdot \frac{v^4 |w_{\sigma_j^2}^{U_j}(v)| |w_{\sigma_j^2}^{U_j}(w)|}{K_{j-l}(v)^2 K_{j-l}(w)^2} dv dw \\
& \lesssim \int_{-U_j}^{U_j} \int_{-U_j}^{U_j} \left[\left(\sum_{i=1}^{m_{j-l}} \delta_{j-l,i}^2 |\mathcal{F}b_{j-l,i}(v)|^2 \right) \left(\sum_{k=1}^{m_{j-l}} \delta_{j-l,k}^2 |\mathcal{F}b_{j-l,k}(w)|^2 \right) + \|\delta_{j-l}\|_\infty^2 \Delta_{j-l}^4 + \Delta_{j-l}^8 \right] \\
& \quad \cdot \frac{v^4 |w_{\sigma_j^2}^{U_j}(v)| |w_{\sigma_j^2}^{U_j}(w)|}{K_{j-l}(v)^2 K_{j-l}(w)^2} dv dw \\
& = \left[\int_{U_j}^{U_j} \sum_{k=1}^{m_{j-l}} \delta_{j-l,k}^2 |\mathcal{F}b_{j-l,k}(v)|^2 \frac{v^4 |w_{\sigma_j^2}^{U_j}(v)|}{K_{j-l}(v)^2} dv \right]^2 + (\|\delta_{j-l}\|_\infty^2 \Delta_{j-l}^4 + \Delta_{j-l}^8) \left[\int_{U_j}^{U_j} \frac{v^4 |w_{\sigma_j^2}^{U_j}(v)|}{K_{j-l}(v)^2} dv \right]^2
\end{aligned}$$

It is possible to bound the first integral in terms of the second one, because

$$\begin{aligned}
& \int_{U_j}^{U_j} \sum_{k=1}^{m_{j-l}} \delta_{j-l,k}^2 |\mathcal{F}b_{j-l,k}(v)|^2 \frac{v^4 |w_{\sigma_j^2}^{U_j}(v)|}{K_{j-l}(v)^2} dv \leq \int_{U_j}^{U_j} \sum_{k=1}^{m_{j-l}} \delta_{j-l,k}^2 \|\mathcal{F}b_{j-l,k}(v)\|_\infty^2 \frac{v^4 |w_{\sigma_j^2}^{U_j}(v)|}{K_{j-l}(v)^2} dv \\
& \lesssim \Delta_{j-l}^2 \int_{-U_j}^{U_j} \sum_{k=1}^{m_{j-l}} \delta_{j-l,k}^2 \frac{v^4 |w_{\sigma_j^2}^{U_j}(v)|}{K_{j-l}(v)^2} dv \lesssim \Delta_{j-l}^2 \|\delta_{j-l}\|_\infty^2 \int_{-U_j}^{U_j} \frac{v^4 |w_{\sigma_j^2}^{U_j}(v)|}{K_{j-l}(v)^2} dv \\
& \lesssim \Delta_{j-l} \|\delta_{j-l}\|_\infty^2 \int_{-U_j}^{U_j} \frac{v^4 |w_{\sigma_j^2}^{U_j}(v)|}{K_{j-l}(v)^2} dv.
\end{aligned}$$

To simplify this common integral, Lemma 3.6 can be used.

Lemma 3.6 For all $j = 1, 2, \dots, n$ the following inequality holds

$$\int_{-U_j}^{U_j} \frac{v^4 |w_{\xi}^{U_j}(v)|}{K_{j-l}(v)^2} dv \lesssim \zeta_j e^{U_j^2 \sum_{i=1}^{j-l} (T_i - T_{i-1}) \sigma_i^2}$$

where $K_{j-l}(v) := K(T_{j-l}, \sigma_{max}, R, v)$, $\xi_j \in \{\sigma_j, \gamma_j, \lambda_j\}$ and respectively $\zeta_j \in \{1, U_j, U_j^2\}$.

Note that Lemma 3.6 is also specified for γ_j and λ_j , which will be investigated at the end of the section. As with all Lemma's, the proof of Lemma 3.6 can be found in the appendix.

Now using the bound for the first integral and Lemma 3.6 the final bound can be found

$$\mathbb{E} \left[\left| \mathcal{R}_{\sigma_j^2}^l \right|^2 \right] \lesssim \left(\|\delta_{j-l}\|_\infty^4 \Delta_{j-l}^2 + \left(\|\delta_{j-l}\|_\infty^2 \Delta_{j-l}^4 + \Delta_{j-l}^8 \right) \right) \left(\int_{-U_j}^{U_j} K_{j-l}(v)^{-2} v^4 |w_{\sigma_j^2}^{U_j}(v)| dv \right)^2$$

$$\lesssim \left(\|\delta_{j-l}\|_\infty^4 \Delta_{j-l}^2 + \|\delta_{j-l}\|_\infty^2 \Delta_{j-l}^4 + \Delta_{j-l}^8 \right) e^{2U_j^2 \cdot \sum_{i=1}^{j-l} (T_i - T_{i-1}) \sigma_i^2}. \quad (3.33)$$

Showing Asymptotic Convergence to Zero

Now with the found bound in expression (3.33) the asymptotic convergence ($U_j \rightarrow \infty, \Delta_j \rightarrow 0$) in probability of the term

$$\frac{U_j^2 e^{-U_j^2 \sum_{i=1}^j (T_i - T_{i-1}) \sigma_i^2 / 2}}{\sqrt{d_{j,j} \Delta_j + d_{j,j-1} \Delta_{j-1} e^{-U_j^2 (T_j - T_{j-1}) \sigma_j^2}}} \cdot \mathcal{R}_{\sigma_j^2}^l \xrightarrow{\mathbb{P}} 0$$

can be proven using Markov's inequality. The terms $d_{j,j}$ and $d_{j,j-1}$ are defined in the same manner as the case of the Linear terms $\mathcal{L}_{\xi_j}^l$ in Proposition 3.3.

Note that the prefactor before $\mathcal{R}_{\sigma_j^2}^l$ is the defined function $f_{\sigma_j^2}(U_j, \Delta_j)$, which was coupled to the asymptotic standard deviation.

Now let us start with the exact derivation. Let $\varepsilon > 0$, then with Markov's inequality and expression (3.33) we can find

$$\begin{aligned} & \mathbb{P} \left(\left| \frac{U_j^2 e^{-U_j^2 \sum_{i=1}^j (T_i - T_{i-1}) \sigma_i^2 / 2}}{\sqrt{d_{j,j} \Delta_j + d_{j,j-1} \Delta_{j-1} e^{-U_j^2 (T_j - T_{j-1}) \sigma_j^2}}} \mathcal{R}_{\sigma_j^2}^l \right| > \varepsilon \right) \\ &= \mathbb{P} \left(\frac{U_j^2 e^{-U_j^2 \sum_{i=1}^j (T_i - T_{i-1}) \sigma_i^2 / 2}}{\sqrt{d_{j,j} \Delta_j + d_{j,j-1} \Delta_{j-1} e^{-U_j^2 (T_j - T_{j-1}) \sigma_j^2}}} \left| \mathcal{R}_{\sigma_j^2}^l \right| > \varepsilon \right) \\ &\stackrel{\text{Markov}}{\leq} \frac{1}{\varepsilon^2} \mathbb{E} \left[\left(\frac{U_j^2 e^{-U_j^2 \sum_{i=1}^j (T_i - T_{i-1}) \sigma_i^2 / 2}}{\sqrt{d_{j,j} \Delta_j + d_{j,j-1} \Delta_{j-1} e^{-U_j^2 (T_j - T_{j-1}) \sigma_j^2}}} \left| \mathcal{R}_{\sigma_j^2}^l \right| \right)^2 \right] \\ &= \frac{1}{\varepsilon^2} \frac{U_j^4 e^{-U_j^2 \sum_{i=1}^j (T_i - T_{i-1}) \sigma_i^2} \mathbb{E} \left[\left| \mathcal{R}_{\sigma_j^2}^l \right|^2 \right]}{d_{j,j} \Delta_j + d_{j,j-1} \Delta_{j-1} e^{-U_j^2 (T_j - T_{j-1}) \sigma_j^2}} \\ &\stackrel{(3.33)}{\lesssim} \frac{1}{\varepsilon^2} \frac{U_j^4 e^{-U_j^2 \sum_{i=1}^j (T_i - T_{i-1}) \sigma_i^2} \left(\|\delta_{j-l}\|_\infty^4 \Delta_{j-l}^2 + \|\delta_{j-l}\|_\infty^2 \Delta_{j-l}^4 + \Delta_{j-l}^8 \right) e^{2U_j^2 \sum_{i=1}^{j-l} (T_i - T_{i-1}) \sigma_i^2}}{d_{j,j} \Delta_j + d_{j,j-1} \Delta_{j-1} e^{-U_j^2 (T_j - T_{j-1}) \sigma_j^2}} \\ &\leq \frac{1}{\varepsilon^2} \frac{U_j^4 \|\delta_{j-l}\|_\infty^4 \Delta_{j-l}^2 e^{2U_j^2 \sum_{i=1}^{j-l} (T_i - T_{i-1}) \sigma_i^2 - U_j^2 \sum_{i=1}^j (T_i - T_{i-1}) \sigma_i^2}}{d_{j,j} \Delta_j} \\ &= \frac{1}{\varepsilon^2} \frac{\|\delta_{j-l}\|_\infty^4 \Delta_{j-l}^2}{d_{j,j} \Delta_j} U_j^4 e^{2U_j^2 \sum_{i=1}^{j-l} (T_i - T_{i-1}) \sigma_i^2 - U_j^2 \sum_{i=1}^j (T_i - T_{i-1}) \sigma_i^2} =: \frac{1}{\varepsilon^2} p_{j,j-l}. \end{aligned}$$

For convergence of both $\mathcal{R}_{\sigma_j^2}^0$ and $\mathcal{R}_{\sigma_j^2}^1$ in the error decomposition, we need to impose that for $l = 0$ and $l = 1$ both respectively $p_{j,j}$ and $p_{j,j-1}$ go to zero. Hence, we need to have the conditions

$$p_{j,j} = \frac{\|\delta_j\|_\infty^4 \Delta_j}{d_{j,j}} U_j^4 e^{U_j^2 \sum_{i=1}^j (T_i - T_{i-1}) \sigma_i^2} \rightarrow 0$$

for $l = 0$, and

$$p_{j,j-1} = \frac{\|\delta_{j-1}\|_\infty^4 \Delta_{j-1}^2}{d_{j,j} \Delta_j} U_j^4 e^{U_j^2 ((\sum_{i=1}^{j-1} (T_i - T_{i-1}) \sigma_i^2) - (T_j - T_{j-1}) \sigma_j^2)} \rightarrow 0$$

for $l = 1$. These conditions impose the restrictions on how fast the convergences of $U_j \rightarrow \infty$ and $\Delta_j \rightarrow 0$ can be compared to each other.

We provide a summary of the conditions imposed and the asymptotic result in Proposition 3.5.

Proposition 3.5 *Let $\varepsilon_{j-l,k}$ be independent centered sub-Gaussian random variables with $\mathbb{V}[\varepsilon_{j-l,k}] = 1$ for all $k = 1, \dots, m_j$, $l = 0, 1$ and let $\delta_{j-l} \in L^{2+\eta}(\mathbb{R}) \cap C^\infty(\mathbb{R})$ for $\eta > 0$, $l = 0, 1$ with $\Delta_j \|\delta_{j-l}\|_{L_2}^2 \leq \|\delta_{j-l}\|_\infty^2$. Furthermore, let the Levy triplets $(\sigma_j, \gamma_j, \lambda_j)$ belong to $\mathcal{G}_{s_j}^n$ and the weight function $(w_{\sigma_j}^1, w_{\gamma_j}^1, w_{\lambda_j}^1)$ belong to $\mathcal{W}_{s_j}^n$. Control $U_j \rightarrow \infty$ and $\Delta_j \rightarrow 0$ such that*

$$\Delta_j U_j^4 e^{U_j^2 \sum_{i=1}^j (T_i - T_{i-1}) \sigma_i^2} \rightarrow 0 \quad \text{and} \quad \frac{\Delta_{j-1}^2}{\Delta_j} U_j^4 e^{U_j^2 (\sum_{i=1}^{j-1} (T_i - T_{i-1}) \sigma_i^2 - (T_j - T_{j-1}) \sigma_j^2)} \rightarrow 0,$$

then we have an asymptotic convergence of

$$\mathcal{R}_{\sigma_j^2}^l \frac{U_j^2 e^{-U_j^2 \sum_{i=1}^j (T_i - T_{i-1}) \sigma_i^2 / 2}}{\sqrt{d_{j,j} \Delta_j + d_{j,j-1} \Delta_{j-1} e^{-U_j^2 (T_j - T_{j-1}) \sigma_j^2}}} \xrightarrow{\mathbb{P}} 0$$

where \mathbb{P} stands for convergence in probability.

The differences in the proof with γ_j and λ_j occur only at a single point. In applying Lemma 6 we get respectively an extra U_j and U_j^2 term. In the next section, it can however be seen that the asymptotic standard deviations of the cases $\tilde{\gamma}_j$ and $\tilde{\lambda}_j$ are coupled to the functions $f_{\gamma_j}(U_j, \Delta_j) = \frac{1}{U_j} f_{\sigma_j^2}(U_j, \Delta_j)$ and $f_{\lambda_j}(U_j, \Delta_j) = \frac{1}{U_j^2} f_{\sigma_j^2}(U_j, \Delta_j)$. Hence, these cut-off factors exactly cancel, and under the same assumptions as Proposition 3.5, it can be concluded that

$$\mathcal{R}_{\gamma_j}^l \frac{1}{U_j} \frac{U_j^2 e^{-U_j^2 \sum_{i=1}^j (T_i - T_{i-1}) \sigma_i^2 / 2}}{\sqrt{d_{j,j} \Delta_j + d_{j,j-1} \Delta_{j-1} e^{-U_j^2 (T_j - T_{j-1}) \sigma_j^2}}} \xrightarrow{\mathbb{P}} 0 \quad (3.34)$$

and

$$\mathcal{R}_{\lambda_j}^l \frac{1}{U_j^2} \frac{U_j^2 e^{-U_j^2 \sum_{i=1}^j (T_i - T_{i-1}) \sigma_i^2 / 2}}{\sqrt{d_{j,j} \Delta_j + d_{j,j-1} \Delta_{j-1} e^{-U_j^2 (T_j - T_{j-1}) \sigma_j^2}}} \xrightarrow{\mathbb{P}} 0 \quad (3.35)$$

Moreover, note that we have constructed a proof for the absolute value of the remainder. Therefore, this proof works for both the real part of the remainder as well as the imaginary part of the remainder.

Asymptotic Normality of $(\tilde{\sigma}_j, \tilde{\gamma}_j, \tilde{\lambda}_j)$

Now all tools have been acquired to state the asymptotic normality of the estimators $(\tilde{\sigma}_j, \tilde{\gamma}_j, \tilde{\lambda}_j)$ while controlling the growth of $U_j \rightarrow \infty$ with the shrinkage of $\Delta_j \rightarrow 0$.

3.3.5 Normality of $\tilde{\sigma}_j$

First, the normality of the estimator $\tilde{\sigma}_j$ will be evaluated. Recall the error decomposition (3.9) that remarked

$$\tilde{\sigma}_j^2 - \sigma_j^2 = \mathcal{L}_{\sigma_j^2}^0 - \mathcal{L}_{\sigma_j^2}^1 + \mathcal{R}_{\sigma_j^2}^0 - \mathcal{R}_{\sigma_j^2}^1 + \mathcal{B}_{\sigma_j^2}. \quad (3.36)$$

Following Proposition (3.3) it is found that, under certain conditions, we have

$$\frac{\mathcal{L}_{\sigma_j^2}^0}{s_{n,0}} \xrightarrow{d} \mathcal{N}(0, 1) \quad \text{and} \quad \frac{\mathcal{L}_{\sigma_j^2}^1}{s_{n,1}} \xrightarrow{d} \mathcal{N}(0, 1),$$

with

$$s_{n,l}^2 = w_{\sigma_j}^1(1)^2 d_{j,j-l} \Delta_{j-l} U_j^{-4} \exp(A_{j-l} U_j^2),$$

where we defined

$$d_{j,j-l} := 2 \|\delta_{j-l}\|_{L^2}^2 (T_j - T_{j-1})^{-2} A_{j-l}^{-2} \exp(-2C_{j-l}),$$

and the terms A_{j-l} and C_{j-l} are as in expression (3.14).

Note that because $(\varepsilon_{j-l,k})$ are independent for different l , the linear terms $\mathcal{L}_{\sigma_j^2}^0$ and $\mathcal{L}_{\sigma_j^2}^1$ – which were only non-deterministic because of these $(\varepsilon_{j-l,k})$ – inherit this independence. Hence, $\mathcal{L}_{\sigma_j^2}^0 - \mathcal{L}_{\sigma_j^2}^1$ is asymptotically a sum of independent normally distributed random variables with variances $s_{n,0}^2$ and $s_{n,1}^2$, and, therefore,

$$\frac{\mathcal{L}_{\sigma_j^2}^0 - \mathcal{L}_{\sigma_j^2}^1}{\sqrt{s_{n,0}^2 + s_{n,1}^2}} \xrightarrow{d} \mathcal{N}(0, 1). \quad (3.37)$$

Recalling that from (3.14),

$$A_{j-l} := \sum_{i=1}^{j-l} (T_i - T_{i-1}) \sigma_i^2,$$

the inverse of the asymptotic standard deviation s_n can be written as:

$$\begin{aligned} \frac{1}{s_n} &:= \frac{1}{\sqrt{s_{n,0}^2 + s_{n,1}^2}} = \frac{U_j^2}{|w_{\sigma_j}^1(1)| \sqrt{d_{j,j} \Delta_j e^{U_j^2 A_j} + d_{j,j-1} \Delta_{j-1} e^{U_j^2 A_{j-1}}}}, \\ &= \frac{U_j^2}{|w_{\sigma_j}^1(1)| \sqrt{d_{j,j} \Delta_j + d_{j,j-1} \Delta_{j-1} e^{U_j^2 (A_{j-1} - A_j)}}}, \\ &= \frac{U_j^2}{|w_{\sigma_j}^1(1)| \sqrt{d_{j,j} \Delta_j + d_{j,j-1} \Delta_{j-1} e^{-U_j^2 \sum_{i=1}^j (T_i - T_{i-1}) \sigma_i^2 / 2}}}. \end{aligned} \quad (3.38)$$

Now let us write the error decomposition resembling the normality in (3.37),

$$\frac{\tilde{\sigma}_j^2 - \sigma_j^2}{s_n} = \frac{\mathcal{L}_{\sigma_j^2}^0 - \mathcal{L}_{\sigma_j^2}^1}{s_n} + \frac{1}{s_n} \mathcal{R}_{\sigma_j^2}^0 - \frac{1}{s_n} \mathcal{R}_{\sigma_j^2}^1 + \frac{1}{s_n} \mathcal{B}_{\sigma_j^2}.$$

In Proposition 3.5 it is stated that asymptotically we have the following convergence in probability

$$\frac{1}{s_n} \mathcal{R}_{\sigma_j^2}^0 \xrightarrow{\mathbb{P}} 0 \quad \text{and} \quad \frac{1}{s_n} \mathcal{R}_{\sigma_j^2}^1 \xrightarrow{\mathbb{P}} 0,$$

whenever the following conditions are satisfied asymptotically

$$\Delta_j U_j^4 e^{U_j^2 \sum_{i=1}^j (T_i - T_{i-1}) \sigma_i^2} \rightarrow 0 \quad \text{and} \quad \frac{\Delta_{j-1}^2}{\Delta_j} U_j^4 e^{U_j^2 (\sum_{i=1}^{j-1} (T_i - T_{i-1}) \sigma_i^2 - (T_j - T_{j-1}) \sigma_j^2)} \rightarrow 0.$$

Furthermore, from Proposition 3.4 it was stated that

$$\mathcal{B}_{\sigma_j^2} \lesssim U_j^{-(s_j+3)},$$

the asymptotic term then simplifies to

$$\begin{aligned} \frac{1}{s_n} \mathcal{B}_{\sigma_j^2} &= \frac{U_j^2}{|w_{\sigma_j}^1(1)|} \frac{\mathcal{B}_{\sigma_j^2}}{\sqrt{d_{j,j} \Delta_j e^{U_j^2 A_j} + d_{j,j-1} \Delta_{j-1} e^{U_j^2 A_{j-1}}}} \\ &\lesssim \frac{U_j^{-(s_j+1)}}{\sqrt{d_{j,j} \Delta_j e^{U_j^2 \sum_{i=1}^j (T_i - T_{i-1}) \sigma_i^2} + d_{j,j-1} \Delta_{j-1} e^{U_j^2 \sum_{i=1}^{j-1} (T_i - T_{i-1}) \sigma_i^2}}} \end{aligned}$$

$$\lesssim \left(U_j^{2(s_j+1)} \left\{ d_{j,j} \Delta_j e^{U_j^2 \sum_{i=1}^j (T_i - T_{i-1}) \sigma_i^2} + d_{j,j-1} \Delta_{j-1} e^{U_j^2 \sum_{i=1}^{j-1} (T_i - T_{i-1}) \sigma_i^2} \right\} \right)^{-1/2}.$$

If the following condition is imposed,

$$U_j^{2(s_j+1)} \left\{ \Delta_j e^{U_j^2 \sum_{i=1}^j (T_i - T_{i-1}) \sigma_i^2} + \Delta_{j-1} e^{U_j^2 \sum_{i=1}^{j-1} (T_i - T_{i-1}) \sigma_i^2} \right\} \rightarrow \infty, \quad (3.39)$$

then the desired result is found

$$\frac{1}{s_n} \mathcal{B}_{\sigma_j^2} \rightarrow 0,$$

whenever $s_j \geq 2$.

From the fact that convergence in probability is stronger than convergence in distribution, all elements can be combined to come to the result that asymptotically

$$\frac{\tilde{\sigma}_j^2 - \sigma_j^2}{s_n} \xrightarrow{d} \mathcal{N}(0, 1), \quad (3.40)$$

or, written differently remembering (3.38),

$$U_j^2 \Xi_j (\tilde{\sigma}_j^2 - \sigma_j^2) \xrightarrow{d} |w_{\sigma_j}^1(1)| Z_1,$$

where $Z_1 \sim \mathcal{N}(0, 1)$ and we defined

$$\Xi_j := \frac{e^{-U_j^2 \sum_{i=1}^j (T_i - T_{i-1}) \sigma_i^2 / 2}}{\sqrt{d_{j,j} \Delta_j + d_{j,j-1} \Delta_{j-1} e^{-U_j^2 (T_j - T_{j-1}) \sigma_j^2}}}. \quad (3.41)$$

The reason that we have written it in this way becomes clear when evaluating $\tilde{\gamma}_j$ and $\tilde{\lambda}_j$, these cases will namely resemble the same asymptotic term Ξ_j . Also, the exact conditions that imply this result will be summarized in a main theorem at the end of the section, together with the cases $\tilde{\gamma}_j$ and $\tilde{\lambda}_j$.

3.3.6 Normality of $\tilde{\gamma}_j$

The case of $\tilde{\gamma}_j$ follows a similar line of thought as the case of σ_j . However, there is a difference in the error decomposition of $\tilde{\gamma}_j$, given in expression (3.10),

$$(\tilde{\gamma}_j + \tilde{\sigma}_j^2) - (\gamma_j + \sigma_j^2) = \mathcal{L}_{\gamma_j^2}^0 - \mathcal{L}_{\gamma_j^2}^1 + \mathcal{R}_{\gamma_j^2}^0 - \mathcal{R}_{\gamma_j^2}^1 + \mathcal{B}_{\gamma_j^2}$$

which depends on the $\tilde{\sigma}_j$ case.

From Proposition 3.3 and the independence of $\mathcal{L}_{\gamma_j}^0$ and $\mathcal{L}_{\gamma_j}^1$, it can be deduced that

$$\frac{\mathcal{L}_{\gamma_j}^0 - \mathcal{L}_{\gamma_j}^1}{U_j s_n} \xrightarrow{d} \mathcal{N}(0, 1),$$

where the only difference is in the used weight function

$$\frac{1}{s_n} := \frac{1}{\sqrt{s_{n,0}^2 + s_{n,1}^2}} = \frac{U_j^2}{|w_{\gamma_j}^1(1)|} \frac{e^{-U_j^2 \sum_{i=1}^j (T_i - T_{i-1}) \sigma_i^2 / 2}}{\sqrt{d_{j,j} \Delta_j + d_{j,j-1} \Delta_{j-1} e^{-U_j^2 (T_j - T_{j-1}) \sigma_j^2}}}.$$

Let us first write the error decomposition in a way that resembles this normality,

$$\frac{1}{U_j s_n} ((\tilde{\gamma}_j + \tilde{\sigma}_j^2) - (\gamma_j + \sigma_j^2)) = \frac{\mathcal{L}_{\gamma_j^2}^0 - \mathcal{L}_{\gamma_j^2}^1}{U_j s_n} + \frac{1}{U_j s_n} \mathcal{R}_{\gamma_j^2}^0 - \frac{1}{U_j s_n} \mathcal{R}_{\gamma_j^2}^1 + \frac{1}{U_j s_n} \mathcal{B}_{\gamma_j^2}$$

Using Proposition 3.5 and expression 3.34 it follows that

$$\frac{1}{U_j s_n} \mathcal{R}_{\gamma_j}^0 \xrightarrow{\mathbb{P}} 0 \quad \text{and} \quad \frac{1}{U_j s_n} \mathcal{R}_{\gamma_j}^1 \xrightarrow{\mathbb{P}} 0,$$

whenever the same asymptotic conditions are satisfied

$$\Delta_j U_j^4 e^{U_j^2 \sum_{i=1}^j (T_i - T_{i-1}) \sigma_i^2} \rightarrow 0 \quad \text{and} \quad \frac{\Delta_{j-1}^2}{\Delta_j} U_j^4 e^{U_j^2 (\sum_{i=1}^{j-1} (T_i - T_{i-1}) \sigma_i^2 - (T_j - T_{j-1}) \sigma_j^2)} \rightarrow 0.$$

Proposition 3.4 provides that $\mathcal{B}_{\gamma_j} \lesssim U_j^{-(s_j+2)}$ such that $\frac{1}{U_j s_n} \mathcal{B}_{\gamma_j} \rightarrow 0$, whenever the same condition is as in expression (3.39) is satisfied. The reason for this is that $\frac{1}{U_j}$ and $U_j^{-(s_j+2)}$ combine to get the same factor $U_j^{-(s_j+3)}$ as in the case $\tilde{\sigma}_j^2$.

From the fact that convergence in probability is stronger than convergence in distribution and using the same definition of Ξ_j as in (3.41), the following result follows

$$U_j \Xi_j ((\tilde{\gamma}_j + \tilde{\sigma}_j^2) - (\gamma_j + \sigma_j^2)) \xrightarrow{d} |w_{\gamma_j}^1(1)| Z_2, \quad (3.42)$$

where $Z_2 \sim \mathcal{N}(0, 1)$.

Expression (3.42) is first rewritten such that it resembles the term $\tilde{\gamma}_j - \gamma_j$ and the normality results in (3.40) and (3.42),

$$U_j \Xi_j ((\tilde{\gamma}_j + \tilde{\sigma}_j^2) - (\gamma_j + \sigma_j^2)) = U_j \Xi_j (\tilde{\gamma}_j - \gamma_j) + \frac{1}{U_j} U_j^2 \Xi_j (\tilde{\sigma}_j - \sigma_j).$$

Now using the previous expression with the convergence results of (3.40) and (3.42) we can see that the term $(\tilde{\gamma}_j - \gamma_j)$ is a factor U_j slower in convergence than the term $(\tilde{\sigma}_j - \sigma_j)$. Therefore, asymptotically the first term with $|w_{\gamma_j}^1(1)|$ dominates the second term with $|w_{\sigma_j}^1(1)|$, because $U_j \rightarrow \infty$. Thus we get

$$U_j \Xi_j (\tilde{\gamma}_j - \gamma_j) \xrightarrow{d} |w_{\gamma_j}^1(1)| Z_2,$$

where $Z_2 \sim \mathcal{N}(0, 1)$.

3.3.7 Normality of $\tilde{\lambda}_j$

For the case of $\tilde{\lambda}_j$ we first recall the error decomposition (3.11),

$$(\tilde{\lambda}_j - \tilde{\sigma}_j^2/2 - \tilde{\gamma}_j) - (\lambda_j - \sigma_j^2/2 - \gamma_j) = \mathcal{L}_{\lambda_j}^0 - \mathcal{L}_{\lambda_j}^1 + \mathcal{R}_{\lambda_j}^0 - \mathcal{R}_{\lambda_j}^1 + \mathcal{B}_{\lambda_j}^2.$$

Following a similar approach to $\tilde{\gamma}_j$, Proposition 3.3 with the independence of $\mathcal{L}_{\lambda_j}^0$ and $\mathcal{L}_{\lambda_j}^1$ gives

$$\frac{\mathcal{L}_{\lambda_j}^0 - \mathcal{L}_{\lambda_j}^1}{U_j^2 s_n} \xrightarrow{d} \mathcal{N}(0, 1),$$

where the only difference is again in the weight function

$$\frac{1}{s_n} := \frac{1}{\sqrt{s_{n,0}^2 + s_{n,1}^2}} = \frac{U_j^2}{|w_{\lambda_j}^1(1)|} \frac{e^{-U_j^2 \sum_{i=1}^j (T_i - T_{i-1}) \sigma_i^2 / 2}}{\sqrt{d_{j,j} \Delta_j + d_{j,j-1} \Delta_{j-1} e^{-U_j^2 (T_j - T_{j-1}) \sigma_j^2}}}.$$

Rewriting the error decomposition to resemble the normality results gives

$$\begin{aligned} & \frac{1}{U_j^2 s_n} \left((\tilde{\lambda}_j - \tilde{\sigma}_j^2/2 - \tilde{\gamma}_j) - (\lambda_j - \sigma_j^2/2 - \gamma_j) \right) \\ &= \frac{\mathcal{L}_{\lambda_j}^0 - \mathcal{L}_{\lambda_j}^1}{U_j^2 s_n} + \frac{1}{U_j^2 s_n} \mathcal{R}_{\lambda_j}^0 - \frac{1}{U_j^2 s_n} \mathcal{R}_{\lambda_j}^1 + \frac{1}{U_j^2 s_n} \mathcal{B}_{\lambda_j}^2. \end{aligned}$$

Using Proposition 3.5 and expression 3.35 it follows that

$$\frac{1}{U_j^2 s_n} \mathcal{R}_{\lambda_j}^0 \xrightarrow{\mathbb{P}} 0 \quad \text{and} \quad \frac{1}{U_j^2 s_n} \mathcal{R}_{\lambda_j}^1 \xrightarrow{\mathbb{P}} 0,$$

whenever the same asymptotic conditions are satisfied

$$\Delta_j U_j^4 e^{U_j^2 \sum_{i=1}^j (T_i - T_{i-1}) \sigma_i^2} \rightarrow 0 \quad \text{and} \quad \frac{\Delta_j^2}{\Delta_j} U_j^4 e^{U_j^2 (\sum_{i=1}^{j-1} (T_i - T_{i-1}) \sigma_i^2 - (T_j - T_{j-1}) \sigma_j^2)} \rightarrow 0.$$

Proposition 3.4 provides that $\mathcal{B}_{\lambda_j} \lesssim U_j^{-(s_j+1)}$ such that $\frac{1}{U_j^2 s_n} \mathcal{B}_{\lambda_j} \rightarrow 0$, if the same condition is as in expression (3.39) is satisfied. The reason for this is that again $\frac{1}{U_j^2}$ and $U_j^{-(s_j+1)}$ combine to get the same factor $U_j^{-(s_j+3)}$ as in the case $\tilde{\sigma}_j^2$.

Hence, combining all these results and remembering that convergence in probability is stronger than convergence in distribution, it can be concluded that

$$\Xi_j \left((\tilde{\lambda}_j - \tilde{\sigma}_j^2/2 - \tilde{\gamma}_j) - (\lambda_j - \sigma_j^2/2 - \gamma_j) \right) \xrightarrow{d} |w_{\lambda_j}^1(1)| Z_3 \quad (3.43)$$

with $Z_3 \sim \mathcal{N}(0, 1)$ independent of Z_1 and Z_2 .

Expression (3.43) is first rewritten such that it resembles the term $\tilde{\lambda}_j - \lambda_j$ and the normality results in (3.40) and (3.42),

$$\begin{aligned} & \Xi_j \left((\tilde{\lambda}_j - \tilde{\sigma}_j^2/2 - \tilde{\gamma}_j) - (\lambda_j - \sigma_j^2/2 - \gamma_j) \right) \\ &= \Xi_j(\tilde{\lambda}_j - \lambda_j) - \frac{1}{U_j} U_j \Xi_j((\tilde{\gamma}_j + \tilde{\sigma}_j^2) - (\gamma_j - \sigma_j)) + \frac{1}{U_j^2} U_j^2 \Xi_j(\tilde{\sigma}_j - \sigma_j). \end{aligned}$$

Now using the normality expressions (3.40), (3.42) and (3.43), it can be derived that the term with $(\tilde{\lambda}_j - \lambda_j)$ is respectively U_j and U_j^2 slower than the terms $((\tilde{\gamma}_j + \tilde{\sigma}_j^2) - (\gamma_j - \sigma_j))$ and $(\tilde{\sigma}_j - \sigma_j)$. Therefore, the second term with $|w_{\gamma_j}^1(1)|$ and the third term with $|w_{\sigma_j}^1(1)|$ both converge to 0 faster when $U_j \rightarrow \infty$. Hence,

$$\Xi_j(\tilde{\lambda}_j - \lambda_j) \xrightarrow{d} |w_{\lambda_j}^1(1)| Z_3,$$

where $Z_3 \sim \mathcal{N}(0, 1)$.

3.4 Asymptotic Normality of $\tilde{\mu}_j(x)$

This section is devoted to showing the asymptotic normality of the estimator $(\tilde{\mu}_j(x))_{j=1, \dots, n}$ for $(\mu_j(x))_{j=1, \dots, n}$. From theoretical considerations, it is advised to look at the error decomposition of the exponentially weighted jump density $\tilde{\mu}_j(x) = e^x \tilde{\nu}_j(x)$ instead of the jump density $\tilde{\nu}_j(x)$. The reason for this is that the shifted estimator $\tilde{\psi}_{\nu_j}(v) = \psi_j(v + i)$ used for $\tilde{\nu}_j(x)$ will result in a term $\mathcal{F}b_{j-l,k}(v + i)$ instead of $\mathcal{F}b_{j-l,k}(v)$. This term will give an e^{-x} term which makes the analysis considerably less comparable to the triplet $(\tilde{\sigma}_j, \tilde{\gamma}_j, \tilde{\lambda}_j)$ and also more difficult. Therefore, it is advised to look at $\tilde{\mu}_j(x)$, and when the result for $\tilde{\mu}_j(x)$ is derived it is easy to get the result for $\tilde{\nu}_j(x)$.

The case of $(\tilde{\mu}_j(x))_{j=1, \dots, n}$ bears resemblance with the asymptotic normality of the estimators $(\tilde{\sigma}_j^2, \tilde{\gamma}_j, \tilde{\lambda}_j)_{j=1, \dots, n}$ in the fact that again an error decomposition will be made into a Bias term, Remainder term and Linear term. Thereafter it will be shown that the Bias and Remainder terms are asymptotically negligible, whereas the Linear term will asymptotically admit a normal distribution.

The difference with the cases of $(\tilde{\sigma}_j^2, \tilde{\gamma}_j, \tilde{\lambda}_j)_{j=1, \dots, n}$ is mostly in the spectral estimation part where now a smoothed inverse Fourier transform is used (2.17),

$$\tilde{\mu}_j(x) = \mathcal{F}^{-1} \left[\left(\tilde{\psi}_j(\cdot) + \frac{\tilde{\sigma}_j^2}{2}(\cdot - i)^2 - i\tilde{\gamma}_j(\cdot - i) + \tilde{\lambda}_j \right) w_{\mu_j}^{U_j}(\cdot) \right] (x)$$

where w_μ is a symmetric weight function supported on $[-1, 1]$.

Error Decomposition of $\tilde{\mu}_j(x)$

The error decomposition of $\tilde{\mu}_j(x)$ will be made by looking upon the term $\tilde{\mu}_j(x) - \mu_j(x)$,

$$\begin{aligned} \tilde{\mu}_j(x) - \mu_j(x) &= \mathcal{F}^{-1} \left[\left(\tilde{\psi}_j(\cdot) + \frac{\tilde{\sigma}_j^2}{2}(\cdot - i)^2 - i\tilde{\gamma}_j(\cdot - i) + \tilde{\lambda}_j \right) w_{\mu_j}^{U_j}(\cdot) \right] (x) \\ &\quad - \mathcal{F}^{-1} \left[\left(\psi_j(\cdot) + \frac{\sigma_j^2}{2}(\cdot - i)^2 - i\gamma_j(\cdot - i) + \lambda_j \right) \right] (x). \end{aligned}$$

Recalling the definition of the inverse Fourier transform

$$\mathcal{F}^{-1} f(x) = \frac{1}{2\pi} \int_{\mathbb{R}} f(v) e^{-ivx} dx$$

and the fact that the weight function $w_{\mu_j}^{U_j}(v)$ is 0 outside the region $[-U_j, U_j]$, then with the linearity of \mathcal{F}^{-1} the term $\tilde{\mu}_j(x) - \mu_j(x)$ can be written as

$$\begin{aligned} \tilde{\mu}_j(x) - \mu_j(x) &= \frac{1}{2\pi} \left[\int_{-U_j}^{U_j} (\tilde{\psi}_j(v) - \psi_j(v)) w_{\mu_j}^{U_j}(v) e^{-ivx} dv + \frac{\tilde{\sigma}_j^2 - \sigma_j^2}{2} \int_{-U_j}^{U_j} (v - i)^2 w_{\mu_j}^{U_j}(v) e^{-ivx} dv \right. \\ &\quad - i(\tilde{\gamma}_j - \gamma_j) \int_{-U_j}^{U_j} (v - i) w_{\mu_j}^{U_j}(v) e^{-ivx} dv + (\tilde{\lambda}_j - \lambda_j) \int_{-U_j}^{U_j} w_{\mu_j}^{U_j}(v) e^{-ivx} dv \\ &\quad \left. + \int_{\mathbb{R} \setminus [-U_j, U_j]} \left(\psi_j(v) + \frac{\sigma_j^2}{2}(v - i)^2 - i\gamma_j(v - i) + \lambda_j \right) (1 - w_{\mu_j}^{U_j}(v)) e^{-ivx} dv \right] \\ &=: \Psi + \Sigma + \Gamma + \Lambda + \mathcal{B}. \end{aligned} \tag{3.44}$$

First of all, note that in the decomposition \mathcal{B} is a Bias term and does not behave stochastically.

From the assumption of $w_{\mu_j}^{U_j} \in \mathcal{W}_n^{s_j}$, we can see that the integrals in the terms of Σ , Γ and Λ exist and are well-defined functions in x . Furthermore, we have already proven the asymptotic normality of $\tilde{\sigma}_j^2 - \sigma_j^2$, $\tilde{\gamma}_j - \gamma_j$ and $\tilde{\lambda}_j - \lambda_j$, thus the terms Σ , Γ and Λ follow the same normality multiplied by this well-defined function.

It will later be shown that the term Ψ converges in a slower manner than the terms Σ , Γ and Λ , such that Ψ dominates the asymptotic behaviour of $\tilde{\mu}_j(x) - \mu_j(x)$.

Asymptotic Normality Result of $\tilde{\mu}_j(x)$

We need to show the convergence of the Bias term \mathcal{B} to 0 and the asymptotic behavior of Ψ composed in a linear and remainder term. The line of thought in these two derivations is similar to the cases of $(\tilde{\sigma}_j, \tilde{\gamma}_j, \tilde{\lambda}_j)$ and the exact derivations is for the sake of not repeating arguments placed in the appendix. Below, we will summarize the results found in the appendix.

In section B we can write Ψ into linear terms and remainder terms

$$\begin{aligned} 2\pi\Psi &= \int_{-U_j}^{U_j} [\mathcal{L}_j^0(v) - \mathcal{L}_j^1(v) + \mathcal{R}_j^0(v) - \mathcal{R}_j^1(v)] w_{\mu_j}^{U_j}(v) e^{-ivx} dv \\ &=: \mathcal{L}_{\mu_j}^0 - \mathcal{L}_{\mu_j}^1 + \mathcal{R}_{\mu_j}^0 - \mathcal{R}_{\mu_j}^1. \end{aligned}$$

Using the Lyapunov Central Limit theorem, the linear terms converge to a normal distribution

$$\frac{\mathcal{L}_{\mu_j}^l}{U_j^3 s_{n,l}} = \frac{T_m}{U_j^3 s_{n,l}} \xrightarrow{d} \mathcal{N}(0, 1), \quad \text{for } l = 0, 1.$$

with asymptotic variance $s_{n,l}^2$ similar to the previously found asymptotic variance of $\tilde{\sigma}_j^2$.

Then, for the remainder terms, it can be shown that, in probability, the following convergence with s_n as in (3.38) can be found:

$$\frac{1}{U_j^3 s_n} \mathcal{R}_{\mu_j}^0 \xrightarrow{\mathbb{P}} 0 \quad \text{and} \quad \frac{1}{U_j^3 s_n} \mathcal{R}_{\mu_j}^1 \xrightarrow{\mathbb{P}} 0,$$

whenever the following conditions are satisfied asymptotically

$$\Delta_j U_j^4 e^{U_j^2 \sum_{i=1}^j (T_i - T_{i-1}) \sigma_i^2} \rightarrow 0 \quad \text{and} \quad \frac{\Delta_j^2}{\Delta_j} U_j^4 e^{U_j^2 (\sum_{i=1}^{j-1} (T_i - T_{i-1}) \sigma_i^2 - (T_j - T_{j-1}) \sigma_j^2)} \rightarrow 0.$$

In section B.1 the result is found that the Bias term can be bounded by

$$|\mathcal{B}| \leq \frac{1}{2\pi} U_j^{-2s_j} \|\mu_j^{s_j}\|_{L^2(\mathbb{R})},$$

such that

$$\frac{|\mathcal{B}|}{U_j^3 s_n} \rightarrow 0$$

whenever for $s_j > 2$,

$$U_j^{2(s_j+1)} \left\{ \Delta_j e^{U_j^2 \sum_{i=1}^j (T_i - T_{i-1}) \sigma_i^2} + \Delta_{j-1} e^{U_j^2 \sum_{i=1}^{j-1} (T_i - T_{i-1}) \sigma_i^2} \right\} \rightarrow \infty.$$

Thus, in the same spirit as the other parameters, from the fact that convergence in probability is stronger than convergence in distribution, all elements can be combined to come to the result that asymptotically

$$2\pi \frac{\Psi}{U_j^3 s_n} \xrightarrow{d} \mathcal{N}(0, 1)$$

or, written differently remembering (3.41),

$$\frac{1}{U_j} \Xi_j \Psi \xrightarrow{d} \frac{1}{2\pi} |w_{\mu_j}^1(1)| Z_4,$$

where $Z_4 \sim \mathcal{N}(0, 1)$.

Recalling the asymptotic results of $\tilde{\sigma}_j^2 - \sigma_j$, $\tilde{\gamma}_j - \gamma_j$, and $\tilde{\lambda}_j - \lambda_j$ that are respectively portrayed in the factors Σ , Γ and Λ in (3.44), it can be seen that the asymptotic convergence rate of Ψ is the slowest and dominates the asymptotic behavior when $U_j \rightarrow \infty$. Hence, it can be concluded that

$$\frac{1}{U_j} \Xi_j (\tilde{\mu}_j(x) - \mu_j(x)) \xrightarrow{d} \frac{1}{2\pi} |w_{\mu_j}^1(1)| Z_4.$$

The result of $\tilde{\nu}_j(x)$ can easily be deduced after recalling that $\nu_j(x) = e^x \mu_j(x)$ and using the continuous mapping theorem,

$$\frac{1}{U_j} \Xi_j e^x (\tilde{\nu}_j(x) - \nu_j(x)) \xrightarrow{d} \frac{1}{2\pi} |w_{\nu_j}^1(1)| Z_4.$$

where the exact specification of the weight function for μ_j and ν_j can be chosen equivalently, i.e., $w_{\nu_j}^1 = w_{\mu_j}^1$.

3.5 Concluding Theorem of Normality Results

All found results of Propositions 3.1, 3.3, 3.4, and 3.5 will be combined to make a final theorem about the asymptotic normality of the Lévy triplet. Note that in Proposition 3.1 the condition was imposed

$$\Delta_j U_j^4 \log U_j e^{U_j^2 \sum_{r=1}^j (T_r - T_{r-1}) \sigma_r^2} \rightarrow 0,$$

and in Proposition 3.3 the condition,

$$\Delta_j U_j^4 e^{U_j^2 \sum_{i=1}^j (T_i - T_{i-1}) \sigma_i^2} \rightarrow 0,$$

when $U_j \rightarrow \infty$ and $\Delta_j \rightarrow 0$. The first condition incorporates the second condition when $U_j \rightarrow \infty$ – the $\log U_j$ only makes the convergence slower.

Using this fact, the combination of all Propositions and expression (3.39) result in Theorem 3.2.

Theorem 3.2 *Let $\varepsilon_{j-l,k}$ be independent centered sub-Gaussian random variables with $\mathbb{V}[\varepsilon_{j-l,k}] = 1$ for all $k = 1, \dots, m_j$, $l = 0, 1$ and let $\delta_{j-l} \in L^{2+\eta}(\mathbb{R}) \cap C^\infty(\mathbb{R})$ for $\eta > 0$, $l = 0, 1$ with $\Delta_j \|\delta_{j-l}\|_{L_2}^2 \leq \|\delta_{j-l}\|_\infty^2$. Furthermore, let the Levy triplets $(\sigma_j, \gamma_j, \mu_j)$ belong to $\mathcal{G}_{s_j}^n$ and the weight function $(w_{\sigma_j}^1, w_{\gamma_j}^1, w_{\lambda_j}^1, w_{\mu_j}^1)$ belong to $\mathcal{W}_{s_j}^n$. Control $U_j \rightarrow \infty$ and $\Delta_j \rightarrow 0$ such that for $j = 1, \dots, n$,*

$$\Delta_j U_j^4 \log U_j e^{U_j^2 \sum_{i=1}^j (T_i - T_{i-1}) \sigma_i^2} \rightarrow 0$$

and for $j = 2, \dots, n$,

$$\begin{aligned} \frac{\Delta_{j-1}^2}{\Delta_j} U_j^4 e^{U_j^2 (\sum_{i=1}^{j-1} (T_i - T_{i-1}) \sigma_i^2 - (T_j - T_{j-1}) \sigma_j^2)} &\rightarrow 0, \\ U_j^{2(s_j+1)} \left\{ \Delta_j e^{U_j^2 \sum_{i=1}^j (T_i - T_{i-1}) \sigma_i^2} + \Delta_{j-1} e^{U_j^2 \sum_{i=1}^{j-1} (T_i - T_{i-1}) \sigma_i^2} \right\} &\rightarrow \infty, \quad s_j \geq 2. \end{aligned}$$

Then we have the asymptotic convergence for all $j = 1, \dots, n$ of

$$\begin{aligned} U_j^2 \Xi_j (\tilde{\sigma}_j^2 - \sigma_j) &\xrightarrow{d} |w_{\sigma_j}^1(1)| Z_1, \\ U_j \Xi_j (\tilde{\gamma}_j - \gamma_j) &\xrightarrow{d} |w_{\gamma_j}^1(1)| Z_2, \\ \Xi_j (\tilde{\lambda}_j - \lambda_j) &\xrightarrow{d} |w_{\lambda_j}^1(1)| Z_3, \\ \frac{1}{U_j} \Xi_j (\tilde{\mu}_j(x) - \mu_j(x)) &\xrightarrow{d} \frac{1}{2\pi} |w_{\mu_j}^1(1)| Z_4, \end{aligned}$$

with $Z_i \sim \mathcal{N}(0, 1)$, $i = 1, 2, 3, 4$ and

$$\Xi_j := \frac{e^{-U_j^2 \sum_{i=1}^j (T_i - T_{i-1}) \sigma_i^2 / 2}}{\sqrt{d_{j,j} \Delta_j + d_{j,j-1} \Delta_{j-1} e^{-U_j^2 (T_j - T_{j-1}) \sigma_j^2}}}.$$

with, for $l = 0, 1$, $d_{j,0} = 0$, and

$$d_{j,j-l} := 2 \|\delta_{j-l}\|_{L_2}^2 \frac{e^{\sum_{i=1}^{j-l} (T_i - T_{i-1}) (\sigma_i^2 / 2 + \gamma_i - \lambda_i)}}{(T_j - T_{j-1})^2 \left(\sum_{i=1}^{j-l} (T_i - T_{i-1}) \sigma_i^2 \right)^2}$$

3.6 Difficulty of Inverse Calibration Problem

An important factor in all the results is parameter Ξ_j which was defined by

$$\Xi_j := \frac{e^{-U_j^2 \sum_{i=1}^j (T_i - T_{i-1}) \sigma_i^2 / 2}}{\sqrt{d_{j,j} \Delta_j + d_{j,j-1} \Delta_{j-1} e^{-U_j^2 (T_j - T_{j-1}) \sigma_j^2}}}. \quad (3.45)$$

with, for $l = 0, 1$,

$$d_{j,j-l} := 2 \|\delta_{j-l}\|_{L^2}^2 \frac{e^{\sum_{i=1}^{j-l} (T_i - T_{i-1}) (\sigma_i^2 / 2 + \gamma_i - \lambda_i)}}{(T_j - T_{j-1})^2 \left(\sum_{i=1}^{j-l} (T_i - T_{i-1}) \sigma_i^2 \right)^2}.$$

We want to write the term Ξ_j in such a way that we can say something about the difficulty of the problem with increasing j . The asymptotic variance of all problems will be influenced by $\frac{1}{\Xi_j}$, which can be written as

$$\begin{aligned} \frac{1}{\Xi_j} &= \frac{\sqrt{2}}{(T_j - T_{j-1})} \left(\|\delta_j\|_{L^2}^2 \frac{e^{\sum_{i=1}^j (T_i - T_{i-1}) (\sigma_i^2 / 2 + \gamma_i - \lambda_i)}}{\left(\sum_{i=1}^j (T_i - T_{i-1}) \sigma_i^2 \right)^2} \Delta_j e^{U_j^2 \sum_{i=1}^j (T_i - T_{i-1}) \sigma_i^2} \right. \\ &\quad \left. + \|\delta_{j-1}\|_{L^2}^2 \frac{e^{\sum_{i=1}^{j-1} (T_i - T_{i-1}) (\sigma_i^2 / 2 + \gamma_i - \lambda_i)}}{\left(\sum_{i=1}^{j-1} (T_i - T_{i-1}) \sigma_i^2 \right)^2} \Delta_{j-1} e^{U_j^2 \sum_{i=1}^{j-1} (T_i - T_{i-1}) \sigma_i^2} \right)^{1/2}. \end{aligned}$$

The factors that mostly influence the size with increasing j are

$$\frac{e^{\sum_{i=1}^j (T_i - T_{i-1}) (\sigma_i^2 / 2 + \gamma_i - \lambda_i)}}{\left(\sum_{i=1}^j (T_i - T_{i-1}) \sigma_i^2 \right)^2} e^{U_j^2 \sum_{i=1}^j (T_i - T_{i-1}) \sigma_i^2},$$

and

$$\frac{e^{\sum_{i=1}^{j-1} (T_i - T_{i-1}) (\sigma_i^2 / 2 + \gamma_i - \lambda_i)}}{\left(\sum_{i=1}^{j-1} (T_i - T_{i-1}) \sigma_i^2 \right)^2} e^{U_j^2 \sum_{i=1}^{j-1} (T_i - T_{i-1}) \sigma_i^2}.$$

Note that in the asymptotics $U_j \rightarrow \infty$, thus the terms

$$e^{U_j^2 \sum_{i=1}^j (T_i - T_{i-1}) \sigma_i^2} \quad \text{and} \quad e^{U_j^2 \sum_{i=1}^{j-1} (T_i - T_{i-1}) \sigma_i^2}$$

dominate. Of course, in these terms, Δ_j and Δ_{j-1} have been left out, because if we multiplied these terms respectively with the grid sizes, then we demanded that they went to 0. However, here we are most interested in the complexity of the problem with increasing j and Δ_j and Δ_{j-1} do not necessarily change in the same manner as these terms with increasing j .

The convergence of the asymptotic variance of the time-inhomogeneous Lévy model with increasing j is thus coupled to the factors in the exponential $\sum_{i=1}^{j-l} (T_i - T_{i-1}) \sigma_i^2$ with $l = 0, 1$. Note that this term contains the time differences $(T_i - T_{i-1})$ and volatilities σ_i^2 of all previous calibrations $i = 1, \dots, j$.

Belomestny et al. [4] and Söhl and Trabs [44] already point out that in the case of the homogeneous Lévy model, i.e. one Lévy process between 0 and end time $T_n = T$, the difficulty of the inverse calibration problem is coupled to $\sigma^2 T$. It is easy to see by filling in $j = 1$ that the time-inhomogeneous model also incorporates the time-homogeneous model and we only have the term $\sum_{i=1}^1 (T_i - T_{i-1}) \sigma_i^2 = \sigma_1^2 T_1 =: \sigma^2 T$. Thus, a theoretical argument is found why the difficulty of the time-homogeneous problem is coupled to $\sigma^2 T$.

Furthermore, the difficulty of the time-inhomogeneous inverse calibration problem is coupled to $\sum_{i=1}^{j-l} (T_i - T_{i-1}) \sigma_i^2$ with $l = 0, 1$. This term grows for increasing j and the problem becomes more difficult when calibration occurs for higher j . This fact will be clearly shown in the practical side of the thesis, which contains the simulations and the empirical results.

3.7 Convergence Rates

Let us recall the asymptotic assumptions on $U_j \rightarrow \infty$ and $\Delta_j \rightarrow 0$ that needed to be made for the convergence to hold. For the well-definedness of ψ_j and the remainder terms \mathcal{R}_j^l divided by the asymptotic variance to converge to 0 in probability, we needed to impose the conditions

$$\Delta_j U_j^4 \log U_j e^{U_j^2 \sum_{i=1}^j (T_i - T_{i-1}) \sigma_i^2} \rightarrow 0 \quad \text{and} \quad \frac{\Delta_j^2}{\Delta_j} U_j^4 e^{U_j^2 (\sum_{i=1}^{j-1} (T_i - T_{i-1}) \sigma_i^2 - (T_j - T_{j-1}) \sigma_j^2)} \rightarrow 0. \quad (3.46)$$

Furthermore, for the bias \mathcal{B}_j divided by the asymptotic variance to become 0, we also needed to have

$$U_j^{2(s_j+1)} \left\{ \Delta_j e^{U_j^2 \sum_{i=1}^j (T_i - T_{i-1}) \sigma_i^2} + \Delta_{j-1} e^{U_j^2 \sum_{i=1}^{j-1} (T_i - T_{i-1}) \sigma_i^2} \right\} \rightarrow \infty, \quad (3.47)$$

which was only possible with $s_j \geq 2$. These 3 conditions imply under what conditions the convergence rates must be found.

The idea is that we want to find $U_j = f(\Delta_j)$ for some function $f : \mathbb{R}^+ \rightarrow \mathbb{R}^+$ such that all 3 conditions are satisfied and optimal convergence is found. The assumption still holds that all Lévy triplets $(\sigma_j, \gamma_j, \mu_j)_{j=1, \dots, n}$ belong to $\mathcal{G}_{s_j}^n$ as in Definition 1.1.

Define $f : [0, 1] \rightarrow \mathbb{R}^+$ as

$$U_{j, \sigma_{\max}} = f(\Delta_j) := \frac{1}{\sigma_{\max}} \sqrt{\frac{\log(1/\Delta_j)}{T_j}}. \quad (3.48)$$

We will show that this choice gives the desired convergence rate. The domain $[0, 1]$ is chosen such that $\log(1/\Delta_j) \geq 0$ and the square root is well-defined. Note that the restriction of the domain is minor because we are interested in the case $\Delta_j \rightarrow 0$.

Let us verify if the limited relations in expressions (3.46) and (3.47) are satisfied for this choice of $U_j = U_{j, \sigma_{\max}}$. First, note that

$$\begin{aligned} \Delta_j e^{U_j^2 \sum_{i=1}^j (T_i - T_{i-1}) \sigma_i^2} &= \Delta_j e^{\frac{1}{T_j \sigma_{\max}^2} \log(1/\Delta_j) \sum_{i=1}^j (T_i - T_{i-1}) \sigma_i^2} = \Delta_j \Delta_j^{-\frac{\sum_{i=1}^j (T_i - T_{i-1}) \sigma_i^2}{T_j \sigma_{\max}^2}} \\ &= \Delta_j \frac{1 - \frac{\sum_{i=1}^j (T_i - T_{i-1}) \sigma_i^2}{T_j \sigma_{\max}^2}}{T_j \sigma_{\max}^2} = \Delta_j \frac{\sum_{i=1}^j (T_i - T_{i-1}) \sigma_{\max}^2 - \sum_{i=1}^j (T_i - T_{i-1}) \sigma_i^2}{T_j \sigma_{\max}^2} \\ &= \Delta_j \frac{\sum_{i=1}^j (T_i - T_{i-1}) (\sigma_{\max}^2 - \sigma_i^2)}{T_j \sigma_{\max}^2} \rightarrow 0 \quad \text{as} \quad \Delta_j \rightarrow 0, \end{aligned}$$

because, by the definition of $\mathcal{G}_{s_j}^n$, we have $\sigma_{\max}^2 > \sigma_i^2$ for all $i = 1, \dots, n$, and thereby $\sum_{i=1}^j (T_i - T_{i-1}) (\sigma_{\max}^2 - \sigma_i^2) / (T_j \sigma_{\max}^2) > 0$. The first relation in (3.46) can then be verified

$$\lim_{\Delta_j \rightarrow 0} \Delta_j U_j^4 \log U_j e^{U_j^2 \sum_{i=1}^j (T_i - T_{i-1}) \sigma_i^2} = \lim_{\Delta_j \rightarrow 0} U_j^4 \log U_j \Delta_j \frac{\sum_{i=1}^j (T_i - T_{i-1}) (\sigma_{\max}^2 - \sigma_i^2)}{T_j \sigma_{\max}^2} = 0,$$

where the last limit can be proven by using a power series expansion or L'Hôpital's rule to note that the exponential term dominates. For the second limiting relation in (3.46), the following expression is useful

$$\begin{aligned} \Delta_j e^{U_j^2 (\sum_{i=1}^{j-1} (T_i - T_{i-1}) \sigma_i^2 - (T_j - T_{j-1}) \sigma_j^2)} &= \Delta_j \frac{\sum_{i=1}^{j-1} (T_i - T_{i-1}) \sigma_{\max}^2 - (\sum_{i=1}^{j-1} (T_i - T_{i-1}) \sigma_i^2 - (T_j - T_{j-1}) \sigma_j^2)}{T_j \sigma_{\max}^2} \\ &= \Delta_j \frac{\sum_{i=1}^{j-1} (T_i - T_{i-1}) \sigma_{\max}^2 - \sum_{i=1}^{j-1} (T_i - T_{i-1}) \sigma_i^2 + (T_j - T_{j-1}) \sigma_{\max}^2 + (T_j - T_{j-1}) \sigma_j^2}{T_j \sigma_{\max}^2} \\ &= \Delta_j \frac{\sum_{i=1}^j (T_i - T_{i-1}) (\sigma_{\max}^2 - \sigma_i^2) + (T_j - T_{j-1}) (\sigma_{\max}^2 + \sigma_j^2)}{T_j \sigma_{\max}^2} \rightarrow 0 \quad \text{as} \quad \Delta_j \rightarrow 0, \end{aligned}$$

because the exponent is positive again. The minor assumption is made that the factor $\frac{\Delta_{j-1}}{\Delta_j} \leq C$ for some $C \in \mathbb{R}$. Then the second limit can be shown by observing the bounds

$$\begin{aligned} 0 &\leq \lim_{\Delta_j \rightarrow 0} \frac{\Delta_{j-1}^2}{\Delta_j} U_j^4 e^{U_j^2 (\sum_{i=1}^{j-1} (T_i - T_{i-1}) \sigma_i^2 - (T_j - T_{j-1}) \sigma_j^2)} \\ &= \lim_{\Delta_j \rightarrow 0} \left(\frac{\Delta_{j-1}}{\Delta_j} \right)^2 U_j^4 \Delta_j e^{U_j^2 (\sum_{i=1}^{j-1} (T_i - T_{i-1}) \sigma_i^2 - (T_j - T_{j-1}) \sigma_j^2)} \\ &= \frac{1}{\sigma_{\max}^4 T_j^2} \lim_{\Delta_j \rightarrow 0} \left(\frac{\Delta_{j-1}}{\Delta_j} \right)^2 \log(\Delta_j)^2 \Delta_j \frac{\sum_{i=1}^j (T_i - T_{i-1}) (\sigma_{\max}^2 - \sigma_i^2) + (T_j - T_{j-1}) (\sigma_{\max}^2 + \sigma_j^2)}{T_j \sigma_{\max}^2} \\ &\leq C^2 \frac{1}{\sigma_{\max}^4 T_j^2} \lim_{\Delta_j \rightarrow 0} \log(\Delta_j)^2 \Delta_j \frac{\sum_{i=1}^j (T_i - T_{i-1}) (\sigma_{\max}^2 - \sigma_i^2) + (T_j - T_{j-1}) (\sigma_{\max}^2 + \sigma_j^2)}{T_j \sigma_{\max}^2} = 0, \end{aligned}$$

such that the squeeze theorem implies

$$\lim_{\Delta_j \rightarrow 0} \frac{\Delta_{j-1}^2}{\Delta_j} U_j^4 e^{U_j^2 (\sum_{i=1}^{j-1} (T_i - T_{i-1}) \sigma_i^2 - (T_j - T_{j-1}) \sigma_j^2)} = 0.$$

Thus all limited relations of expression (3.46) — the conditions such that $\tilde{\psi}_j$ is well-defined and the remainder terms divided by the asymptotic variance converge to 0 in \mathbb{P} — are satisfied for this choice of $U_{j, \sigma_{\max}}$.

Remind that for the domain $[0, 1]$ it holds that $\log(1/\Delta_j) \geq 0$. For the condition of the Bias term divided by the standard deviation (3.47) it follows that for $U_j = U_{j, \sigma_{\max}}$ we have

$$\begin{aligned} &\lim_{\Delta_j \rightarrow 0} U_j^{2(s_j+1)} \left\{ \Delta_j e^{U_j^2 \sum_{i=1}^j (T_i - T_{i-1}) \sigma_i^2} + \Delta_{j-1} e^{U_j^2 \sum_{i=1}^{j-1} (T_i - T_{i-1}) \sigma_i^2} \right\} \\ &= \lim_{\Delta_j \rightarrow 0} \log(1/\Delta_j)^{s_j+1} \left\{ \Delta_j e^{U_j^2 \sum_{i=1}^j (T_i - T_{i-1}) \sigma_i^2} + \frac{\Delta_{j-1}}{\Delta_j} \Delta_j e^{U_j^2 \sum_{i=1}^{j-1} (T_i - T_{i-1}) \sigma_i^2} \right\} \\ &= \lim_{\Delta_j \rightarrow 0} \log(1/\Delta_j)^{s_j+1} \left\{ \Delta_j \frac{\sum_{i=1}^j (T_i - T_{i-1}) (\sigma_{\max}^2 - \sigma_i^2)}{T_j \sigma_{\max}^2} \right. \\ &\quad \left. + \frac{\Delta_{j-1}}{\Delta_j} \Delta_j \frac{\sum_{i=1}^{j-1} (T_i - T_{i-1}) (\sigma_{\max}^2 - \sigma_i^2) + (T_j - T_{j-1}) \sigma_{\max}^2}{T_j \sigma_{\max}^2} \right\} = 0, \end{aligned}$$

where the squeeze theorem was used

$$\begin{aligned} 0 &\leq \lim_{\Delta_j \rightarrow 0} \log(1/\Delta_j)^{s_j+1} \frac{\Delta_{j-1}}{\Delta_j} \Delta_j \frac{\sum_{i=1}^{j-1} (T_i - T_{i-1}) (\sigma_{\max}^2 - \sigma_i^2) + (T_j - T_{j-1}) \sigma_{\max}^2}{T_j \sigma_{\max}^2} \\ &\leq C \lim_{\Delta_j \rightarrow 0} \log(1/\Delta_j)^{s_j+1} \Delta_j \frac{\sum_{i=1}^{j-1} (T_i - T_{i-1}) (\sigma_{\max}^2 - \sigma_i^2) + (T_j - T_{j-1}) \sigma_{\max}^2}{T_j \sigma_{\max}^2} \end{aligned}$$

and for general $\alpha > 0$ we have

$$\lim_{\Delta_j \rightarrow 0} \log(1/\Delta_j)^{s_j+1} \Delta_j^\alpha = 0.$$

This last limit can easily be proved by a power series expansion or rewriting the term to $(-\log \Delta_j)^{s_j+1} / \Delta_j^{-\alpha}$ and applying L'Hôpital's rule $s_j + 1$ times. Note that the limit goes to 0 and not the required ∞ for convergence of the Bias to 0.

Thus, for the choice of $U_{j, \sigma_{\max}}$ the remainder terms divided by the standard deviation converge to 0 and the bias term divided by the standard deviation does not converge to 0. Therefore, the Bias term dominates the Remainder term.

Intuitively this can also be verified, in the rate $U_{j,\sigma_{\max}} \sim \frac{1}{\sigma_{\max}}$ the fact was used that $\sigma_i^2 < \sigma_{\max}^2$, such that the rate $U_{j,\sigma_{\max}}$ is smaller than the rate U_{j,σ_i} — which can only be known if σ_i^2 is known. Therefore, *oversmoothing* is deployed, and the Bias is dominating.

Using the domination of the Bias term then, for example, with $\tilde{\sigma}_j^2$, it follows with the error decomposition (3.9) that

$$\mathbb{E} \left[\frac{\tilde{\sigma}_j^2 - \sigma_j^2}{s_n} \right] = \underbrace{\frac{\mathbb{E}[\mathcal{L}_{\sigma_j^2}^0 - \mathcal{L}_{\sigma_j^2}^1]}{s_n}}_{=0} + \frac{\mathbb{E}[\mathcal{R}_{\sigma_j^2}^0 - \mathcal{R}_{\sigma_j^2}^1 + \mathcal{B}_{\sigma_j^2}]}{s_n} \approx \frac{\mathcal{B}_{\sigma_j^2}}{s_n},$$

where we used that $\mathcal{B}_{\sigma_j^2}$ and s_n are deterministic. Using Proposition 3.4 it then follows that

$$\mathbb{E}[\tilde{\sigma}_j^2 - \sigma_j^2] = \mathcal{B}_{\sigma_j^2} \lesssim U_{j,\sigma_{\max}}^{-(s_j+3)} = \left(\frac{1}{\sigma_{\max}} \sqrt{\frac{\log(1/\Delta_j)}{T_j}} \right)^{-(s_j+3)} = |\log \Delta_j|^{-(s_j+3)/2}.$$

All the other cases $\gamma_j, \lambda_j, \nu_j$ were dependent on the same limiting relations of (3.46) and (3.47), the only difference occurs in Proposition 3.4. Therefore,

$$\begin{aligned} \mathbb{E}[\tilde{\gamma}_j - \gamma_j] &= \mathcal{B}_{\gamma_j} \lesssim U_{j,\sigma_{\max}}^{-(s_j+2)} = |\log \Delta_j|^{-(s_j+2)/2}, \\ \mathbb{E}[\tilde{\lambda}_j - \lambda_j] &= \mathcal{B}_{\lambda_j} \lesssim U_{j,\sigma_{\max}}^{-(s_j+1)} = |\log \Delta_j|^{-(s_j+1)/2}, \\ \mathbb{E}[\tilde{\mu}_j(x) - \mu_j(x)] &= \mathcal{B}_{\nu_j(x)} \lesssim U_{j,\sigma_{\max}}^{-s_j} = |\log \Delta_j|^{-s_j/2}. \end{aligned}$$

The rates given by $U_{j,\sigma_{\max}}$ in expression (3.48) are also optimal. The reason for this is that if U_j is chosen slightly larger than $U_{j,\sigma_{\max}}$, then it is not guaranteed that the remainder asymptotic relations in (3.46) hold. The cut-off U_j can only be chosen larger if σ_i^2 is *exactly* known, which is not the case in practical problems. Furthermore, if U_j is chosen slightly smaller than $U_{j,\sigma_{\max}}$, then the bound on the Bias terms becomes larger, such that the rate is less optimal. Hence, $U_{j,\sigma_{\max}}$ is the optimal rate. These rates agree with Belomestny and Reiß [7, p.459], which proved these rates for the time-homogeneous model.

All the findings of this section are summarized in Theorem 3.3.

Theorem 3.3 *Let $\Delta_{j-1}/\Delta_j \leq C$ for some $C \in \mathbb{R}$ and let the Lévy triplets $(\sigma_j^2, \gamma_j, \nu_j)_{j=1,2,\dots,n}$ belong to $\mathcal{G}_{s_j}^n$. Define $U_{j,\sigma_{\max}}$ with the function $f : [0, 1] \rightarrow \mathbb{R}^+$ by*

$$U_{j,\sigma_{\max}} := f(\Delta_j) = \frac{1}{\sigma_{\max}} \sqrt{\frac{\log(1/\Delta_j)}{T_j}},$$

then $U_{j,\sigma_{\max}}$ is the optimal choice of the cut-off value in terms of Δ_j for all Lévy triplets $(\sigma_j^2, \gamma_j, \mu_j)_{j=1,2,\dots,n}$. The convergence rates are governed by the biases and are given by

$$\begin{aligned} \mathbb{E}[\tilde{\sigma}_j^2 - \sigma_j^2] &\lesssim U_{j,\sigma_{\max}}^{-(s_j+2)} = |\log \Delta_j|^{-(s_j+2)/2}, \\ \mathbb{E}[\tilde{\gamma}_j - \gamma_j] &\lesssim U_{j,\sigma_{\max}}^{-(s_j+2)} = |\log \Delta_j|^{-(s_j+2)/2}, \\ \mathbb{E}[\tilde{\lambda}_j - \lambda_j] &\lesssim U_{j,\sigma_{\max}}^{-(s_j+1)} = |\log \Delta_j|^{-(s_j+1)/2}, \\ \mathbb{E}[\tilde{\mu}_j(x) - \mu_j(x)] &\lesssim U_{j,\sigma_{\max}}^{-s_j} = |\log \Delta_j|^{-s_j/2}. \end{aligned}$$

Chapter 4

Confidence Intervals with Finite Sample Variance

The asymptotic standard deviation of the asymptotic normality results (Theorem 3.2) can be used to make $(100 - \vartheta)\%$ (asymptotic) confidence intervals. This can be done by using the continuous mapping theorem and Slutsky's theorem.

From practical applications, however, it is found that these confidence intervals are not necessarily satisfactory in terms of coverage probabilities. The reason for this is that the estimation of the finite sample by its limit, as in the normality part has been done, is not a good practice in real-life/finite sample applications. Therefore, this practice has been left out of the thesis, and a new more practical side, where the variance is not estimated by its limit, will be investigated.

The new approach of creating confidence intervals by estimating the variance of a finite sample will be called *finite sample variance*. On the practical side of the report, it can be seen that this method works particularly well in terms of coverage probabilities.

Söhl and Trabs [44] already derived confidence intervals for finite samples by using a simplified continuous scheme. The exact simplification is that [44] made an idealized continuous observation scheme of the regression model (2.9),

$$\mathcal{O}_{j,k} = \mathcal{O}_j(x_{j,k}) + \delta_{j,k}\varepsilon_{j,k},$$

by using the Gaussian white noise model,

$$d\mathcal{O}_k(x) = \mathcal{O}(x)dx + \varepsilon_k\delta_k(x)dW(x),$$

where W is a two-sided Brownian motion, $\delta_k \in L^2(\mathbb{R})$, and $\varepsilon_k > 0$. Transferring asymptotic results from the Gaussian white noise model to the regression model is formally justified by the concept of asymptotic equivalence [13] – this result only holds when the errors are Gaussian. Nevertheless, as [41] points out, it is an idealized model and the ultimate interest is in the regression model with discrete observations. This would lead to less asymptotic results and assumptions.

Therefore, Tendijck [46] made a start obtaining finite sample variance confidence intervals by directly using the regression model (2.9), i.e., the discrete case is investigated instead of making a simplified continuous case. In this section, we will clarify, improve and complete the work he started.

The idea of the method is to build confidence intervals by estimating the variance of the stochastic error. The same error decomposition as in the asymptotic normality case will be used, i.e., the error decomposition where we split into a linear, a remainder, and a bias term. Now the *important assumption* will be made that for the finite/non-asymptotic case the bias and remainder term can be neglected ¹. The reason behind this assumption is that in the theoretic results, we have already seen that these terms converge to 0 in the limit compared to the linear terms. After neglecting these terms, the variance s_n^2 (as in the linear term) will

¹ This assumption will be further inspected in the practical side of the thesis. Sometimes bias can be observed and the assumption does not always hold, however, the coverage probabilities can still be satisfactory.

be estimated for the finite case, i.e. not its limiting behavior, and used to make confidence intervals.

First, the case of $\tilde{\sigma}_j$ will be inspected, and thereafter the cases of $\tilde{\gamma}_j$ and $\tilde{\lambda}_j$ which bear great resemblances to $\tilde{\sigma}_j$. In the end, a point-wise confidence interval for $\tilde{\nu}_j(x)$ for a certain point x will also be constructed.

4.1 Confidence Intervals for $\tilde{\sigma}_j$

For constructing confidence intervals, the variance of the estimator $\tilde{\sigma}_j^2$ will be estimated,

$$s_{\tilde{\sigma}_j^2}^2 \approx \mathbb{V}(\tilde{\sigma}_j^2) = \mathbb{E} \left[(\tilde{\sigma}_j^2 - \mathbb{E}[\tilde{\sigma}_j^2])^2 \right],$$

where after the assumptions we will later see that $\mathbb{E}[\tilde{\sigma}_j^2] = \sigma_j^2$.

The method starts with the same error decomposition (3.9) as the linearity results, which was given by

$$\tilde{\sigma}_j^2 - \sigma_j^2 = \mathcal{L}_{\sigma_j^2}^0 - \mathcal{L}_{\sigma_j^2}^1 + \mathcal{R}_{\sigma_j^2}^0 - \mathcal{R}_{\sigma_j^2}^1 + \mathcal{B}_{\sigma_j^2}. \quad (4.1)$$

The assumption is made that the bias term $\mathcal{B}_{\sigma_j^2}$ and the remainder terms $\mathcal{R}_{\sigma_j^2}^0, \mathcal{R}_{\sigma_j^2}^1$ can be neglected, such that

$$\tilde{\sigma}_j^2 - \sigma_j^2 \approx \mathcal{L}_{\sigma_j^2}^0 - \mathcal{L}_{\sigma_j^2}^1,$$

where for $l = 0, 1$ one should recall the definitions

$$\mathcal{L}_{\sigma_j^2}^l = \int_{-U_j}^{U_j} w_{\sigma_j^2}^{U_j}(v) \operatorname{Re}(\mathcal{L}_j^l(v)) dv \quad \text{with} \quad \mathcal{L}_j^l(v) = \frac{1}{T_j - T_{j-1}} \frac{\tilde{\varphi}_{T_{j-l}}(v-i) - \varphi_{T_{j-l}}(v-i)}{\varphi_{T_{j-l}}(v-i)}.$$

Using (3.2) the stochastic term $\tilde{\varphi}_{T_{j-l}}(v-i) - \varphi_{T_{j-l}}(v-i)$ will be written in the more basic form

$$\tilde{\varphi}_{T_{j-l}}(v-i) - \varphi_{T_{j-l}}(v-i) = iv(1+iv) \sum_{k=1}^{m_{j-l}} \delta_{j-l,k} \varepsilon_{j-l,k} \mathcal{F} b_{j-l,k}(v),$$

such that

$$\mathcal{L}_j^l(v) = \frac{1}{T_j - T_{j-1}} \frac{iv(1+iv) \sum_{k=1}^{m_{j-l}} \delta_{j-l,k} \varepsilon_{j-l,k} \mathcal{F} b_{j-l,k}(v)}{\varphi_{T_{j-l}}(v-i)}.$$

Note that it is easy to see that $\mathbb{E}[\mathcal{L}_j^l(v)] = 0$ for $l = 0, 1$, and thereby $\mathbb{E}[\tilde{\sigma}_j^2] = \sigma_j^2$.

Recall that the linear cubic spline interpolation scheme (2.12) is used, such that $b_{j-l,k}(x) = \Lambda\left(\frac{x-x_{j-l,k}}{\Delta_{j-l}}\right)$ with $\Lambda(x) = (1-|x|)\mathbb{1}_{|x|\leq 1}$. Now the Fourier transform will be approximated

$$\mathcal{F} b_{j-l,k}(v) = \int_{\mathbb{R}} b_{j-l,k}(x) e^{ivx} dx \approx \frac{x_{j-l,k+1} - x_{j-l,k-1}}{2} e^{ivx_{j-l,k}} = \Delta_{j-l} e^{ivx_{j-l,k}} \quad (4.2)$$

where we used the equidistant grid $\Delta_{j-l} = |x_{j-l,k+1} - x_{j-l,k}| = |x_{j-l,k} - x_{j-l,k-1}|$.

The following convenient function $f_{\sigma_j}^l$ is defined as

$$f_{\sigma_j}^l(v) := w_{\sigma_j^2}^{U_j}(v) \frac{iv(1+iv)}{(T_j - T_{j-1})\varphi_{T_{j-l}}(v-i)},$$

then also using (4.2) the term $\mathcal{L}_{\sigma_j^2}^l$ can be written as

$$\begin{aligned} \mathcal{L}_{\sigma_j^2}^l &= \int_{-U_j}^{U_j} w_{\sigma_j^2}^{U_j}(v) \operatorname{Re}(\mathcal{L}_j^l(v)) dv \\ &= \int_{-U_j}^{U_j} w_{\sigma_j^2}^{U_j}(v) \operatorname{Re} \left(\frac{1}{T_j - T_{j-1}} \frac{iv(1+iv) \sum_{k=1}^{m_{j-l}} \delta_{j-l,k} \varepsilon_{j-l,k} \mathcal{F} b_{j-l,k}(v)}{\varphi_{T_{j-l}}(v-i)} \right) dv \end{aligned}$$

$$\begin{aligned}
&= \int_{-U_j}^{U_j} \operatorname{Re} \left(f_{\sigma_j}^l(v) \sum_{k=1}^{m_{j-l}} \delta_{j-l,k} \varepsilon_{j-l,k} \mathcal{F} b_{j-l,k}(v) \right) dv \\
&\approx \int_{-U_j}^{U_j} \operatorname{Re} \left(f_{\sigma_j}^l(v) \sum_{k=1}^{m_{j-l}} \delta_{j-l,k} \varepsilon_{j-l,k} \Delta_{j-l} e^{ivx_{j-l,k}} \right) dv \\
&= \sum_{k=1}^{m_{j-l}} \delta_{j-l,k} \varepsilon_{j-l,k} \Delta_{j-l} \operatorname{Re} \left(\int_{-U_j}^{U_j} f_{\sigma_j}^l(v) e^{ivx_{j-l,k}} dv \right). \tag{4.3}
\end{aligned}$$

Note that by the definition of the class $\mathcal{W}_{s_j}^n$, it was that $w_{\sigma_j}^{U_j} \in \mathcal{W}_{s_j}^n$ is 0 outside the region $[-U_j, U_j]$, thus

$$\int_{-U_j}^{U_j} f_{\sigma_j}^l(v) e^{ivx_{j-l,k}} dv = 2\pi \frac{1}{2\pi} \int_{\mathbb{R}} f_{\sigma_j}^l(v) e^{ivx_{j-l,k}} dv = 2\pi \mathcal{F}^{-1} f_{\sigma_j}^l(-x_{j-l,k})$$

and the following expression is found

$$\mathcal{L}_{\sigma_j^2}^l = 2\pi \sum_{k=1}^{m_{j-l}} \delta_{j-l,k} \varepsilon_{j-l,k} \Delta_{j-l} \operatorname{Re} \left(\mathcal{F}^{-1} f_{\sigma_j}^l(-x_{j-l,k}) \right).$$

Using the fact that $(\varepsilon_{j,k})$ are independent centered sub-Gaussian random variables with $\mathbb{V}[\varepsilon_{j,k}] = 1$, it follows that $\mathcal{L}_{\sigma_j^2}^0$ and $\mathcal{L}_{\sigma_j^2}^1$ are independent, and the estimated variance becomes

$$\begin{aligned}
\mathbb{V}(\tilde{\sigma}_j^2) &= \mathbb{E} \left[(\tilde{\sigma}_j^2 - \mathbb{E}[\tilde{\sigma}_j^2])^2 \right] = \mathbb{E} \left[(\tilde{\sigma}_j^2 - \sigma_j^2)^2 \right] \approx \mathbb{E} \left[(\mathcal{L}_{\sigma_j^2}^0 - \mathcal{L}_{\sigma_j^2}^1)^2 \right] \\
&\approx \mathbb{E} \left[(\mathcal{L}_{\sigma_j^2}^0)^2 \right] + \mathbb{E} \left[(\mathcal{L}_{\sigma_j^2}^1)^2 \right] - \underbrace{2 \mathbb{E}[\mathcal{L}_{\sigma_j^2}^0] \mathbb{E}[\mathcal{L}_{\sigma_j^2}^1]}_{=0} \\
&\approx \mathbb{E} \left[\left(2\pi \sum_{k=1}^{m_j} \delta_{j,k} \varepsilon_{j,k} \Delta_j \operatorname{Re} \left(\mathcal{F}^{-1} f_{\sigma_j}^l(-x_{j,k}) \right) \right)^2 \right] \\
&\quad + \mathbb{E} \left[\left(2\pi \sum_{k=1}^{m_{j-1}} \delta_{j-1,k} \varepsilon_{j-1,k} \Delta_{j-1} \operatorname{Re} \left(\mathcal{F}^{-1} f_{\sigma_j}^l(-x_{j-1,k}) \right) \right)^2 \right] \\
&\approx 4\pi^2 \sum_{k=1}^{m_j} \delta_{j,k}^2 \Delta_j^2 \operatorname{Re} \left(\mathcal{F}^{-1} f_{\sigma_j}^0(-x_{j,k}) \right)^2 + 4\pi^2 \sum_{k=1}^{m_{j-1}} \delta_{j-1,k}^2 \Delta_{j-1}^2 \operatorname{Re} \left(\mathcal{F}^{-1} f_{\sigma_j}^1(-x_{j-1,k}) \right)^2
\end{aligned}$$

The estimated variance is thus given by

$$s_{\sigma_j}^2 = 4\pi^2 \sum_{k=1}^{m_j} \delta_{j,k}^2 \Delta_j^2 \operatorname{Re} \left(\mathcal{F}^{-1} f_{\sigma_j}^0(-x_{j,k}) \right)^2 + 4\pi^2 \sum_{k=1}^{m_{j-1}} \delta_{j-1,k}^2 \Delta_{j-1}^2 \operatorname{Re} \left(\mathcal{F}^{-1} f_{\sigma_j}^1(-x_{j-1,k}) \right)^2. \tag{4.4}$$

Note that in practical applications the function $\varphi_{T_{j-l}}(v-i)$ in $f_{\sigma_j}^l(v)$ is not available. The estimator $\tilde{\varphi}_{T_{j-l}}(v-i)$ will therefore be used instead of $\varphi_{T_{j-l}}(v-i)$ in the function $f_{\sigma_j}^l(v)$.

Using the continuous mapping theorem and Slutsky's theorem a $(100 - \vartheta)\%$ asymptotic confidence interval for $\tilde{\sigma}_j^2$ can be constructed by

$$\left[\tilde{\sigma}_j^2 + z_{\vartheta/2} \cdot s_{\sigma_j}^2, \quad \tilde{\sigma}_j^2 - z_{100-\vartheta/2} \cdot s_{\sigma_j}^2 \right], \tag{4.5}$$

where z_p is the p th quantile of a standard normal distribution.

4.2 Confidence Intervals for $\tilde{\gamma}_j$

Now let us estimate the variance of $\tilde{\gamma}_j$,

$$s_{\tilde{\gamma}_j}^2 \approx \mathbb{V}(\tilde{\gamma}_j) = \mathbb{E} \left[(\tilde{\gamma}_j - \mathbb{E}[\tilde{\gamma}_j])^2 \right].$$

It has a similar line of thought as the case $\tilde{\sigma}_j^2$, so the calculations will be made more concise.

When combining the error decompositions (3.9) and (3.10),

$$\begin{aligned} \tilde{\sigma}_j^2 - \sigma_j^2 &= \mathcal{L}_{\sigma_j^2}^0 - \mathcal{L}_{\sigma_j^2}^1 + \mathcal{R}_{\sigma_j^2}^0 - \mathcal{R}_{\sigma_j^2}^1 + \mathcal{B}_{\sigma_j^2}, \\ (\tilde{\gamma}_j + \tilde{\sigma}_j^2) - (\gamma_j + \sigma_j^2) &= \mathcal{L}_{\gamma_j}^0 - \mathcal{L}_{\gamma_j}^1 + \mathcal{R}_{\gamma_j}^0 - \mathcal{R}_{\gamma_j}^1 + \mathcal{B}_{\gamma_j}, \end{aligned}$$

a sole expression for $\tilde{\gamma}_j - \gamma_j$ can be found

$$\tilde{\gamma}_j - \gamma_j = \mathcal{L}_{\gamma_j}^0 - \mathcal{L}_{\sigma_j^2}^0 - \mathcal{L}_{\gamma_j}^1 + \mathcal{L}_{\sigma_j^2}^1 + \mathcal{R}_{\gamma_j}^0 - \mathcal{R}_{\sigma_j^2}^0 - \mathcal{R}_{\gamma_j}^1 + \mathcal{R}_{\sigma_j^2}^1 + \mathcal{B}_{\gamma_j} - \mathcal{B}_{\sigma_j^2}.$$

The assumption is made that the remainder terms $\mathcal{R}_{\gamma_j}^0, \mathcal{R}_{\gamma_j}^1, \mathcal{R}_{\sigma_j^2}^0, \mathcal{R}_{\sigma_j^2}^1$ and the bias terms $\mathcal{B}_{\gamma_j}, \mathcal{B}_{\sigma_j^2}$ can again be neglected. Thus,

$$\tilde{\gamma}_j - \gamma_j = \mathcal{L}_{\gamma_j}^0 - \mathcal{L}_{\sigma_j^2}^0 - \mathcal{L}_{\gamma_j}^1 + \mathcal{L}_{\sigma_j^2}^1.$$

Recall that

$$\mathcal{L}_{\sigma_j^2}^l = \int_{-U_j}^{U_j} w_{\sigma_j^2}^{U_j}(v) \operatorname{Re}(\mathcal{L}_j^l(v)) dv \quad \text{and} \quad \mathcal{L}_{\gamma_j}^l = \int_{-U_j}^{U_j} w_{\gamma_j}^{U_j}(v) \operatorname{Im}(\mathcal{L}_j^l(v)) dv,$$

where

$$\mathcal{L}_j^l(v) = \frac{1}{T_j - T_{j-1}} \frac{\tilde{\varphi}_{T_{j-l}}(v-i) - \varphi_{T_{j-l}}(v-i)}{\varphi_{T_{j-l}}(v-i)}.$$

Using expression (3.2) the stochastic term $\tilde{\varphi}_{T_{j-l}}(v-i) - \varphi_{T_{j-l}}(v-i)$ will be written in the more basic form

$$\begin{aligned} \tilde{\varphi}_{T_{j-l}}(v-i) - \varphi_{T_{j-l}}(v-i) &= iv(1+iv) \sum_{k=1}^{m_{j-l}} \delta_{j-l,k} \varepsilon_{j-l,k} \mathcal{F} b_{j-l,k}(v), \\ &\approx iv(1+iv) \sum_{k=1}^{m_{j-l}} \delta_{j-l,k} \varepsilon_{j-l,k} \Delta_{j-l} e^{ivx_{j-l,k}}, \end{aligned}$$

where the Fourier transform was approximated as in (4.2). After defining the function $f_{\gamma_j}^l$ as

$$f_{\gamma_j}^l(v) := w_{\gamma_j}^{U_j}(v) \frac{iv(1+iv)}{(T_j - T_{j-1})\varphi_{T_{j-l}}(v-i)},$$

then $\mathcal{L}_{\gamma_j}^l$ can be written as

$$\begin{aligned} \mathcal{L}_{\gamma_j}^l &= \int_{-U_j}^{U_j} w_{\gamma_j}^{U_j}(v) \operatorname{Im}(\mathcal{L}_j^l(v)) dv, \\ &= \int_{-U_j}^{U_j} \operatorname{Im} \left(f_{\gamma_j}^l(v) \sum_{k=1}^{m_{j-l}} \delta_{j-l,k} \varepsilon_{j-l,k} \mathcal{F} b_{j-l,k}(v) \right) dv, \\ &\approx \sum_{k=1}^{m_{j-l}} \delta_{j-l,k} \varepsilon_{j-l,k} \Delta_{j-l} \operatorname{Im} \left(\int_{-U_j}^{U_j} f_{\gamma_j}^l(v) e^{ivx_{j-l,k}} dv \right), \\ &= 2\pi \sum_{k=1}^{m_{j-l}} \delta_{j-l,k} \varepsilon_{j-l,k} \Delta_{j-l} \operatorname{Im} \left(\mathcal{F}^{-1} f_{\gamma_j}^l(-x_{j-l,k}) \right), \end{aligned} \tag{4.6}$$

where we again used that $w_{\gamma_j}^{U_j}$ is 0 outside the region $[-U_j, U_j]$.

Observing expressions (4.3) and (4.6) it can be seen that the independence of $(\varepsilon_{j,k})$ implies that $\mathcal{L}_{\sigma_j^2}^0, \mathcal{L}_{\gamma_j}^0$ are independent of $\mathcal{L}_{\sigma_j^2}^1, \mathcal{L}_{\gamma_j}^1$. Furthermore, it is easy to see that $\mathbb{E}[\tilde{\gamma}_j] = \gamma_j$. Having this in mind, the variance of $\tilde{\gamma}_j$ takes the form

$$\mathbb{V}(\tilde{\gamma}_j) = \mathbb{E} \left[(\tilde{\gamma}_j - \gamma_j)^2 \right] \approx \mathbb{E}[(\mathcal{L}_{\gamma_j}^0 - \mathcal{L}_{\sigma_j^2}^0)^2] + \mathbb{E}[(\mathcal{L}_{\gamma_j}^1 - \mathcal{L}_{\sigma_j^2}^1)^2].$$

Now using expression (4.3) and (4.6) together with the fact that $(\varepsilon_{j,k})$ are independent and were chosen such that $\mathbb{V}(\varepsilon_{j,k}) = 1$, a final approximation of the variance can be found

$$\begin{aligned} \mathbb{V}(\tilde{\gamma}_j) &\approx \mathbb{E} \left[\left(2\pi \sum_{k=1}^{m_j} \delta_{j,k} \varepsilon_{j,k} \Delta_j \left\{ \operatorname{Im} \left(\mathcal{F}^{-1} f_{\gamma_j}^0(-x_{j,k}) \right) - \operatorname{Re} \left(\mathcal{F}^{-1} f_{\sigma_j}^0(-x_{j,k}) \right) \right\} \right)^2 \right] \\ &+ \mathbb{E} \left[\left(2\pi \sum_{k=1}^{m_{j-1}} \delta_{j-1,k} \varepsilon_{j-1,k} \Delta_{j-1} \left\{ \operatorname{Im} \left(\mathcal{F}^{-1} f_{\gamma_j}^1(-x_{j-1,k}) \right) - \operatorname{Re} \left(\mathcal{F}^{-1} f_{\sigma_j}^1(-x_{j-1,k}) \right) \right\} \right)^2 \right], \\ &\approx 4\pi^2 \sum_{k=1}^{m_j} \delta_{j,k}^2 \Delta_j^2 \left\{ \operatorname{Im} \left(\mathcal{F}^{-1} f_{\gamma_j}^0(-x_{j,k}) \right) - \operatorname{Re} \left(\mathcal{F}^{-1} f_{\sigma_j}^0(-x_{j,k}) \right) \right\}^2 \\ &+ 4\pi^2 \sum_{k=1}^{m_{j-1}} \delta_{j-1,k}^2 \Delta_{j-1}^2 \left\{ \operatorname{Im} \left(\mathcal{F}^{-1} f_{\gamma_j}^1(-x_{j-1,k}) \right) - \operatorname{Re} \left(\mathcal{F}^{-1} f_{\sigma_j}^1(-x_{j-1,k}) \right) \right\}^2. \end{aligned}$$

Thus, the estimation of the variance of γ_j is given by

$$\begin{aligned} s_{\gamma_j}^2 &= 4\pi^2 \sum_{k=1}^{m_j} \delta_{j,k}^2 \Delta_j^2 \left\{ \operatorname{Im} \left(\mathcal{F}^{-1} f_{\gamma_j}^0(-x_{j,k}) \right) - \operatorname{Re} \left(\mathcal{F}^{-1} f_{\sigma_j}^0(-x_{j,k}) \right) \right\}^2 \\ &+ 4\pi^2 \sum_{k=1}^{m_{j-1}} \delta_{j-1,k}^2 \Delta_{j-1}^2 \left\{ \operatorname{Im} \left(\mathcal{F}^{-1} f_{\gamma_j}^1(-x_{j-1,k}) \right) - \operatorname{Re} \left(\mathcal{F}^{-1} f_{\sigma_j}^1(-x_{j-1,k}) \right) \right\}^2. \end{aligned} \quad (4.7)$$

Note that in practical application the function $\varphi_{T_{j-l}}(v-i)$ in $f_{\gamma_j}^l(v)$ and $f_{\sigma_j}^l(v)$ is not available. The estimator $\tilde{\varphi}_{T_{j-l}}(v-i)$ will therefore be used instead of $\varphi_{T_{j-l}}(v-i)$ in these functions.

Using the continuous mapping theorem and Slutsky's theorem a $(100 - \vartheta)\%$ confidence interval for $\tilde{\gamma}_j$ can be constructed by

$$\left[\tilde{\gamma}_j + z_{\vartheta/2} \cdot s_{\gamma_j}, \quad \tilde{\gamma}_j - z_{100-\vartheta/2} \cdot s_{\gamma_j} \right], \quad (4.8)$$

where z_p is the p th quantile of a standard normal distribution.

4.3 Confidence Intervals for $\tilde{\lambda}_j$

Finally, the variance of $\tilde{\lambda}_j$ will be estimated,

$$s_{\lambda_j}^2 \approx \mathbb{V}(\lambda_j) = \mathbb{E} \left[\left(\tilde{\lambda}_j - \mathbb{E}[\lambda_j] \right)^2 \right].$$

Again it has a similar line of thought as the case $\tilde{\sigma}_j^2$ and $\tilde{\gamma}_j$, so the calculations will be made rather quickly.

When combining the error decompositions (3.9), (3.10) and (3.11),

$$\begin{aligned} \tilde{\sigma}_j^2 - \sigma_j^2 &= \mathcal{L}_{\sigma_j^2}^0 - \mathcal{L}_{\sigma_j^2}^1 + \mathcal{R}_{\sigma_j^2}^0 - \mathcal{R}_{\sigma_j^2}^1 + \mathcal{B}_{\sigma_j^2}, \\ (\tilde{\gamma}_j + \tilde{\sigma}_j^2) - (\gamma_j + \sigma_j^2) &= \mathcal{L}_{\gamma_j}^0 - \mathcal{L}_{\gamma_j}^1 + \mathcal{R}_{\gamma_j}^0 - \mathcal{R}_{\gamma_j}^1 + \mathcal{B}_{\gamma_j}, \\ (\tilde{\lambda}_j - \tilde{\sigma}_j^2/2 - \tilde{\gamma}_j) - (\lambda_j - \sigma_j^2/2 - \gamma_j) &= \mathcal{L}_{\lambda_j}^0 - \mathcal{L}_{\lambda_j}^1 + \mathcal{R}_{\lambda_j}^0 - \mathcal{R}_{\lambda_j}^1 + \mathcal{B}_{\lambda_j}, \end{aligned}$$

a sole expression for $\tilde{\lambda}_j - \lambda_j$ can be found

$$\begin{aligned} \tilde{\lambda}_j - \lambda_j &= \mathcal{L}_{\lambda_j}^0 + \mathcal{L}_{\gamma_j}^0 - \frac{1}{2}\mathcal{L}_{\sigma_j^2}^0 - \mathcal{L}_{\lambda_j}^1 - \mathcal{L}_{\gamma_j}^1 + \frac{1}{2}\mathcal{L}_{\sigma_j^2}^1 \\ &\quad + \mathcal{R}_{\lambda_j}^0 + \mathcal{R}_{\gamma_j}^0 - \frac{1}{2}\mathcal{R}_{\sigma_j^2}^0 - \mathcal{R}_{\lambda_j}^1 - \mathcal{R}_{\gamma_j}^1 + \frac{1}{2}\mathcal{R}_{\sigma_j^2}^1 + \mathcal{B}_{\lambda_j} + \mathcal{B}_{\gamma_j} - \frac{1}{2}\mathcal{B}_{\sigma_j^2}. \end{aligned}$$

The assumption is made that the remainder terms $\mathcal{R}_{\lambda_j}^0, \mathcal{R}_{\lambda_j}^1, \mathcal{R}_{\gamma_j}^0, \mathcal{R}_{\gamma_j}^1, \mathcal{R}_{\sigma_j^2}^0, \mathcal{R}_{\sigma_j^2}^1$ and the bias terms $\mathcal{B}_{\lambda_j}, \mathcal{B}_{\sigma_j^2}$ can again be neglected. Thus,

$$\tilde{\lambda}_j - \lambda_j = \mathcal{L}_{\lambda_j}^0 + \mathcal{L}_{\gamma_j}^0 - \frac{1}{2}\mathcal{L}_{\sigma_j^2}^0 - \mathcal{L}_{\lambda_j}^1 - \mathcal{L}_{\gamma_j}^1 + \frac{1}{2}\mathcal{L}_{\sigma_j^2}^1.$$

Recall that

$$\begin{aligned} \mathcal{L}_{\sigma_j^2}^l &= \int_{-U_j}^{U_j} w_{\sigma_j^2}^{U_j}(v) \operatorname{Re}(\mathcal{L}_j^l(v)) dv, \quad \mathcal{L}_{\gamma_j}^l = \int_{-U_j}^{U_j} w_{\gamma_j}^{U_j}(v) \operatorname{Im}(\mathcal{L}_j^l(v)) dv, \quad \text{and} \\ \mathcal{L}_{\lambda_j}^l &= \int_{-U_j}^{U_j} w_{\lambda_j}^{U_j}(v) \operatorname{Re}(\mathcal{L}_j^l(v)) dv \quad \text{with} \quad \mathcal{L}_j^l(v) = \frac{1}{T_j - T_{j-1}} \frac{\tilde{\varphi}_{T_{j-l}}(v-i) - \varphi_{T_{j-l}}(v-i)}{\varphi_{T_{j-l}}(v-i)}. \end{aligned}$$

Using expression (3.2) the stochastic term $\tilde{\varphi}_{T_{j-l}}(v-i) - \varphi_{T_{j-l}}(v-i)$ will again be written in the approximated form

$$\begin{aligned} \tilde{\varphi}_{T_{j-l}}(v-i) - \varphi_{T_{j-l}}(v-i) &= iv(1+iv) \sum_{k=1}^{m_j} \delta_{j-l,k} \varepsilon_{j-l,k} \mathcal{F} b_{j-l,k}(v), \\ &\approx iv(1+iv) \sum_{k=1}^{m_j} \delta_{j-l,k} \varepsilon_{j-l,k} \Delta_{j-l} e^{ivx_{j-l,k}}. \end{aligned}$$

After defining the function $f_{\lambda_j}^l$ as

$$f_{\lambda_j}^l(v) := w_{\lambda_j}^{U_j}(v) \frac{iv(1+iv)}{(T_j - T_{j-1})\varphi_{T_{j-l}}(v-i)},$$

then $\mathcal{L}_{\lambda_j}^l$ can be written as

$$\begin{aligned} \mathcal{L}_{\lambda_j}^l &= \int_{-U_j}^{U_j} w_{\lambda_j}^{U_j}(v) \operatorname{Re}(\mathcal{L}_j^l(v)) dv, \\ &\approx \sum_{k=1}^{m_{j-l}} \delta_{j-l,k} \varepsilon_{j-l,k} \Delta_j \operatorname{Re} \left(\int_{-U_j}^{U_j} f_{\lambda_j}^l(v) e^{ivx_{j-l,k}} dv \right), \\ &= 2\pi \sum_{k=1}^{m_{j-l}} \delta_{j-l,k} \varepsilon_{j-l,k} \Delta_{j-l} \operatorname{Re} \left(\mathcal{F}^{-1} f_{\lambda_j}^l(-x_{j-l,k}) \right), \end{aligned} \tag{4.9}$$

where we again used that $w_{\lambda_j}^{U_j}$ is 0 outside the region $[-U_j, U_j]$.

Observing expressions (4.3), (4.6) and (4.9) it can be seen that the independence of $(\varepsilon_{j,k})$ implies that $\mathcal{L}_{\sigma_j^2}^0, \mathcal{L}_{\gamma_j}^0, \mathcal{L}_{\lambda_j}^0$ are independent of $\mathcal{L}_{\sigma_j^2}^1, \mathcal{L}_{\gamma_j}^1, \mathcal{L}_{\lambda_j}^1$. Furthermore, it is easy to see that $\mathbb{E}[\tilde{\lambda}_j] = \lambda_j$. The variance of $\tilde{\lambda}_j$ then takes the form

$$\mathbb{V}(\tilde{\lambda}_j) = \mathbb{E} \left[\left(\tilde{\lambda}_j - \lambda_j \right)^2 \right] \approx \mathbb{E} \left[\left(\mathcal{L}_{\lambda_j}^0 + \mathcal{L}_{\gamma_j}^0 - \frac{1}{2}\mathcal{L}_{\sigma_j^2}^0 \right)^2 \right] + \mathbb{E} \left[\left(\mathcal{L}_{\lambda_j}^1 + \mathcal{L}_{\gamma_j}^1 - \frac{1}{2}\mathcal{L}_{\sigma_j^2}^1 \right)^2 \right].$$

Now using expression (4.3) and (4.6) together with the fact that $(\varepsilon_{j,k})$ are independent with $\mathbb{V}(\varepsilon_{j,k}) = 1$ a final approximation of the variance can be found

$$\begin{aligned}
\mathbb{V}(\tilde{\lambda}_j) &\approx \mathbb{E} \left[\left(2\pi \sum_{k=1}^{m_j} \delta_{j,k} \varepsilon_{j,k} \Delta_j \left\{ \operatorname{Im} \left(\mathcal{F}^{-1} f_{\gamma_j}^0(-x_{j,k}) \right) \right. \right. \right. \\
&\quad \left. \left. \left. + \operatorname{Re} \left(\mathcal{F}^{-1} f_{\lambda_j}^0(-x_{j,k}) - \frac{1}{2} \mathcal{F}^{-1} f_{\sigma_j}^0(-x_{j,k}) \right) \right\} \right)^2 \right] \\
&\quad + \mathbb{E} \left[\left(2\pi \sum_{k=1}^{m_{j-1}} \delta_{j-1,k} \varepsilon_{j-1,k} \Delta_{j-1} \left\{ \operatorname{Im} \left(\mathcal{F}^{-1} f_{\gamma_j}^1(-x_{j-1,k}) \right) \right. \right. \right. \\
&\quad \left. \left. \left. + \operatorname{Re} \left(\mathcal{F}^{-1} f_{\lambda_j}^1(-x_{j-1,k}) - \frac{1}{2} \mathcal{F}^{-1} f_{\sigma_j}^1(-x_{j-1,k}) \right) \right\} \right)^2 \right] \\
&\approx 4\pi^2 \sum_{k=1}^{m_j} \delta_{j,k}^2 \Delta_j^2 \left\{ \operatorname{Im} \left(\mathcal{F}^{-1} f_{\gamma_j}^0(-x_{j,k}) \right) + \operatorname{Re} \left(\mathcal{F}^{-1} f_{\lambda_j}^0(-x_{j,k}) - \frac{1}{2} \mathcal{F}^{-1} f_{\sigma_j}^0(-x_{j,k}) \right) \right\}^2 \\
&\quad + 4\pi^2 \sum_{k=1}^{m_{j-1}} \delta_{j-1,k}^2 \Delta_{j-1}^2 \left\{ \operatorname{Im} \left(\mathcal{F}^{-1} f_{\gamma_j}^1(-x_{j-1,k}) \right) \right. \\
&\quad \left. + \operatorname{Re} \left(\mathcal{F}^{-1} f_{\lambda_j}^1(-x_{j-1,k}) - \frac{1}{2} \mathcal{F}^{-1} f_{\sigma_j}^1(-x_{j-1,k}) \right) \right\}^2.
\end{aligned}$$

Thus, the estimation of the variance of λ_j is given by

$$\begin{aligned}
s_{\lambda_j}^2 &= 4\pi^2 \sum_{k=1}^{m_j} \delta_{j,k}^2 \Delta_j^2 \left\{ \operatorname{Im} \left(\mathcal{F}^{-1} f_{\gamma_j}^0(-x_{j,k}) \right) + \operatorname{Re} \left(\mathcal{F}^{-1} f_{\lambda_j}^0(-x_{j,k}) - \frac{1}{2} \mathcal{F}^{-1} f_{\sigma_j}^0(-x_{j,k}) \right) \right\}^2 \\
&\quad + 4\pi^2 \sum_{k=1}^{m_{j-1}} \delta_{j-1,k}^2 \Delta_{j-1}^2 \left\{ \operatorname{Im} \left(\mathcal{F}^{-1} f_{\gamma_j}^1(-x_{j-1,k}) \right) \right. \\
&\quad \left. + \operatorname{Re} \left(\mathcal{F}^{-1} f_{\lambda_j}^1(-x_{j-1,k}) - \frac{1}{2} \mathcal{F}^{-1} f_{\sigma_j}^1(-x_{j-1,k}) \right) \right\}^2. \quad (4.10)
\end{aligned}$$

Note that in practical application the function $\varphi_{T_{j-l}}(v-i)$ in $f_{\lambda_j}^l(v)$, $f_{\gamma_j}^l(v)$ and $f_{\sigma_j}^l(v)$ is not available. The estimator $\tilde{\varphi}_{T_{j-l}}(v-i)$ will therefore be used instead of $\varphi_{T_{j-l}}(v-i)$ in these functions.

Using the continuous mapping theorem and Slutsky's theorem a $(100 - \vartheta)\%$ confidence interval for $\tilde{\lambda}_j$ can be constructed by

$$\left[\tilde{\lambda}_j + z_{\vartheta/2} \cdot s_{\lambda_j}, \quad \tilde{\lambda}_j - z_{100-\vartheta/2} \cdot s_{\lambda_j} \right], \quad (4.11)$$

where z_p is the p th quantile of a standard normal distribution.

4.4 Confidence Intervals for $\tilde{\nu}_j(x)$

In the theoretical part, out of convenience, we derived the asymptotic normality of the exponentially weighted jump density $\tilde{\mu}_j(x) = e^x \tilde{\nu}_j(x)$, instead of the density $\nu_j(x)$. However, in the statistical model, we already mentioned that estimating $\tilde{\nu}_j(x)$ directly in practical cases is more stable than estimating $\tilde{\mu}_j(x)$. Therefore, the finite sample variance confidence intervals will also be made for $\tilde{\nu}_j(x)$ directly.

For constructing confidence intervals the variance of the estimator $\tilde{\nu}_j^2$ at a certain point x will be estimated,

$$s_{\nu_j}^2(x) \approx \mathbb{V}(\tilde{\nu}_j(x)) = \mathbb{E} \left[(\tilde{\nu}_j(x) - \mathbb{E}[\tilde{\nu}_j(x)])^2 \right],$$

where after the assumptions we will later see that $\mathbb{E}[\tilde{\nu}_j(x)] = \nu_j(x)$. The case of $\tilde{\nu}_j$ is different from previous cases, because – as can be seen in expression (2.17) – here we had the shifted estimator $\tilde{\psi}_{\nu_j}(v) = \tilde{\psi}_j(v + i)$ and an inverse Fourier transform \mathcal{F}^{-1} . Similar to $\tilde{\mu}_j(x)$ the error decomposition of $\tilde{\nu}_j(x)$ can be written as

$$\begin{aligned} \tilde{\nu}_j(x) - \nu_j(x) &= \frac{1}{2\pi} \left[\int_{-U_j}^{U_j} (\tilde{\psi}_{\nu_j}(v) - \psi_{\nu_j}(v)) w_{\nu_j}^{U_j}(v) e^{-ivx} dv + \frac{\tilde{\sigma}_j^2 - \sigma_j^2}{2} \int_{-U_j}^{U_j} v^2 w_{\nu_j}^{U_j}(v) e^{-ivx} dv \right. \\ &\quad - i(\tilde{\gamma}_j - \gamma_j) \int_{-U_j}^{U_j} v w_{\nu_j}^{U_j}(v) e^{-ivx} dv + (\tilde{\lambda}_j - \lambda_j) \int_{-U_j}^{U_j} w_{\nu_j}^{U_j}(v) e^{-ivx} dv \\ &\quad \left. + \int_{\mathbb{R} \setminus [-U_j, U_j]} \left(\psi_{\nu_j}(v) + \frac{\sigma_j^2}{2} v^2 - i\gamma_j v + \lambda_j \right) (1 - w_{\nu_j}^{U_j}(v)) e^{-ivx} dv \right] \\ &=: \Psi + \Sigma + \Gamma + \Lambda + \mathcal{B}, \end{aligned}$$

where Ψ can be written in linear terms $\mathcal{L}_j^0, \mathcal{L}_j^1$ and remainder terms $\mathcal{R}_j^0, \mathcal{R}_j^1$,

$$\begin{aligned} \Psi &= \frac{1}{2\pi} \int_{-U_j}^{U_j} [\mathcal{L}_j^0(v) - \mathcal{L}_j^1(v) + \mathcal{R}_j^0(v) - \mathcal{R}_j^1(v)] w_{\nu_j}^{U_j}(v) e^{-ivx} dv, \\ &=: \mathcal{L}_{\nu_j}^0 - \mathcal{L}_{\nu_j}^1 + \mathcal{R}_{\nu_j}^0 - \mathcal{R}_{\nu_j}^1. \end{aligned}$$

Note that in $\tilde{\nu}_j(x) - \nu_j(x)$ all the other terms $\tilde{\sigma}_j^2 - \sigma_j^2$, $\tilde{\gamma}_j - \gamma_j$ and $\tilde{\lambda}_j - \lambda_j$ appear. All these terms are multiplied by integrals, which can be recognized as inverse Fourier Transforms. These transforms are well-defined by the conditions $w_{\nu_j}^{U_j} \in \mathcal{W}_{s_j}^n$. For conciseness of notation of these transforms, the function $g_{U_j}^k$ for $k = 0, 1, 2$ will be introduced as

$$g_{U_j}^{(k)}(x) := \mathcal{F}^{-1} \left[v^k w_{\nu_j}^{U_j}(v) \right] (x). \quad (4.12)$$

For general weight functions, $w_{\nu_j}^{U_j}(v)$ the function $g_{U_j}^k(x)$ is not necessarily analytically solvable, and will therefore be approximated numerically in the computer script. If, as with the previous cases, the assumptions are made that the bias term \mathcal{B} and remainder terms $\mathcal{R}_j^0, \mathcal{R}_j^1$ can be neglected, together with expression (4.12), then $\tilde{\nu}_j(x) - \nu_j(x)$ can be written as

$$\tilde{\nu}_j(x) - \nu_j(x) = \mathcal{L}_{\nu_j}^0 - \mathcal{L}_{\nu_j}^1 + \frac{\tilde{\sigma}_j^2 - \sigma_j^2}{2} g_{U_j}^{(2)}(x) - i(\tilde{\gamma}_j - \gamma_j) g_{U_j}^{(1)}(x) + (\tilde{\lambda}_j - \lambda_j) g_{U_j}^{(0)}(x).$$

From the previous sections, recall the approximations

$$\begin{aligned} \tilde{\sigma}_j^2 - \sigma_j^2 &\approx \mathcal{L}_{\sigma_j^2}^0 - \mathcal{L}_{\sigma_j^2}^1, \\ \tilde{\gamma}_j - \gamma_j &\approx \mathcal{L}_{\gamma_j}^0 - \mathcal{L}_{\sigma_j^2}^0 - \mathcal{L}_{\gamma_j}^1 + \mathcal{L}_{\sigma_j^2}^1 \\ \tilde{\lambda}_j - \lambda_j &\approx \mathcal{L}_{\lambda_j}^0 + \mathcal{L}_{\gamma_j}^0 - \frac{1}{2} \mathcal{L}_{\sigma_j^2}^0 - \mathcal{L}_{\lambda_j}^1 - \mathcal{L}_{\gamma_j}^1 + \frac{1}{2} \mathcal{L}_{\sigma_j^2}^1. \end{aligned}$$

Substituting these expressions and aligning all the terms with $l = 0$ and $l = 1$, then gives

$$\begin{aligned} \tilde{\nu}_j(x) - \nu_j(x) &= \left\{ \mathcal{L}_{\nu_j}^0 + \mathcal{L}_{\sigma_j^2}^0 \left(\frac{1}{2} g_{U_j}^{(2)}(x) + i g_{U_j}^{(1)}(x) - \frac{1}{2} g_{U_j}^{(0)}(x) \right) + \mathcal{L}_{\gamma_j}^0 \left(-i g_{U_j}^{(1)}(x) + g_{U_j}^{(0)}(x) \right) \right. \\ &\quad \left. + \mathcal{L}_{\lambda_j}^0 g_{U_j}^{(0)}(x) \right\} - \left\{ \mathcal{L}_{\nu_j}^1 + \mathcal{L}_{\sigma_j^2}^1 \left(\frac{1}{2} g_{U_j}^{(2)}(x) + i g_{U_j}^{(1)}(x) - \frac{1}{2} g_{U_j}^{(0)}(x) \right) \right. \\ &\quad \left. + \mathcal{L}_{\gamma_j}^1 \left(-i g_{U_j}^{(1)}(x) + g_{U_j}^{(0)}(x) \right) + \mathcal{L}_{\lambda_j}^1 g_{U_j}^{(0)}(x) \right\}. \quad (4.13) \end{aligned}$$

Simplified expression for $\mathcal{L}_{\sigma_j^2}^l$, $\mathcal{L}_{\gamma_j}^l$ and $\mathcal{L}_{\lambda_j}^l$ were already respectively derived in expression (4.3), (4.6) and (4.9). Thus, we only still need to derive a simplified expression for $\mathcal{L}_{\nu_j}^l$. In persuasion of this, recall that

$$\mathcal{L}_{\nu_j}^l = \frac{1}{2\pi} \int_{-U_j}^{U_j} \mathcal{L}_{\nu_j}^l(v) w_{\nu_j}^{U_j}(v) e^{-ivx} dv,$$

with

$$\mathcal{L}_{\nu_j}^l(v) = \frac{1}{T_j - T_{j-1}} \frac{\tilde{\varphi}_{\nu_j, T_{j-l}}(v-i) - \varphi_{\nu_j, T_{j-l}}(v-i)}{\varphi_{\nu_j, T_{j-l}}(v-i)} = \frac{1}{T_j - T_{j-1}} \frac{\tilde{\varphi}_{T_{j-l}}(v) - \varphi_{T_{j-l}}(v)}{\varphi_{T_{j-l}}(v)}.$$

Using expression (3.2) the stochastic term $\tilde{\varphi}_{T_{j-l}}(v) - \varphi_{T_{j-l}}(v)$ will be written in the more basic form

$$\tilde{\varphi}_{T_{j-l}}(v) - \varphi_{T_{j-l}}(v) = -v(v+i) \sum_{k=1}^{m_j} \delta_{j-l, k} \varepsilon_{j-l, k} \mathcal{F} b_{j-l, k}(v+i).$$

Following the same line of thought as (4.2), but then with $\mathcal{F} b_{j-l, k}(v+i)$ instead of $\mathcal{F} b_{j-l, k}(v)$, an approximation for $\mathcal{F} b_{j-l, k}(v+i)$ is

$$\begin{aligned} \mathcal{F} b_{j-l, k}(v+i) &= \int_{\mathbb{R}} b_{j-l, k}(x) e^{i(v+i)x} dx = \int_{\mathbb{R}} b_{j-l, k}(x) e^{-x} e^{ivx} dx \\ &\approx \frac{x_{j-l, k+1} - x_{j-l, k-1}}{2} e^{-x_{j-l, k}} e^{ivx_{j-l, k}} = \Delta_{j-l} e^{-x_{j-l, k}} e^{ivx_{j-l, k}} \end{aligned} \quad (4.14)$$

where we used the equidistant grid $\Delta_{j-l} = |x_{j-l, k+1} - x_{j-l, k}| = |x_{j-l, k} - x_{j-l, k-1}|$.

The following convenient function $f_{\nu_j}^l$ is defined as

$$f_{\nu_j}^l(v) := -w_{\nu_j}^{U_j}(v) \frac{v(v+i)}{(T_j - T_{j-1}) \varphi_{T_{j-l}}(v-i)},$$

then also using (4.14) the term $\mathcal{L}_{\nu_j}^l$ can be written as

$$\begin{aligned} \mathcal{L}_{\nu_j}^l &= \frac{1}{2\pi} \int_{-U_j}^{U_j} \mathcal{L}_{\nu_j}^l(v) w_{\nu_j}^{U_j}(v) e^{-ivx} dv \\ &= \frac{1}{2\pi} \int_{-U_j}^{U_j} w_{\nu_j}^{U_j}(v) \frac{1}{T_j - T_{j-1}} \frac{-v(v+i) \sum_{k=1}^{m_j-l} \delta_{j-l, k} \varepsilon_{j-l, k} \mathcal{F} b_{j-l, k}(v+i)}{\varphi_{T_{j-l}}(v)} e^{-ivx} dv \\ &= \frac{1}{2\pi} \int_{-U_j}^{U_j} f_{\nu_j}^l(v) \sum_{k=1}^{m_j-l} \delta_{j-l, k} \varepsilon_{j-l, k} \mathcal{F} b_{j-l, k}(v+i) e^{-ivx} dv \\ &\approx \frac{1}{2\pi} \int_{-U_j}^{U_j} f_{\nu_j}^l(v) \sum_{k=1}^{m_j-l} \delta_{j-l, k} \varepsilon_{j-l, k} \Delta_j e^{-x_{j-l, k}} e^{ivx_{j-l, k}} e^{-ivx} dv \\ &= \frac{1}{2\pi} \sum_{k=1}^{m_j-l} \delta_{j-l, k} \varepsilon_{j-l, k} \Delta_j e^{-x_{j-l, k}} \int_{-U_j}^{U_j} f_{\nu_j}^l(v) e^{-iv(x-x_{j-l, k})} dv. \end{aligned} \quad (4.15)$$

Note that by the definition of the class $\mathcal{W}_{s_j}^n$, it was that $w_{\nu_j}^{U_j} \in \mathcal{W}_{s_j}^n$ is 0 outside the region $[-U_j, U_j]$, thus

$$\int_{-U_j}^{U_j} f_{\nu_j}^l(v) e^{-iv(x-x_{j-l, k})} dv = 2\pi \frac{1}{2\pi} \int_{\mathbb{R}} f_{\nu_j}^l(v) e^{-iv(x-x_{j-l, k})} dv = 2\pi \mathcal{F}^{-1} f_{\nu_j}^l(x - x_{j-l, k})$$

and the following expression for (4.3) is found

$$\mathcal{L}_{\nu_j^2}^l = 2\pi \sum_{k=1}^{m_j-l} \frac{e^{-x_{j-l,k}}}{2\pi} \delta_{j-l,k} \varepsilon_{j-l,k} \Delta_{j-l} \mathcal{F}^{-1} f_{\nu_j}^l(x - x_{j-l,k}). \quad (4.16)$$

Observing expressions (4.3), (4.6), (4.9) and (4.16) it can be seen that the independence of $(\varepsilon_{j,k})$ implies that $\mathcal{L}_{\sigma_j^2}^0, \mathcal{L}_{\gamma_j}^0, \mathcal{L}_{\lambda_j}^0$ and $\mathcal{L}_{\nu_j}^0$ are independent of $\mathcal{L}_{\sigma_j^2}^1, \mathcal{L}_{\gamma_j}^1, \mathcal{L}_{\lambda_j}^1$ and $\mathcal{L}_{\nu_j}^1$. Furthermore, it is easy to see in (4.13) that $\mathbb{E}[\tilde{\nu}_j(x)] = \nu_j(x)$, because $\mathbb{E}[\mathcal{L}_{\xi_j}^l] = 0$ for all $\xi_j \in \{\sigma_j^2, \gamma_j, \lambda_j, \nu_j\}$. Having this in mind and using expression (4.13) the variance of $\tilde{\nu}_j$ at a certain point x takes the form

$$\begin{aligned} \mathbb{V}(\tilde{\nu}_j(x)) &\approx \mathbb{E} \left[(\tilde{\nu}_j(x) - \nu_j(x))^2 \right] \\ &\approx \mathbb{E} \left[\left\{ \mathcal{L}_{\nu_j}^0 + \mathcal{L}_{\sigma_j^2}^0 \left(\frac{1}{2} g_{U_j}^{(2)}(x) + i g_{U_j}^{(1)}(x) - \frac{1}{2} g_{U_j}^{(0)}(x) \right) + \mathcal{L}_{\gamma_j}^0 \left(-i g_{U_j}^{(1)}(x) + g_{U_j}^{(0)}(x) \right) \right. \right. \\ &\quad \left. \left. + \mathcal{L}_{\lambda_j}^1 g_{U_j}^{(0)}(x) \right\}^2 \right] + \mathbb{E} \left[\left\{ \mathcal{L}_{\nu_j}^1 + \mathcal{L}_{\sigma_j^2}^1 \left(\frac{1}{2} g_{U_j}^{(2)}(x) + i g_{U_j}^{(1)}(x) - \frac{1}{2} g_{U_j}^{(0)}(x) \right) \right. \right. \\ &\quad \left. \left. + \mathcal{L}_{\gamma_j}^1 \left(-i g_{U_j}^{(1)}(x) + g_{U_j}^{(0)}(x) \right) + \mathcal{L}_{\lambda_j}^1 g_{U_j}^{(0)}(x) \right\}^2 \right]. \end{aligned}$$

Substituting all approximations for $\mathcal{L}_{\sigma_j^2}^l, \mathcal{L}_{\gamma_j}^l, \mathcal{L}_{\lambda_j}^l$ and $\mathcal{L}_{\nu_j}^l$ (respectively given in expression (4.3), (4.6), (4.9) and (4.16)) into the approximation of $\mathbb{V}(\tilde{\nu}_j(x))$ gives

$$\begin{aligned} \mathbb{V}(\tilde{\nu}_j(x)) &\approx \mathbb{E} \left[\left\{ 2\pi \sum_{k=1}^{m_j} \delta_{j,k} \varepsilon_{j,k} \Delta_j \left(\frac{e^{-x_{j,k}}}{2\pi} \mathcal{F}^{-1} f_{\nu_j}^0(x - x_{j,k}) \right. \right. \right. \\ &\quad \left. \left. + \operatorname{Re} \left(\mathcal{F}^{-1} f_{\sigma_j}^0(-x_{j,k}) \right) \left(\frac{1}{2} g_{U_j}^{(2)}(x) + i g_{U_j}^{(1)}(x) - \frac{1}{2} g_{U_j}^{(0)}(x) \right) \right. \right. \\ &\quad \left. \left. + \operatorname{Im} \left(\mathcal{F}^{-1} f_{\gamma_j}^0(-x_{j,k}) \right) \left(-i g_{U_j}^{(1)}(x) + g_{U_j}^{(0)}(x) \right) + \operatorname{Re} \left(\mathcal{F}^{-1} f_{\lambda_j}^0(-x_{j,k}) \right) g_{U_j}^{(0)}(x) \right\}^2 \right] \\ &+ \mathbb{E} \left[\left\{ 2\pi \sum_{k=1}^{m_j-1} \delta_{j-1,k} \varepsilon_{j-1,k} \Delta_{j-1} \left(\frac{e^{-x_{j-1,k}}}{2\pi} \mathcal{F}^{-1} f_{\nu_j}^1(x - x_{j-1,k}) \right. \right. \right. \\ &\quad \left. \left. + \operatorname{Re} \left(\mathcal{F}^{-1} f_{\sigma_j}^1(-x_{j-1,k}) \right) \left(\frac{1}{2} g_{U_j}^{(2)}(x) + i g_{U_j}^{(1)}(x) - \frac{1}{2} g_{U_j}^{(0)}(x) \right) \right. \right. \\ &\quad \left. \left. + \operatorname{Im} \left(\mathcal{F}^{-1} f_{\gamma_j}^1(-x_{j-1,k}) \right) \left(-i g_{U_j}^{(1)}(x) + g_{U_j}^{(0)}(x) \right) + \operatorname{Re} \left(\mathcal{F}^{-1} f_{\lambda_j}^1(-x_{j-1,k}) \right) g_{U_j}^{(0)}(x) \right\}^2 \right]. \end{aligned}$$

Now using that $(\varepsilon_{j,k})$ were centered independent random variables with $\mathbb{V}[\varepsilon_{j,k}] = 1$ gives the approximation $s_{\nu_j}^2(x)$ of the variance $\mathbb{V}(\tilde{\nu}_j(x))$,

$$\begin{aligned} s_{\nu_j}^2(x) &\approx 4\pi^2 \sum_{k=1}^{m_j} \delta_{j,k}^2 \Delta_j^2 \left(\frac{e^{-x_{j,k}}}{2\pi} \mathcal{F}^{-1} f_{\nu_j}^0(x - x_{j,k}) \right. \\ &\quad \left. + \operatorname{Re} \left(\mathcal{F}^{-1} f_{\sigma_j}^0(-x_{j,k}) \right) \left(\frac{1}{2} g_{U_j}^{(2)}(x) + i g_{U_j}^{(1)}(x) - \frac{1}{2} g_{U_j}^{(0)}(x) \right) \right. \\ &\quad \left. + \operatorname{Im} \left(\mathcal{F}^{-1} f_{\gamma_j}^0(-x_{j,k}) \right) \left(-i g_{U_j}^{(1)}(x) + g_{U_j}^{(0)}(x) \right) + \operatorname{Re} \left(\mathcal{F}^{-1} f_{\lambda_j}^0(-x_{j,k}) \right) g_{U_j}^{(0)}(x) \right)^2 \\ &+ 4\pi^2 \sum_{k=1}^{m_j-1} \delta_{j-1,k}^2 \Delta_{j-1}^2 \left(\frac{e^{-x_{j-1,k}}}{2\pi} \mathcal{F}^{-1} f_{\nu_j}^1(x - x_{j-1,k}) \right. \end{aligned}$$

$$\begin{aligned}
& + \operatorname{Re} \left(\mathcal{F}^{-1} f_{\sigma_j}^1(-x_{j-1,k}) \right) \left(\frac{1}{2} g_{U_j}^{(2)}(x) + i g_{U_j}^{(1)}(x) - \frac{1}{2} g_{U_j}^{(0)}(x) \right) \\
& + \operatorname{Im} \left(\mathcal{F}^{-1} f_{\gamma_j}^1(-x_{j-1,k}) \right) \left(-i g_{U_j}^{(1)}(x) + g_{U_j}^{(0)}(x) \right) + \operatorname{Re} \left(\mathcal{F}^{-1} f_{\lambda_j}^1(-x_{j-1,k}) \right) g_{U_j}^{(0)}(x) \Big)^2.
\end{aligned}$$

Note that in practical application the function $\varphi_{T_{j-l}}(v)$ in $f_{\lambda_j}^l(v)$, $f_{\gamma_j}^l(v)$, $f_{\sigma_j}^l(v)$ and $f_{\nu_j}^l(v)$ is not available. The estimator $\tilde{\varphi}_{T_{j-l}}(v)$ will therefore be used instead of $\varphi_{T_{j-l}}(v)$ in these functions.

Using the continuous mapping theorem and Slutsky's theorem a $(100 - \vartheta)\%$ confidence interval for $\tilde{\nu}_j(x)$ can be constructed by

$$\left[\tilde{\nu}_j(x) + z_{\vartheta/2} \cdot s_{\nu_j}(x), \quad \tilde{\nu}_j(x) - z_{100-\vartheta/2} \cdot s_{\nu_j}(x) \right], \quad (4.17)$$

where z_p is the p th quantile of a standard normal distribution.

Expression (4.17) is a confidence interval for $\tilde{\nu}_j(x)$ at a *fixed point* x , and is *not* a confidence band. In applications, we, therefore, need to choose points x in which at every point x expression (4.17) is evaluated — we do not have an upper and lower function.

Chapter 5

Simulations

In this chapter, we will test the calibration model with simulated data ¹. The goal is to evaluate how accurate the estimations are, inspect the difficulty of the inverse calibration problem, look at how the bias and stochastic variance trade-off takes place for finite samples, and test the performance of the finite sample confidence intervals. At the end of the chapter, we want to have a general insight into the properties and performance of the time-inhomogeneous model, such that we can apply the model to market data in the next chapter.

Before the calibrations take place, we first need to construct an underlying model. Some open-ended questions need to be addressed for constructing this model, e.g., which underlying time-inhomogeneous price process S_t will be used and how do we construct the option prices \mathcal{O}_j from S_t . Furthermore, some calibration settings also need to be addressed, e.g., how do we choose the cut-off value U_j in a data-driven manner, and what weight functions are appropriate? All these questions will first be answered in section 5.1, hereafter we will evaluate the results in section 5.2.

5.1 Simulation Settings

Before the calibration algorithm can be tested on simulations, there are some important decisions and settings to be made, namely

1. How do we choose the cut-off parameters U_j and U_{ν_j} ?
2. Which weight functions in the classes $\mathcal{W}_{s_j}^n$ do we choose?
3. What underlying time-inhomogeneous Lévy model S_t will be calibrated?
4. How are the option prices \mathcal{O} simulated from S_t and how do we choose the design points $\mathcal{O}_{j,k}$, distribution of the noise $(\varepsilon_{j,k})$, and magnitude of the noise $\delta_{j,k}$?
5. How do we numerically approximate the Fourier transform \mathcal{F} ?

All these questions will respectively be elucidated in the following sections.

5.1.1 Choice of Cut-off Parameters U_j and U_{ν_j}

The most important tuning parameters are the cut-off frequencies U_j for $(\tilde{\sigma}_j^2, \tilde{\gamma}_j, \tilde{\lambda}_j)$ and U_{ν_j} for $\tilde{\nu}_j$ in the time period $T_j - T_{j-1}$. Note that, due to the underlying nonlinear 'change point detection'-structure, a proper mathematical analysis for the data-driven parameters U_j and U_{ν_j} — even in the idealized linear setting — is not found yet [24]. However, we can propose some well-known methods that choose U_j and U_{ν_j} in a data-driven practical manner.

An intuitive method that comes to mind in simulations is the *oracle* method, in which the a priori knowledge of the parameters is used to find the best cut-off value.

Method 5.1 (Oracle) Choose U_j^* and $U_{\nu_j}^*$ such that the L^1 -distance off the estimators $(\tilde{\sigma}_j^2, \tilde{\gamma}_j, \tilde{\lambda}_j)$ and $\tilde{\nu}_j$ with respect to the true values $(\sigma_j^2, \gamma_j, \lambda_j)$ and ν_j is minimized,

¹ Computer code has been made in the computational program R. The code can be found at the GitHub page: <https://github.com/Loek44/Spectral-Calibration-of-Time-Inhomogeneous-Levy-processes>

$$U_j^* = \arg \min_{U_j > 0} \|(\tilde{\sigma}_j^2, \tilde{\gamma}_j, \tilde{\lambda}_j) - (\sigma_j^2, \gamma_j, \lambda_j)\|_{L^1} \quad \text{and} \quad U_{\nu_j}^* = \arg \min_{U_j > 0} \|\tilde{\nu}_j(x) - \tilde{\nu}_j(x)\|_{L^1}.$$

A drawback of this method is that it cannot be used in the case of empirical data because the underlying parameters are unknown. The *flat* method can be used in such a case. The flat method finds the flattest region for all estimates of the parameters, i.e., the region where the estimators stabilize.

Method 5.2 (Flat) Choose U_j^* and $U_{\nu_j}^*$ that correspond to the point where the estimators stabilize,

$$U_j^* = \arg \min_{U_j > 0} \left(\left| \frac{d}{dU_j} \sigma_j(U_j) \right| + \alpha U_j \right), \quad \alpha > 0 \quad \text{and} \quad U_{\nu_j}^* = \arg \min_{0 < U_{\nu_j} < U_j^*} \left\| \frac{d}{dU_j} \nu_j(U_j) \right\|_{L^2}.$$

From practical results, it is found that this method works well in practice where the underlying model follows an exponential Lévy model (See Bauer and Reiß [1] for theoretical arguments why this is the case). However, with empirical data, it is less obvious to find the region where the estimators stabilize because the data is only approximated by a time-inhomogeneous Exponential Lévy model. For empirical data, the next method is preferred.

The last method, introduced by Cont and Tankov [16], is the partial least squares (*PLS*) method, which chooses the best Lévy triplet $(\sigma_j^2, \gamma_j, \nu_j)$ whose implied option function $\tilde{\mathcal{O}}_{(\sigma_j^2, \gamma_j, \nu_j)}$ is closest, in L^2 sense, to the smoothed spline $\tilde{\mathcal{O}}_j$.

Method 5.3 (PLS) Choose U_j^* that minimizes the L^2 -distance between the implied option function $\tilde{\mathcal{O}}_{(\sigma_j^2, \gamma_j, \nu_j)}$ and the smoothing spline $\tilde{\mathcal{O}}_j$ where over-fitting is penalized by the factor α ,

$$U_j^* = \arg \min_{U_j > 0} \left[\left\| \tilde{\mathcal{O}}_{(\sigma_j^2, \gamma_j, \nu_j)}(x) - \tilde{\mathcal{O}}_j(x) \right\|_{L^2} + \alpha \int_{\mathbb{R}} |\tilde{\nu}_{U_j}''(x)|^2 dx \right].$$

The over-fitting parameter α was introduced by [10] for theoretical consideration to avoid over-fitting. Nevertheless, [44] show from practical experience with this method that the correction procedure of the Lévy densities for the shape restriction (2.18) leads to an auto-penalization. Due to the Fourier techniques, a rigorous fit leads to high fluctuations of the estimator of the nonparametric part. Thus, the correction procedure has a significant effect, which in turn worsens the fit.

The PLS method needs a minimization procedure to find the implied option function and is therefore considerably slower than the other two methods. Furthermore, the PLS method better fits the option price function, whereas the oracle and flat method better fit the Lévy triplet for simulations. Note that the PLS method, by the excellent estimation of the option price function, opens a way to estimate the underlying noise with real data – this noise can be used in the construction of confidence intervals.

5.1.2 Choice of Weight Functions

The literature of Belomestny and Reiß [7] and Söhl and Trabs [44] both provide different choices of the weight functions that satisfy the conditions of the set $\mathcal{W}_{s_j}^n$ in definition (3.2). The weight functions of [44] are however preferred to the weight functions of [7]. The reason is that the noise is particularly large in the high frequencies and thus it is desirable to assign less weight to these frequencies. Smoothly transitioning the weight function to 0 at the cut-off value slightly improves the results. With this in mind, we would like the weight functions and the first two derivatives of the weight functions to be 0 at the cut-off value.

The weight functions then become

$$\begin{aligned}
w_{\sigma_j}^1(v) &= c_{\sigma} \left((2s_j + 1)v^{2s_j} - (8s_j + 12)v^{2s_j+2} + (12s_j + 30)v^{2s_j+4} \right. \\
&\quad \left. - (8s_j + 32)v^{2s_j+6} + (2s_j + 9)v^{2s_j+8} \right) \mathbb{1}_{\{|v| \leq 1\}}, \\
w_{\gamma_j}^1(v) &= c_{\gamma} (v^{2s_j+1} - 3v^{2s_j+3} + 3v^{2s_j+5} - v^{2s_j+7}) \mathbb{1}_{\{|v| \leq 1\}}, \\
w_{\lambda_j}^1(v) &= c_{\lambda} \left((2s_j + 3)v^{2s_j} - (8s_j + 20)v^{2s_j+2} + (12s_j + 42)v^{2s_j+4} \right. \\
&\quad \left. - (8s_j + 36)v^{2s_j+6} + (2s_j + 11)v^{2s_j+8} \right) \mathbb{1}_{\{|v| \leq 1\}}, \\
w_{\nu_j}^1(v) &= \mathbb{1}_{\{|v| \leq 0.05\}} + \exp \left(-\frac{e^{-(|v|-0.05)^{-2}}}{(|v|-1)^2} \right) \mathbb{1}_{\{0.05 < |v| < 1\}},
\end{aligned}$$

where c_{σ} , c_{γ} and c_{λ} are normalization constants such that the conditions in section 2.4 of the weight functions are satisfied. Note that w_{ν_j} is just the flat top kernel. Figure 5.1 shows, for example, a plot of the weight functions $w_{\sigma_j}^1(v)$, $w_{\gamma_j}^1(v)$, $w_{\lambda_j}^1(v)$ functions with $s_j = 2$.

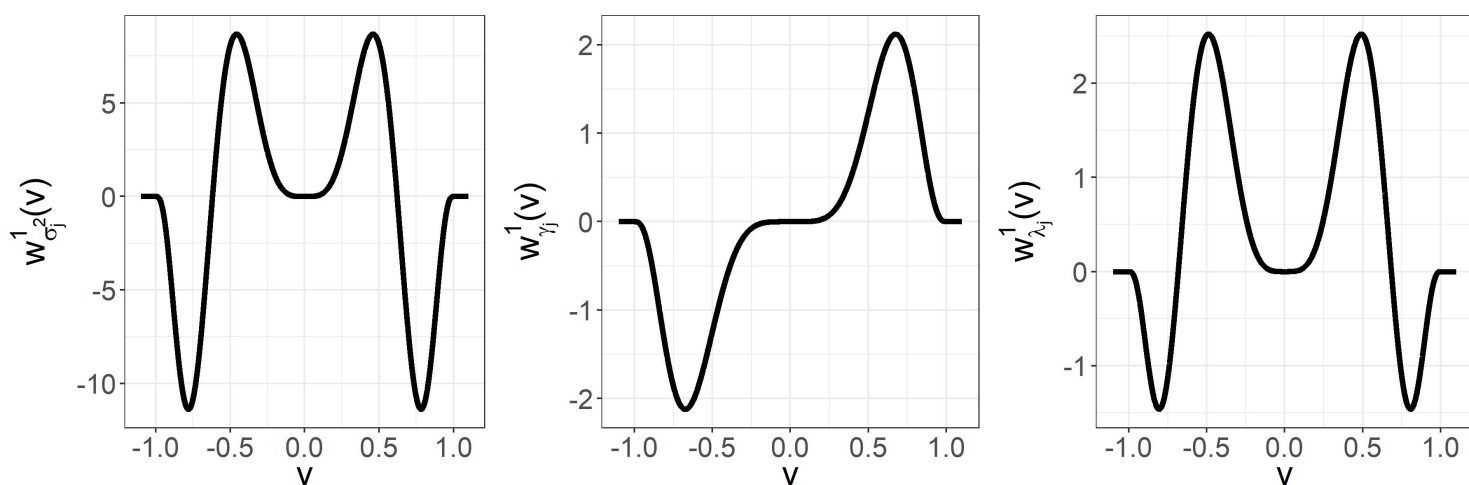


Fig. 5.1: Plots of the weight functions $w_{\sigma_j}^1(v)$, $w_{\gamma_j}^1(v)$ and $w_{\lambda_j}^1(v)$ proposed by [44] with underlying smoothness assumption of the density $s_j = 2$.

An important point to make is that one should remember that for the theoretical results the weight functions are forbidden from being zero at the cut-off value. This is an argument to use the weight functions of [7]. However, practical results show that the usage of weight functions that equal zero at the cut-off value improves upon the theoretical results, i.e., the root-mean-square errors of the estimators become smaller.

The value s_j in the weight functions denotes the smoothness of the underlying jump density ν_j and has the same meaning as the order of the kernel in nonparametric estimation. As with classical kernel estimators, the exact choice of the weight functions in spectral estimation is not very critical, although, as argued, the weight functions of [44] are slightly preferred. Still, the global error will be mostly due to the estimation of the cut-off value U_j .

5.1.3 Simulation of Exponential Time-Inhomogeneous Lévy Model

A time-inhomogeneous exponential Lévy model $S_t = S_0 e^{rt + X_t}$ with X_t a time-inhomogeneous Lévy process, as in Definition 1.4, needs to be constructed to test our calibrations. In other words, we need to provide maturities $(T_j)_{j=1, \dots, n}$ and provide within these maturities $T_j - T_{j-1}$ exponential Lévy processes with triplet $(\sigma_j^2, \gamma_j, \nu_j)$.

The spectral calibration algorithm was derived to be applicable to Lévy processes with a jump component of finite activity and an absolutely continuous jump measure. The reason for this was that empirical financial data also mostly satisfies these properties, e.g., infinitely many small jumps are generally not observed in financial data. For interest in the theoretical infinite activity in a homogeneous setting see [4].

Typical parametric sub-models of the finite activity case are the Merton model [33] and the double exponential/Kou model [31].

Model 5.1 (Merton) *The Merton model is a jump-diffusion finite activity Lévy process with volatility σ , drift γ , and jump intensity λ , where the jumps are normally distributed with mean μ and standard deviation δ , or, equivalently, the Lévy density is*

$$\nu(x) = \frac{\lambda}{\delta\sqrt{2\pi}} e^{-\frac{(x-\mu)^2}{2\delta^2}}.$$

An easy derivation is to obtain that the martingale condition (2.4) for the Merton model is satisfied whenever

$$\frac{\sigma^2}{2} + \gamma + \lambda(e^{\frac{\delta^2}{2} + \mu} - 1) = 0. \quad (5.1)$$

Model 5.2 (Kou) *The double exponential or Kou model is a jump-diffusion finite activity Lévy process with volatility σ , drift γ , and jump intensity λ , where the jumps are double exponentially distributed with positive intensity λ_+ , negative intensity λ_- , and probability parameter $p \in [0, 1]$, this gives the Lévy density*

$$\nu(x) = \lambda (p\lambda_+ e^{-\lambda_+ x} \mathbb{1}_{\{x \in [0, \infty)\}} + (1-p)\lambda_- e^{\lambda_- x} \mathbb{1}_{\{x \in (-\infty, 0)\}}).$$

First of all, we want the Kou model to be continuous at $x = 0$, this is the case if we choose $p = \frac{\lambda_-}{\lambda_+ + \lambda_-}$. Furthermore, the Kou model satisfies the martingale condition (2.4) whenever,

$$\frac{\sigma^2}{2} + \gamma + \lambda \left(\frac{p}{\lambda_+ - 1} - \frac{1-p}{\lambda_- + 1} \right) = 0. \quad (5.2)$$

The double exponential jump density in the Kou model is difficult — but still significantly accurate — to estimate because of the non-differentiability at zero. Smoother estimates than the Kou model correspond to better representations seen from empirical data and, therefore, the Merton model is preferred to calibrate the simulations.

For example, we will construct a model with three maturities $(T_j)_{j=1,2,3}$ with homogeneous spacings of a week apart $T_j - T_{j-1} = \frac{1}{52}$ for all $j = 1, 2, 3$. Between these maturities, three Merton models operate with parameters $(\sigma_j, \gamma_j, \lambda_j, \mu_j, \delta_j)_{j=1,2,3}$ given in Table 5.1. The drift parameters $(\gamma_j)_{j=1,2,3}$ were calculated such that the martingale condition of the Merton model (5.1) is satisfied.

The importance of the satisfaction of the martingale condition lies in the fact that if the martingale condition is unsatisfied, then the right expression of the pricing formula in Proposition 2.9 (iv), i.e.

$$\mathcal{F}(\mathcal{O}_j(x))(v) = \int_{-\infty}^{\infty} \mathcal{O}_j(x) e^{ivx} dx = \frac{1 - \varphi_{T_j}(v - i)}{v(v - i)},$$

might have a singularity at zero. We can then not apply the inverse Fourier transform to construct an option function for simulations.

	σ_j	γ_j	λ_j	μ_j	δ_j
$j = 1$	0.2	0.3644183	5	-0.1	0.2
$j = 2$	0.1	0.1597298	2	-0.2	0.4
$j = 3$	0.3	0.1155446	3	-0.1	0.3

Table 5.1: Parameters of the three Merton models used to produce the sample path of the price process S_t in Figure 5.2.

Figure 5.2 shows a sample path of the price process S_t against the time t where the grey lines portray the maturities $(T_j)_{j=0,1,2,3}$ with $T_0 = 0$. The risk-free interest rate and initial price were respectively set to $r = 0.06$ and $S_0 = 100$.

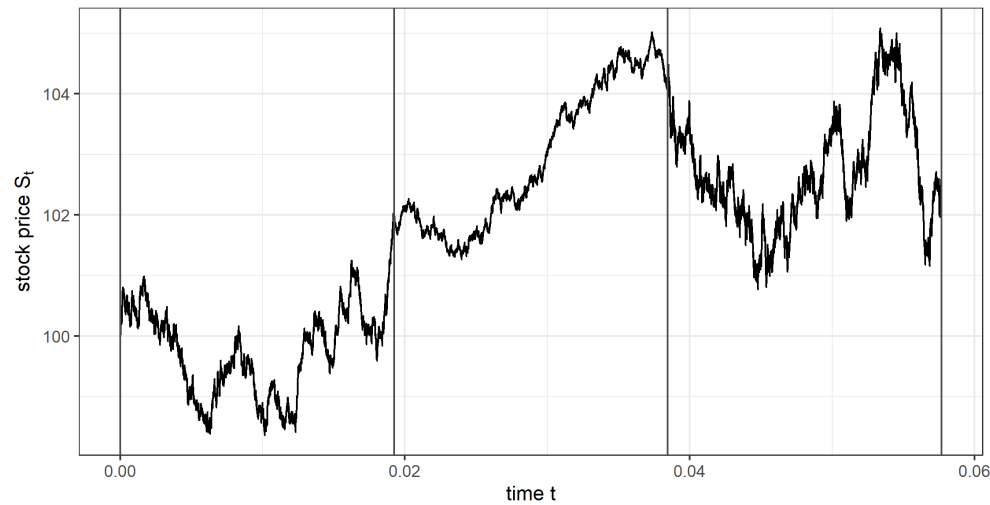


Fig. 5.2: Sample path of the time-inhomogeneous exponential model used for the construction of the price process S_t built up from three Merton models with parameters given in Table 5.1.

5.1.4 Simulation of Noised Option Prices from Models

Simulated noised option prices from a proposed model are needed to execute the calibration. The model for noised option prices, given in (2.9), is

$$\mathcal{O}_{j,k} = \mathcal{O}_j(x_{j,k}) + \delta_{j,k}\varepsilon_{j,k}, \quad k = 1, \dots, m_j,$$

where we defined $\mathcal{O}_{j,k} := \mathcal{C}(x_{j,k}, T_j)/S_0$ and $\delta_{j,k} := \zeta_{j,k}/S_0$. Put prices $\mathcal{P}(x_{j,k}, T_j)$ can also be used by first transferring them to call prices $\mathcal{C}(x_{j,k}, T_j)$ using the put-call parity (2.6).

For making noised observations we need to 1) calculate the option function $\mathcal{O}_j(x)$ from the simulation model, 2) decide on the spacing and number of design points $(x_{j,k})_{k=1, \dots, m_j}$, and 3) decide on the distributions of $(\varepsilon_{j,k})_{k=1, \dots, m_j}$ and magnitude $(\delta_{j,k})_{k=1, \dots, m_j}$.

For 1), Proposition 2.1 (iv) provides a direct way to calculate the function $\mathcal{O}_j(x)$ from a given characteristic function φ_{T_j} by

$$\mathcal{O}_j(x) = \mathcal{F}^{-1} \left[\frac{1 - \varphi_{T_j}(v - i)}{v(v - i)} \right] (x).$$

Now for 2), the number of design points $(x_{j,k})_{k=1, \dots, m_j}$ is chosen to be $m_j = 150$ for all $j = 1, 2, 3$. This is also around the number of design points that we will encounter in empirical data. Furthermore, empirical data has the property that more option prices are found at the money (i.e. at $x=0$) than further in or out the money (i.e. $x \ll 0$ and $x \gg 0$). Therefore, the design points $(x_{j,k})_{k=1, \dots, m_j}$ have been obtained by a random sample which yields more option prices at the money.

And for 3), the distributions of $(\varepsilon_{j,k})_{k=1, \dots, m_j}$ are chosen to be Gaussian $\mathcal{N}(0, 1)$ and the magnitude $\delta_{j,k}$ is chosen proportional to the underlying value of $\mathcal{O}_j(x_{j,k})$ with a noise level α , i.e., $\delta_{j,k} = \alpha \mathcal{O}_j(x_{j,k})$. The noise level α decides the percentage of noise that will be added to the underlying option function, in practice we will choose $0.005 \leq \alpha \leq 0.03$.

5.1.5 Numerical Approximation Fourier Transform

In the construction of the calibration model using option prices, the Fourier transforms

$$\mathcal{F}f(v) = \int_{-\infty}^{\infty} f(x)e^{ivx} dx \quad \text{and} \quad \mathcal{F}^{-1}F(x) = \frac{1}{2\pi} \int_{-\infty}^{\infty} F(v)e^{-ivx} dv$$

are used regularly. In practice, these Fourier transforms need to be (mostly) calculated numerically. This process can be rather fast due to the usage of the Fast Fourier Transform *FFT* algorithm. This section will concisely elaborate on this numerical approximation.

An efficient way to calculate the Fourier transforms is by the usage of the discrete Fourier transform *DFT*,

$$\mathbf{F}f_k = \sum_{k=0}^{N-1} f_k e^{-2\pi i n k / N}, \quad n = 0, \dots, N-1.$$

Generically, the computation of F_0, \dots, F_{N-1} needs N^2 operations a priori. However, when N is a power of 2, the FFT algorithm can be implemented to reduce the complexity from N^2 to $O(N \log N)$ operations (see, for example, [51]). The FFT algorithm is implemented in almost all high-level scientific computation environments.

Suppose that we want to find the inverse Fourier transform of $f(x)$ using the DFT. In persuasion of this, the integral needs to be truncated and discretized as follows:

$$\int_{-\infty}^{\infty} f(x) e^{-ivx} dx \approx \int_{-L/2}^{L/2} f(x) e^{-ivx} dx \approx \frac{L}{N} \sum_{k=0}^{N-1} w_k f(x_k) e^{ivx_k}$$

where $x_k = -A/2 + k\Delta$, $\Delta = A/(N-1)$ is the discretization step and w_k the weights that correspond to the particular integration rule, e.g., for the trapezoidal rule $w_0 = w_{N-1} = 1$ and $w_{1, \dots, N-2} = \frac{1}{2}$. The substitution of $u_n = \frac{2\pi n}{N\Delta}$ in the sum will make the expression in the DFT take the form:

$$\mathbf{F}f(u_n) \approx \frac{L}{N} e^{iuL/2} \sum_{k=0}^{N-1} w_k f(x_k) e^{-2\pi i n k / N}.$$

Thus, the FFT algorithm allows to compute $\mathbf{F}f(u)$ at the points $u_n = \frac{2\pi n}{N\Delta}$. The relation between the grid step d in the Fourier space and the initial grid step Δ_j is given by:

$$d\Delta_j = \frac{2\pi}{N}.$$

The above expression implies that if option prices need to be computed on a fine grid of strikes and, at the same time, the discretization error needs to be kept low, then numerous points need to be used. An additional limitation of the FFT method is that the grid must always be uniform and the grid size must always be a power of 2. The functions that need to be integrated with this report are in general irregular at the money and smooth elsewhere. However, it is impossible to increase the resolution close to the money without doing it elsewhere. These observations show that the use of FFT is only justified when one has many options with the same maturity (somewhat more than 10) available. Luckily, we mostly calibrate to empirical results and simulations with numerous option prices, so this is not a problem here.

5.2 Simulation Results

The underlying model that will be calibrated is the model of section 5.1.3, i.e., a time-inhomogeneous Lévy model which is built up from maturities $(T_1, T_2, T_3) = (1/52, 2/52, 3/52)$ where the Lévy processes between the maturities are given by Merton models with parameters $(\sigma_j, \gamma_j, \lambda_j, \mu_j, \delta_j)_{j=1,2,3}$ and their values displayed in Table 5.1.

Furthermore, as was explained in section 5.1.4, the sample size/number of design points is chosen to be $m_j = 150$, the distribution of $(\varepsilon_{j,k})$ is chosen to be Gaussian $\mathcal{N}(0, 1)$, and the magnitude is chosen to be proportional to the option function $\delta_{j,k} = \alpha \mathcal{O}_j(x_{j,k})$ with $\alpha = 0.010$.

For the general parameters, we choose the risk-free rate as $r = 0.06$ and the initial stock price as $S = 100$.

The code written for the simulations is generic and all simulation settings can be adjusted to inspect certain dependencies, e.g., all cut-off schemes have been implemented, both the weight function of [44] and [7] can be chosen, all model parameters can be varied, the

distribution and the magnitude of the noise can be adjusted, the interpolation scheme can be varied, the design can be chosen in a deterministic or random manner, different underlying time-inhomogeneous models with Merton and/or Kou, and more.

After inspecting all the different dependencies, we find that the code runs cleanly for all cases. One important thing to note is that the difficulty of the inverse problem for the Lévy process that governs the dynamics in $(T_j - T_{j-1})$ relates to the factor $\sum_{i=1}^j \sigma_i^2(T_i - T_{i-1})$. The bigger $\sum_{i=1}^j \sigma_i^2(T_i - T_{i-1})$ becomes, the more difficult the problem is. We, therefore, advise keeping these values small enough for sensible results.

The major new subjects of this thesis are the fact that we used a time-inhomogeneous Lévy model and the first usage of the finite sample variance method to create confidence intervals. Thus, we are most interested in looking into these new practices in the simulation results.

The simulation results are constructed as follows 1) the estimators $(\tilde{\psi}_j)_{j=1,2,3}$ for $(\psi_j)_{j=1,2,3}$ will be inspected, 2) from $(\tilde{\psi}_j)_{j=1,2,3}$ the estimators $(\tilde{\sigma}_j, \tilde{\gamma}_j, \tilde{\lambda}_j)_{j=1,2,3}$ are estimated and we compare them to $(\sigma_j, \gamma_j, \lambda_j)_{j=1,2,3}$, 3) the estimator $\tilde{\nu}_j$ for ν_j will thereafter be individually inspected, and 4) the confidence intervals will be added and coverage probabilities inspected.

All the above steps will be done for multiple Monte-Carlo simulations to get an idea of the bias-variance trade-off and underlying distributions of the estimators. In every Monte-Carlo simulation, we first calibrate all results in the order $j = 1, 2, 3$, i.e. one time-inhomogeneous Lévy model at a time, and then move on to the next simulation.

An important decision for all simulation steps is the choice of the scheme for choosing the cut-off values $(U_j)_{j=1,2,3}$. All different schemes for choosing U_j , i.e. oracle method, flat method, and PLS method, have been implemented and coded. As mentioned in section 5.1.1, the flat method works particularly well for simulations and is used for calibration.

Another important choice for 4) is the fact if one should use the "known" error distribution, where the error is exactly known, or one should use the PLS method to estimate the error — which is also necessary for empirical results where the underlying error is unknown. Consequently, step 4) will be analyzed for both scenarios, and both scenarios are implemented in the code.

5.2.1 Estimating $(\tilde{\psi}_j)_{j=1,2,3}$ for $(\psi_j)_{j=1,2,3}$

The performance of the estimator $\tilde{\psi}_j$ for ψ_j needs to be analyzed, because this estimator is at the root of the estimation of the triplet $(\tilde{\sigma}_j^2, \tilde{\gamma}_j, \tilde{\lambda}_j)$. Remember that $\tilde{\sigma}_j^2$ and $\tilde{\lambda}_j$ are estimated using the real part $\text{Re}(\tilde{\psi}_j(v))$ and $\tilde{\gamma}_j$ using the imaginary part $\text{Im}(\tilde{\psi}_j(v))$. These parts are therefore inspected separately.

Figure 5.3 shows the results of estimating the real Re and imaginary parts Im of ψ_j with $\tilde{\psi}_j$ for $j = 1, 2, 3$. In these plots, the grey circles depict the estimation grid of $\tilde{\psi}_j$ and the black lines depict the known underlying ψ_j function.

In these plots we have zoomed in to the region of $[-40, 40]$. This region depicts the common range where the calibration algorithm chooses the cut-off frequencies $[-U_j, U_j]$. Outside of these ranges, a large deviation of $\tilde{\psi}_j$ from ψ_j can occur. Because of the exponential growth of the deviation in v whenever $\sigma_j > 0$ (See Belomestny et al. [4]).

The approximate ranges that are *well-behaved*, i.e. good ranges where the cut-off frequency U_j is chosen in, is mostly due to the difficulty of the inverse problem at the moment $\sum_{i=1}^j \sigma_i^2(T_i - T_{i-1})$. The bigger the sum is, the more difficult it becomes to get an accurate representation for a certain j of $\tilde{\psi}_j$ for ψ_j on an adequate range.

Figures 5.3a, 5.3b and 5.3c show that the estimation of the ψ_j function in the range $[-40, 40]$ is adequate and that the values are mostly well-predicted. An important remark to see in these figures is that the estimation of ψ_j becomes more difficult for increasing j , i.e. predicting ψ_1 is more accurate than predicting ψ_3 . This is a direct consequence of the difficulty of the inverse problem for increasing j .

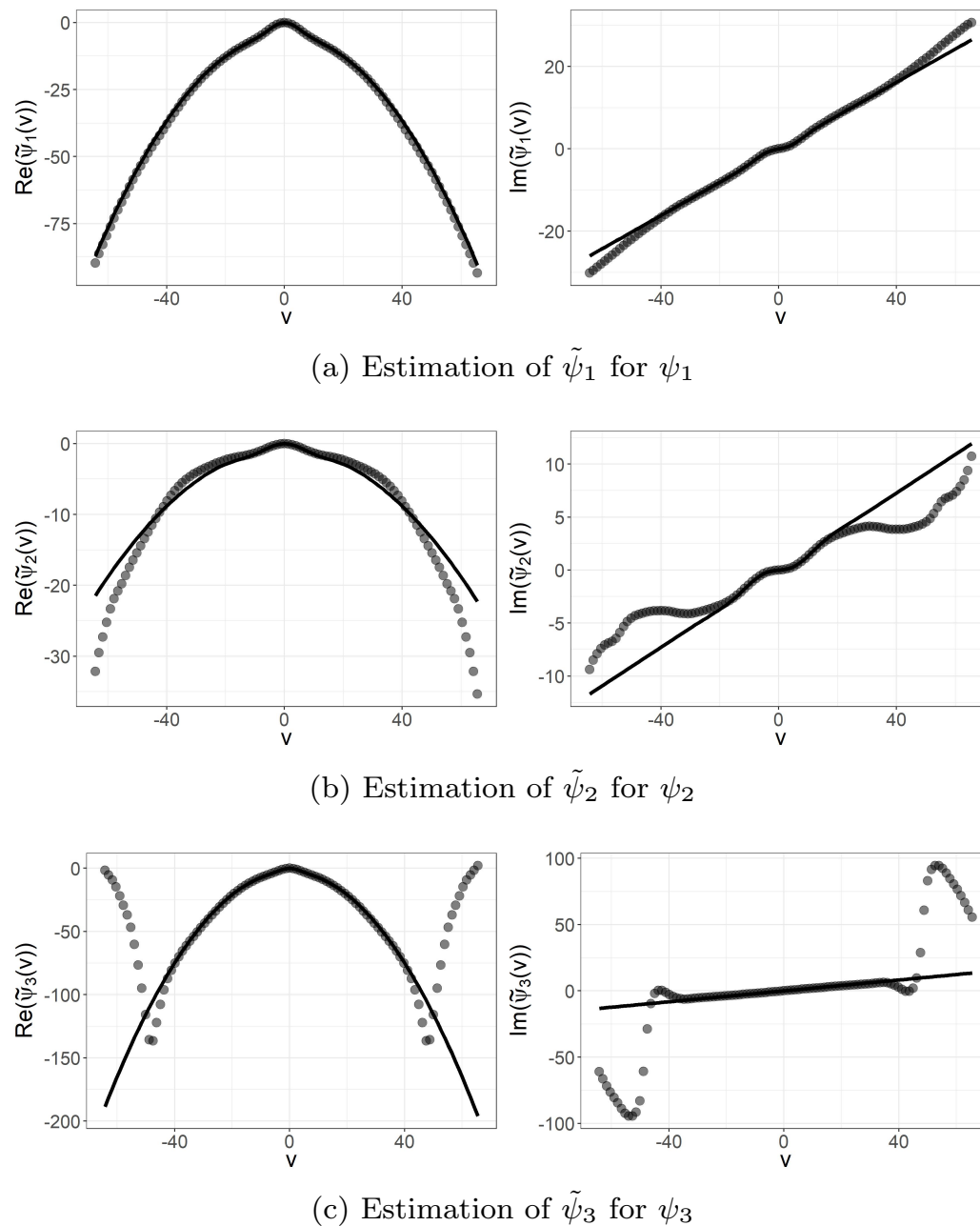


Fig. 5.3: These plots show the estimation of the real Re and imaginary part Im of $\tilde{\psi}_j$ portrayed by grey circles for ψ_j portrayed by a black line for $j = 1, 2, 3$.

5.2.2 Estimating $(\tilde{\sigma}_j, \tilde{\gamma}_j, \tilde{\lambda}_j)_{j=1,2,3}$ for $(\sigma_j, \gamma_j, \lambda_j)_{j=1,2,3}$

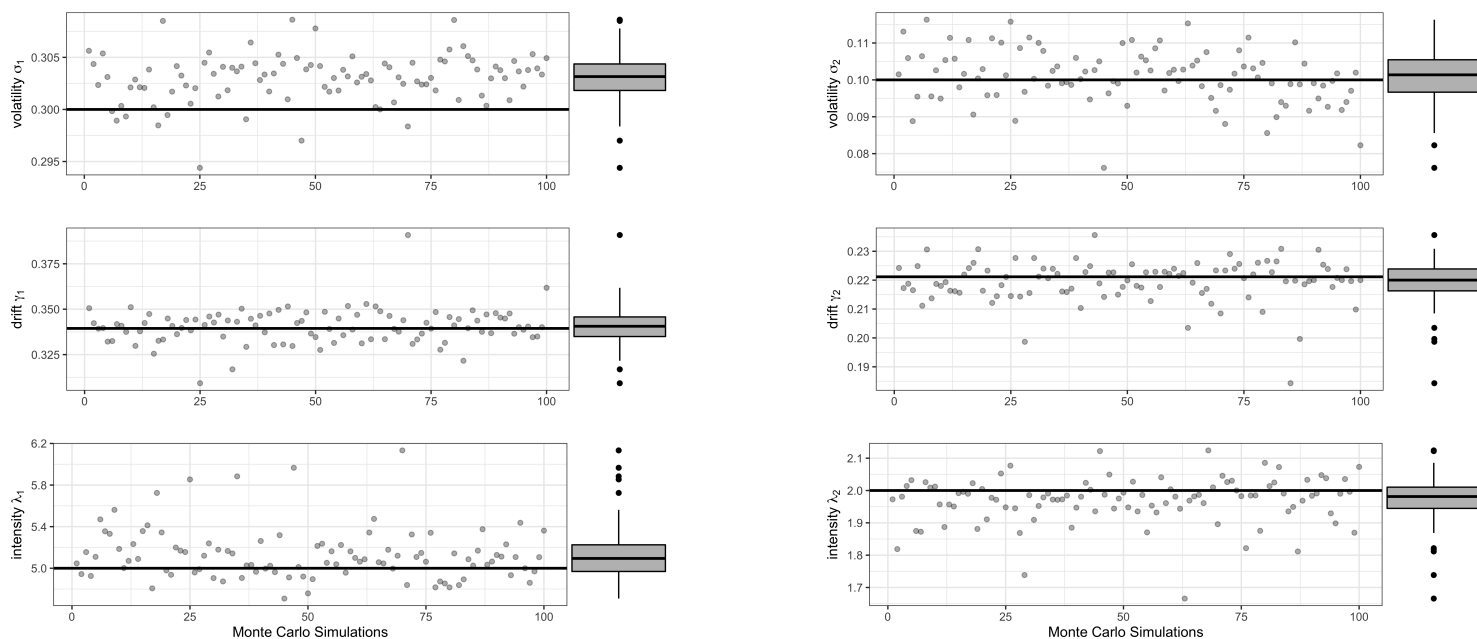
To get a general idea of the performance of the estimators $(\tilde{\sigma}_j, \tilde{\gamma}_j, \tilde{\lambda}_j)_{j=1,2,3}$ for $(\sigma_j, \gamma_j, \lambda_j)_{j=1,2,3}$ one hundred Monte-Carlo simulations will be executed and analyzed. In every Monte-Carlo simulation, new random noise is generated and we look at how this affects the spectral calibration.

Figure 5.4 displays the result of the 100 spectral calibrations in 3 sub-figures. Every subfigure displays for a certain $j = 1, 2, 3$ the results for the accompanying triplet $(\tilde{\sigma}_j, \tilde{\gamma}_j, \tilde{\lambda}_j)$ through separate scatter-plots. A black line has been added in these scatterplots to display the underlying theoretical value that needs to be estimated. Furthermore, a boxplot has been added to the right of every scatterplot to give insight into the distribution of the 100 estimates.

Before we go into the details of Figure 5.4, it is important to have an intuition about what values the flat method chose as cut-off values. The cut-off values determine the bias and stochastic variance trade-off for the practical case, i.e., U_j finite and $\Delta_j \neq 0$. Figure 5.5 shows the values of U_j that correspond to the scatter-plots in Figure 5.4.

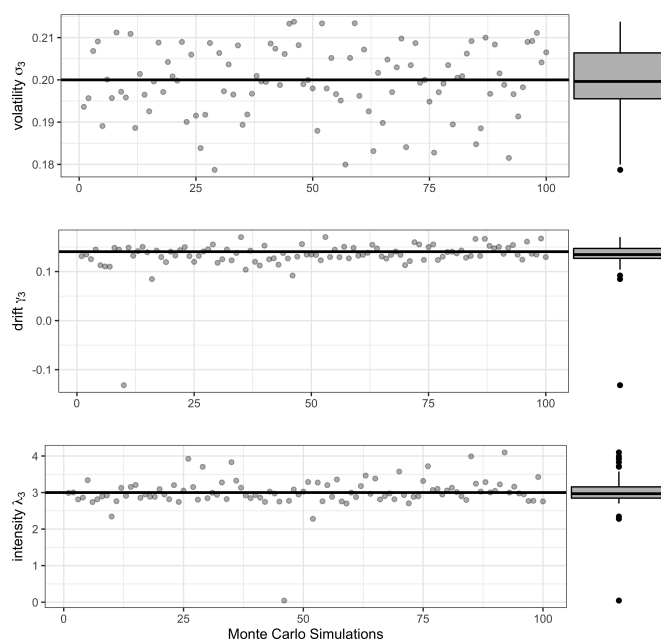
First and foremost, Figures 5.4a, 5.4b, and 5.4c show that most estimators behave well and that the values are generically well predicted, i.e., not many outliers or insensible results are displayed. The only insensible results would be the estimation of $\tilde{\lambda}_3$ to be zero one time.

From the y-axis in Figures 5.4a, 5.4b and 5.4c we see that in every case $j = 1, 2, 3$ the accuracy of the estimators is respectively decreasing in the order $\sigma_j, \gamma_j, \lambda_j$. This fact was



(a) 100 hundred Monte-Carlo estimates
 $(\tilde{\sigma}_1, \tilde{\gamma}_1, \tilde{\lambda}_1)$ for $(\sigma_1, \gamma_1, \lambda_1) \approx (0.2, 0.36, 5)$

(b) 100 hundred Monte-Carlo estimates
 $(\tilde{\sigma}_2, \tilde{\gamma}_2, \tilde{\lambda}_2)$ for $(\sigma_2, \gamma_2, \lambda_2) \approx (0.1, 0.16, 2)$



(c) 100 hundred Monte-Carlo estimates
 $(\tilde{\sigma}_3, \tilde{\gamma}_3, \tilde{\lambda}_3)$ for $(\sigma_3, \gamma_3, \lambda_3) \approx (0.3, 0.12, 3)$

Fig. 5.4: These scatterplots show the result of 100 Monte-Carlo simulations of $(\tilde{\sigma}_j, \tilde{\gamma}_j, \tilde{\lambda}_j)_{j=1,2,3}$ for $(\sigma_j, \gamma_j, \lambda_j)_{j=1,2,3}$. In every plot, the black line portrays the theoretical value. Furthermore, to the right of every plot, a boxplot has been added to display the underlying distribution of the estimators.

also encountered in the speed of convergence proven in the theoretical part (see Theorem 3.2).

In section 3.5 we saw that the difficulty of the time-inhomogeneous inverse calibration problem is coupled to $\sum_{i=1}^j (T_i - T_{i-1})\sigma_i^2$. This term grows for increasing j and the problem becomes more difficult when calibration occurs for higher j . In Figure 5.4 we can see this decreasing accuracy of the parameters σ_j , γ_j , or λ_j in j . For example, σ_1 is more accurately determined than σ_2 in the stochastic variance sense, disregarding the bias, which will be the topic of the next paragraph.

An obvious fact that can be seen is that in some scatterplots we can note general bias in the estimators, e.g., in the scatterplot of $\tilde{\sigma}_1$ all estimators are above the theoretical value which corresponds to a bias term. In the theoretical part, we showed that the bias asymptotically goes to 0. However, in the practical results, bias can occur. An easy way to see the general bias is to compare the boxplots with the theoretical values displayed by the black line. The cut-off value U_j is the parameter that governs the bias and stochastic error

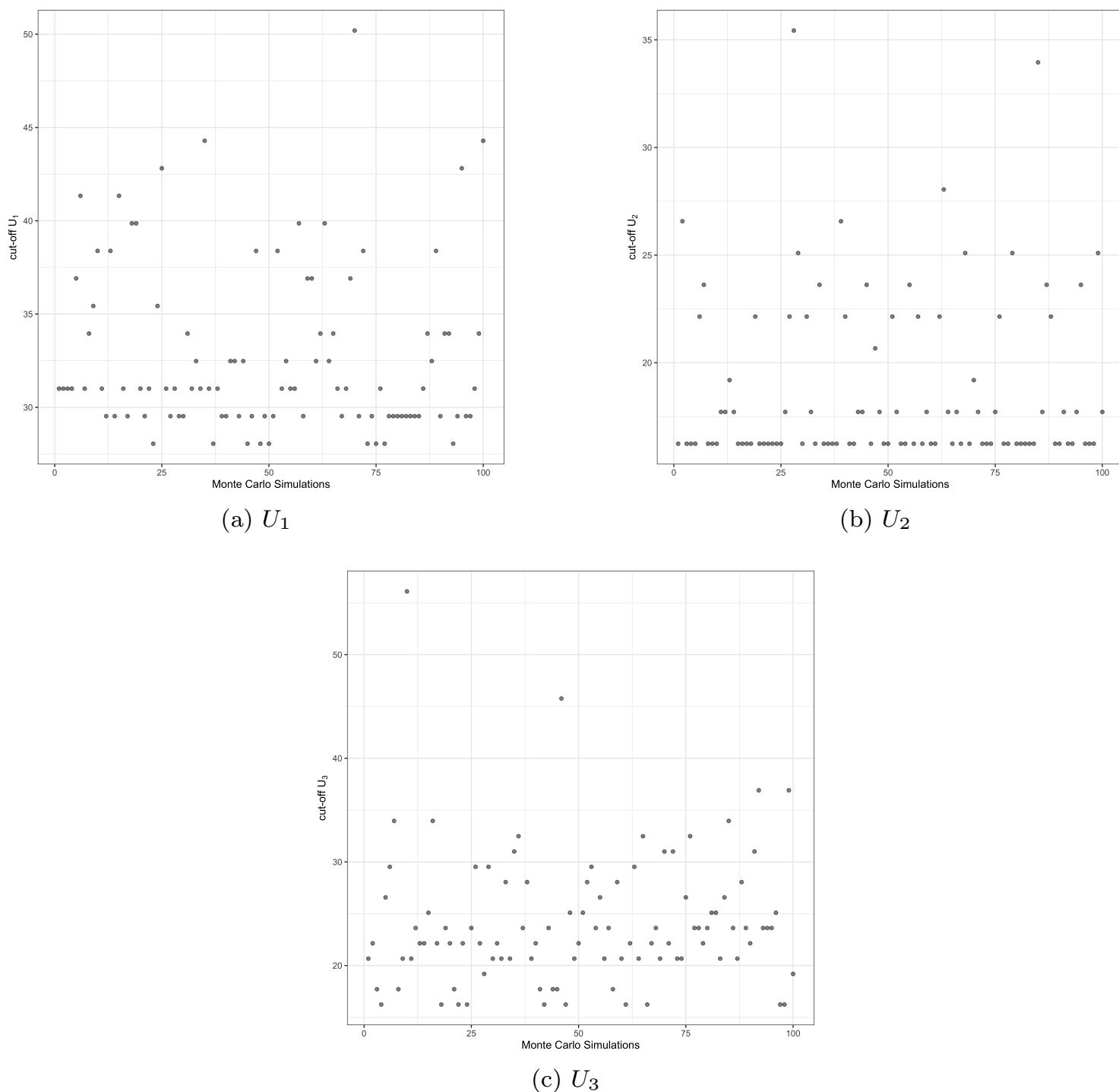


Fig. 5.5: Scatterplots of cutoff values $(U_j)_{j=1,2,3}$ for 100 Monte-Carlo simulations.

trade-off — in the same way the bandwidth h plays in kernel estimation in nonparametric statistics. The bias decreases and the stochastic error increases when U_j increases.

When comparing the results of Figure 5.4 with the corresponding cut-off values in Figure 5.5, it can be seen that all outliers correspond to large values of U_j . General practical advice is therefore to not let U_j become too large for preventing the stochastic error to be too big. This is also an important point when making finite sample confidence intervals. Here we made the assumption that the Bias can be neglected, and this assumption is more true when U_j is larger, but we also do not want U_j to become too large. More about this later when building confidence intervals.

5.2.3 Estimating $(\tilde{\nu}_j)_{j=1,2,3}$ for $(\nu_j)_{j=1,2,3}$

The estimator for the jump density $\tilde{\nu}_j$ needs to be estimated by taking an inverse Fourier transform,

$$\tilde{\nu}_j(x) = \mathcal{F}^{-1} \left[\left(\psi_{\nu_j}(\cdot) + \frac{\tilde{\sigma}_j^2}{2}(\cdot)^2 - i\tilde{\gamma}_j(\cdot) + \tilde{\lambda}_j \right) w_{\nu_j}(\cdot) \right] (x), \quad x \in \mathbb{R},$$

and is therefore different from the other estimators. This is the reason why we analyze this estimator on itself.

To calibrate $\tilde{\nu}_j$ the shifted calibration function ψ_{ν_j} is used and therefore a separate calibration is carried out for better stability. In general, the cut-off value U_{ν_j} that is chosen for calibrating $\tilde{\nu}_j$ is smaller than the cut-off value U_j .

The Lévy density estimates $\tilde{\nu}_j(x)$ for $\nu_j(x)$ are calculated with the same 100 Monte-Carlo simulations. The 100 results of the estimates $\tilde{\nu}_j(x)$ are shown as grey lines and the underlying known density $\nu_j(x)$ is shown as a black line in Figure 5.6.

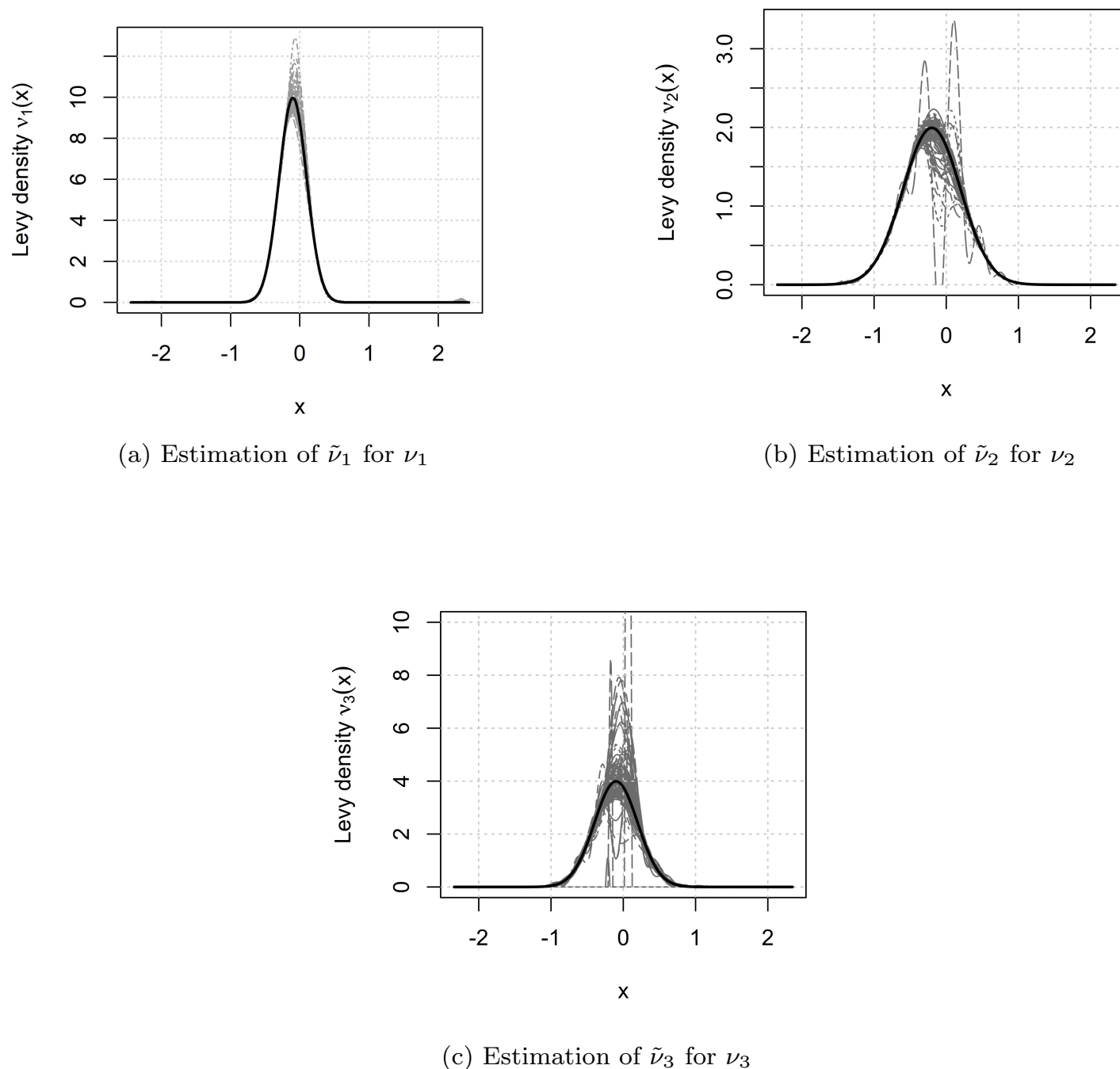


Fig. 5.6: These plots show the estimation of 100 Monte-Carlo simulated Lévy densities $\tilde{\nu}_j(x)$, portrayed by grey lines, for $\nu_j(x)$, portrayed by a black line, for $j = 1, 2, 3$.

Figure 5.6a shows that the 100 estimates $\tilde{\nu}_1(x)$ look satisfactory, 5.6b deteriorates a little but still looks satisfactory, and 5.6c looks quite chaotic. The theoretical results already point out that the performance of the estimators is in the following chronological order $\sigma_j^2, \gamma_j, \lambda_j, \gamma_j, \nu_j$ for a certain j . Thus, the estimation part of $\nu_j(x)$ is the most difficult.

We already discussed that the accuracy of the estimators deteriorates with increasing j because of the difficulty of the inverse problem. Hence, from both considerations, $\tilde{\nu}_3(x)$ in Figure 5.6c should be the most difficult to estimate. It can be noted in all 3 figures that there can still be bumps of mass found in the tails. These bumps relate to the fact that we used

a normal Fourier transform \mathcal{F} for getting into the spectral domain, then did the estimation in this domain, and to get the Lévy density back we then needed to use an inverse Fourier transform \mathcal{F}^{-1} . These tail bumps are thus the result of little errors in the tails that are portrayed as sine and cosine waves in the densities after transforming back.

The most variance for every $j = 1, 2, 3$ is found at $\tilde{\nu}_j(0)$ and deteriorates — if the masses in the tails are neglected — when we move away from 0. This is the result of the smoothness of the estimated curves, the larger variance of $\tilde{\nu}_j(0)$ leads to an increased variance of $\tilde{\nu}_j(x)$ in the neighborhood of 0.

Although the estimates of $\tilde{\nu}_3(x)$ in Figure 5.6c appear chaotic, most estimates are sensible. Figure 5.7 shows a boxplot of the 100 Monte estimates $\tilde{\nu}_3(x)$ at the point of $\mu_3 = -0.1$.

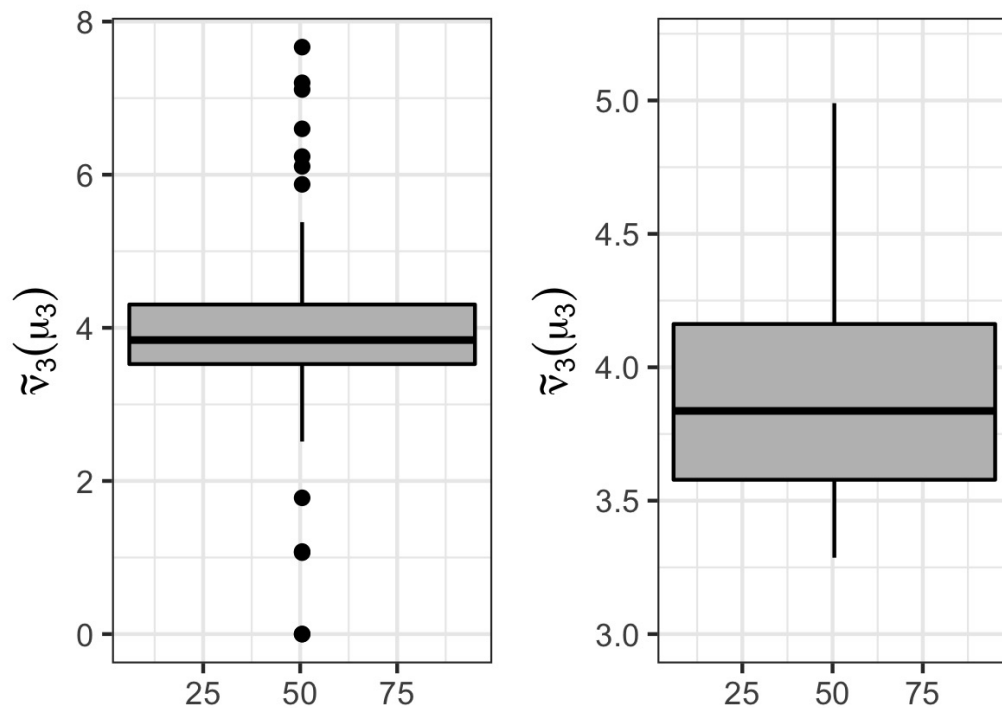


Fig. 5.7: Boxplots of the 100 Monte-Carlo estimates $\tilde{\nu}_3(\mu_3)$ in Figure 5.6c. The left shows all estimates, whereas the right shows a zoomed-in version.

In the boxplots of Figure 5.7, we see that the 25% and 75% percentiles are respectively at around 3.27 and 4.98. Consequently, most estimates are well-behaved. In total, there are 10 outliers on 100 Monte-Carlo estimates. Not all outliers also give odd estimates, some are due to already displayed errors in the approximation of $\tilde{\lambda}_3$, which makes the mass of the estimates different. This is due to the correction procedure of $\tilde{\nu}_j(x)$ in expression (2.18), which made sure that $\tilde{\nu}_j(x) \geq 0$ for all $x \in \mathbb{R}$ and $\tilde{\lambda}_3 = \|\tilde{\nu}_3\|_{L_1(\mathbb{R})}$.

All 100 estimates $\tilde{\nu}_j(x)$ are inspected individually and three *odd* cases that can occur are shown in Figure 5.8.

All three odd cases in Figure 5.8 display something that can go wrong. The first plot shows a peak at 0 that is too large and is one of the outliers in the boxplot. This effect is already due to the miss estimation of $\tilde{\lambda}_j$. The second plot shows an oscillating curve, these are due to miss estimations in the Fourier transforms \mathcal{F} , such that when estimating $\tilde{\nu}_j(x)$ with \mathcal{F}^{-1} the underlying function is, because of errors, not well-behaved to transform. The third plot shows the case where both problems in estimating occur in an extreme sense.

If the cut-off values U_3 of these simulations 85, 16, and 10 are looked upon in the code or Figure 5.5, then the results are respectively 33.96, 33.96, and even 56.10. Note that these cut-off values are all bigger than the generally chosen cut-off values. Also in Figure 5.4 we can already see that for these estimates the parameters $(\tilde{\sigma}_j^2, \tilde{\gamma}_j, \tilde{\lambda}_j)$ are also outliers.²

These miss-estimates make the plot of $\tilde{\nu}_3(x)$ in Figure 5.6c look chaotic, where more than 90% are well-behaved and accurate.

² In the section on the confidence intervals, we will see that large cut-off values will lead to large intervals such that we can account for this misbehavior.

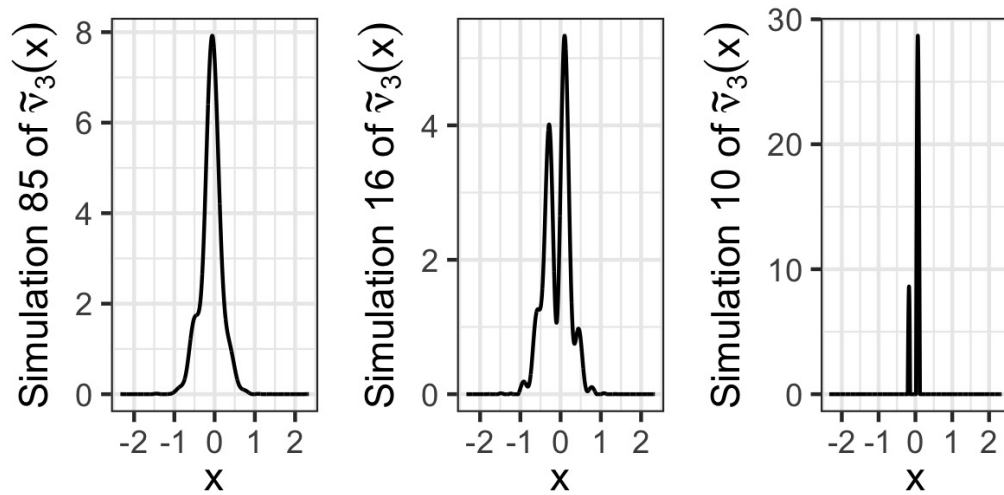


Fig. 5.8: Plots of three odd estimates $\tilde{\nu}_3(x)$ for $\nu_3(x)$ in the simulation results in Figure 5.6c.

It was on purpose that we made plots that showed these misbehaviors. If the factor $\sum_{i=1}^j \sigma_i^2(T_i - T_{i-1})$ or the magnitude of errors $(\delta_{j,k})$ are chosen small enough, then these odd plots do not occur. However, to have an understanding of what can go wrong in empirical calibration, it is good to already have seen these extreme cases in simulations. Although, as will be shown in the next section, empirical cases are generally more well-behaved than the simulations shown here.

5.2.4 Confidence Intervals and Coverage Probabilities

In all statistical procedures, it is common to get a feeling about how accurate the estimation is. A raw estimation without any confidence can be misleading, especially if the underlying value as validation is unknown. In section 4 we already discussed that using the derived asymptotic confidence intervals is not good practice in finite sample cases, and we produced new confidence intervals with the *Finite Sample Variance* practice.

The derived $(100 - \vartheta)\%$ confidence intervals for $\tilde{\sigma}_j^2$, $\tilde{\gamma}_j$, $\tilde{\lambda}_j$ and $\tilde{\nu}_j(x)$ in the Finite Sample case were respectively derived and given in expressions (4.5), (4.8), (4.11) and (4.17). We will choose $\vartheta = 0.05$ such that 95% confidence intervals are strived for. Recall that $\nu_j(x)$ was a point-wise confidence interval and not a confidence band. The coverage probabilities will be analysed for the vector $(\tilde{\sigma}_j^2, \tilde{\gamma}_j, \tilde{\lambda}_j, \tilde{\nu}_j(\mu_j), \tilde{\nu}_j(\delta_j))$ for $j = 1, 2, 3$, where in the Merton model μ_j was the mean and δ_j the standard deviation.

The main underlying assumption of this practice was that the Remainder terms and Bias terms are neglected. The reasoning was that in the Theoretical Results these terms converge to 0 and the Linear terms dominate the asymptotic behavior. As the reader can probably imagine, this assumption can be quite strong and an analysis of the derived confidence intervals must be verified, we will do this by using *Coverage Probabilities*.

Another important point is that for deriving the confidence intervals, the magnitude of the error $(\delta_{j,k})$ is needed. Note that in the simulations these errors were simulated by using the proportional relation to the option price function $\delta_{j,k} = \alpha \mathcal{O}_j(x_{j,k})$ at the design points $(x_{j,k})$ with $\alpha = 0.010$. These values have been saved and can be used. However, in the empirical part, we need a manner to estimate these magnitudes. We discussed that the PLS method is the preferred method for estimating this noise. In the simulation part here, both the cases of *known* error magnitudes and *estimated* error magnitudes will be analyzed.

Thus, in this section, we will investigate the confidence intervals created and verify these with coverage probabilities for the known and estimated error magnitudes $(\delta_{j,k})$. An important fact that will be encountered is that we can only reach the coverage probabilities with exact error magnitudes when undersmoothing is used, i.e. the cut-off value U_j must not be *too small*. Otherwise, the Bias term, which was neglected, can dominate.

Exact Error Distribution

To first get a general feeling and not introduce more randomness into the model with the PLS method, the situation with the exact/known error distribution will be analyzed. For conciseness, the first ten Monte-Carlo simulations are analyzed, i.e., the same first 10 estimates as Figure 5.4.

For the first 10 Monte-Carlo simulations Table 5.2 shows the cut-off values $(U_j)_{j=1,2,3}$ and Figure 5.9 shows the accompanying ten 95% confidence intervals for $(\tilde{\sigma}_j^2, \tilde{\gamma}_j, \tilde{\lambda}_j, \tilde{\nu}_j(\mu_j), \tilde{\nu}_j(\mu_j + \delta_j))_{j=1,2,3}$ where the grey lines portray the underlying values of $(\sigma_j^2, \gamma_j, \lambda_j, \nu_j(\mu_j), \nu_j(\mu_j + \delta_j))_{j=1,2,3}$.³

	1	2	3	4	5	6	7	8	9	10
U_1	38.9	26.8	28.2	26.8	40.3	30.9	41.6	33.6	25.5	26.8
U_2	20.1	22.8	14.8	14.8	14.8	20.1	20.1	30.9	20.1	14.8
U_3	21.5	16.1	26.8	18.8	18.8	20.1	22.8	18.8	21.5	26.8

Table 5.2: Cut-off values $(U_j)_{j=1,2,3}$ chosen by the flat method for the 10 Monte-Carlo simulations in Figure 5.9.

Furthermore, Figure 5.10 shows for the first Monte-Carlo simulation the estimates $(\tilde{\nu}_j(x))_{j=1,2,3}$ in gray with confidence intervals in black and the underlying density $(\nu_j(x))_{j=1,2,3}$ in red. All the estimates appear accurate and well-behaved. Next to that $\nu_j(x)$ is contained in almost all ranges of the confidence interval, only at $\nu_3(x)$ in the left tail a bump can be seen that the confidence interval does not capture.

Note in Figure 5.9 that the size of the underlying confidence interval for every estimate is different. This is mostly due to the difference in cut-off value U_j portrayed in Table 5.2. The larger U_j , the larger the confidence interval. For example, we can see this in the 7th observation with $U_1 = 41.6$.

Next to that, we can see that some confidence intervals of these small samples are not close to the 95% coverage that they should have. The most extreme cases of $\tilde{\sigma}_1^2$ in Figure 5.9a only have 70% coverage. On the contrary, some other confidence intervals, e.g. $\tilde{\lambda}_2$, even get 100% coverage. The goal is to find confidence intervals where all parameters exceed 95%, i.e. we want to be conservative. The reason is that when considering the empirical data we can have some certainty in the lower bound of the coverage probability in the results.

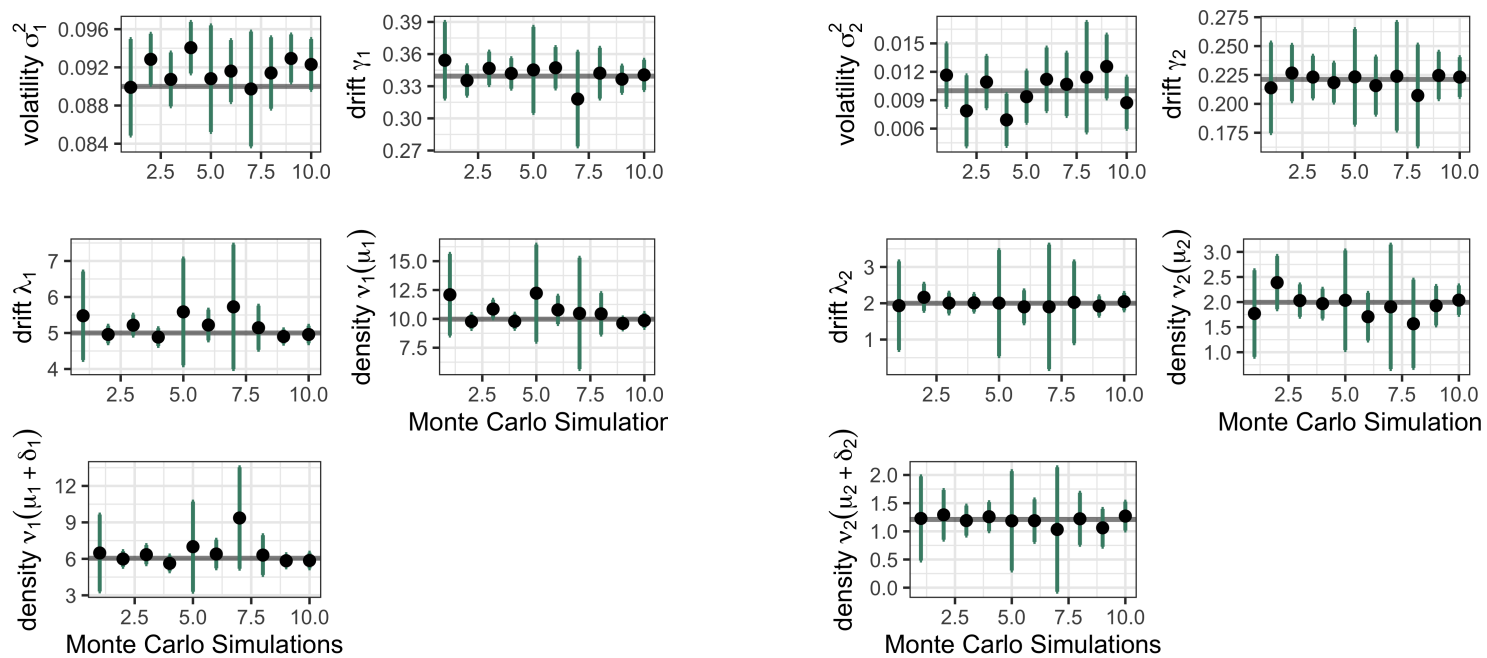
The example case of $\tilde{\sigma}_j^2$ provides an answer to why some intervals are inaccurate. We can see that some estimates of $\tilde{\sigma}_j^2$ display the same kind of bias, they are all portrayed above the theoretical value. Now recall that in the construction of the Finite Sample confidence intervals the assumption was made that the bias can be neglected. This might, however, as can be seen here, not be the case.

Söhl and Trabs [44] provide a manner in which accurate practical confidence intervals can still be created. For example, recall that the error decomposition

$$\tilde{\sigma}_j^2 - \sigma_j^2 = \underbrace{\int_{-U_j}^{U_j} w_{\sigma_j^{U_j}} \operatorname{Re}(\tilde{\psi}_j^0(v) - \psi_j^0(v)) dv + \int_{-U_j}^{U_j} w_{\sigma_j^{U_j}} \operatorname{Re}(\tilde{\psi}_j^1(v) - \psi_j^1(v)) dv}_{\text{Stochastic Error}} + \underbrace{\int_{-U_j}^{U_j} w_{\sigma_j^{U_j}} \operatorname{Re}(\mathcal{F}\mu_j(v)) dv}_{\text{Bias}},$$

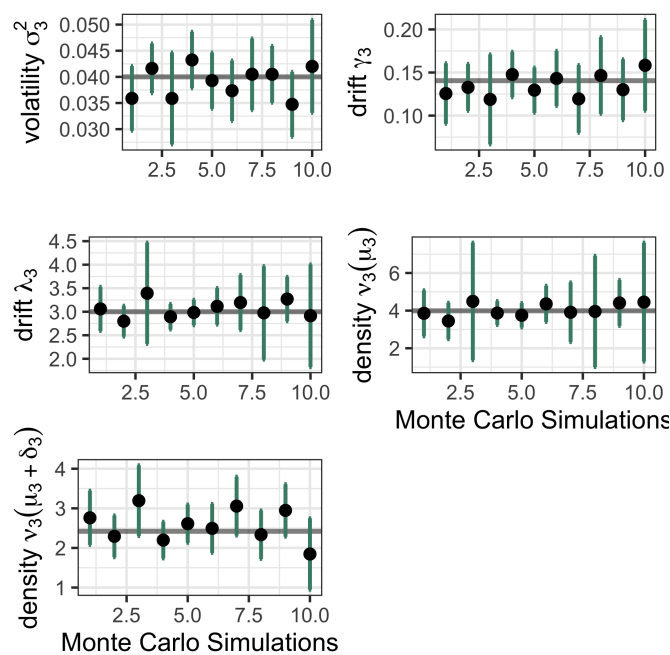
was decomposed into a stochastic part and a deterministic bias term. The choice of the cut-off value U_j allows a trade-off between these two terms. Larger U_j correspond to larger stochastic errors and smaller bias, whereas smaller U_j the case is vice versa. Deliberately

³ With a little abuse of notation remind that $(\delta_{j,k})$ were the error magnitudes and δ_j was the standard deviation of the Merton model.



(a) 10 Monte-Carlo estimates
 $(\tilde{\sigma}_1, \tilde{\gamma}_1, \tilde{\lambda}_1, \tilde{\nu}_1(\mu_1), \tilde{\nu}_1(\mu_1 + \delta_1))$ with
 confidence intervals for
 $(\sigma_1, \gamma_1, \lambda_1, \nu_1(\mu_1), \nu_1(\mu_1 + \delta_1)) \approx$
 $(0.2, 0.36, 5, -0.1, 0.2)$.

(b) 10 Monte-Carlo estimates
 $(\tilde{\sigma}_2, \tilde{\gamma}_2, \tilde{\lambda}_2, \tilde{\nu}_2(\mu_2), \tilde{\nu}_2(\mu_2 + \delta_2))$ with
 confidence intervals for
 $(\sigma_2, \gamma_2, \lambda_2, \nu_2(\mu_2), \nu_2(\mu_2 + \delta_2)) \approx$
 $(0.1, 0.16, 2, -0.2, 0.4)$.



(c) 10 Monte-Carlo estimates
 $(\tilde{\sigma}_3, \tilde{\gamma}_3, \tilde{\lambda}_3, \tilde{\nu}_3(\mu_3), \tilde{\nu}_3(\mu_3 + \delta_3))$ with
 confidence intervals for
 $(\sigma_3, \gamma_3, \lambda_3, \nu_3(\mu_3), \nu_3(\mu_3 + \delta_3)) \approx$
 $(0.3, 0.12, 3, -0.1, 0.3)$.

Fig. 5.9: These plots show the result of 10 Monte-Carlo simulations of $(\tilde{\sigma}_j^2, \tilde{\gamma}_j, \tilde{\lambda}_j, \tilde{\nu}_j(\mu_j), \tilde{\nu}_j(\mu_j + \delta_j))_{j=1,2,3}$ with 95% confidence intervals. In every plot, the thick grey lines portray the theoretical values $(\sigma_j, \gamma_j, \lambda_j, \nu_j(\mu_j), \nu_j(\mu_j + \delta_j))_{j=1,2,3}$.

choosing U_j larger to counter the bias is a common practice in nonparametric statistics and is called *undersmoothing*.

Using larger U_j the confidence intervals are widened but the deterministic term reduces. This provides a way to obtain practically usable confidence intervals that attain the coverage probabilities. Let us propose choosing the new cut-off values:

$$U_j = \zeta U_j^{\text{flat}}$$

with $\zeta > 1$ to provide undersmoothing. Söhl and Trabs [44] do not provide exact argumentation for their exact choice of $\zeta = 4/3$, which they used in the time-homogeneous

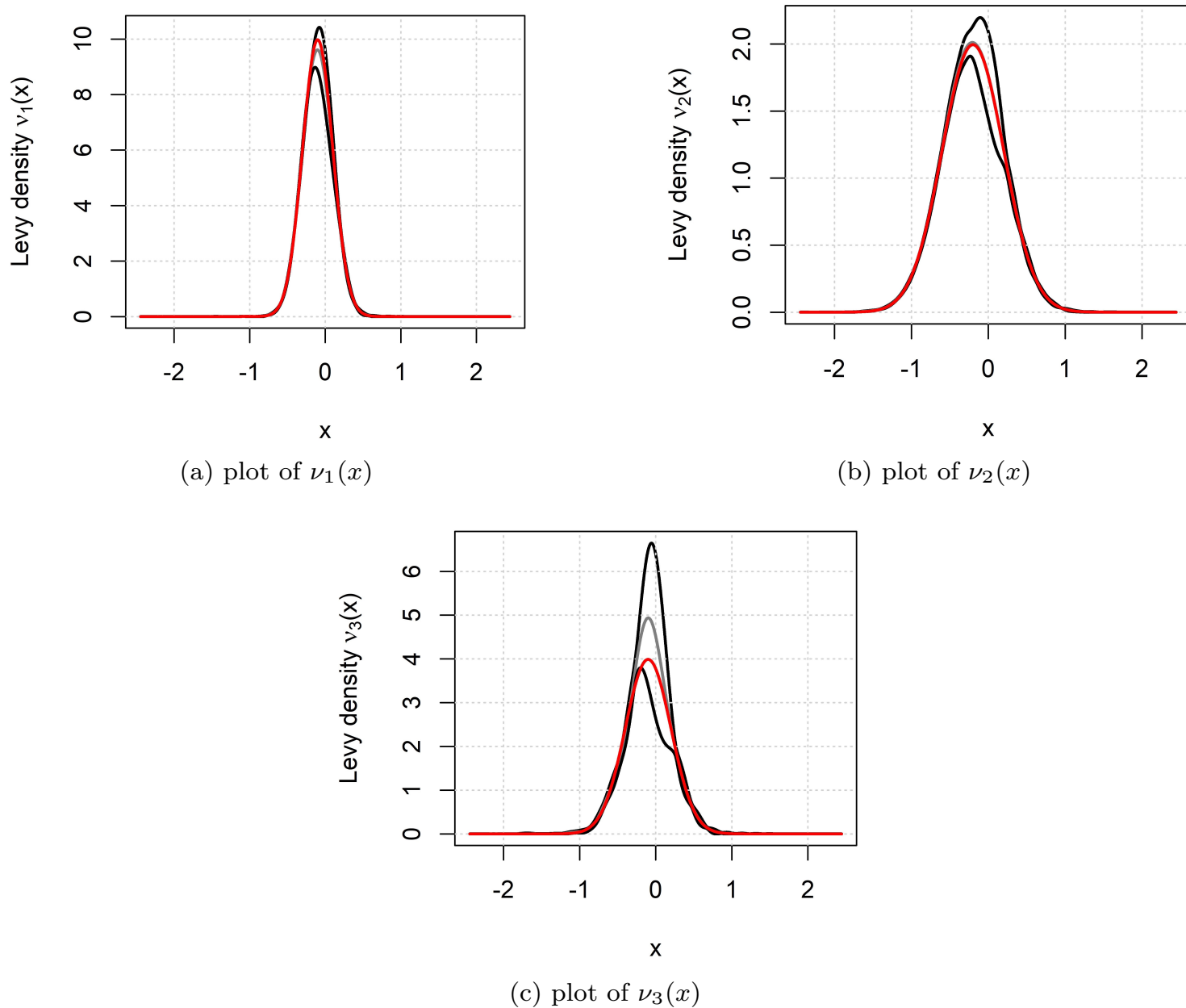


Fig. 5.10: For the first Monte-Carlo simulation these plots show the estimates $(\tilde{\nu}_j(x))_{j=1,2,3}$ in gray with confidence intervals in black and the underlying densities $(\nu_j(x))_{j=1,2,3}$ in red.

model. Mostly, this value is chosen in a practical manner such that the required coverage probabilities are attained. Therefore, multiple simulations with different values of ζ will be evaluated.

Recall that the densities ν_j required a different calibration with $\tilde{\psi}_{\nu_j}$ and thereby chose a cut-off value U_{ν_j} . For the parameter U_{ν_j} we will use the same undersmoothing with ζ .

To clarify, first all calibrations are done with the *flat* method, then all cut-off values $(U_j^{\text{flat}})_{j=1,2,3}$ for every Monte-Carlo simulation are subtracted, and then a new calibration for every Monte-Carlo simulation and $j = 1, 2, 3$ is done with the new fixed cut-off values $U_j = \zeta U_j^{\text{flat}}$.

Table 5.3 shows the coverage results $(\tilde{\sigma}_j^2, \tilde{\gamma}_j, \tilde{\lambda}_j, \tilde{\nu}_j(\mu_j), \tilde{\nu}_j(\mu_j + \delta_j))$ of 100 Monte-Carlo simulations using the flat method and thereafter under-smoothing with ζ . For more accurate results, more Monte-Carlo simulations need to be evaluated. However, the evaluated time already gets quite large, because two calibrations for every Monte-Carlo simulation have been done, i.e., one with the flat methods to find U_j and one with the fixed method with ζU_j . The table provides a rough estimate in which range ζ should be evaluated with more Monte-Carlo simulations.

From Table 5.3 it can be seen that the results get better and better for increasing values of ζ . This result is most clearly seen in $\tilde{\sigma}_1^2$. Larger ζ means undersmoothing, but also larger confidence intervals. It appears that the 95% coverage probability for $\tilde{\sigma}_1^2$ is attained conservatively for all parameters for $\zeta = 1.2$.

	1.1				1.2				1.3								
$j = 1$	87	100	100	98	100	96	97	100	98	100	98	100	98	100	100	98	100
$j = 2$	98	100	100	99	99	99	100	100	99	99	99	100	100	99	99	99	99
$j = 3$	99	100	96	95	98	100	100	100	98	97	100	100	100	100	99	98	98

Table 5.3: Coverage probabilities of $(\tilde{\sigma}_j^2, \tilde{\gamma}_j, \tilde{\lambda}_j, \tilde{\nu}_j(\mu_j), \tilde{\nu}_j(\mu_j + \delta_j))_{j=1,2,3}$ in % for 100 Monte-Carlo simulations and undersmoothing $U_j = \zeta U_j^{\text{flat}}$ with the value $\zeta \in \{1.1, 1.2, 1.3\}$.

To obtain a more accurate coverage probability 1000 Monte-Carlo simulations will be carried out for $\zeta = 1.2$. The results are shown in Table 5.4 and the width of the first 10 confidence intervals can be seen in Figure 5.11.

$\zeta = 1.2$	$\tilde{\sigma}_j^2$	$\tilde{\gamma}_j$	$\tilde{\lambda}_j$	$\tilde{\nu}_j(\mu_j)$	$\tilde{\nu}_j(\mu_j + \delta_j)$
$j = 1$	95.3%	99.2%	99.3%	98.0%	99.6%
$j = 2$	99.3%	99.9%	100.0%	98.8%	99.4%
$j = 3$	99.3%	98.9%	98.8%	97.6%	96.1%

Table 5.4: Coverage probabilities of $(\tilde{\sigma}_j^2, \tilde{\gamma}_j, \tilde{\lambda}_j, \tilde{\nu}_j(\mu_j), \tilde{\nu}_j(\mu_j + \delta_j))_{j=1,2,3}$ for 1000 Monte-Carlo simulations and undersmoothing $U_j = \zeta U_j^{\text{flat}}$ with the value $\zeta = 1.2$.

Figure 5.11 shows that most bias now has disappeared when using undersmoothing with $\zeta = 1.2$. Furthermore, the confidence intervals are bigger. In Figure 5.8 it was shown that sometimes calibration can go wrong. However, it is satisfactory to see that this can be seen in the large confidence intervals, this opens a way to detect misleading calibrations.

The main practical result is that conservative adequate confidence intervals can be created using undersmoothing with $\zeta = 1.2$. Note that different parameters might need a different value of ζ . Although, after multiple simulations with different parameters, the undersmoothing of $\zeta = 1.2$ is found to be generally satisfactory.

PLS Estimated Error Distribution

In the previous section, we used that the error magnitudes $(\delta_{j,k})$ are known a priori in constructing confidence intervals. However, outside of the simulations, the error magnitudes are unknown. Therefore, we construct an estimator for these error magnitudes.

The regression model for the noise in the option prices was given by (2.9), i.e.,

$$\mathcal{O}_{j,k} = \mathcal{O}_j(x_{j,k}) + \delta_{j,k}\varepsilon_{j,k}, \quad k = 1, \dots, m_j.$$

In a similar fashion as the simulations, we assumed that the error magnitudes are proportional to the underlying option function:

$$\delta_{j,k} = \delta_j \mathcal{O}_j(x_{j,k}).$$

Plugging this assumption into the regression model, we get

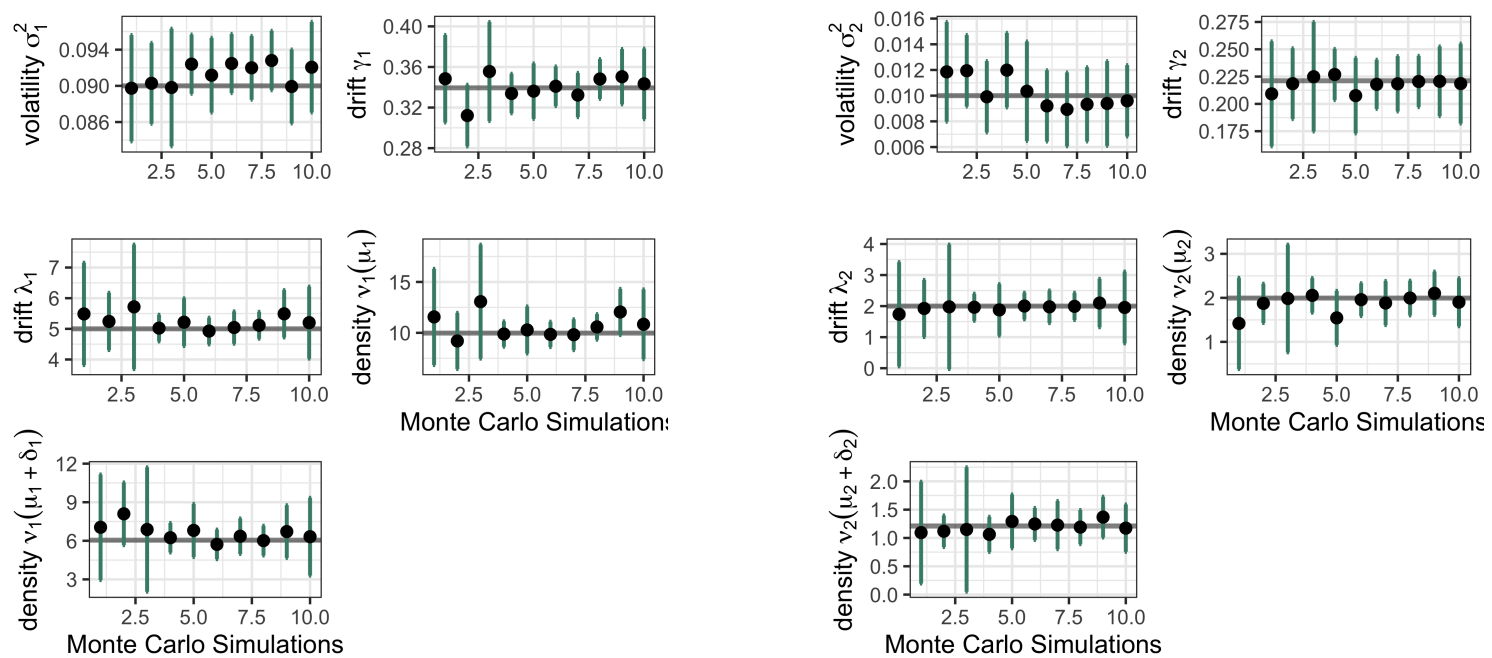
$$\mathcal{O}_{j,k} = \mathcal{O}_j(x_{j,k}) + \delta_j \mathcal{O}_j(x_{j,k})\varepsilon_{j,k}$$

Rewriting to get an expression for δ_j gives

$$\delta_j \varepsilon_{j,k} = \frac{\mathcal{O}_{j,k}}{\mathcal{O}_j(x_{j,k})} - 1 = \frac{\mathcal{O}_{j,k} - \mathcal{O}_j(x_{j,k})}{\mathcal{O}_j(x_{j,k})}.$$

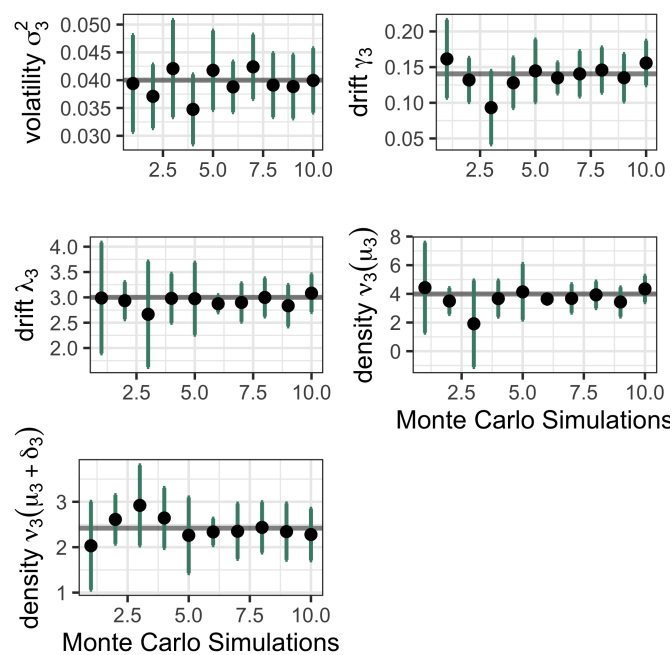
Using the fact that the error distribution was centered and had unit variance, we can then write

$$\delta_j = \sqrt{\mathbb{E}[\delta_j^2 \varepsilon_{j,k}^2]} = \sqrt{\mathbb{E}\left[\left(\frac{\mathcal{O}_{j,k} - \mathcal{O}_j(x_{j,k})}{\mathcal{O}_j(x_{j,k})}\right)^2\right]}.$$



(a) 10 Monte-Carlo estimates
 $(\tilde{\sigma}_1, \tilde{\gamma}_1, \tilde{\lambda}_1, \tilde{\nu}_1(\mu_1), \tilde{\nu}_1(\mu_1 + \delta_1))$ with
 confidence intervals for
 $(\sigma_1, \gamma_1, \lambda_1, \nu_1(\mu_1), \nu_1(\mu_1 + \delta_1)) \approx$
 $(0.2, 0.36, 5, -0.1, 0.2)$.

(b) 10 Monte-Carlo estimates
 $(\tilde{\sigma}_2, \tilde{\gamma}_2, \tilde{\lambda}_2, \tilde{\nu}_2(\mu_2), \tilde{\nu}_2(\mu_2 + \delta_2))$ with
 confidence intervals for
 $(\sigma_2, \gamma_2, \lambda_2, \nu_2(\mu_2), \nu_2(\mu_2 + \delta_2)) \approx$
 $(0.1, 0.16, 2, -0.2, 0.4)$.



(c) 10 Monte-Carlo estimates
 $(\tilde{\sigma}_3, \tilde{\gamma}_3, \tilde{\lambda}_3, \tilde{\nu}_3(\mu_3), \tilde{\nu}_3(\mu_3 + \delta_3))$ with
 confidence intervals for
 $(\sigma_3, \gamma_3, \lambda_3, \nu_3(\mu_3), \nu_3(\mu_3 + \delta_3)) \approx$
 $(0.3, 0.12, 3, -0.1, 0.3)$.

Fig. 5.11: These plots show the result of 10 Monte-Carlo simulations of
 $(\tilde{\sigma}_j^2, \tilde{\gamma}_j, \tilde{\lambda}_j, \tilde{\nu}_j(\mu_j), \tilde{\nu}_j(\mu_j + \delta_j))_{j=1,2,3}$ with 95% confidence intervals and undersmoothing
 with $\zeta = 1.2$. In every plot, the thick grey lines portray the theoretical values
 $(\sigma_j, \gamma_j, \lambda_j, \nu_j(\mu_j), \nu_j(\mu_j + \delta_j))_{j=1,2,3}$.

Approximating the expected value \mathbb{E} by the mean gives an estimator $\tilde{\delta}_j$ for δ_j ,

$$\tilde{\delta}_j = \sqrt{\frac{1}{m_j} \sum_{k=1}^{m_j} \left(\frac{\mathcal{O}_{j,k} - \mathcal{O}_j(x_{j,k})}{\mathcal{O}_j(x_{j,k})} \right)^2}.$$

Note that for the estimator $\tilde{\delta}_j$ and the approximation of the error magnitudes $\tilde{\delta}_{j,k} = \tilde{\delta}_j \mathcal{O}_j(x_{j,k})$ the function $\mathcal{O}_j(x_{j,k})$ is needed. This function is however unknown.

Recall that the Penalized Least Squares method was the method that minimized the L^2 -distance between the implied option function $\tilde{\mathcal{O}}_{(\sigma_j^2, \gamma_j, \nu_j)}$ and the smoothing spline $\tilde{\mathcal{O}}_j$.

Therefore, using the PLS method the final estimator of the error magnitudes can be given as

$$\tilde{\delta}_{j,k} = \tilde{\delta}_j \tilde{\mathcal{O}}_{(\sigma_j^2, \gamma_j, \nu_j)}(x_{j,k}) \quad \text{with} \quad \tilde{\delta}_j = \sqrt{\frac{1}{m_j} \sum_{k=1}^{m_j} \left(\frac{\mathcal{O}_{j,k} - \tilde{\mathcal{O}}_{(\sigma_j^2, \gamma_j, \nu_j)}(x_{j,k})}{\tilde{\mathcal{O}}_{(\sigma_j^2, \gamma_j, \nu_j)}(x_{j,k})} \right)^2}. \quad (5.3)$$

Figure 5.12 shows the PLS-estimated functions $\tilde{\mathcal{O}}_{(\sigma_j^2, \gamma_j, \nu_j)}(x_{j,k})$ in black and the observed points $\mathcal{O}_{j,k}$ in grey for the cases $j = 1, 2, 3$. In these plots, the x -axis is limited to values that are not too close to 0. These values can result in an unstable estimator of $\tilde{\delta}_j$. This is mostly because the Fourier transform can imply bumps in the tails of $\tilde{\mathcal{O}}_{(\sigma_j^2, \gamma_j, \nu_j)}(x_{j,k})$, which can result in unrealistic large values of

$$\frac{\mathcal{O}_{j,k} - \tilde{\mathcal{O}}_{(\sigma_j^2, \gamma_j, \nu_j)}(x_{j,k})}{\tilde{\mathcal{O}}_{(\sigma_j^2, \gamma_j, \nu_j)}(x_{j,k})},$$

in the tails.

Figure 5.12 shows that the PLS-estimate $\tilde{\mathcal{O}}_{(\sigma_j^2, \gamma_j, \nu_j)}(x_{j,k})$ is quite stable and accurate in portraying the underlying denoised function of the observed points $\mathcal{O}_{j,k}$. Only at the point of the peaks, the values are underestimated and some bias can be noticed. This can be mostly seen in Figure 5.12a, and decreases in 5.12b, and decreases even more in 5.12c.

Using expression (5.3) the underlying error factor $\tilde{\delta}_j$ can be calculated. For 100 Monte-Carlo simulations, this error factor is calculated and the estimated mean $\mu_{\tilde{\delta}_j}$ and standard deviation $\sigma_{\tilde{\delta}_j}$ are given in Table 5.5.

	$j = 1$	$j = 2$	$j = 3$
$\mu_{\tilde{\delta}_j}$	0.019	0.015	0.013
$\sigma_{\tilde{\delta}_j}$	0.003	0.002	0.003

Table 5.5: Mean $\mu_{\tilde{\delta}_j}$ and standard deviation $\sigma_{\tilde{\delta}_j}$ of the estimator $(\tilde{\delta}_j)_{j=1,2,3}$ for 100 Monte-Carlo simulations.

Recall that the underlying noise factor was given by $\delta_j = 0.010$ for $j = 1, 2, 3$. Table 5.5 shows that all estimates are above the underlying theoretical value. As mentioned, this bias is mostly due to the miss-estimation of the PLS method at the peaks in Figure 5.12.

Overestimating $\tilde{\delta}_j$ is not necessarily a problem, the confidence intervals just become more conservative. This opens a way that the Bias in the estimation of the triplet $(\tilde{\sigma}_j, \tilde{\gamma}_j, \tilde{\nu}_j)_{j=1,2,3}$ can already be captured in the overestimation of $\tilde{\delta}_j$. Thus, the undersmoothing parameter ζ – which governed the Bias and Stochastic Error trade-off – might not be needed anymore.

To verify this, using 1000 Monte-Carlo simulations, calculating δ_j in every Monte-Carlo simulation, the same Figure as in 5.11 can be created. The new coverage probabilities are given in Table 5.6.

Table 5.6 shows that all coverage probabilities are above the implied 95% confidence interval without using undersmoothing. So if expression (5.3) is used to estimate δ_j , one

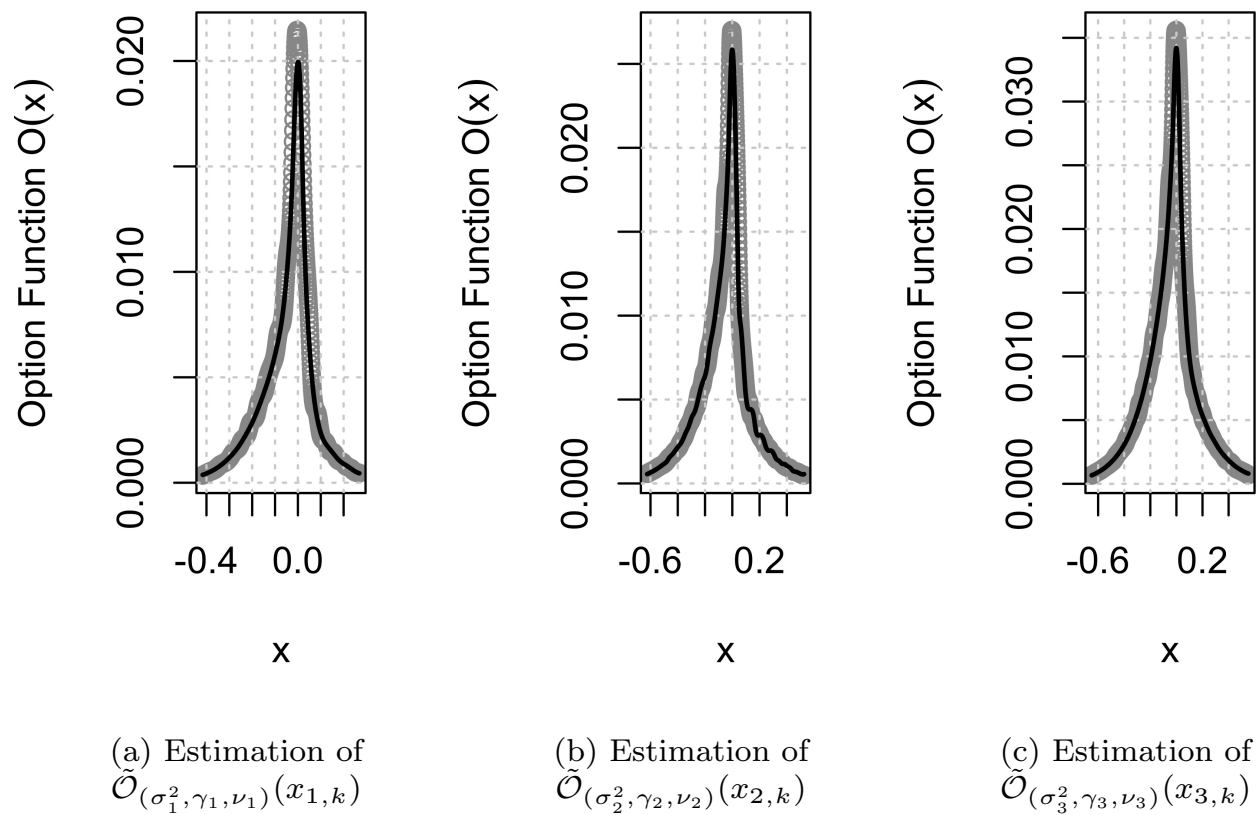


Fig. 5.12: These plots show the PLS-estimation of the function $\tilde{\mathcal{O}}_{(\sigma_j^2, \gamma_j, \nu_j)}(x_{j,k})$ as a black line for the observed grey points $\mathcal{O}_{j,k}$ for the cases $j = 1, 2, 3$.

	$\tilde{\sigma}_j^2$	$\tilde{\gamma}_j$	$\tilde{\lambda}_j$	$\tilde{\nu}_j(\mu_j)$	$\tilde{\nu}_j(\mu_j + \delta_j)$
$j = 1$	97.3%	99.1%	99.4%	98.9%	99.9%
$j = 2$	99.9%	99.6%	99.8%	98.8%	99.4%
$j = 3$	96.9%	97.4%	95.4%	96.1%	99.2%

Table 5.6: Coverage probabilities of $(\tilde{\sigma}_j^2, \tilde{\gamma}_j, \tilde{\lambda}_j, \tilde{\nu}_j(\mu_j), \tilde{\nu}_j(\mu_j + \delta_j))_{j=1,2,3}$ for 1000 Monte-Carlo simulations while estimating $\tilde{\delta}_j$ with expression (5.3).

does not in general also need to employ undersmoothing to reduce the bias, because the bias is already captured in the estimation error of $\tilde{\delta}_j$.

Chapter 6

Empirical Results

The constructed time-inhomogeneous calibration model will be applied to empirical data in this chapter. The data set that will be used is downloaded from the website <https://historicaloptiondata.com>, which is run by an enterprise that has been actively providing historical option prices and historical stock prices for over twenty years.¹

For the choice of the data, it is advised to choose a liquid product such that numerous stable option prices are provided for the underlying asset. The ticker SPY — the most popular exchange-traded fund of the S&P500 — is generally considered to have the most liquid on-screen traded options and is therefore a natural choice.

The SPY data that has been downloaded contains call and put option prices with quote dates in August 2022 and maturities running up to December 2024. More about the specifics of the data, the cleaning of the data, and the amount of data, in the upcoming section *Underlying Data Set*.

The empirical settings resemble in many parts the same simulation settings section as in 5.1, e.g., the weight functions are chosen similarly. Therefore, the differences with respect to the simulations will first be discussed in section 6.1. The calibration results in a similar setting as the simulations, i.e. three maturities one week apart, will be shown in section 6.2. In the last section 6.3, a calibration will be evaluated using all maturities in the data set to test the full capacity of the model and provide insight into the time dependency of the parameters.

6.1 Empirical Settings

6.1.1 Underlying Data Set

Figure 6.1 shows a snapshot of the data that has been downloaded. The data frame contains the underlying ticker (*underlying*), the quote date (*quotedate*), the last price of the underlying on the quote date (*underlying_last*), the type of option call or put (*type*), the strike price (*strike*), the last (*last*), bid (*bid*) and ask (*ask*) prices, and the underlying volume (*volume*).

underlying	underlying_last	type	expiration	quotedate	strike	last	bid	ask	volume
SPY	408.15	call	08/05/2022	08/02/2022	416	0.69	0.67	0.68	10025
SPY	408.15	put	08/05/2022	08/02/2022	416	8.67	8.63	8.77	749
SPY	408.15	call	08/05/2022	08/02/2022	417	0.52	0.51	0.52	11193
SPY	408.15	put	08/05/2022	08/02/2022	417	9.30	9.48	9.63	799
SPY	408.15	call	08/05/2022	08/02/2022	418	0.40	0.39	0.40	18794
SPY	408.15	put	08/05/2022	08/02/2022	418	10.29	10.36	10.53	275

Fig. 6.1: Snapshot of S&P500 ETF (SPY) market options data set used for empirical calibrations.

¹ Downloading the data costs a fee to provide the underlying company for running the data services.

The data frame contained much more information, such as the contract number, the exchange the product is traded on, the greeks, and the implied volatility, which are not of interest to our calibration.

Some products portrayed prices with low volume, these are however not actively traded and not accurately priced. Therefore, all contracts with a volume of less than 5 have been filtered out of the data.

For the actual price of the call and put options, the mid-price will be taken, i.e., the mean of the bid and ask prices. This is the most natural choice of what the product should be worth.

The quote date is taken as the first available quote date namely 2nd of August 2022. The available expiration/maturity dates and the underlying number of call and put options with volume > 5 for this quote day are

"08/03/2022":128, "08/05/2022":160, "08/08/2022":126, "08/10/2022":135,
 "08/12/2022":165, "08/15/2022":123, "08/17/2022":101, "08/19/2022":214,
 "08/22/2022":74, "08/24/2022":96, "08/26/2022":145, "08/29/2022":102,
 "08/31/2022":111, "09/02/2022":136, "09/06/2022":60, "09/07/2022":15,
 "09/09/2022":109, "09/16/2022":288, "09/30/2022":168, "10/21/2022":210,
 "11/18/2022":76, "12/16/2022":198, "12/30/2022":76, "01/20/2023":104,
 "03/17/2023":72, "03/31/2023":26, "06/16/2023":78, "06/30/2023":9,
 "09/15/2023":24, "12/15/2023":42, "01/19/2024":28, "06/21/2024":4,
 "12/20/2024":14.

It can be seen that the amount of call and put options can change from expiration to expiration. In general, as with the simulations, the maturities containing more than 100 data points will be considered for stability.

Using the put-call parity it is possible to use both the call and put prices. The dynamic parameter that governs the same prices of calls and puts with the same strike is the interest rate r – if the interest rate r is not adequately chosen the put-call parity might not be satisfied.

6.1.2 Interest Rate r

The risk-free interest rate underlying the price process will be inferred from the option prices. Recall that the put-call parity in expression (2.6) was given by

$$\mathcal{C}(x_{j,k}, T_j) - \mathcal{P}(x_{j,k}, T_j) = S_0 \mathbb{E} \left[e^{X_{T_j}} - e^{x_{j,k}} \right] = S_0 (1 - e^{x_{j,k}}).$$

with

$$x_{j,k} = \log(K_{j,k}/S_0) - r_{j,k}T_j,$$

where $r_{j,k}$ is denoted instead of r to clarify the dependency on j and k . The dependency on j means that for different maturities T_j the interest rate may change over time. The parameter k models that for the same maturity T_j there might still be noise in the interest rates implied by the option prices for different strike prices.

Rewriting (2.6) to isolate $r_{j,k}$ results in

$$r_{j,k} = -\frac{1}{T_j} \log \left(\frac{S_0 - \mathcal{C}(x_{j,k}, T_j) + \mathcal{P}(x_{j,k}, T_j)}{K_{j,k}} \right).$$

For every maturity T_j there should be one interest rate r_j displayed by the multiple option prices $\mathcal{C}(x_{j,k}, T_j)$ and $\mathcal{P}(x_{j,k}, T_j)$ for $k = 1, \dots, m_j$. Let us, therefore, approximate the interest rate r_j by the mean of the observations $r_{j,k}$,

$$r_j = -\frac{1}{m_j T_j} \sum_{k=1}^{m_j} \log \left(\frac{S_0 - \mathcal{C}(x_{j,k}, T_j) + \mathcal{P}(x_{j,k}, T_j)}{K_{j,k}} \right). \quad (6.1)$$

Calculating r_j for the option prices with maturity "08/31/2022" gives the estimate of 0.0126. A plot of the price of the call options against the strikes can be found in Figure 6.2a. A plot of the put prices converted to calls with the put-call parity with this interest rate r_j against strikes can be found in Figure 6.2b.

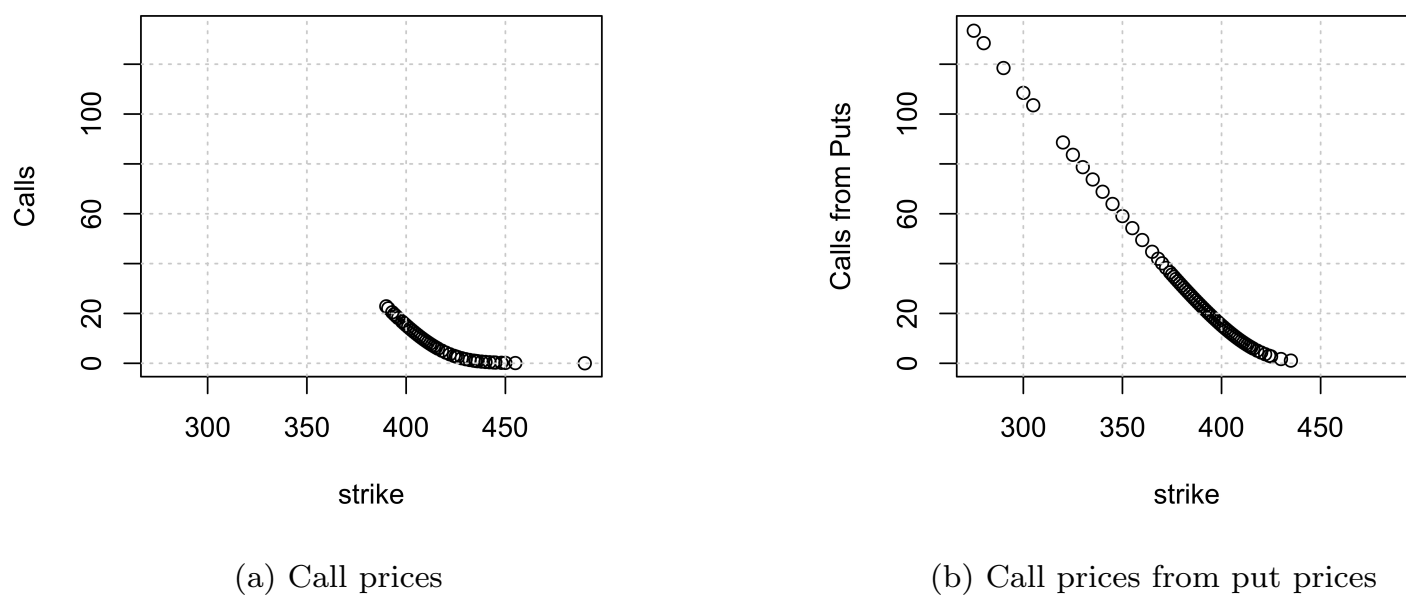


Fig. 6.2: Call prices (left) and call prices from puts by put-call parity (right) against strike price for maturity "08/31/2022" and interest rate $r_j \approx 0.01$.

From Figure 6.2 it appears that a lot of put prices with a relatively small strike price are sold more than call prices with a relatively high strike price – both cases are the out-of-the-money regions. This is due to hedging from risk-averse agents, which get insurance with these puts in the case when the index drops majorly.

Combining Figures 6.2a and 6.2b gives us a wide range of option prices that will be used in constructing the option function \mathcal{O}_j for the calibration process.

6.1.3 Smoothness Parameter s_j

The underlying smoothness parameter s_j was an important parameter that governed the convergence in the theoretical results. The parameter in the simulations for the Merton model is, for example, infinitely smooth, but we chose the parameter to be 6. In the empirical results, we assume that the underlying densities are at least 2 times differentiable and we take $s_j = 2$ for all maturities.

6.1.4 Choice of Cut-Off Parameters U_j and U_{ν_j}

In the case of real data, the Lévy model serves as an approximation only. The real underlying dynamics of the stock process do not necessarily have to be exactly portrayed by an Lévy model, as with the simulations. Consequently, the *flat* method of section 5.1.1 does not have to stabilize and does not necessarily lead to sensible results in estimating U_j and U_{ν_j} as it did with the simulations. The preferred method for choosing U_j and U_{ν_j} with real data is, therefore, the PLS method.

6.2 Empirical Results

In the same manner as with the simulations, we would like to calibrate a process that has three maturities approximately a week apart and more than 100 data points per maturity. Looking at the data displayed in section 6.1.1 the maturities can be taken as $(T_1, T_2, T_3) =$

(08/08/2022, 08/15/2022, 08/26/2022) with the quote date $T_0 = 08/02/2022$. The amount of data points per maturity is respectively 126, 123, and 145, which are all quite close to the amount of 150 data points in the simulations.

The risk-free rate r_j is chosen between every two maturities $(T_{j-1}, T_j)_{j=1,2,3}$ as in expression (6.1) and from the data it follows that $S = 408.15$ at T_0 .

Most theoretical considerations have been explained in the simulations and will therefore not be repeated in the real-life data. Mostly, the results and differences with respect to the simulations will be shown.

Estimation of $\tilde{\psi}_j$ for ψ_j

The estimators $(\tilde{\psi}_j)_{j=1,2,3}$ will first be investigated because it is at the root of the estimation procedure of the triplets $(\tilde{\sigma}_j, \tilde{\gamma}_j, \tilde{\lambda}_j)_{j=1,2,3}$. Recall that $\tilde{\sigma}_j$ and $\tilde{\lambda}_j$ were estimated with the real part $\text{Re}(\tilde{\psi}_j)$ and $\tilde{\gamma}_j$ was estimated with the imaginary part $\text{Im}(\tilde{\psi}_j)$. Figure 6.3 shows the real and imaginary parts of $(\tilde{\psi}_j)_{j=1,2,3}$ that follow from the data for the different maturities.

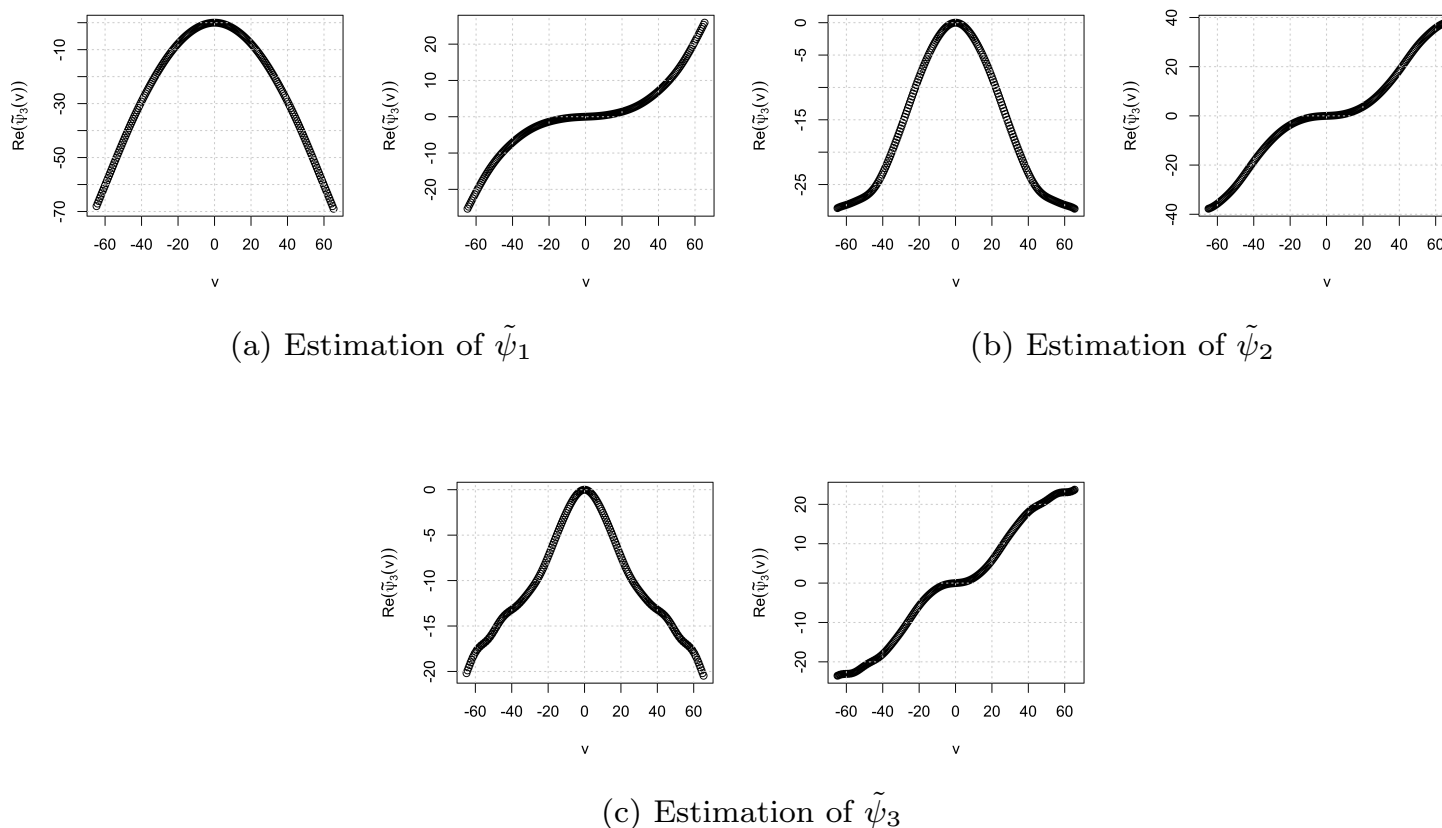


Fig. 6.3: These plots show the estimation of the real Re and imaginary part Im of the calibration function $\tilde{\psi}_j$ for $j = 1, 2, 3$.

Note that in Figure 6.3 all estimations look stable and similar to the simulation plots of 5.3.

Calibration of \mathcal{O}_j Functions by PLS Method

Both the cut-off parameters $(U_j)_{j=1,2,3}$ that will be used for estimating the triplets $(\tilde{\sigma}_j, \tilde{\gamma}_j, \tilde{\lambda}_j)_{j=1,2,3}$ and the underlying noise parameter $(\tilde{\delta}_j)_{j=1,2,3}$ – as in expression (5.3) – need to follow from the PLS-method, which minimized the Residual Sum of Square in the option function, i.e.,

$$U_j^* = \inf_{U_j > 0} \left[\left\| \tilde{\mathcal{O}}_{(\sigma_j^2, \gamma_j, \nu_j)}(x_{j,k}) - \tilde{\mathcal{O}}_{j,k} \right\|_{l^2} \right].$$

The best estimated implied option function $\tilde{\mathcal{O}}_{(\sigma_j^2, \gamma_j, \nu_j)}(x)$ to the underlying data $\tilde{\mathcal{O}}_{j,k}$ chosen by the PLS-method for $j = 1, 2, 3$ is shown in Figure 6.4. The data $\tilde{\mathcal{O}}_{j,k}$ is displayed as grey points and the function $\tilde{\mathcal{O}}_{(\sigma_j^2, \gamma_j, \nu_j)}(x)$ is displayed as a black line.

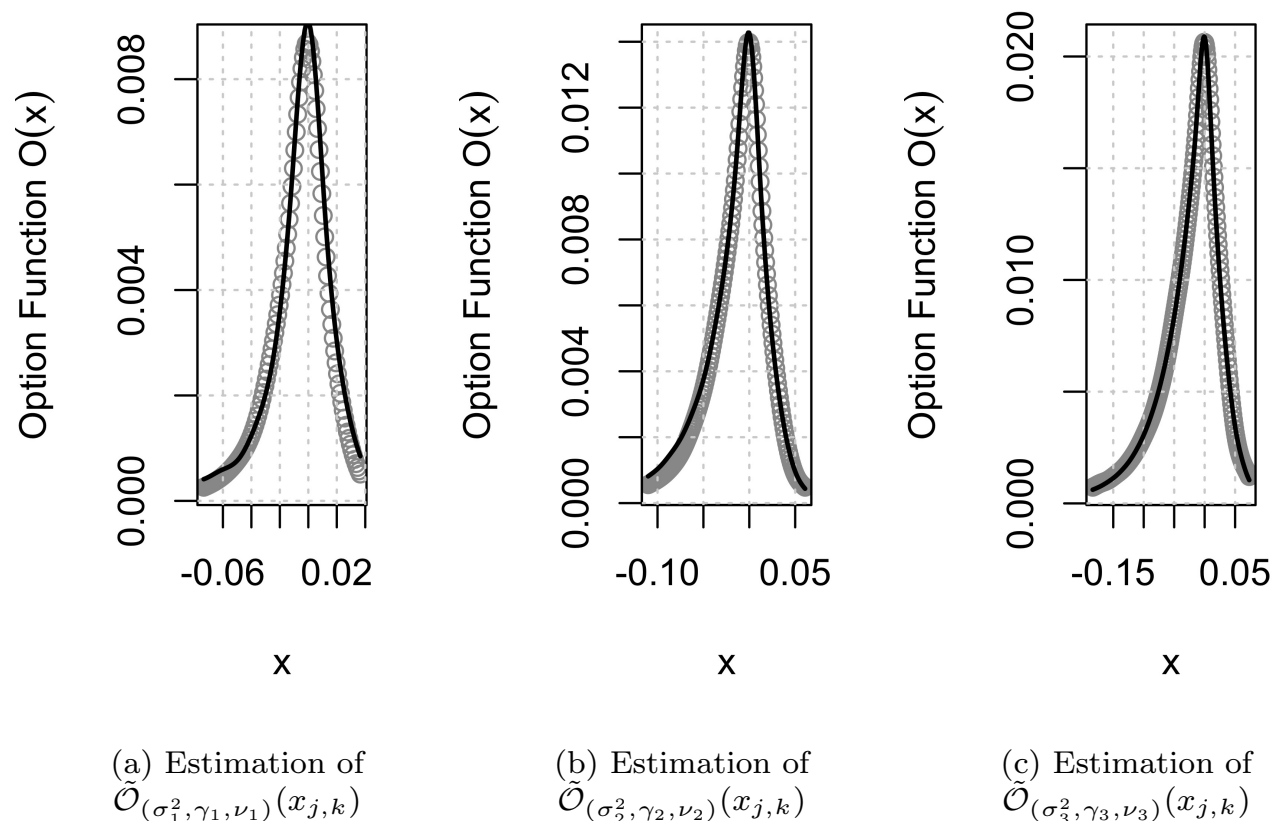


Fig. 6.4: These plots show the PLS-estimation of the function $\tilde{\mathcal{O}}_{(\sigma_j^2, \gamma_j, \nu_j)}(x_{j,k})$ as a black line for the observed grey points $\mathcal{O}_{j,k}$ for the cases $j = 1, 2, 3$.

In the simulations at Figure 5.12, we noted the fact that the PLS method underestimates the peak of the observations and [46] did support this fact. However, it can be seen in the real-life data that this is not necessarily the case. This is probable since the real-life data is not necessarily portrayed by an exponential Lévy process as the simulations were.

The cut-off parameters $(U_j)_{j=1,2,3}$ that follow from the best fits of the PLS method in Figure 6.4 are given by:

$$U_1 = 35.5, \quad U_2 = 61.4 \quad \text{and} \quad U_3 = 55.3. \quad (6.2)$$

Furthermore, the underlying noise parameters, as in expression (5.3), are given by

$$\tilde{\delta}_1 = 0.057, \quad \tilde{\delta}_2 = 0.050, \quad \text{and} \quad \tilde{\delta}_3 = 0.020, \quad (6.3)$$

such that we can construct the noise to form confidence intervals. [16], [44], and [46] all used the rule of thumb that $\tilde{\delta}_j = 0.01$ in constructing their results, which this historical empirical data set does not support. We also used the calibration procedure on live data, i.e. option prices that are listed today for maturities in the future, and in this case, even more noise exists.

Estimation of $(\tilde{\sigma}_j^2, \tilde{\gamma}_j, \tilde{\lambda}_j)$

The estimation of the triplets $(\tilde{\sigma}_j^2, \tilde{\gamma}_j, \tilde{\lambda}_j)_{j=1,2,3}$ with the PLS-method together with the confidence intervals as constructed in expression (5.3) are plotted in Figure 6.5.

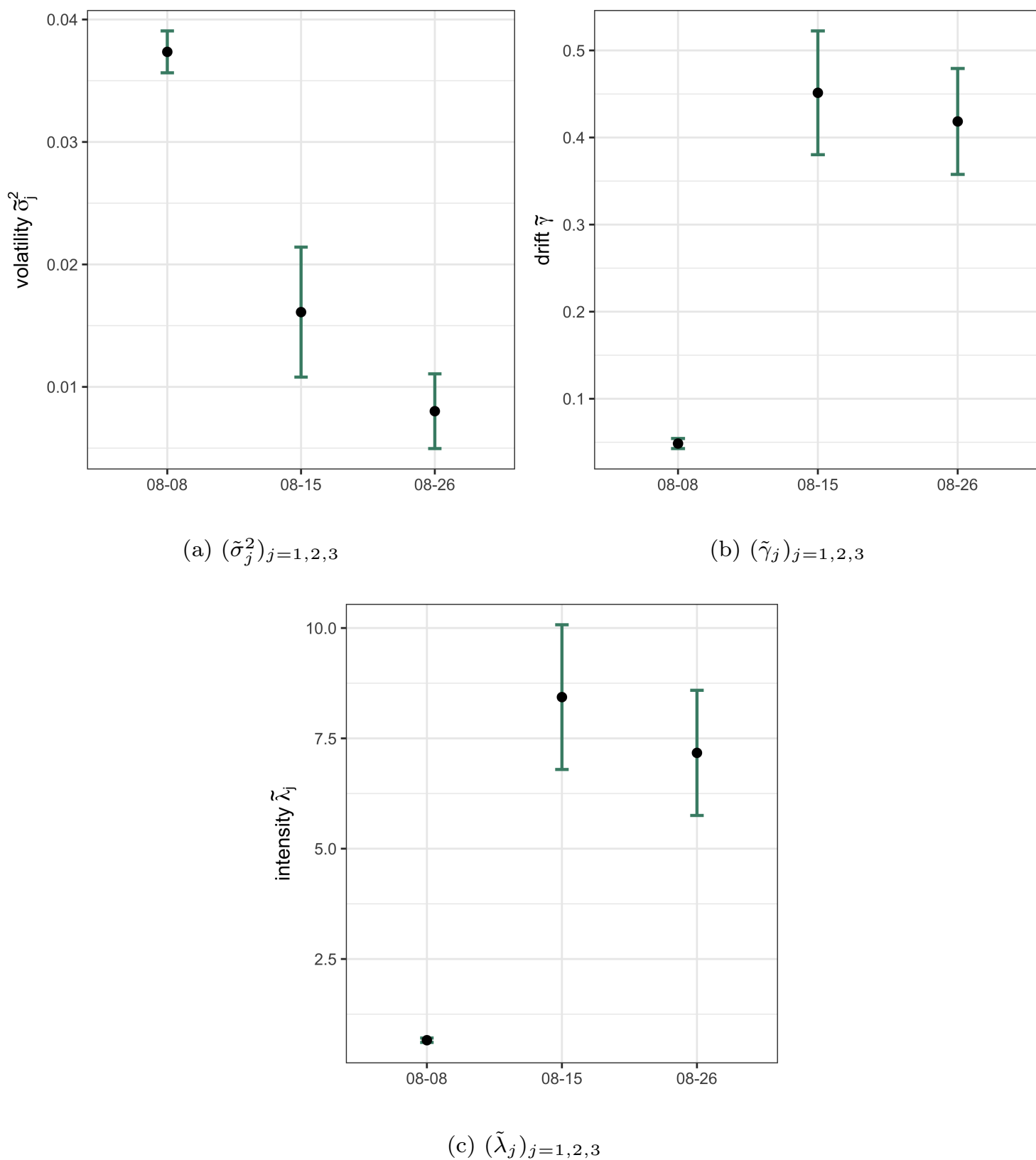


Fig. 6.5: Plots of the estimation of the triplets $(\tilde{\sigma}_j^2, \tilde{\gamma}_j, \tilde{\lambda}_j)_{j=1,2,3}$ for the empirical data as black points with confidence intervals in green.

In Figure 6.5 it can be seen that for the closest maturity of $T_1 = 08/08/2022$ the volatility $\tilde{\sigma}_1$ is highest but the drift $\tilde{\gamma}_1$ and intensity $\tilde{\lambda}_1$ are lowest. Whereas with the cases of $j = 2, 3$ we can notice the opposite effect. This effect can be seen in more real-life data and can provide an argument for time-inhomogeneous models instead of homogeneous models. However, a more detailed analysis must be carried out to support and verify this argument. In the next section, we will investigate a calibration with 19 maturities for a closer look at the time dependencies of the parameters.

The finite-sample confidence intervals for these triplets (4.5), (4.8) and (4.11) were mostly dependent on the underlying noise parameter $\delta_{j,k}$ – and thereby $\tilde{\delta}_j$ – and the chosen cut-off frequency U_j . Furthermore, the confidence intervals also had a term with the previous calibration $j - 1$ for $j > 1$. Recalling the estimated values in (6.2) and (6.3) it makes sense that the first one has the lowest confidence intervals, the second one the highest, and the third one just lower than the second.

Estimation of $\nu_j(x)$

The estimators of $(\nu_j(x))_{j=1,2,3}$ were estimated by an inverse Fourier transform with separate cut-off values $(U_{\nu_j})_{j=1,2,3}$ to gain more accurate results. The constructed Lévy densities by the PLS method and their confidence intervals (4.17) are plotted in Figure 6.6. All these densities have a similar shape to what [10] and [44] already captured in the homogeneous model.

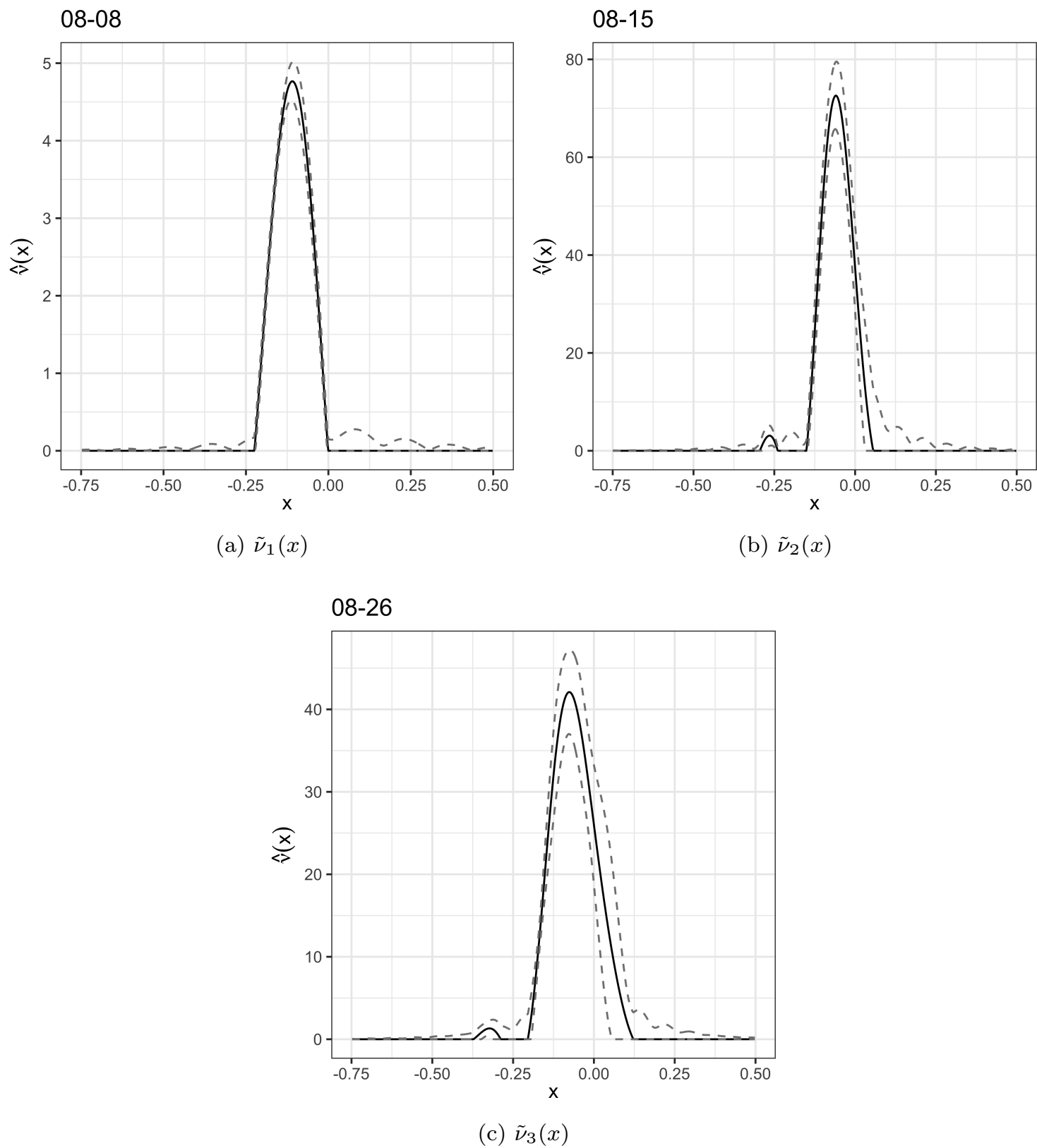


Fig. 6.6: Plots of the estimation of the jump densities $(\tilde{\nu}_j)_{j=1,2,3}$ in black with confidence intervals in grey.

Figure 6.6 shows that there can be some fluctuations in the confidence intervals at the tails of the density. The difference between these confidence intervals compared to the simulations with the Merton model is that they do not look normally distributed. At a certain moment, they look to hinge to 0 instead of a gradual convergence to 0. The confidence intervals then get these minor fluctuations at 0 and take these into account in the confidence intervals.

At the confidence intervals at $T_2 = 08/15/2022$ and $T_3 = 08/26/2022$ a bump can be noticed before $x = -0.25$. These densities appear to be unimodal or have only minor additional modes in the tails, which may be described as artifacts of the spectral calibration model – these results were also shown by [44]. However, these modes scarcely occur on the positive x-axis. A stylized fact from real-life data is that in price processes small jumps mostly occur downwards, as is displayed by the peaks that are all centered at the negative x-axis.

Construction of path S_t

Figures 6.5 and 6.6 show the Lévy triplets $(\tilde{\sigma}_j, \tilde{\gamma}_j, \tilde{\nu}_j)_{j=1,2,3}$ that governs the price dynamics in every interval $(T_j - T_{j-1})_{j=1,2,3}$ as described by the time-inhomogeneous model. Using these parameters, paths of the price process using this time-inhomogeneous exponential Lévy model can be constructed. Figure 6.7 shows two paths where in Figure 6.7a no jump occurs and in 6.7b a jump occurs. The grey lines portray the maturities of $T_1, T_2,$ and T_3 where the first grey line at 0 portrays T_0 .

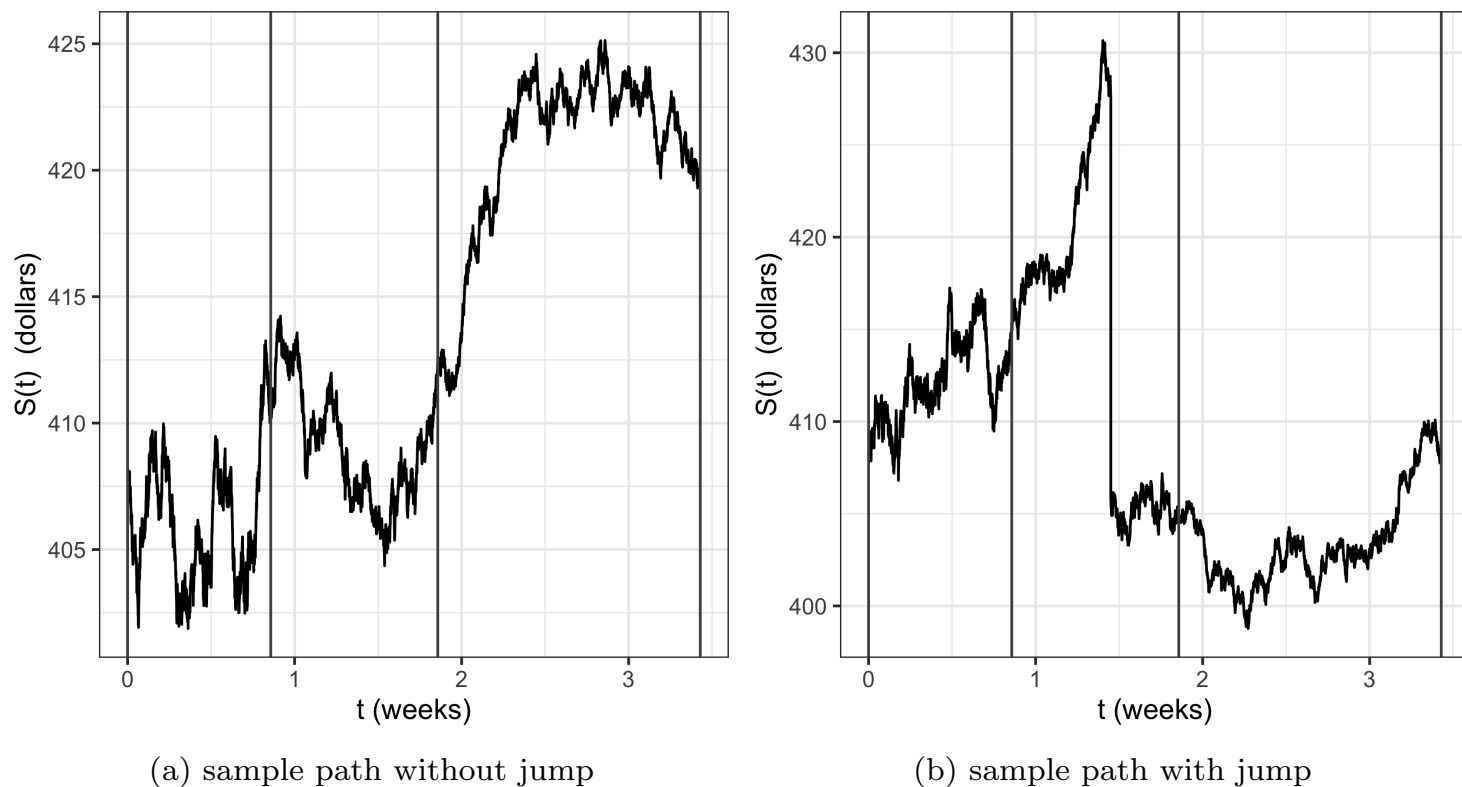


Fig. 6.7: Two sample paths of the price dynamics S_t against time modeled by a time-inhomogeneous exponential Lévy model that follow from calibration of real-life data of SPY options. The grey lines portray the 3 used maturities of the options.

The strength of the time-inhomogeneous Lévy models compared to the homogeneous Lévy models was in the fact that it allows us to preserve almost all the tractability of Lévy models — as with the homogeneous case — but it also enables us to reproduce the whole range of option prices across all maturities by dynamics that specifically describe the process between two maturities.

6.3 Real-Life Parameters over Time

To test the full capacity of the model and use all the data, let us consider calibrating a time-inhomogeneous model with numerous maturities. This will also give insight into how the parameters may change over time. The maturities and the number of data points at these maturities that will be considered are:

"08/03/2022":128, "08/05/2022":160, "08/08/2022":126, "08/10/2022":135,
 "08/12/2022":165, "08/15/2022":123, "08/17/2022":101, "08/19/2022":214,
 "08/22/2022":74, "08/24/2022":96, "08/29/2022":102, "08/31/2022":111,

"09/02/2022":136, "09/06/2022":60, "09/09/2022":109, "09/16/2022":288,
 "09/30/2022":168, "10/21/2022":210, "11/18/2022":76.

We use the PLS method to calibrate all these Lévy processes to the underlying option prices between all time intervals $[T_{j-1}, T_j]_{j=1, \dots, 19}$. Note that the time intervals are not equidistant, in the month of August we have a lot of expiration days only several days apart, but afterward the maturities can even be a week or more apart. In general, the closer to the quote date of 2nd of August, the more maturities and options listed at these maturities an agent can find.

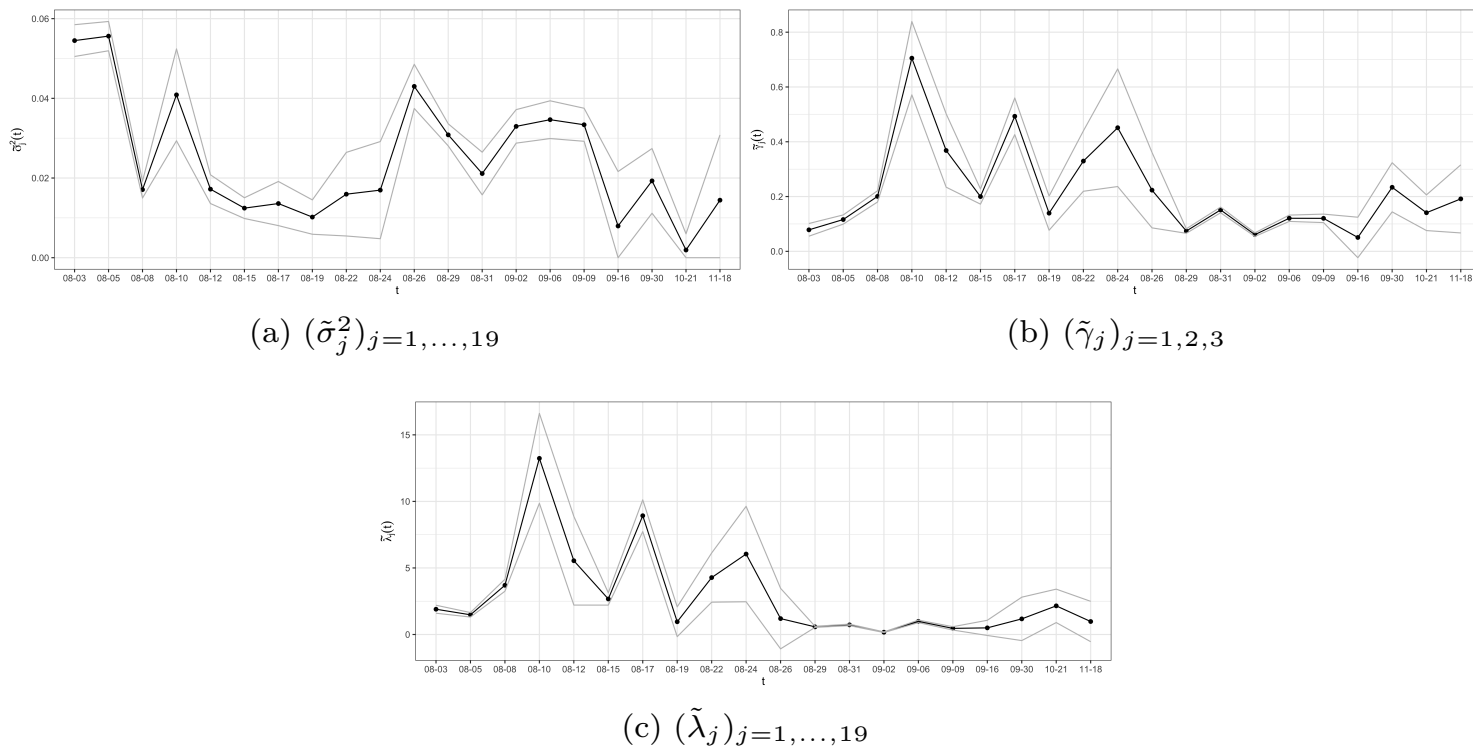


Fig. 6.8: Plots of the estimation of the triplets $(\tilde{\sigma}_j^2, \tilde{\gamma}_j, \tilde{\lambda}_j)_{j=1, \dots, 19}$ for the empirical data as black points with confidence intervals in grey.

Figure 6.8 shows the results of the estimation of the triplet $(\tilde{\sigma}_j, \tilde{\gamma}_j, \tilde{\lambda}_j)_{j=1, \dots, 19}$ with confidence intervals over the period of all maturities. Recall that in the previous section in Figure 6.5 we got the estimates of $(\tilde{\sigma}_j, \tilde{\gamma}_j, \tilde{\lambda}_j)$ at the dates 08/08/2022, 08/15/2022, and 08/26/2022. When comparing these to Figure 6.8 we can see that the estimates differ. The reason behind this is that now we use much more maturities and the intervals between the maturities are much shorter, such that the calibration takes place between different maturities with different characteristic functions. The coefficient over a longer period can be seen as the average over all the shorter periods.

Furthermore, Figure 6.8 shows that the estimates and confidence intervals can significantly differ over time, especially close to the quote date. This confirms that the time-inhomogeneous model is preferred over the time-homogeneous model where the parameters are constant and only calibrated from the quote day until a certain maturity.

The time-homogeneous model would take the intervals $[T_0, T_j]_{j=1, \dots, 19}$ for calibrating and one could make a time-dependent model by combining all triplets as suggested by Cont and Tankov [16, Chapter 14.2.2]. However, the dynamics between maturities are then neglected or over-counted, one would have an overlap between maturities, e.g., would the volatility calibrated on the period $[08/02/2022, 08/15/2022]$ be a good estimate of the volatility on $[08/08/2022, 08/15/2022]$. The time-inhomogeneous model carefully uses all data to calibrate between two maturities and would take certain events between maturities better into account in the dynamics.

In Figure 6.9 all jump densities $(\tilde{\nu}_j(x))_{j=1, \dots, 19}$ with confidence intervals have been plotted. It is visible that the width of the densities differs per maturity, some maturities are narrow and peaked, while some are broader and more spread out. Therefore some Lévy densities give more weight to more negative jumps than others.

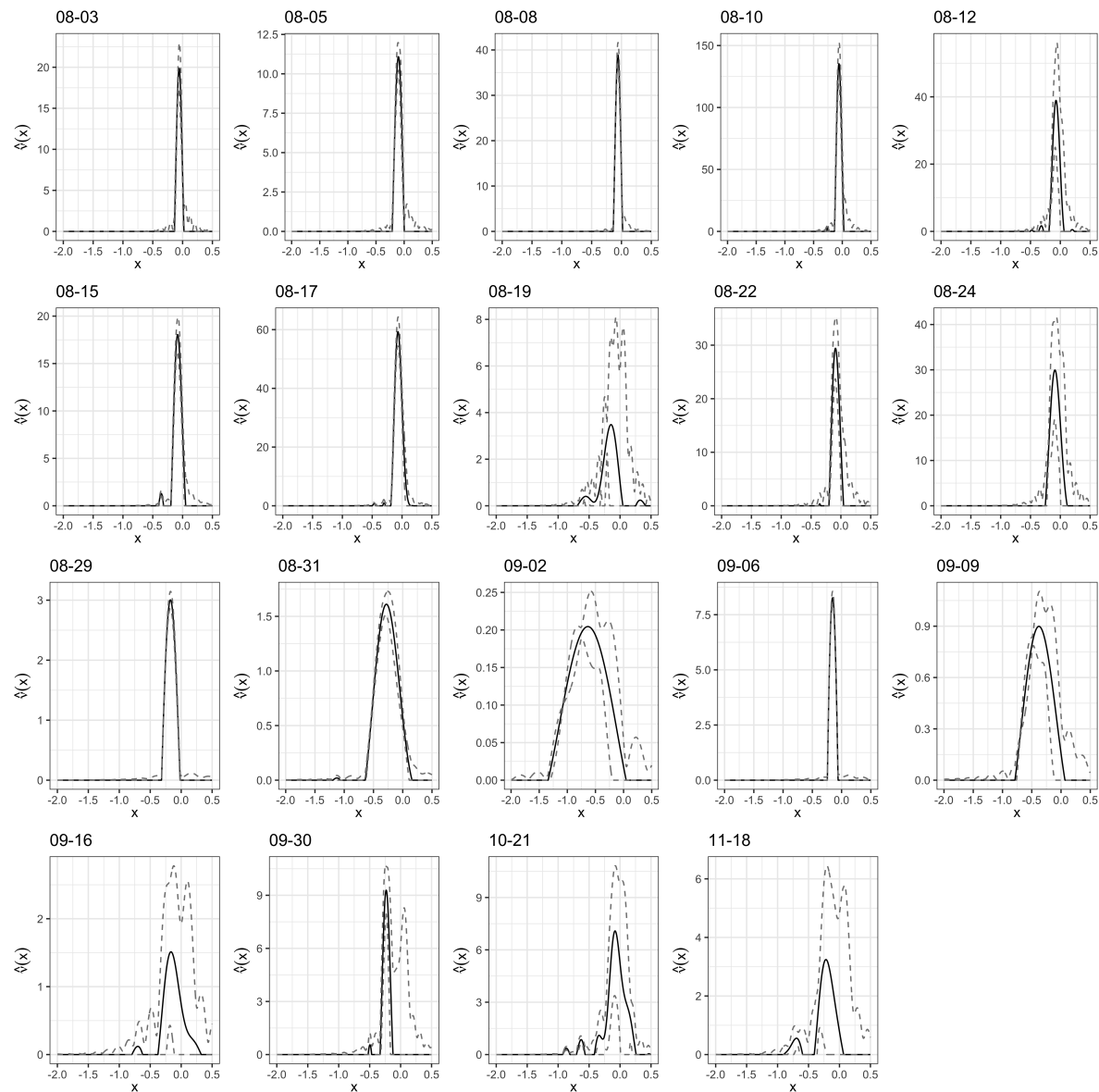


Fig. 6.9: Plots of the estimation of the jump densities $(\tilde{\nu}_j)_{j=1,\dots,19}$ in black with confidence intervals in grey.

The confidence intervals in Figure 6.9 also differ quite much from maturity to maturity. For example, "08/17/2022" is accurate where the next maturity "08/19/2022" is less precise, and then "08/22/2022" is accurate again. This is due to the different underlying noise and chosen cut-off values per calibration. Also, the confidence intervals for the last 4 plots "09/16/2022", "09/30/2022", "10/21/2022", and "10/21/2022" look rather imprecise. The reason here is that the calibration gets more difficult because the time frame is in the units of weeks now instead of several days.

Using the results of Figures 6.8 and 6.9 paths of the underlying price process can be constructed. Figure 6.10 shows two of these paths, where in 6.10a a path without jumps is presented and in 6.10b a path with jumps is presented. The grey lines portray the different maturities. In the beginning there are a lot of maturity dates and it decreases over time.

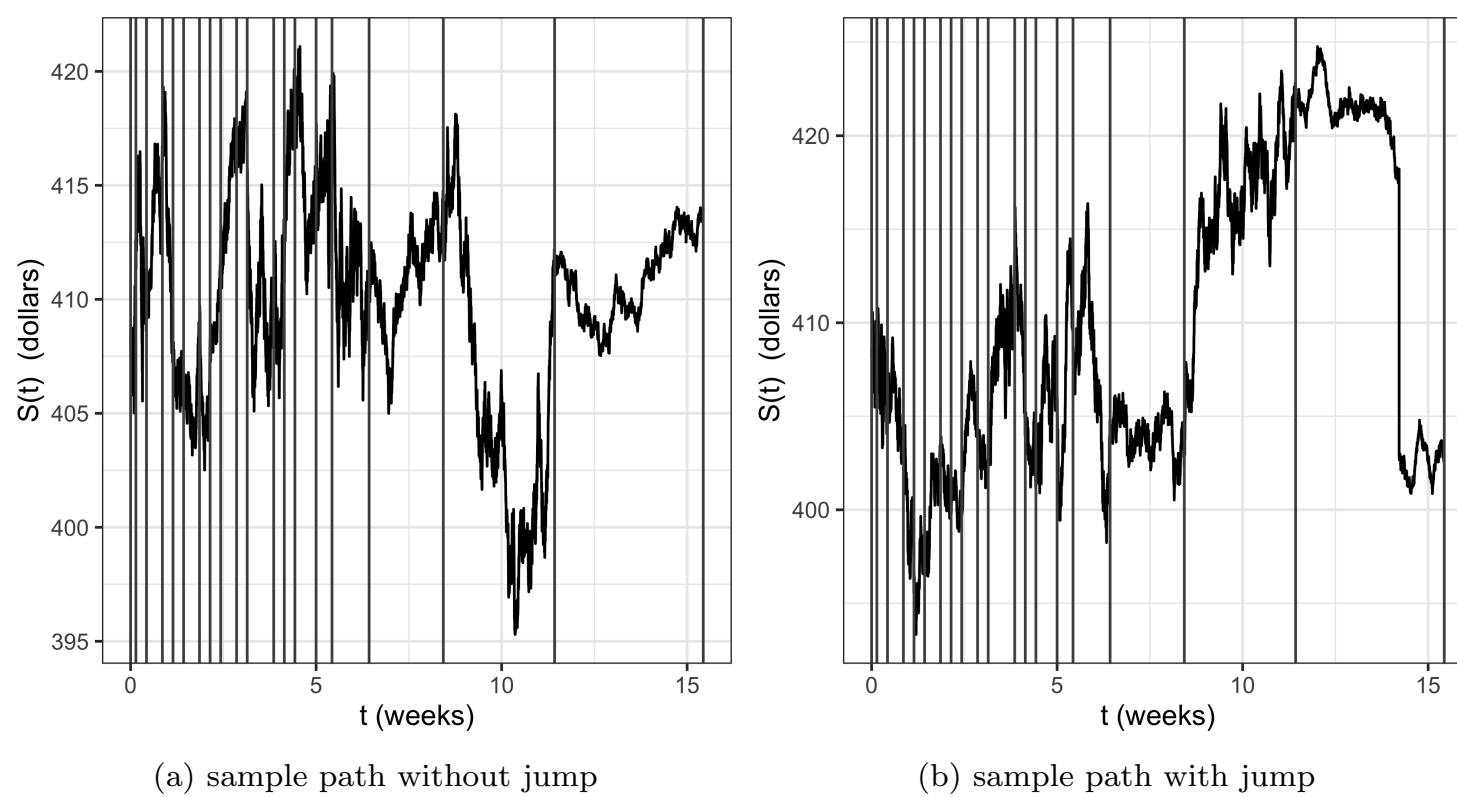


Fig. 6.10: Two sample paths of the price dynamics S_t against time modeled by a time-inhomogeneous exponential Lévy model that follows from calibration of real-life data of SPY options. The grey lines portray the 19 used maturities of the options.

Chapter 7

Conclusion

In this thesis, the time-inhomogeneous exponential Lévy model was introduced as a discrete additive process. An estimation procedure for the nonparametric calibration using option prices of these time-inhomogeneous models was constructed with the usage of the spectral domain. The time-inhomogeneous model can incorporate all option prices over all maturities and strike prices, which makes it a natural extension of the homogeneous model.

The underlying estimators of the process are asymptotically normally distributed under certain conditions of the increasing cut-off parameter and decreasing grid size. Furthermore, the calibration is well-defined, optimal convergence rates are found, and the inverse calibration problem has been inspected. From the difficulty of the inverse calibration, we found that the calibration works sufficiently whenever the time between maturities- and volatilities do not become too large.

Using the asymptotic variance of the normality results to create confidence intervals was not sufficient. The limiting result does not necessarily portray the finite sample cases. Thus, a new method that constructs the finite sample variance while disregarding the bias and remainder terms was built.

In the simulations, options have been extracted from a time-inhomogeneous Lévy process based on Merton models with 3 maturities a week apart. The calibration works for the majority of the Monte-Carlo simulations, but some odd cases/miss-calibrations could be noted. These odd cases could however be easily identified by the larger chosen cut-off values and the in turn widened confidence intervals. For the usage of the exact error distribution in the confidence intervals, undersmoothing should be employed to deal with the neglected bias term. Whereas the Penalised Least Squares estimated error distribution leads to an overestimation and an auto-penalization of this bias term.

Finally, the application of the constructed model to option prices of the S&P500 ETF (SPY) provided us with the insight that the model and confidence intervals work well in practice whenever enough option prices at different maturities are listed. The calibration of many maturities of the inhomogeneous model with confidence intervals showed us that the parameters differ over time, and this provided us with an argument for the time-inhomogeneous model.

For future research, we recommend investigating the performance of the time-inhomogeneous model in the pricing of exotic options, hedging, and risk management. Next to that, the constructed non-parametric spectral calibration method could also be used to construct goodness-of-fit tests to parametric time-inhomogeneous exponential Lévy models. As a last note, the extension of the inhomogeneous model to the case of infinite jump activity might also be theoretically interesting (See Trabs [48] for an extension for the homogeneous model).

References

- [1] Bauer, F. and Reiß, M.: 2008, Regularization independent of the noise level: an analysis of quasi-optimality, *Inverse Problems* **24**(5), 055009.
- [2] Bellamy, N. and Jeanblanc, M.: 2000, Incompleteness of markets driven by a mixed diffusion., *Finance & Stochastics* **4**(2).
- [3] Belomestny, D.: 2010, Spectral estimation of the fractional order of a Lévy process, *Ann. Statist.* **38**(1), 317–351.
- [4] Belomestny, D., Comte, F., Genon-Catalot, V., Masuda, H. and Reiß, M.: 2015, Lévy matters iv, *Lecture Notes in Mathematics. Springer* .
- [5] Belomestny, D., Gugushvili, S., Schauer, M. and Spreij, P.: 2019, Nonparametric Bayesian inference for Gamma-type Lévy subordinators, *Communications in Mathematical Sciences* **17**(3), 781–816.
- [6] Belomestny, D. and Reiß, M.: 2005, *Optimal calibration for exponential Lévy models*, WIAS.
- [7] Belomestny, D. and Reiß, M.: 2006aa, *Spectral calibration of exponential Lévy models*, Vol. 10, Springer.
- [8] Belomestny, D. and Reiß, M.: 2006ab, Spectral calibration of exponential Lévy models, *Financ. Stoch.* **10**(4), 449–474.
- [9] Belomestny, D. and Reiß, M.: 2006ba, Spectral calibration of exponential Lévy Models [2], *SFB 649 Discussion Paper 2006-035*, Sonderforschungsbereich 649, Humboldt Universität zu Berlin, Germany. available at <http://sfb649.wiwi.hu-berlin.de/papers/pdf/SFB649DP2006-035.pdf>.
- [10] Belomestny, D. and Reiß, M.: 2006bb, Spectral calibration of exponential lévy models [2], *SFB 649 Discussion Paper 2006-035* . Available at <http://sfb649.wiwi.hu-berlin.de/papers/pdf/SFB649DP2006-035.pdf>.
- [11] Belomestny, D. and Reiß, M.: 2015, Estimation and calibration of Lévy models via Fourier methods, *Lévy Matters IV*, Vol. 2128 of *Lecture Notes in Math.*, Springer, Cham, pp. 1–76.
- [12] Boyarchenko, S. and Levendorskiĭ, S.: 2002, Barrier options and touch-and-out options under regular Lévy processes of exponential type, *Ann. Appl. Probab.* **12**(4), 1261–1298.
- [13] Brown, L. D. and Low, M. G.: 1996, Asymptotic equivalence of nonparametric regression and white noise, *The Annals of Statistics* **24**(6), 2384–2398.
- [14] Carr, P. and Madan, D.: 1999, Option valuation using the fast fourier transform, *Journal of computational finance* **2**(4), 61–73.
- [15] Coca, A. J.: 2018, Efficient nonparametric inference for discretely observed compound Poisson processes, *Probab. Theory Related Fields* **170**(1-2), 475–523.
- [16] Cont, R. and Tankov, P.: 2004, *Financial modelling with jump-diffusions*. chapman.
- [17] Cont, R. and Tankov, P.: 2004b, Nonparametric calibration of jump-diffusion option pricing models, *J. Comput. Financ.* **7**(3), 1–49.
- [18] Cont, R. and Tankov, P.: 2006, Retrieving Lévy processes from option prices: Regularization of an ill-posed inverse problem, *SIAM Journal on Control and Optimization* **45**(1), 1–25.

- [19] Cont, R. and Voltchkova, E.: 2005a, A finite difference scheme for option pricing in jump diffusion and exponential Lévy models, *SIAM J. Numer. Anal.* **43**(4), 1596–1626.
- [20] Cont, R. and Voltchkova, E.: 2005b, Integro-differential equations for option prices in exponential Lévy models, *Financ. Stoch.* **9**(3), 299–325.
- [21] Eberlein, E. and Jacod, J.: 1997, On the range of options prices, *Finance and Stochastics* **1**(2), 131–140.
- [22] Emmer, S. and Klüppelberg, C.: 2004, Optimal portfolios when stock prices follow an exponential Lévy process, *Financ. Stoch.* **8**(1), 17–44.
- [23] Figueroa-López, J.: 2011, Sieve-based confidence intervals and bands for Lévy densities, *Bernoulli* **17**(2), 643–670.
- [24] Goldenshluger, A., Tsybakov, A. and Zeevi, A.: 2006, Optimal change-point estimation from indirect observations, *The Annals of Statistics* **34**(1), 350–372.
- [25] Green, P. J. and Silverman, B. W.: 2019, *Nonparametric regression and generalized linear models: a roughness penalty approach*, Chapman and Hall/CRC.
- [26] Gugushvili, S.: 2009, Nonparametric estimation of the characteristic triplet of a discretely observed Lévy process, *J. Nonparametr. Stat.* **21**(3), 321–343.
- [27] Gugushvili, S., van der Meulen, F. and Spreij, P.: 2015, Nonparametric Bayesian inference for multidimensional compound Poisson processes, *Mod. Stoch. Theory Appl.* **2**(1), 1–15.
- [28] Kallsen, J.: 2000, Optimal portfolios for exponential Lévy processes, *Math. Methods Oper. Res.* **51**(3), 357–374.
- [29] Kato, K. and Kurisu, D.: 2019, Bootstrap confidence bands for spectral estimation of Lévy densities under high-frequency observations, *To appear in Stochastic Processes and their Applications*.
- [30] Kawata, T.: 2014, *Fourier analysis in probability theory*, Vol. 15, Academic Press.
- [31] Kou, S. G.: 2002, A jump-diffusion model for option pricing, *Management science* **48**(8), 1086–1101.
- [32] Merton, R. C.: 1976a, Option pricing when underlying stock returns are discontinuous, *J. Financ. Econ.* **3**(1-2), 125–144.
- [33] Merton, R. C.: 1976b, Option pricing when underlying stock returns are discontinuous, *Journal of financial economics* **3**(1-2), 125–144.
- [34] Mordecki, E.: 2002, Optimal stopping and perpetual options for Lévy processes, *Finance Stoch.* **6**(4), 473–493.
- [35] Neumann, M. H. and Reiß, M.: 2009, Nonparametric estimation for Lévy processes from low-frequency observations, *Bernoulli* **15**(1), 223–248.
- [36] Nickl, R. and Reiß, M.: 2012, A Donsker theorem for Lévy measures, *J. Funct. Anal.* **263**(10), 3306–3332.
- [37] Nickl, R. and Söhl, J.: 2019, Bernstein - von Mises theorems for statistical inverse problems II: Compound Poisson processes, *To appear in Electronic Journal of Statistics*.
- [38] Qin, L. and Todorov, V.: 2019, Nonparametric implied Lévy densities, *Ann. Statist.* **47**(2), 1025–1060.
- [39] Renault, E.: 1997, Econometric models of option pricing errors, *Econometric Society Monographs* **28**, 223–278.
- [40] Söhl, J.: 2010, Polar sets for anisotropic gaussian random fields, *Statistics & probability letters* **80**(9-10), 840–847.
- [41] Söhl, J.: 2012, Confidence sets in nonparametric calibration of exponential lévy models, *Finance and Stochastics* **18**(3), 617–649.
- [42] Söhl, J.: 2014, Confidence sets in nonparametric calibration of exponential Lévy models, *Financ. Stoch.* **18**(3), 617–649.
- [43] Söhl, J. and Trabs, M.: 2014a, Option calibration of exponential Lévy models: Confidence intervals and empirical results, *J. Comput. Financ.* **18**(2), 91–119.
- [44] Söhl, J. and Trabs, M.: 2014b, Option calibration of exponential lévy models: Confidence intervals and empirical results, *Journal of Computational Finance* **18**(2).

- [45] Tankov, P.: 2011, Pricing and hedging in exponential Lévy models: review of recent results, *Paris-Princeton Lectures on Mathematical Finance 2010*, Vol. 2003 of *Lecture Notes in Math.*, Springer, Berlin, pp. 319–359.
- [46] Tendijck, S.: 2018, *Nonparametric calibration of inhomogeneous lévy processes using fourier techniques*, Master's thesis, Delft University of Technology.
- [47] Todorov, V.: 2019, Nonparametric spot volatility from options, *Preprint* .
- [48] Trabs, M.: 2014, Calibration of self-decomposable Lévy models, *Bernoulli* **20**(1), 109–140.
- [49] Trabs, M.: 2015, Quantile estimation for Lévy measures, *Stochastic Process. Appl.* **125**(9), 3484–3521.
- [50] van der Vaart, A. and Wellner, J. A.: 1997, Weak convergence and empirical processes with applications to statistics, *Journal of the Royal Statistical Society-Series A Statistics in Society* **160**(3), 596–608.
- [51] Van Loan, C.: 1992, *Computational frameworks for the fast Fourier transform*, SIAM.
- [52] Zheng, W. and Kwok, Y. K.: 2014, Fourier transform algorithms for pricing and hedging discretely sampled exotic variance products and volatility derivatives under additive processes, *J. Comput. Financ.* **18**(2), 3–30.

Appendix A

Proofs of Lemmata

Proof (Lemma 3.1) (Proof by Contradiction) Suppose that $\sup_{t \in [0, T]} |\arg g(t) - \arg f(t)| > \pi$. Then by the continuity of $\arg g(t)$ and $\arg f(t)$ we can employ the Mean Value Theorem to conclude that there exists a $t_0 \in [0, T]$ such that $|\arg g(t_0) - \arg f(t_0)| = \pi$. This is equivalent with $g(t_0) = -rf(t_0)$ for some $r \in \mathbb{R}_{>0}$. But then

$$|f(t_0) - g(t_0)| = (1 + r)|f(t_0)| > |f(t_0)| \geq C.$$

This contradicts the assumption $|f(t_0) - g(t_0)| \leq C$ for all $t \in [0, T]$. \square

Proof (Lemma 3.2) For the case of $q = 0$, the bound becomes

$$(x^2 + c)^0 = 1 \leq \max(2^{0-1}, 1)((x^2)^0 + c^0) = 1,$$

and the inequality holds. Now let $q \in \mathbb{R} \setminus \{0\}$. Define $y := x^2$ and instead of considering x it is easier to consider $y \geq 0$. Define $f_c : \mathbb{R}_{\geq 0} \rightarrow \mathbb{R}_{\geq 0}$ as

$$f_c(y) = \frac{(y + c)^{2q}}{y^{2q} + c^{2q}}.$$

Note that the function f_c has no singularities and that the derivative can be given by

$$\begin{aligned} \frac{df_c(y)}{dy} &= \frac{(y^{2q} + c^{2q})2q(y + c)^{2q-1} - (y + c)^{2q}2qy^{2q-1}}{(y^{2q} + c^{2q})^2} \\ &= \frac{2q(y + c)^{2q-1}((y^{2q} + c^{2q}) - (y + c)y^{2q-1})}{(y^{2q} + c^{2q})^2} \\ &= \frac{2qc(y + c)^{2q-1}(c^{2q-1} - y^{2q-1})}{(y^{2q} + c^{2q})^2}. \end{aligned}$$

Furthermore, the function f_c also satisfies

$$\lim_{y \rightarrow \infty} f_c(y) = 1,$$

and $f_c(0) = 1$. Thus, we must either have that $|f_c(y)| \leq 1$ for all $y > 0$ or $|f_c(y)| \leq f_c(z)$ with z a zero of $df_c(y)/dy$. From the expression of the derivative, it is clear that $df_c(y)/dy$ only has one zero on its domain which equals c . The value of this zero of the function is a maximum and has the value $f(c) = 2^{2q-1}$. Hence, for any $q, x \in \mathbb{R}$ and $c > 0$ we have that

$$|f_c(y)| \leq \max(2^{2q-1}, 1)$$

holds, substituting $y := x^2$ back and rearranging then completes the proof

$$(x^2 + c)^{2q} \leq \max(2^{2q-1}, 1)((x^2)^{2q} + c^{2q}).$$

\square

Proof (Lemma 3.3) By the monotonicity property of integrals, it follows that

$$\begin{aligned} & \lim_{U \rightarrow \infty} \left| \int_{(0,1)^2 \setminus (0,1-h(U))^2} f_U(v,w) g_U(v,w) d(v,w) \right| \\ & \leq \lim_{U \rightarrow \infty} C \int_{(0,1)^2 \setminus (0,1-h(U))^2} f_U(v,w) d(v,w) = 0. \end{aligned}$$

Thus,

$$\lim_{U \rightarrow \infty} \int_0^1 \int_0^1 f_U(v,w) g_U(v,w) dv dw = \lim_{U \rightarrow \infty} \int_{1-h(U)}^1 \int_{1-h(U)}^1 f_U(v,w) g_U(v,w) dv dw$$

Now it will be proven that this integral equals $g(1,1)$ by looking at the difference

$$\begin{aligned} & \lim_{U \rightarrow \infty} \left| \int_{1-h(U)}^1 \int_{1-h(U)}^1 f_U(v,w) (g_U(v,w) - g_U(1,1)) dv dw \right| \\ & \leq \lim_{U \rightarrow \infty} \int_{1-h(U)}^1 \int_{1-h(U)}^1 f_U(v,w) dv dw \sup_{(u,v) \in [1-h(U),1]^2} |g_U(v,w) - g_U(1,1)| \\ & = 0, \end{aligned}$$

by the assumptions in the Lemma. Concluding we have

$$\lim_{U \rightarrow \infty} \int_0^1 \int_0^1 f_U(v,w) g_U(v,w) dv dw = \lim_{U_j \rightarrow \infty} g_U(1,1).$$

□

Proof (Lemma 3.4) For the proof, we will show that the difference

$$\begin{aligned} & \lim_{U_j \rightarrow \infty} \Delta_{j-l}^{-1} \sum_{k=1}^{m_{j-l}} \delta_{j-l,k}^2 \left(A_{j-l}^2 e^{-A_{j-l} U_j^2} I_v^2 - e^{-2C_{j-l}} w_{\sigma_j}^1(1)^2 \mathcal{F} b_{j-l,k}(U_j)^2 e^{-2iB_{j-l} U_j} \right) \\ & = \lim_{U_j \rightarrow \infty} \sum_{k=1}^{m_{j-l}} \delta_{j-l,k}^2 \Delta_{j-l} \left(A_{j-l}^2 e^{-A_{j-l} U_j^2} I_v^2 \Delta_{j-l}^{-2} - e^{-2C_{j-l}} w_{\sigma_j}^1(1)^2 \mathcal{F} b_{j-l,k}(U_j)^2 e^{-2iB_{j-l} U_j} \Delta_{j-l}^{-2} \right) \end{aligned}$$

will be 0. By the assumption that $\delta_{j-l} \in L^{2+\eta}(\mathbb{R})$ with $\eta > 0$ we can see by the Riemann Integral that $\lim_{U_j \rightarrow \infty} \sum_{k=1}^{m_{j-l}} \delta_{j-l,k}^2 \Delta_{j-l} = \|\delta_{j-l}\|_{L^2}^2 < \infty$. Therefore, it is enough to show that the second part of the summation becomes 0 asymptotically,

$$\lim_{U_j \rightarrow \infty} \sum_{k=1}^m A_{j-l}^2 e^{-A_{j-l} U_j^2} I_v^2 \Delta_{j-l}^{-2} - e^{-2C_{j-l}} w_{\sigma_j}^1(1)^2 \mathcal{F} b_{j-l,k}(U_j)^2 e^{-2iB_{j-l} U_j} \Delta_{j-l}^{-2} = 0.$$

This is similar to bounding the term by any $\varepsilon > 0$ provided that $U_j > 0$ is large enough. Thereafter, letting ε converge to 0 completes the proof. In expression (3.18) we already proved the case without the term Δ_{j-l}^{-2} , thus it is enough to show that the second term is bounded, indeed because if $f_n/g_n \rightarrow 1$, $h_n \in \mathbb{C}$ and $|g_n h_n| \leq C$, then

$$\lim_{n \rightarrow \infty} |f_n h_n - g_n h_n| = \lim_{n \rightarrow \infty} |g_n h_n| |f_n/g_n - 1| \leq C \lim_{n \rightarrow \infty} |f_n/g_n - 1| = 0.$$

Inserting $\mathcal{F} b_{j-l,k}(U_j) = \Delta_{j-l} e^{iU_j x_{j,k}} \text{sinc}^2(U_j \Delta_{j-l})$, gives

$$\lim_{U_j \rightarrow \infty} \sum_{k=1}^m A_{j-l}^2 e^{-A_{j-l} U_j^2} I_v^2 \Delta_{j-l}^{-2} - e^{-2C_{j-l}} w_{\sigma_j}^1(1)^2 e^{2iU_j x_{j,k}} \text{sinc}^4(U_j \Delta_{j-l}) e^{-2iB_{j-l} U_j}.$$

The absolute value of the second part converges to $e^{-2C_{j-1}}w_{\sigma_j}^1(1)^2$, so it is easily bounded, which concludes the proof. \square

Proof (Lemma 3.5) Without loss of generality, we can assume that $C = 1$, because if $C \neq 1$ then we can replace z and \tilde{z} by z/C and \tilde{z}/C . Furthermore, the result only needs to be proven for positive real z , the rest of the complex plane for z thereafter follows by a rotational argument $ze^{i\varphi}$ and rotating \tilde{z} in a similar manner.

So, without loss of generality, we assume $C = 1$ and $z \in \mathbb{R}^+$. Let us write $\tilde{z} = x + iy$ with $(x, y) \in \mathbb{R}^2$. We then want to have $|z| > 2$, $|\tilde{z}| = x^2 + y^2 > 1$, and $|\arg z - \arg \tilde{z}| \leq 2\pi$. The proof is based on showing that $1/4$ bounds the real-valued function that satisfies these conditions,

$$f : (\mathbb{R}^2 \setminus \{(x, y) : x^2 + y^2 < 1\}) \times [2, \infty) \rightarrow \mathbb{R}^+$$

defined by

$$f(x, y, z) = \frac{|\log(x + iy) - \log(z) - (x + iy - z)z^{-1}|^2}{|x + iy - z|^4}.$$

The optimization of the function is difficult and will be done by the computer. From the computer, it is believed that the maximum of the function is attained at $z = 2$ and $x^2 + y^2 = 1$. Moreover, the maximum will be located at the point such that the difference in the argument is maximized. In our example this would be $x = -1$ and $y = 0$, leading to a difference in the argument of π . Hence, combining everything results in

$$f(z) \leq \frac{(3/2 - \log 2)^2 + \pi^2}{3^4} \approx 0.1299 \leq \frac{1}{4},$$

which completes the proof. \square

Proof (Lemma 3.6) The result will first be proven for the case $\xi_j = \sigma_j$, thereafter the differences for the proves of γ_j and λ_j will be pointed out. Define $A_j = \sum_{i=1}^j (T_i - T_{i-1})\sigma_i^2$ and recall

$$K_j(v) := 2^{j-1}e^{-v^2 A_j/2 + 2RT_j}.$$

It is easy to see that

$$\frac{1}{K_j(v)^2} = \frac{1}{2^{2j-2}}e^{v^2 A_j - 4RT_j} \lesssim e^{v^2 A_j}.$$

Using the symmetry of $w_{\sigma_j}^{U_j}$, $w_{\sigma_j}^{U_j}(v) = w_{\sigma_j}^1/U_j^3$, and the properties of $w_{\sigma_j}^1 \in \mathcal{W}_{s_j}^n$, then for the desired bound it follows that

$$\begin{aligned} \int_{-U_j}^{U_j} \frac{v^4 |w_{\sigma_j}^{U_j}(v)|}{K_j(v)^2} dv &\lesssim \int_{-U_j}^{U_j} e^{v^2 A_j} v^4 |w_{\sigma_j}^{U_j}(v)| dv \lesssim \int_{-U_j}^{U_j} e^{v^2 A_j} v^4 \frac{v^4}{U_j^{s_j+3}} |v|^{s_j} dv \\ &\lesssim U_j^{-(s_j+3)} \int_0^{U_j} v^{3+s_j} 2A_j v e^{A_j v^2} dv \leq \int_0^{U_j} 2A_j v e^{A_j v^2} dv = \left[e^{A_j v^2} \right]_{v=0}^{U_j} = e^{A_j U_j^2}. \end{aligned}$$

For the cases of γ_j and λ_j the proofs are almost analogous, only use that $w_{\gamma_j}^{U_j}$ is anti-symmetric and $w_{\gamma_j}^{U_j} = w_{\gamma_j}^1/U_j^2$ for γ_j , and $w_{\lambda_j}^{U_j} = w_{\lambda_j}^1/U_j$ for λ_j . \square

Appendix B

Additional Details Asymptotic Normality $\tilde{\mu}_j(x)$

B.1 Bias Term \mathcal{B}

The Bias term \mathcal{B} is given by

$$\mathcal{B} = \frac{1}{2\pi} \int_{\mathbb{R} \setminus [-U_j, U_j]} \left(\psi_j(v) + \frac{\sigma_j^2}{2}(v-i)^2 - i\gamma_j(v-i) + \lambda_j \right) (1 - w_{\mu_j}^{U_j}(v)) e^{-ivx} dv.$$

To show the asymptotic rate of the Bias term it is easier to analyze \mathcal{B}^2 , by the triangle rule for integration and the properties of $w_{\mu_j}^{U_j} \in \mathcal{W}_n^{s_j}$, it follows that

$$\begin{aligned} 4\pi^2 \mathcal{B}^2 &\leq \int_{\mathbb{R} \setminus [-U_j, U_j]} \left| \left(\psi_j(v) + \frac{\sigma_j^2}{2}(v-i)^2 - i\gamma_j(v-i) + \lambda_j \right) (1 - w_{\mu_j}^{U_j}(v)) e^{-ivx} \right|^2 dv \\ &\leq \int_{\mathbb{R}} \left| \left(\psi_j(v) + \frac{\sigma_j^2}{2}(v-i)^2 - i\gamma_j(v-i) + \lambda_j \right) (1 - w_{\mu_j}^{U_j}(v)) e^{-ivx} \right|^2 dv \\ &= \int_{\mathbb{R}} \left| \left(\psi_j(v) + \frac{\sigma_j^2}{2}(v-i)^2 - i\gamma_j(v-i) + \lambda_j \right) (1 - w_{\mu_j}^{U_j}(v)) \right|^2 dv \\ &= \int_{\mathbb{R}} \left| \mathcal{F}\mu_j(v)(1 - w_{\mu_j}^{U_j}(v)) \right|^2 dv \leq \int_{\mathbb{R}} |\mathcal{F}\mu_j(v)|^2 \frac{v^{2s_j}}{U_j^{2s_j}} dv. \end{aligned}$$

Now using the Fourier property $\mathcal{F}f^{(k)}(v) = (iv)^k \mathcal{F}f(v)$,

$$4\pi^2 \mathcal{B}^2 \leq \frac{1}{U_j^{2s_j}} \int_{\mathbb{R}} \left| \frac{\mathcal{F}\mu_j^{s_j}(v)}{(-iv)^{s_j}} \right|^2 v^{2s_j} dv = \frac{1}{U_j^{2s_j}} \int_{\mathbb{R}} |\mathcal{F}\mu_j^{s_j}(v)|^2 dv = U_j^{-2s_j} \|\mu_j^{s_j}\|_{L^2(\mathbb{R})}^2.$$

The properties of $\mu_j \in \mathcal{G}_n^{s_j}$ imply that $\|\mu_j^{s_j}\|_{L^2(\mathbb{R})}^2$ is a constant. Hence, it follows that

$$|\mathcal{B}| \leq \frac{1}{2\pi} U_j^{-s_j} \|\mu_j^{s_j}\|_{L^2(\mathbb{R})}.$$

B.2 Decomposition of Ψ Term

The Ψ term was defined by

$$\Psi = \frac{1}{2\pi} \int_{-U_j}^{U_j} (\tilde{\psi}_j(v) - \psi_j(v)) w_{\mu_j}^{U_j}(v) e^{-ivx} dv.$$

To show the asymptotic normality of the Ψ term we again split up Ψ in Linear parts $\mathcal{L}_{\mu_j}^0, \mathcal{L}_{\mu_j}^1$ and Remainder parts $\mathcal{R}_{\mu_j}^0, \mathcal{R}_{\mu_j}^1$, whereafter we will show that $\mathcal{L}_{\mu_j}^l$ is asymptotically normal and $\mathcal{R}_{\mu_j}^l$ is asymptotically negligible for $l = 0, 1$.

Note that the Ψ term bears a lot of resemblance with the cases of $(\tilde{\sigma}_j^2, \tilde{\gamma}_j, \tilde{\gamma}_j)$. The difference is in the fact that we now have a different weight function $w_{\mu_j}^{U_j}(v)$ and an extra term e^{-ivx} .

Recalling the definition of $\tilde{\psi}_j = \tilde{\psi}_j^0 - \tilde{\psi}_j^1$ and $\psi_j = \psi_j^0 - \psi_j^1$ and neglecting the stabilisation of $\kappa(v, T_{j-l})$ in the log, we can write

$$\Psi = \frac{1}{2\pi} \int_{-U_j}^{U_j} \left[\frac{1}{T_j - T_{j-1}} \log \left(\frac{\tilde{\varphi}_{T_j}(v-i)}{\varphi_{T_j}(v-i)} \right) - \frac{1}{T_j - T_{j-1}} \log \left(\frac{\tilde{\varphi}_{T_{j-1}}(v-i)}{\varphi_{T_{j-1}}(v-i)} \right) \right] w_{\mu_j}^{U_j}(v) e^{-ivx} dv.$$

Splitting the log into linear terms and remainder terms with a Taylor expansion opens up a way to write Ψ as

$$\begin{aligned} \Psi &= \frac{1}{2\pi} \int_{-U_j}^{U_j} [\mathcal{L}_j^0(v) - \mathcal{L}_j^1(v) + \mathcal{R}_j^0(v) - \mathcal{R}_j^1(v)] w_{\mu_j}^{U_j}(v) e^{-ivx} dv \\ &=: \mathcal{L}_{\mu_j}^0 - \mathcal{L}_{\mu_j}^1 + \mathcal{R}_{\mu_j}^0 - \mathcal{R}_{\mu_j}^1, \end{aligned} \quad (\text{B.1})$$

where for $l = 0, 1$ we have

$$\mathcal{L}_j^l(v) = \frac{1}{T_j - T_{j-1}} \frac{\tilde{\varphi}_{T_{j-l}}(v-i) - \varphi_{T_{j-l}}(v-i)}{\varphi_{T_{j-l}}(v-i)} \quad \text{and} \quad \mathcal{R}_j^l(v) = \tilde{\psi}_j^l - \psi_j^l(v) - \mathcal{L}_j^l(v).$$

The goal is to show that the linearized terms $\mathcal{L}_{\mu_j}^0(v), \mathcal{L}_{\mu_j}^1(v)$ are asymptotic normal and that the remainder terms $\mathcal{R}_{\mu_j}^0(v), \mathcal{R}_{\mu_j}^1(v)$ are asymptotically negligible.

B.3 Normality of Terms $\mathcal{L}_{\mu_j}^l(v)$ in Ψ

Firstly, the normality of the linearized terms $\mathcal{L}_{\mu_j}^0(v), \mathcal{L}_{\mu_j}^1(v)$ will be evaluated. This will be done by writing $\mathcal{L}_{\mu_j}^l(v)$ for $l = 0, 1$ as a sum of the error distribution of the regression model $(\varepsilon)_{j,k}$ – recall that these were centered independent sub-Gaussian random variables with $\mathbb{V}[\varepsilon_{j,k}] = 1$. Then we again show that the conditions of the Lyapunov Central limit Theorem – given in 3.1 – again hold and we can imply asymptotic normality.

As in (3.14) the deterministic characteristic function will again be written as

$$\begin{aligned} \varphi_{T_{j-l}}(v-i) &= \exp \left(\frac{-v^2}{2} \left(\sum_{r=1}^{j-l} (T_r - T_{r-1}) \sigma_r^2 \right) + iv \left(\sum_{r=1}^{j-l} (T_r - T_{r-1}) (\sigma_r^2 + \gamma_r) \right) \right. \\ &\quad \left. + \left(\sum_{r=1}^{j-l} (T_r - T_{r-1}) \left(\frac{\sigma_r^2}{2} + \gamma_r - \lambda_r \right) \right) + \left(\sum_{r=1}^m (T_r - T_{r-1}) \mathcal{F} \mu_r(v) \right) \right) \\ &=: \exp \left(-\frac{v^2}{2} A_{j-l} + iv B_{j-l} + C_{j-l} + D_{j-l}(v) \right). \end{aligned}$$

At this moment, the goal is to write \mathcal{L}_j^l as a sum of the independent $(\varepsilon_{j,k})$, such that we are in the form of Theorem 3.1. Using the properties of the weight function $w_{\mu_j} \in \mathcal{W}_{s_j}^n$ gives the result

$$\begin{aligned} \mathcal{L}_{\mu_j}^l &= \frac{1}{2\pi} \int_{-U_j}^{U_j} \mathcal{L}_j^l(v) w_{\mu_j}^{U_j}(v) e^{-ivx} dv = \frac{1}{2\pi} U_j \int_{-1}^1 \mathcal{L}_j^l(v U_j) w_{\mu_j}^1(v) e^{-iv U_j x} dv \\ &= \frac{1}{2\pi} U_j \int_0^1 \mathcal{L}_j^l(v U_j) w_{\mu_j}^1(v) e^{-iv U_j x} dv + \frac{1}{2\pi} U_j \int_0^1 \mathcal{L}_j^l(-v U_j) w_{\mu_j}^1(-v) e^{iv U_j x} dv \end{aligned}$$

$$\begin{aligned} &= \frac{1}{2\pi} U_j \int_0^1 \mathcal{L}_j^l(vU_j) w_{\mu_j}^1(v) e^{-ivU_j x} dv + \frac{1}{2\pi} U_j \int_0^1 \overline{\mathcal{L}_{\nu_j}^l(vU_j)} w_{\mu_j}^1(v) e^{ivU_j x} dv \\ &= \frac{1}{\pi} U_j \int_0^1 \operatorname{Re}(\mathcal{L}_j^l(vU_j) e^{-ivU_j x}) w_{\mu_j}^1(v) dv \end{aligned}$$

Using expression (3.2), we can write $\mathcal{L}_j^l(v)$ in a more basic form

$$\mathcal{L}_j^l(v) = \frac{1}{T_j - T_{j-1}} \frac{iv(1+iv) \sum_{k=1}^m \delta_{j-l,k} \varepsilon_{j-l,k} \mathcal{F}b_{j-l,k}(v)}{\varphi_{T_{j-l}}(v-i)}.$$

Substituting this, switching summation and integration, and switching integration and taking the real part, we can find

$$\begin{aligned} \mathcal{L}_{\mu_j}^l &= \frac{1}{\pi} \frac{U_j}{T_j - T_{j-1}} \sum_{k=1}^{m_{j-l}} \delta_{j-l,k} \varepsilon_{j-l,k} \int_0^1 \operatorname{Re} \left(\frac{ivU_j(1+ivU_j) \mathcal{F}b_{j-l,k}(vU_j)}{\varphi_{T_{j-l}}(vU_j-i)} e^{-ivU_j x} \right) w_{\mu_j}^1(v) dv, \\ &= \frac{1}{\pi} \frac{U_j}{T_j - T_{j-1}} \sum_{k=1}^{m_{j-l}} \delta_{j-l,k} \varepsilon_{j-l,k} \operatorname{Re} \left(\int_0^1 \frac{ivU_j(1+ivU_j) \mathcal{F}b_{j-l,k}(vU_j)}{\varphi_{T_{j-l}}(vU_j-i)} e^{-ivU_j x} w_{\mu_j}^1(v) dv \right). \end{aligned}$$

If, for $k = 1, \dots, m_{j-l}$, we define random variables

$$X_k := \frac{1}{\pi} \frac{U_j}{T_j - T_{j-1}} \delta_{j-l,k} \varepsilon_{j-l,k} \operatorname{Re} \left(\int_0^1 \frac{ivU_j(1+ivU_j) \mathcal{F}b_{j-l,k}(vU_j)}{\varphi_{T_{j-l}}(vU_j-i)} e^{-ivU_j x} w_{\mu_j}^1(v) dv \right),$$

then, from the properties that $(\varepsilon_{j,k})$ are independent centered random variables with $\mathbb{V}[\varepsilon_{j,k}] = 1$, it follows that (X_k) are independent centred random variables with $\mathbb{V}[X_k] = \sigma_k^2 < \infty$. Note that this is exactly the setting of Theorem 3.1 where $\mathcal{L}_{\mu_j}^l = T_m = \sum_{k=1}^m X_k$.

The Lyapunov conditions in Theorem 3.1 need to be shown. Firstly, the variance $s_{n,l}^2$ of $\mathcal{L}_{\mu_j}^l$ will be looked upon. The result is stated as a proposition because the proof is rather tedious and enduring.

Proposition B.1 *Let $s_{n,l}^2 = \sum_{k=1}^{m_{j-l}} \sigma_k^2$ with $\sigma_k^2 = \mathbb{V}[X_k^2] < \infty$ for $k = 1, \dots, m$ and let $\delta_{j-l} \in L^\eta(\mathbb{R})$ for $\eta \geq 2$ and $l = 0, 1$. As U_j tends to infinity, then*

$$s_{n,l}^2 = w_{\sigma_j}^1(1)^2 d_{j,j-l} \Delta_{j-l} U_j^{-4} \exp(A_{j-l} U_j^2),$$

where we defined the constant

$$d_{j,j-l} := 2 \|\delta_{j-l}\|_{L^2}^2 (T_j - T_{j-1})^{-2} A_{j-l}^{-2} \exp(-2C_{j-l}),$$

and the terms A_{j-l} and C_{j-l} are as in expression (3.14).

Proof (Proposition B.1) Using that $\mathbb{E}[\varepsilon_{j-l,k}] = 0$ and $\mathbb{V}[\varepsilon_{j-l,k}] = 1$, it follows that

$$\begin{aligned} s_{n,l}^2 &= \sum_{k=1}^{m_{j-l}} \sigma_k^2 \\ &= \frac{U_j^2}{\pi^2 (T_j - T_{j-1})^2} \sum_{k=1}^m \delta_{j-l,k}^2 \operatorname{Re}^2 \left(\int_0^1 \frac{ivU_j(1+ivU_j) \mathcal{F}b_{j-l,k}(vU_j)}{\varphi_{T_{j-l}}(vU_j-i)} e^{-ivU_j x} w_{\mu_j}^1(v) dv \right). \end{aligned}$$

Instead of computing the real part immediately, we will make use of the following identity

$$\operatorname{Re}^2 z = \left(\frac{z + \bar{z}}{2} \right)^2 = \frac{1}{4} (z^2 + 2z\bar{z} + \bar{z}^2),$$

and compute the three different parts instead. The problem can then be decomposed to

$$s_{n,l}^2 = \frac{U_j^2}{4\pi^2 (T_j - T_{j-1})^2} \sum_{k=1}^m \delta_{j-l,k}^2 (\mathcal{I}_v^2 + 2\mathcal{I}_v \mathcal{I}_{\bar{v}} + \mathcal{I}_{\bar{v}}^2) \quad (\text{B.2})$$

with $\mathcal{I}_v := \int_0^1 f(v)dv$ and $\mathcal{I}_{\bar{v}} := \overline{\int_0^1 f(v)dv}$ for the function

$$f(x, v) := \frac{ivU_j (1 + ivU_j) \mathcal{F}b_{j-l,k}(vU_j)}{\varphi_{T_{j-l}}(vU_j - i)} e^{-ivU_j x} w_{\mu_j}^1(v).$$

We start with the simplification of the term \mathcal{I}_v^2 ,

$$\begin{aligned} \mathcal{I}_v^2 &:= \left(\int_0^1 \frac{ivU_j (1 + ivU_j) \mathcal{F}b_{j-l,k}(vU_j)}{\exp(-v^2 U_j^2 A_{j-l}/2 + ivU_j B_{j-l} + C_{j-l} + D_{j-l}(vU_j))} e^{-ivU_j x} w_{\mu_j}^1(v) dv \right)^2 \\ &= \int_0^1 \int_0^1 \frac{ivU_j (1 + ivU_j) iwU_j (1 + iwU_j) \mathcal{F}b_{j-l,k}(vU_j) \mathcal{F}b_{j-l,k}(wU_j)}{\exp(-(v^2 + w^2) U_j^2 A_{j-l}/2 + i(v+w)U_j B_{j-l} + 2C_{j-l} + D_{j-l}(vU_j) + D_{j-l}(wU_j))} \\ &\quad e^{-ivU_j x} e^{-iwU_j x} w_{\mu_j}^1(v) w_{\mu_j}^1(w) dv dw \\ &= -U_j^2 \exp(-2C_{j-l}) \int_0^1 \int_0^1 vw \exp(A_{j-l}(v^2 + w^2) U_j^2/2) (1 + ivU_j) (1 + iwU_j) g(v, w) dv dw \\ &= -U_j^2 \exp(-2C_{j-l}) \left(\int_0^1 \int_0^1 vw \exp(A_{j-l}(v^2 + w^2) U_j^2/2) g(v, w) dv dw \right. \\ &\quad \left. + iU_j \int_0^1 \int_0^1 vw \exp(A_{j-l}(v^2 + w^2) U_j^2/2) (v+w) g(v, w) dv dw \right. \\ &\quad \left. - U_j^2 \int_0^1 \int_0^1 vw \exp(A_{j-l}(v^2 + w^2) U_j^2/2) \cdot vwg(v, w) dv dw \right), \end{aligned}$$

with g defined as

$$g(v, w) := \frac{\mathcal{F}b_{j-l,k}(vU_j) \mathcal{F}b_{j-l,k}(wU_j) e^{-ivU_j x} e^{-iwU_j x}}{\exp(i(v+w)U_j B_{j-l} + D_{j-l}(vU_j) + D_{j-l}(wU_j))} w_{\mu_j}^1(v) w_{\mu_j}^1(w).$$

In a similar manner, the terms $\mathcal{I}_{\bar{v}}^2$ and $\mathcal{I}_z \mathcal{I}_{\bar{z}}$ can be expressed as

$$\begin{aligned} \mathcal{I}_{\bar{z}^2} &= -U_j^2 \exp(-2C_{j-l}) \left(\int_0^1 \int_0^1 vw \exp(A_{j-l}(v^2 + w^2) U_j^2/2) g(-v, -w) dv dw \right. \\ &\quad \left. + iU_j \int_0^1 \int_0^1 vw \exp(A_{j-l}(v^2 + w^2) U_j^2/2) (-v-w) g(-v, -w) dv dw \right. \\ &\quad \left. - U_j^2 \int_0^1 \int_0^1 vw \exp(A_{j-l}(v^2 + w^2) U_j^2/2) vwg(-v, -w) dv dw \right) \end{aligned}$$

and

$$\begin{aligned} \mathcal{I}_z \mathcal{I}_{\bar{z}} &= U_j^2 \exp(-2C_{j-l}) \cdot \left(\int_0^1 \int_0^1 vw \exp(A_{j-l}(v^2 + w^2) U_j^2/2) \cdot g(v, -w) dv dw \right. \\ &\quad \left. + iU_j \int_0^1 \int_0^1 vw \exp(A_{j-l}(v^2 + w^2) U_j^2/2) (v-w) g(v, -w) dv dw \right. \\ &\quad \left. - U_j^2 \int_0^1 \int_0^1 vw \exp(A_{j-l}(v^2 + w^2) U_j^2/2) \cdot -vwg(v, -w) dv dw \right). \end{aligned}$$

For evaluating these integrals even further Lemma 3.3 will again be used as in the case of $\tilde{\sigma}_j^2$, only now the function $g(v, w)$ is slightly different.

Remembering the solution of the Fourier transform $\mathcal{F}b_{j,k}(v)$ in expression (3.3), it can be shown that $\lim_{U_j \rightarrow \infty} g(v, w)$ is not necessarily finite.

For applying Lemma 3.3, the function $\tilde{g}_{U_j}(v, w)$ will be defined as

$$\tilde{g}_{U_j}(v, w) := vw \exp(2iU_j(B_{j-l} + x)) \mathcal{F}b_{j,k}(U_j)^{-2} g(v, w).$$

With this new addition, $\lim_{U_j \rightarrow \infty} \tilde{g}_{U_j}(1, 1)$ exists and is finite. Hence, we need to check the conditions on \tilde{g}_{U_j} and we need to find functions f_{U_j} which converge to a Dirac delta function at $(1, 1)$. Rescaling the other factors in the integrals, such that these integrals are in the form of Lemma 3.3, gives

$$f_{U_j}(v, w) := A_{j-l}^2 U_j^4 \exp(-A_{j-l} U_j^2) vw \exp(A_{j-l}(v^2 + w^2) U_j^2 / 2) =: F(v) \cdot F(w).$$

The $h(x)$ function in Lemma 3.3 will be chosen to be $h(x) = x^{-3/2}$, it is easy to see that $h(x) \downarrow 0$ as $x \rightarrow \infty$. Now the conditions of Lemma 3.3 will be checked on this particular $f_{U_j}(u, v)$ function

$$\begin{aligned} \lim_{U_j \rightarrow \infty} \int_{1-U_j^{-3/2}}^1 \int_{1-U_j^{-3/2}}^1 f_{U_j}(v, w) dv dw &= \lim_{U_j \rightarrow \infty} \left(\int_{1-U_j^{-3/2}}^1 F(v) dv \right)^2 = 1, \\ \lim_{U_j \rightarrow \infty} \int_0^1 \int_0^1 f_{U_j}(v, w) dv dw &= \lim_{U_j \rightarrow \infty} \left(\int_0^1 F(v) dv \right)^2 = 1, \end{aligned}$$

where it was used that

$$\begin{aligned} \int_{b(U_j)}^1 F(v) dv &= \exp(-A_{j-l} U_j^2 / 2) \int_{b(U_j)}^1 v A_{j-l} U_j^2 \exp(A_{j-l} v^2 U_j^2 / 2) dv \\ &= \exp(-A_{j-l} U_j^2 / 2) \cdot \left[\exp(A_{j-l} v^2 U_j^2 / 2) \right]_{b(U_j)}^1 \\ &= \exp(-A_{j-l} U_j^2 / 2) \cdot \left[\exp(A_{j-l} U_j^2 / 2) - \exp\left(A_{j-l} (b(U_j))^2 U_j^2 / 2\right) \right] \\ &= 1 - \exp(-A_{j-l} U_j^2 [1 - b(U_j)^2] / 2). \end{aligned}$$

The function f is thus satisfactory. What remains to check is the boundedness of \tilde{g}_U on the unit square and we need to check that

$$\lim_{U_j \rightarrow \infty} \sup_{(u,v) \in [1-U^{-3/2}, 1]^2} |\tilde{g}_{U_j}(u, v) - \tilde{g}_{U_j}(1, 1)| = 0.$$

First of all recall

$$\begin{aligned} \tilde{g}_{U_j}(v, w) &:= vw \exp(2iU_j(B_{j-l} + x)) \mathcal{F}b_{j,k}(U_j)^{-2} g(v, w) \\ &= vw \frac{\mathcal{F}b_{j-l,k}(vU_j) \mathcal{F}b_{j-l,k}(wU_j)}{\mathcal{F}b_{j-l,k}(U_j)^2} w_{\mu_j}^1(v) w_{\mu_j}^1(w) \frac{\exp(2iU_j(B_{j-l} + x))}{\exp(i(v+w)U_j(B_{j-l} + x))} e^{-D_{j-l}(vU_j) - D_{j-l}(wU_j)} \end{aligned}$$

The assumption is made that $U_j > c$ for a certain $c > 0$. For ease of notation let

$$\begin{aligned} \tilde{g}_1(v, w) &= vw, \quad \tilde{g}_2(v, w) = \frac{\mathcal{F}b_{j-l,k}(vU_j) \mathcal{F}b_{j-l,k}(wU_j)}{\mathcal{F}b_{j-l,k}(U_j)^2}, \quad \tilde{g}_3(v, w) = w_{\mu_j}^1(v) w_{\mu_j}^1(w) \\ \tilde{g}_4(v, w) &= \exp(i(2 - v - w)U_j(B_{j-l} + x)), \quad \tilde{g}_5(v, w) = \exp(-D_{j-l}(vU_j) - D_{j-l}(wU_m)) \end{aligned}$$

Note that \tilde{g}_1, \tilde{g}_3 and \tilde{g}_4 are uniformly bounded on the unit square. Also note that $\mathcal{F}\mu_j(x) \rightarrow 0$ for $x \rightarrow \infty$. Hence, D_{j-l} is a bounded function, which implies that \tilde{g}_5 is bounded uniformly. Proving boundedness of \tilde{g}_2 , recall expression (3.3), then

$$\tilde{g}_2(v, w) = \exp(-i(v+w-2)U_j x_{j,k} \Delta_{j,k}) \cdot \frac{\text{sinc}^2(vU_j \Delta_{j-l}/2) \text{sinc}^2(wU_j \Delta_{j,k}/2)}{\text{sinc}^2(U_j \Delta_{j,k}/2)} \quad (\text{B.3})$$

where $\Delta_{j-l} = |x_{j,k-1} - x_{j,k}|$. We can find a $c > 0$, such that for all $U_j > c$ we have $\text{sinc}^2(U_j \Delta_{j-l}) \geq 1/2$, which leads to the bound

$$|\tilde{g}_2(v, w)| \leq \left| \frac{\text{sinc}^2(vU_j\Delta_{j-l}/2) \text{sinc}^2(wU_j\Delta_{j-l}/2)}{\text{sinc}^2(U_j\Delta_{j-l}/2)} \right| \leq \left| \frac{1}{\text{sinc}^2(U_j\Delta_{j-l}/2)} \right| \leq 2.$$

So, \tilde{g}_2 is bounded on the unit square. Putting everything together we can conclude that $\tilde{g}(v, w)$ is bounded on the unit square.

We note that $\tilde{g}_1 \cdot \tilde{g}_3$ is continuous in $(1, 1)$. Moreover, the second part of \tilde{g}_2 in expression (B.3) also behaves satisfactory. Thus these factors can be taken out of the equation. Note that, \tilde{g}_5 converges uniformly to 1 for $U_j \rightarrow \infty$ because of the smoothness of $\mu_j(x)$. The only problems thus occur in the first part of \tilde{g}_2 in expression (B.3) and in \tilde{g}_4 ,

$$\begin{aligned} \sup_{(v,w) \in [1-U_j^{-3/2}, 1]^2} |\tilde{g}_4(v, w) - 1| &= \left| \exp\left(i\left(2 - \left(1 - U_j^{-3/2}\right) - \left(1 - U_j^{-3/2}\right)\right)U_j(B_{j-l} + x)\right) - 1 \right| \\ &= \left| \exp\left(i \cdot U_j^{-1/2}(B_{j-l} + x)\right) - \exp(i \cdot 0) \right| \leq \left| U_j^{-1/2}(B_{j-l} + x) \right| \rightarrow 0. \end{aligned}$$

Similarly, the first part of \tilde{g}_2 can be controlled. This completes all the conditions of the function $\tilde{g}_{U_j}(v, w)$ in Lemma 3.3. To conclude, now we have found and checked the functions $f_{U_j}(v, w)$ and $\tilde{g}_{U_j}(v, w)$ in Lemma 3.3 and we can use these functions to solve the desired integrals.

From this Lemma, it appears that all the integrals in the final expressions for \mathcal{I}_v^2 , $\mathcal{I}_{\bar{v}}^2$ and $\mathcal{I}_v\mathcal{I}_{\bar{v}}$ converge equally fast to 0 and the dominating term is the last one with the U_j^4 factor in front of it. Henceforth, the first two integrals will be left out of the equation. Reminding the extra term of $\tilde{g}_{U_j}(v, w)$ with respect to $g(v, w)$, using Lemma 3.3 the limit is found to be

$$\begin{aligned} &\lim_{U_j \rightarrow \infty} \mathcal{I}_{\bar{v}}^2 A_{j-l}^2 \exp(-A_{j-l}U_j^2) \mathcal{F}b_{j-l,k}(U_j)^{-2} \exp(2iU_j(B_{j-l} + x)) \\ &= \lim_{U_j \rightarrow \infty} \exp(-2C_{j-l}) \int_0^1 \int_0^1 f_{U_j}(v, w) \tilde{g}_{U_j}(v, w) dv dw = \exp(-2C_{j-l}) \lim_{U_j \rightarrow \infty} \tilde{g}_{U_j}(1, 1) \\ &= \exp(-2C_{j-l}) w_{\mu_j}^1(1)^2 \lim_{U_j \rightarrow \infty} \exp(-2D_{j-l}(U_j)) = \exp(-2C_{j-l}) w_{\mu_j}^1(1)^2. \end{aligned}$$

In a similar manner, the other terms $\mathcal{I}_{\bar{v}}^2$ and $\mathcal{I}_v\mathcal{I}_{\bar{v}}$ their convergence can be deduced

$$\begin{aligned} &\lim_{U_j \rightarrow \infty} \mathcal{I}_{\bar{v}}^2 A_{j-l}^2 \exp(-A_{j-l}U_j^2) \overline{\mathcal{F}b_{j,k}(U_j)^{-2}} \exp(-2iU_j(B_{j-l} + x)) = \exp(-2C_{j-l}) w_{\mu_j}^1(1)^2, \\ &\lim_{U_j \rightarrow \infty} \mathcal{I}_v\mathcal{I}_{\bar{v}} A_{j-l}^2 \exp(-A_{j-l}U_j^2) |\mathcal{F}b_{j,k}(U_j)|^{-2} = \exp(-2C_{j-l}) w_{\mu_j}^1(1)^2. \end{aligned}$$

Recalling expression (B.2) for $s_{n,l}^2$, the asymptotic variance $s_{n,l}^2$ will be found by considering the following adapted limit

$$\lim_{U_j \rightarrow \infty} \frac{s_{n,l}^2}{\Delta_{j-l}U_j^{-4}A_{j-1}^{-2} \exp(A_{j-1}U_j^2)} \tag{B.4}$$

$$= \frac{1}{(T_j - T_{j-1})^2} \lim_{U_j \rightarrow \infty} \Delta_{j-l}^{-1} \sum_{k=1}^{m_{j-l}} \delta_{j-l,k}^2 A_{j-1}^2 \exp(-A_{j-1}U_j^2) (\mathcal{I}_v^2 + 2\mathcal{I}_v\mathcal{I}_{\bar{v}} + \mathcal{I}_{\bar{v}}^2). \tag{B.5}$$

An important remark to make is that when $U_j \rightarrow \infty$ the maximum distance between the grid points needs to go to zero $\Delta_{j-l} \rightarrow 0$, and thereby the number of observations needs to go infinity $m_{j-l} \rightarrow \infty$.

All the different limits for \mathcal{I}_v^2 , $\mathcal{I}_v\mathcal{I}_{\bar{v}}$ and $\mathcal{I}_{\bar{v}}^2$ will be individually considered by replacing the summands by their respective asymptotic behavior. Note that this is not a trivial step and should be proven. The result is given in Lemma (B.1).

Lemma B.1 *Under the assumptions of Proposition 3.2,*

$$\begin{aligned} & \lim_{U_j \rightarrow \infty} \Delta_{j-l}^{-1} \sum_{k=1}^{m_{j-l}} \delta_{j-l,k}^2 A_{j-l}^2 e^{-A_{j-l} U_j^2} \mathcal{I}_v^2 \\ &= \lim_{U \rightarrow \infty} \Delta_{j-l}^{-1} \sum_{k=1}^{m_{j-l}} \delta_{j-l,k}^2 e^{-2C_{j-l}} w_{\mu_j}^1(1)^2 \mathcal{F} b_{j-l,k}(U_j)^2 e^{-2i(B_{j-l}+x)U_j} \end{aligned}$$

The steps of the proof of Lemma B.1 are completely similar to the steps of the proof of Lemma 3.4 – the different term $e^{-2i(B_{j-l}+x)U_j}$ cancels while taking the absolute value of the second term as in the proof of Lemma 3.4.

Recalling the Fourier transform of $b_{j-l,k}$ in (3.3) and the definition of the Riemann integral, we can derive

$$\begin{aligned} & \lim_{U_j \rightarrow \infty} \Delta_{j-l}^{-1} \sum_{k=1}^{m_{j-l}} \delta_{j-l,k}^2 A_{j-l}^2 e^{-A_{j-l} U_j^2} \mathcal{I}_v^2 \\ &= e^{-2C_{j-l}} w_{\mu_j}^1(1)^2 \lim_{U_j \rightarrow \infty} e^{-2i(B_{j-l}+x)U_j} \Delta_{j-l}^{-1} \sum_{k=1}^{m_{j-l}} \delta_{j-l,k}^2 \mathcal{F} b_{j-l,k}(U_j)^2 \\ &= e^{-2C_{j-l}} w_{\mu_j}^1(1)^2 \lim_{U_j \rightarrow \infty} e^{-2i(B_{j-l}+x)U_j} \operatorname{sinc}^4(U_j \Delta_{j-l}/2) \sum_{k=1}^{m_{j-l}} \delta_{j-l,k}^2 e^{2iU_j x_{j-l,k}} \Delta_{j-l} \\ &= e^{-2C_{j-l}} w_{\mu_j}^1(1)^2 \lim_{U_j \rightarrow \infty} e^{-2i(B_{j-l}+x)U_j} \operatorname{sinc}^4(U_j \Delta_{j-l}/2) \int_{-\infty}^{\infty} \delta_{j-l}(x)^2 e^{2iU_j x} dx \\ &= e^{-2C_{j-l}} w_{\mu_j}^1(1)^2 \lim_{U_j \rightarrow \infty} e^{-2i(B_{j-l}+x)U_j} \operatorname{sinc}^4(U_j \Delta_{j-l}/2) \mathcal{F} \delta_{j-l}^2(2U_j). \end{aligned} \quad (\text{B.6})$$

In a similar manner,

$$\begin{aligned} & \lim_{U_j \rightarrow \infty} \Delta_{j-l}^{-1} \sum_{k=1}^{m_{j-l}} \delta_{j-l,k}^2 A_{j-l}^2 e^{-A_{j-l} U_j^2} \mathcal{I}_{\bar{v}}^2 \\ &= e^{-2C_{j-l}} w_{\mu_j}^1(1)^2 \lim_{U_j \rightarrow \infty} e^{2i(B_{j-l}+x)U_j} \Delta_{j-l}^{-1} \sum_{k=1}^{m_{j-l}} \delta_{j-l,k}^2 \mathcal{F} b_{j-l,k}(-U_j)^2 \\ &= e^{-2C_{j-l}} w_{\mu_j}^1(1)^2 \lim_{U_j \rightarrow \infty} e^{2i(B_{j-l}+x)U_j} \operatorname{sinc}^4(-U_j \Delta_{j-l}/2) \mathcal{F} \delta_{j-l}^2(-2U_j) \end{aligned} \quad (\text{B.7})$$

and

$$\begin{aligned} & \lim_{U_j \rightarrow \infty} \Delta_{j-l}^{-1} \sum_{k=1}^{m_{j-l}} \delta_{j-l,k}^2 A_{j-l}^2 e^{-A_{j-l} U_j^2} \mathcal{I}_v \mathcal{I}_{\bar{v}} \\ &= e^{-2C_{j-l}} w_{\mu_j}^1(1)^2 \lim_{U_j \rightarrow \infty} \Delta_{j-l}^{-1} \sum_{k=1}^{m_{j-l}} \delta_{j-l,k}^2 |\mathcal{F} b_{j-l,k}(U_j)|^2 \\ &= e^{-2C_{j-l}} w_{\mu_j}^1(1)^2 \lim_{U_j \rightarrow \infty} \operatorname{sinc}^4(U_j \Delta_{j-l}/2) \int_{-\infty}^{\infty} \delta_{j-l}(x)^2 dx \\ &= e^{-2C_{j-l}} w_{\mu_j}^1(1)^2 \lim_{U_j \rightarrow \infty} \operatorname{sinc}^4(U_j \Delta_{j-l}/2) \|\delta_{j-l}\|_{L^2}^2. \end{aligned} \quad (\text{B.8})$$

We have assumed δ to be an $L^{2+\eta}$ with $\eta > 0$ function, hence $\mathcal{F} \delta_{j-l}^2(2U_j) \rightarrow 0$ as $U_j \rightarrow \infty$. Moreover, $U_j \Delta_{j-l} \rightarrow 0$, thus $\operatorname{sinc}^4(U_j \Delta_{j-l}/2) \rightarrow 1$ as $U_j \rightarrow \infty$. So, we can conclude that expressions (B.6) and (B.7) are equal to 0 in the limit. Furthermore, expression (B.8) becomes

$$\lim_{U_j \rightarrow \infty} \Delta_{j-l}^{-1} \sum_{k=1}^{m_{j-l}} \delta_{j-l,k}^2 A_{j-l}^2 e^{-A_{j-l} U_j^2} \mathcal{I}_v \mathcal{I}_{\bar{v}} = e^{-2C_{j-l}} w_{\mu_j}^1(1)^2 \lim_{U_j \rightarrow \infty} \operatorname{sinc}^4(U_j \Delta_{j-l}/2) \|\delta_{j-l}\|_{L^2}^2.$$

Using expression (B.5) the asymptotic variance $s_{n,l}^2$ is then found to be

$$\begin{aligned} s_{n,l}^2 &= \Delta_{j-l} U_j^{-4} A_{j-l}^{-2} \exp(A_{j-l} U^2) \cdot \frac{1}{4} \left(0 + 2 \cdot 4 (T_j - T_{j-1})^{-2} e^{-2C_{j-l}} w_{\mu_j}^1(1)^2 \|\delta_{j-l}\|_{L^2}^2 + 0 \right) \\ &= 2 \|\delta_{j-l}\|_{L^2}^2 (T_j - T_{j-1})^{-2} A_{j-l}^{-2} e^{-2C_{j-l}} w_{\mu_j}^1(1)^2 \cdot \Delta_{j-l} U_j^{-4} e^{A_{j-l} U_j^2} \\ &= w_{\mu_j}^1(1)^2 d_{j,j-l} \Delta_{j-l} U_j^{-4} e^{A_{j-l} U_j^2} \end{aligned}$$

where we had the constant

$$d_{j,j-l} = 2 \|\delta_{j-l}\|_{L^2}^2 (T_j - T_{j-1})^{-2} A_{j-l}^{-2} e^{-2C_{j-l}}.$$

□

This asymptotic variance $s_{n,l}^2$ is the same as we found earlier for the case in the main body of σ_j^2 . In the Lyapunov Central Limit Theorem 3.1 next to the variance also a bound for $\mathbb{E}|X_r|^{2+\eta}$ needed to be found. Note that the only difference with the case with $\mu_j(x)$ compared to $\sigma_j(x)$ in X_k is the different weight function $w_{\mu_j}^1$ and the factor $e^{-iU_j v x}$. This last factor cancels in the absolute signs and the weight function is again bounded. Thus, the derivation becomes similar and we find the same expression as in (3.23). The verification of the Lyapunov condition is therefore also completely similar.

Hence, with Theorem 3.1 we can imply that

$$\frac{\mathcal{L}_{\mu_j}^l}{U_j^3 s_{n,l}} = \frac{T_{j-l}}{U_j^3 s_{n,l}} \xrightarrow{d} \mathcal{N}(0, 1), \quad \text{for } l = 0, 1.$$

B.4 Remainder Terms $\mathcal{R}_{\mu_j}^l$ in Ψ

In this section, we want to investigate if and under which conditions the asymptotic remainder term will be negligible asymptotically.

The idea is again going to be that we are going to look at certain conditions such that asymptotically when $U_j \rightarrow \infty$ and $\Delta_j \rightarrow 0$ we have

$$\mathcal{R}_{\mu_j}^l f_{\mu_j}(U_j, \Delta_j) \xrightarrow{\mathbb{P}} 0,$$

where the function $f_{\mu_j}(U_j, \Delta_j)$ is given by

$$f_{\mu_j}(U_j, \Delta_j) = \frac{1}{U_j^3} \frac{U_j^2 e^{-U_j^2 \sum_{i=1}^j (T_i - T_{i-1}) \sigma_i^2 / 2}}{\sqrt{d_{j,j} \Delta_j + d_{j,j-1} \Delta_{j-1} e^{-U_j^2 (T_j - T_{j-1}) \sigma_j^2}}}$$

Note that $f_{\mu_j}(U_j, \Delta_j)$ is a positive deterministic function and \mathbb{P} stands for convergence in probability.

This function $f_{\mu_j}(U_j, \Delta_j)$ may feel arbitrary now, but it will be shown that this function is coupled to the asymptotic variance s_n^2 of the previously considered $\tilde{\sigma}_j^2$ by $f_{\mu_j}(U_j, \Delta_j) = \frac{|w_{\mu_j}^1(1)|}{s_n^2}$. We actually want $\frac{\mathcal{R}_{\mu_j}^l}{s_n^2}$ to become 0, because then we can conclude that $\frac{\tilde{\mu}_j(x) - \mu_j(x)}{s_n^2} \xrightarrow{d} \mathcal{N}(0, 1)$.

Markov's inequality will be used with the convex function x^2 to bound the convergence in probability, i.e., let $\varepsilon > 0$ then

$$\mathbb{P} \left(\left| \mathcal{R}_{\mu_j}^l f_{\mu_j}(U_j, \Delta_j) \right| > \varepsilon \right) \leq \frac{1}{\varepsilon^2} \mathbb{E} \left[\left| \mathcal{R}_{\mu_j}^l f_{\mu_j}(U_j, \Delta_j) \right|^2 \right] = \frac{|f_{\mu_j}(U_j, \Delta_j)|^2}{\varepsilon^2} \mathbb{E} \left[\left| \mathcal{R}_{\mu_j}^l \right|^2 \right].$$

So we want to find a bound for $\mathbb{E} \left[\left| \mathcal{R}_{\mu_j}^l \right|^2 \right]$. Fortunately, it will be shown that the derivation will be identical to the triplet in the main part of the thesis.

Before we begin, recall that we did define

$$\mathcal{R}_j^l(v) = \tilde{\psi}_j^l(v) - \psi_j^l(v) - \mathcal{L}_j^l(v) \quad \text{and} \quad \mathcal{R}_{\mu_j}^l = \int_{-U_j}^{U_j} \mathcal{R}_j^l(v) w_{\mu_j}^{U_j}(v) e^{-ivx} dv.$$

Note that $\mathcal{R}_{\mu_j}^l$ is a random variable, because it is connected to the error terms $(\varepsilon_{j,k})$.

The term $\mathcal{R}_j^l(v)$ is exactly the same as in the case σ_j^2 . In expression (3.26) we already derived the bound

$$\begin{aligned} |\mathcal{R}_j^l| &\leq \frac{1}{2} (T_j - T_{j-1})^{-1} K_{j-l}(v)^{-2} (v^4 + v^2) \left| \mathcal{F}(\tilde{\mathcal{O}}_{j-l} - \mathcal{O}_{j-l})(v) \right|^2 \\ &\lesssim K_{j-l}(v)^{-2} (v^4 + v^2) \left| \mathcal{F}(\tilde{\mathcal{O}}_{j-l} - \mathcal{O}_{j-l})(v) \right|^2. \end{aligned}$$

Now for $\mathbb{E} \left[|\mathcal{R}_{\mu_j}^l|^2 \right]$ we get the bound:

$$\mathbb{E} \left[|\mathcal{R}_{\mu_j}^l|^2 \right] = \mathbb{E} \left[\left| \int_{-U_j}^{U_j} \mathcal{R}_j^l(v) w_{\mu_j}^{U_j}(v) e^{-ivx} dv \right|^2 \right] \leq \mathbb{E} \left[\left(\int_{-U_j}^{U_j} |\mathcal{R}_j^l(v)| |w_{\mu_j}^{U_j}(v)| dv \right)^2 \right].$$

We see that the deviating term e^{-ivx} cancels and we are in the same position as with the σ_j case where only the weight function $w_{\mu_j}^{U_j}(v)$ differs.

The only difference thereafter occurs in Lemma 3.6, where it can be shown that for the weight function $w_{\mu_j}^{U_j}(v)$,

$$\int_{-U_j}^{U_j} \frac{v^4 |w_{\mu_j}^{U_j}(v)|}{K_j(v)^2} dv \lesssim \frac{1}{U_j} e^{U_j^2 \sum_{i=1}^j (T_i - T_{i-1}) \sigma_i^2}.$$

Hence, following the same steps with the same conditions imposed we find the result

$$\mathcal{R}_{\mu_j}^l \frac{1}{U_j^3} \frac{U_j^2 e^{-U_j^2 \sum_{i=1}^j (T_i - T_{i-1}) \sigma_i^2 / 2}}{\sqrt{d_{j,j} \Delta_j + d_{j,j-1} \Delta_{j-1} e^{-U_j^2 (T_j - T_{j-1}) \sigma_j^2}}} \xrightarrow{\mathbb{P}} 0. \quad (\text{B.9})$$

whenever the same asymptotic conditions are satisfied

$$\Delta_j U_j^4 e^{U_j^2 \sum_{i=1}^j (T_i - T_{i-1}) \sigma_i^2} \rightarrow 0 \quad \text{and} \quad \frac{\Delta_{j-1}^2}{\Delta_j} U_j^4 e^{U_j^2 (\sum_{i=1}^{j-1} (T_i - T_{i-1}) \sigma_i^2 - (T_j - T_{j-1}) \sigma_j^2)} \rightarrow 0.$$

